TERRAPIN TECHNOLOGIES
MANNED MARS MISSION PROPOSAL

ENAE 412: NASA/USRA Project
Dr. Mark Lewis, Advisor

Period: January 23, 1990 - May 14, 1990

UM-AERO-90-27

The sections of this report represent the individual efforts of the following students:

Amato, Michael
Bryant, Heather
Coleman, Rodney
Compy, Chris
Crouse, Patrick
Crunkleton, Joe
Hurtado, Edgar
Iverson, Eirik
Kamosa, Mike
Kraft, Lauri
Martin, Larry
McCartney, Rick
Miyake, Kaoru
Rosenberg, Evan
Ryan, Darren
Seybold, Calina

The compilation and editing of this report were performed by Lauri Kraft and Calina Seybold.

Acknowledgments

Thanks to Dr. James E. Randolph and Dr. Angus McRonald of the Jet Propulsion Laboratory for suggesting this work; to Ms. Stacy Weinstein, also of the Jet Propulsion Laboratory, for providing trajectory information; and to Dr. Jim Phenix and Dr. Stephen Paddack of the NASA Goddard Space Flight Center for their participation with the USRA Program.

Thanks to Mr. Tom McLaughlin for his time and effort in teaching Rick McCartney and Larry Martin how to use his Waverider generation code, and for the time he spent generating our Waveriders.

Also, thanks to Dr. Ajay Kothari, Dr. Anthony Vizzini, and Dr. John Anderson for their informative lectures and other support of this program. Especially, thanks to Dr. Mark Lewis for lectures, individual help, and other many contributions.

Finally, appreciation is extended to the USRA program, under the direction of John Alred, for supporting this design experience.

Special Notes

I would like to thank Dr. Everett Jones and Dr. David VanWie from the aerospace department here at the University for taking the time to provide me with documentation and insight into the heating problems I encountered. Also, I owe my appreciation to Dr. Mark Lewis and Mr. Charles Lind for their patience in answering my time-consuming questions on everything from computers to chemistry. Finally, a special thanks goes to Mr. James Batt for getting me started. --- Calina Seybold

I would like to thank Mr. Charles Lind for dedicating time to helping me with the various intricacies of document production on the Macintosh and for his invaluable advice. --- Lauri Kraft

Table of Contents

Manned Mars Mission Proposal

I.1 Introduction

Terrapin Technologies is pleased to propose a Manned Mars Mission (M^3) design study. The purpose of M^3 is to transport 10 personnel and a habitat with all required support systems and supplies from low Earth orbit (LEO) to the surface of Mars and, after an eight-man surface expedition of 3 months, to return the personnel safely to LEO. The proposed hardware design is based on systems and components of demonstrated high capability and reliability. The mission design builds on past mission experience, but incorporates innovative design approaches to achieve mission priorities. Those priorities, in decreasing order of importance, are safety, reliability, minimum personnel transfer time, minimum weight, and minimum cost. The design demonstrates the feasibility and flexibility of a Waverider transfer module.

I.2 Mission Overview
(Kraft)

The M^3 begins with the departure of the Landing/Launch Vehicle Module (LLVM) from LEO on a transfer trajectory to Mars. The LLVM is comprised of three submodules: (1) the LLVM Departure/Return Stage, (2) the Lander/Launcher/Habitat Submodule, and (3) the Supply Stage (SS). The Departure/Return Stage provides propulsion and control for the burn out of LEO, as well as propulsion and control for primary burns to achieve a low Mars orbit (LMO) and propulsion and control for the burn to return the Waverider to LEO. The Lander/Launcher/Habitat Submodule provides all life support, logistics, and equipment for the surface expedition, as well as propulsion, thermal protection, parachute braking system, and control for descent to the Mars surface and propulsion and control for liftoff and rendezvous with the Departure/Return Stage in LMO. Finally, the Supply Stage carries supplies for the WOPM return to LEO.

Following departure of the LLVM from LEO and checkout of all systems in Mars orbit, the Waverider Orbital Personnel Module (WOPM) departs LEO for Venus. The WOPM is comprised of two submodules: (1) the WOPM Departure Stage, which provides propulsion and control for the burn out of LEO and separates after that burn is complete, and (2) the Waverider, which provides propulsion and control for transfer into LMO, thermal protection for an aero-assist maneuver in the Venus atmosphere, guidance for all phases of the mission, and accommodations for the ten personnel on both departure and return legs of the mission. After separation from the WOPM near Venus, the Departure stage, with propulsion produced by a nuclear generator, will return autonomously to LEO to be reused for future missions. The

LLVM Departure/Return Stage and the WOPM Departure Stage are of the same design, and, for generic discussions, will be referred to as "the booster."

The WOPM aero-gravity assist (AGA) maneuver at Venus is designed to allow a large change in direction of the orbital velocity without significant change in the magnitude of the velocity. Thus a significant reduction in transfer time and flexibility in mission design are gained relative to a conventional direct transfer from Earth to Mars. After transferring from Venus to LMO, the WOPM performs an aerobrake maneuver and carries out a rendezvous with the LLVM, already in Mars parking orbit. Systems are checked out, and the Waverider, Supply Stage, and Return Stage, now docked together, are separated from the Lander/Launcher, which then descends to the Mars surface with 8 of the 10 crew members. The other 2 crew members remain on board the Waverider to monitor the habitat on Mars and maintain frequent communication with the ground stations on Earth. They will also be responsible for performing scientific experiments and transferring supplies for the return voyage from the Supply Stage portion of the LLVM.

After the 3-month expedition is complete, the Liftoff Submodule rejoins the WOPM in LMO. Personnel transfer to the Waverider, and the empty SS is jettisoned. This allows the WOPM to return to earth without the added weight of the SS, thereby decreasing the necessary amount of return fuel. Finally, the WOPM departs for Earth with the Return Stage providing propulsion.

The entire mission requires a total of 520 days: 258 days for the transfer of the unmanned LLVM to Mars, 135 days for the transfer of the WOPM to Mars, 90 days for the surface expedition, and 137 days for the return of the WOPM to Earth. The manned mission totals only 362 days. A detailed sequence of events is provided in Section II.4, and a detailed description of the design and function of all modules and submodules is provided in Section III.

I.3 Design Concept
(Kraft)

I.3.1 LLVM Design and Function

The LLVM is designed to include a Departure/Return Stage, which provides propulsion for departure from LEO; the Liftoff and Landing Submodules; the Habitat used as a base for the 3-month expedition; supplies and all support systems required by the crew during the surface and return phases of the mission; and the Return Stage, which returns the Waverider from LMO to LEO. It was decided to place these items on the LLVM instead of the WOPM because their weight would be an unnecessary burden for the Waverider, since the crew would not have need of them until LMO is achieved. In addition, the thin, aerodynamic structure of a Waverider of reasonable

proportions is not capable of transporting such large volumes of matter and still achieving the high values of L/D required for the Venus fly-by portion of the mission.

As noted previously, the boosters for the WOPM and the LLVM are of identical design. They utilize nuclear reactors for propulsion. Tank structure for the boosters is based on salvaged STS external tanks. Both boosters are recovered at the end of the mission and can be reused on later missions.

The Launcher/Lander/Habitat is a blunt lifting cone and thus provides a compact, efficient volume for the crew dwelling on the surface. It uses chemical propellants.

I.3.2 WOPM Design and Function

The WOPM is designed to carry the 10-person crew and all of the supplies and equipment needed to reach LMO from LEO. When the Liftoff Subsystem returns to LMO for rendezvous, the WOPM must be capable of adjusting its trajectory to meet that of the Liftoff module. Once the remaining crew reenters the Waverider, it will dock with the booster portion of the LLVM in the proper configuration for the return trip. The mission concept is shown in the sketch below.

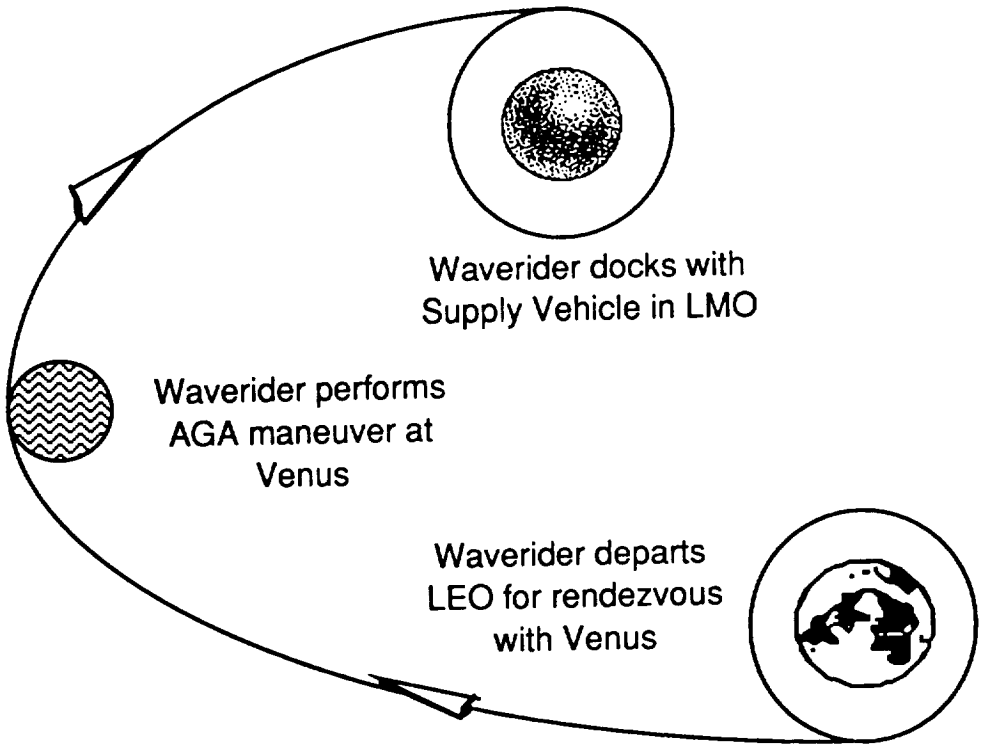

The Waverider approach to the mission design allowed very short transfer times, an important factor in assuring the comfort and safety of the crew. Also, by using aero-gravity maneuvers at planet encounters rather than propellants, the Waverider concept allows reduction in mission mass compared to missions relying solely on propulsion; and the AGA allows more flexibility in choice of launch dates than simple gravity maneuvers.

I.4 Organization
(Kraft)

The Terp Tech organization for the M^3 Project is as follows:

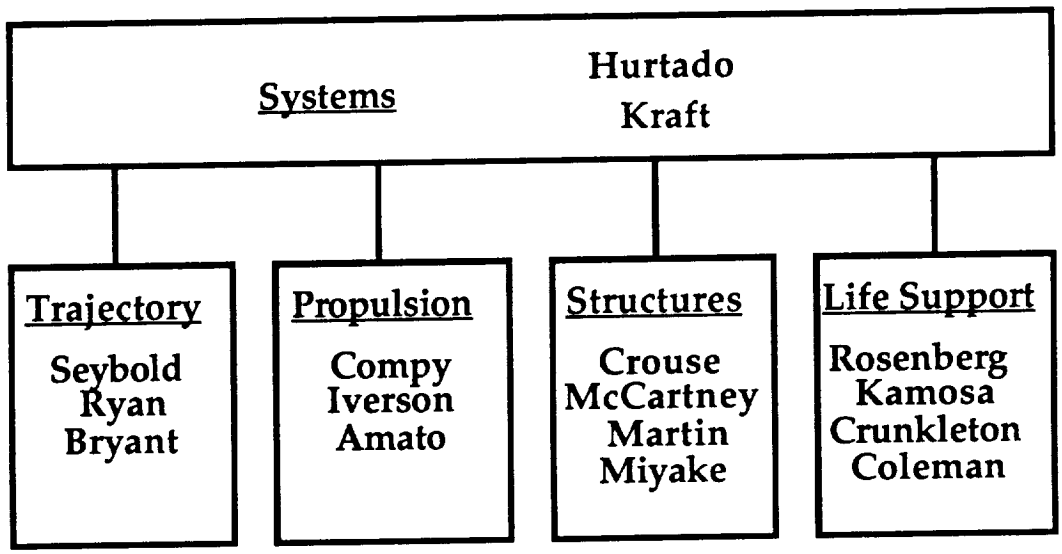

II.1 Mission Analysis

II.2 Trajectory

II.2.1 Trajectory Design

Research has lead us to develop codes to determine parameters for aero-gravity assist (AGA) maneuvers, aerobrake corridors, convective heating rates, rendezvous, and general trajectories. Given below are the results of these calculations for the Waverider.

II.4.1.1 WOPM Trajectory
(Ryan)

The trajectory of the Waverider consists of leaving earth orbit on an elliptical transfer orbit to Venus, performing an aero-gravity assist (AGA) maneuver at Venus, and then travelling to Mars on a new elliptical orbit. Once at Mars, an

aerobrake maneuver will be performed to place the Waverider in a circular orbit around the planet. For the return to earth, the Waverider is placed on an elliptical transfer orbit back to earth, where a velocity increment is applied to slow the vehicle down and place it into orbit about the earth.

The first step in the design of the trajectory was determining how to get to Venus from Earth in the shortest amount of time. In order to find the necessary velocities and the times of flight, a computer code was written using Battin's Universal Formulas (Kaplan, Reference 35). This particular method was chosen because it allows the computation of the final position and velocity vectors of a spacecraft after a given duration of time, if the initial position and velocity vectors are known.

Starting with an initial position vector equal to the orbital radius of the earth about the sun, an initial velocity (relative to the sun) was entered into the code. The time of flight was then varied until the final position vector was equal to the orbital radius vector of Venus about the sun. By repeating this process for various initial velocities, the time of flight to Venus was determined. A graph of the data is shown in Figure II.4.1.1-1 below:

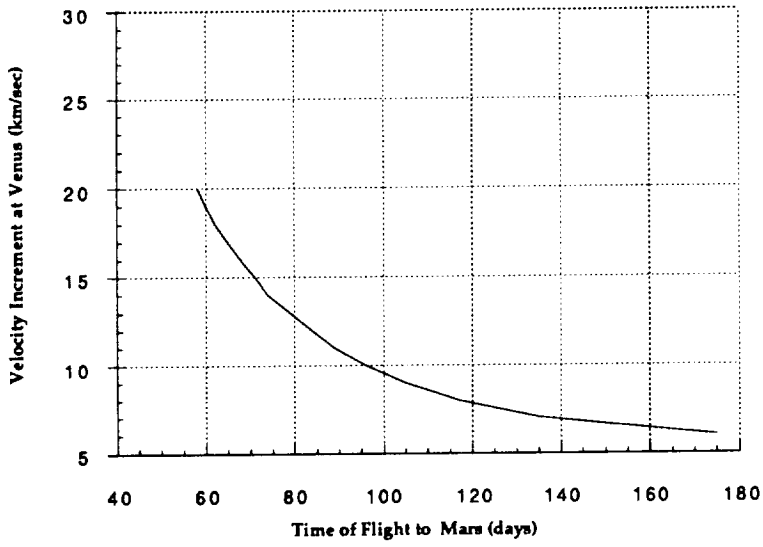

Figure II.4.1.1-1: ΔV vs. Time of Flight

The second step in computing the trajectory of the Waverider was to consider the path between Venus and Mars. The same method was used as before to find the final position and velocity vectors, knowing the initial conditions at Venus. The initial velocity was varied at Venus until the final position of

the spacecraft was equal to the orbital radius of Mars, and a time of flight for this segment of the trajectory was obtained. A graph of the data is shown in Figure II.4.1.1-2 below:

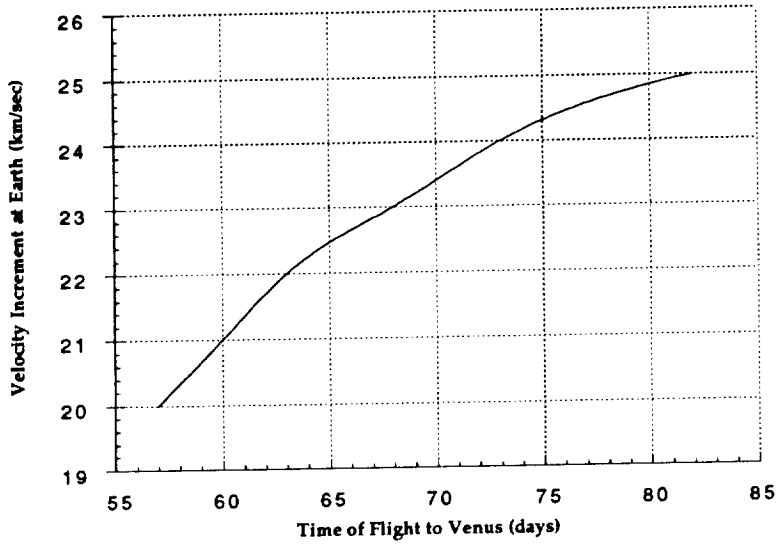

Figure II.4.1.1-2: ΔV at Earth vs. Time of Flight

From the data obtained on the Earth-Venus trajectory , it was found that the final velocities at Venus were much lower than the required velocities needed for the Venus-Mars trajectory. In order to obtain the required velocities, the AGA maneuver design was used. Since the ΔV obtained by an AGA maneuver depends on the angular deflection through the planet's atmosphere, the required deflection angle had to be determined. The deflection angle could not be picked randomly because it depends on the position of the planets. Therefore, the third step in the trajectory determination was to write a computer program to give the heliocentric coordinates of the planets Venus, Earth, and Mars, if a specific month, day and year were entered. The code assumed that the orbits of the planets were circular and coplanar, and the initial starting dates and positions were obtained from the American Ephemeris and Nautical Almanac.

Considering all the variables in the first three steps, the trajectory was then found by trial and error. The position of the planets was computed for various dates, and for each date, the first and second steps were used to determine the flight times, velocity increments, and required deflection angles at Venus. The table below lists dates that best fit our goals:

Earth-Venus-Mars Trajectory

Date	Time	Description
8/22/2026	---	Earth Departure
10/28/2026	69 days	AGA maneuver at Venus
1/02/2027	135 days	Arrive at Mars

Total Period of Trajectory: 135 days

The above trajectory allows the Waverider to reach Mars in 135 days, with a required deflection angle of 82 degrees through the atmosphere of Venus. A schematic of the trajectory is given in Figure II.4.1.1-3.

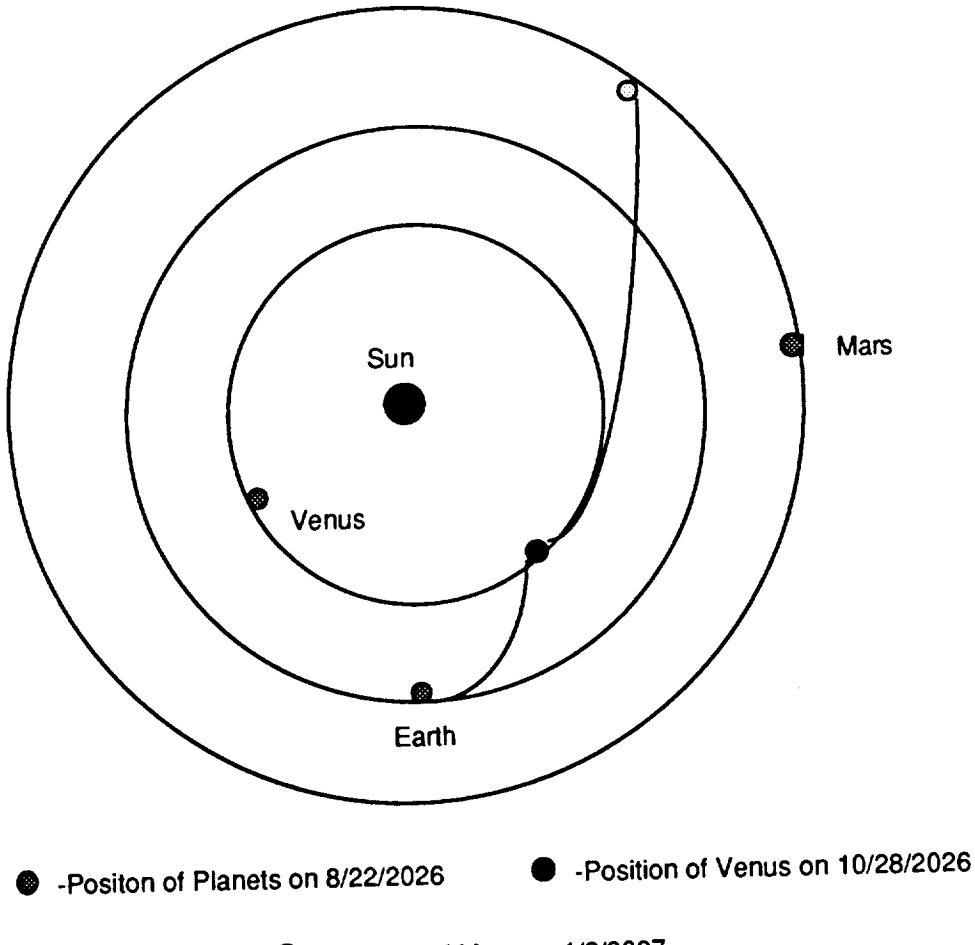

Figure II.4.1.1-3: Waverider Trajectory

II.4.1.1.1 Venus Flyby
(Bryant)

The Waverider configuration will be used to obtain the shortest possible round-trip mission time. Ordinarily, a planetary flyby utilizes a gravity assist maneuver to change the direction of the spacecraft's velocity vector. However, the range of angular deflections possible with such a maneuver is somewhat limited. For a gravity assist trajectory, deflection angle is dependent upon the spacecraft's velocity. For lower velocities, the possible deflection increases with increasing velocity magnitude, reaching a maximum when the spacecraft velocity equals the planet's circular velocity at the radius of passage. If the velocity increases beyond circular velocity, the angular deflection possible with a gravity assist maneuver begins to decrease.

Rather than perform a simple gravity assist, the Waverider employs an aero-gravity assist (AGA) maneuver at Venus to supply the ΔV necessary to reach Mars. The advantage of using the Waverider for this application lies in the fact that it is a lifting body. Since its structure is tailored to "ride" the shock wave at a certain flight condition, the Waverider can enter and fly through the planet's atmosphere without experiencing excessive velocity loss due to drag. The lift vector is directed towards the planet during the atmospheric flyby, thus augmenting gravity and balancing the centrifugal force which tends to propel the Waverider out of the atmosphere. The result is the unique ability of the Waverider to remain at a constant altitude during the atmospheric passage, thus allowing almost any desired angular deflection.

Although the aero-gravity assist maneuver causes velocity losses during the atmospheric flight, the greater range of possible deflection angles it offers over a simple gravity assist make it more desirable for planning missions and for shortening total mission time. With a gravity assist, the planets must be in a specific alignment for the proper deflection angle to be realized; therefore the launch windows for such missions are very short and far apart. For an aero-gravity assist maneuver, however, planetary alignment is not such a crucial issue, so the launch window is increased considerably.

In our Manned Mars Mission, the Waverider will leave low Earth orbit and approach Venus on a hyperbolic trajectory. Upon reaching the planet at a relative velocity of 17.0 km/sec, the vehicle will dive into the atmosphere and perform the AGA maneuver with a total deflection angle of 82 degrees.

For the mathematical analysis of the AGA maneuver, it was first necessary to determine the lift needed to balance the centrifugal force acting on the Waverider at its approach velocity. This was accomplished by use of the following equation:

$$L=m\left(\frac{V_i^2}{R}-\frac{\nu}{R^2}\right)$$

From a calculated value of lift and the definition of lift coefficient,

$$C_L=\frac{2L}{\rho A V_i^2}$$

the density at which the Waverider should fly could be found. Subsequently, from density tables of the Venusian atmosphere (Hunten, Reference 34), the following relationship between density and altitude from 60 km to 140 km was obtained through a computer-generated curve-fit:

$$h = 57.6 - 10.2 \log r$$

A computer code was written to solve these three equations iteratively, obtaining a convergent value of altitude for the AGA maneuver (see Appendix A). For a Waverider mass of 300,000 kg, we found the necessary lift to be 9480 kN, corresponding to an atmospheric density of 0.00139 kg/m3 and a flight altitude of 86.7 km.

Given the total desired deflection angle of 82.0 ° around the planet, it was possible to calculate what portion of the total flyby would occur in the atmosphere. Figure II.4.1.1.1-1 shows the division of the total deflection into the parts taking place inside and outside the Venusian atmosphere.

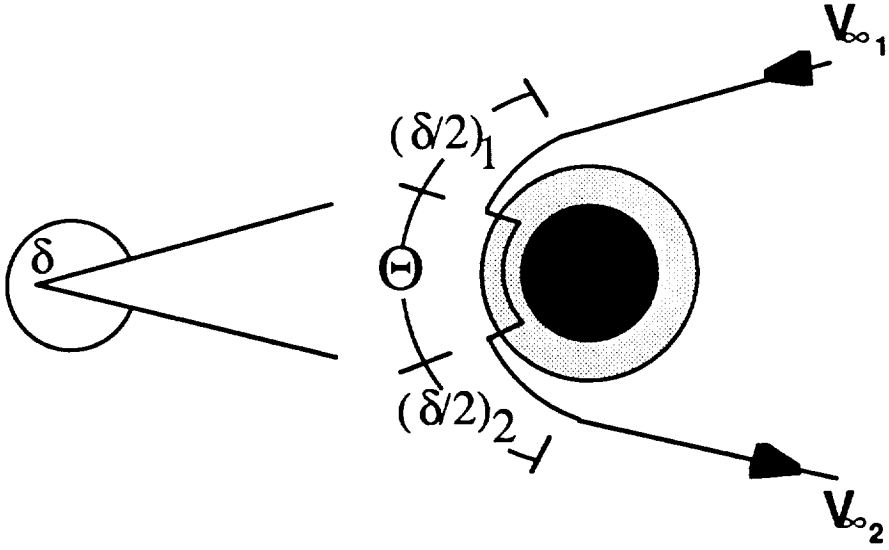

Figure II.4.1.1.1-1: Aero-Gravity Assist Maneuver

With a hyperbolic approach to the planet, the segments of the deflection occurring outside the atmosphere were obtained as follows:

$$\left(\frac{\delta}{2}\right)_1 = \sin^{-1}\left(\frac{1}{1+\overline{V}^2}\right)$$

$$\left(\frac{\delta}{2}\right)_2 = \sin^{-1}\left(\frac{e^{\frac{2\theta}{L/D}}}{1+\overline{V}^2}\right)$$

Since the leading edges of the Waverider will be made of an ablative material that will sublime in a known fashion, we were able to assume that the Waverider lift-to-drag ratio will remain constant at 6.9 throughout the maneuver, in spite of high heating rates. The above-mentioned computer code applied these equations iteratively, and the values of $(\delta/2)_1$ and $(\delta/2)_2$ were determined to be 12.70 ° and 16.66 °, respectively. Finally, the amount of deflection occurring in the atmosphere of Venus (θ) was found to be 52.64 °, for a total atmospheric flight time of 6.1 minutes.

Once the deflection through the atmosphere was known, it was possible to determine the amount of velocity lost during the AGA maneuver. The velocity of the Waverider leaving the atmosphere of Venus is a function of deflection angle and the lift-to-drag ratio:

$$V_2 = \sqrt{\left(e^{\frac{-2\theta}{L/D}}V_1^2\right) - \left(e^{\frac{-2\theta}{L/D}} - 1\right)\frac{V}{R}}$$

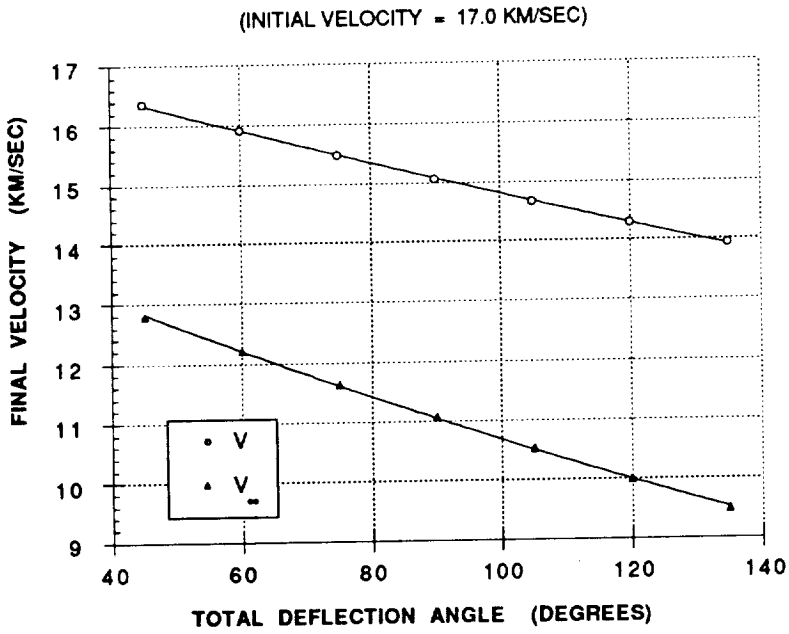

Figure II.4.1.1.1-2: Final Velocity vs Deflection Angle

Figure II.4.1.1.1-2 shows the variation in final velocity with deflection angle. Given the values determined above, the outgoing velocity was found to be 15.3 km/sec, corresponding to a velocity at infinity of 11.4 km/sec relative to Venus. Finally, the Law of Cosines was applied to the incoming and outgoing velocities to obtain the ΔV possible with the AGA maneuver. Figure II.4.1.1.1-3 shows the variation of ΔV with deflection angle. For an angular deflection of 82 degrees, the ΔV obtained is 16.5 km/sec.

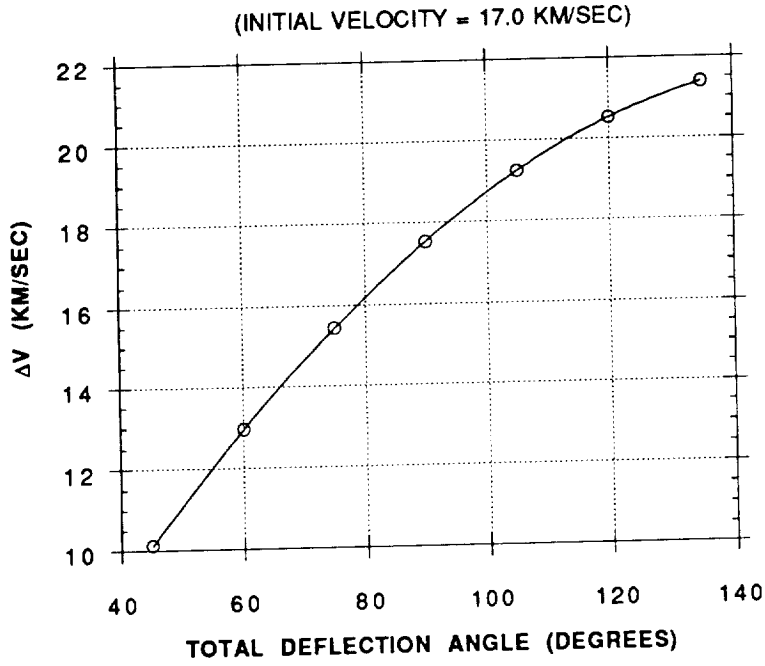

Figure II.4.1.1.1-3: ΔV vs Deflection Angle

II.4.1.1.2 Mars Capture
(Seybold)

In order to achieve a circular orbit around Mars, we need to burn off the excess velocity resulting from our hyperbolic approach from Venus. Since we need to burn off 6-10 km/s, and the Waverider will not have a large enough propulsive system on board to do a retroburn, an aerobrake seems to be the most cost and mass efficient way to slow down. To analyze an aerobrake trajectory, a corridor is found that gives the safest and most effective passage through a planet's atmosphere. This corridor is defined by an overshoot boundary and an undershoot boundary.

The quickest and most effective aerobrake is one in which the vehicle remains in the planet's atmosphere until all of the excess velocity is burned off. The overshoot boundary is the altitude that the incoming vehicle must

remain below in order to prevent it from skipping back out of the atmosphere. In determining our overshoot boundary, the following equation (Tauber, Bowles, and Yang, Reference 69) was used:

$$\rho_{ovr}=\frac{2}{R_o}\left(\frac{m}{C_L A}\right)\left(\frac{V_s^2}{V^2}-1\right)$$

Where: ρ_{ovr} = Density at Overshoot Boundary
R_o = Planetary Radius (Mars = 3390 km)
m = Mass
CL= Lift Coefficient
A = Planform Area
Vs = Circular Satellite Speed (Mars = 3555.9 m/s)
V = Approaching Velocity

This equation gives a density; to find the corresponding altitude, the following atmospheric model is used (Tauber, Bowles, and Yang, Reference 60):

$$\rho= \rho_i e^{-\beta_i y}$$

Where:

Altitude Range (km)	ρ_i (kg/m3)	β_i(m - 1)
> 36	0.03933	0.0001181
9 to 36	0.01901	0.00009804
< 9	0.01501	0.00007124

Using this model, an initial altitude is estimated and the corresponding density obtained. This density is then compared to the density calculated for the overshoot boundary. Through successive iterations of our code, the two densities converge until they fall within a given uncertainty (0.0003). Once within that uncertainty, the code computes the corresponding altitude of the atmospheric model density. This altitude is the overshoot boundary.

The undershoot boundary is the minimum altitude in the corridor, below which the vehicle will be fatally drawn in toward the planet's surface. The procedure for determining this boundary is identical to the one used to determine the overshoot boundary, with the exception that the density for the undershoot boundary is determined from (Tauber, Bowles, and Yang, Reference 60):

$$\rho_{und} = \frac{2}{R_o}\left(\frac{m}{C_D A}\right)\left(\frac{V_s^2}{V^2}\right)\left(\frac{1}{g}\right)\left(\frac{-dV}{dt}\right)$$

Where: CD = Drag Coefficient
g = Gravity of Mars (3.73 m/s2)

To determine the drag coefficient, our code uses the lift coefficient referenced in the overshoot discussion and asks for an L/D ratio as input. Since L/D is also CL/CD, the drag coefficient can be easily obtained. For the -dV/dt term, our code requests an input for the desired multiple of the Martian gravity (the number of "g's") and multiplies that number by 3.73 m/s^2 to get the deceleration the vehicle will undergo.

Both of the inputs mentioned above significantly vary the undershoot boundary and thus the corridor width. Increasing the L/D ratio (Fig. II.4.1.1.2-1) or increasing the deceleration (Fig. II.4.1.1.2-2) will increase the corridor width. Also, increasing the deceleration will decrease the time of flight for the aerobrake. However, it should be noted that the overshoot boundary is not affected by these inputs; the corridor width is increased by going deeper into the atmosphere. Therefore, there is a trade-off between a wider maneuvering corridor and a faster time of flight or lower aerodynamic heating (from the lower densities) and less strain on the astronauts (from the lesser deceleration).

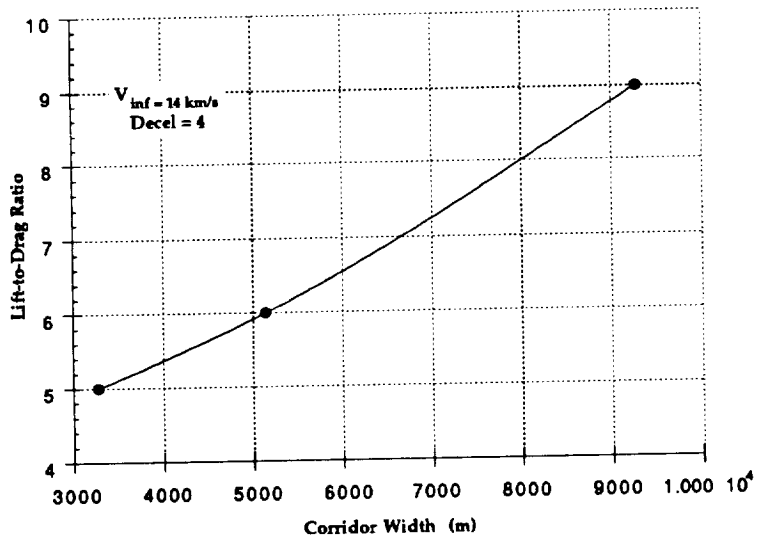

Figure II.4.1.1.2-1: L/D Ratio vs Aerobrake Corridor Width

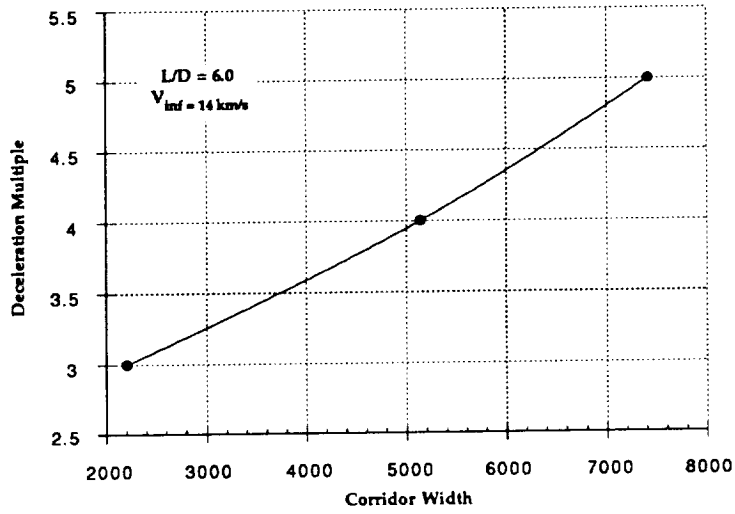

Figure II.4.1.1.2-2: Deceleration Multiple vs Aerobrake Corridor Width

From the expected parameters (m=300,000 kg, A=1,428.87 m2, V=13,200 m/s) and the lift coefficient obtained from the AGA design, the overshoot boundary turned out to be 17,680 m. Choosing a deceleration multiple of 4 (dV/dt = 14.92 m/s2) and assuming--even though we will be off optimum--that the L/D will be about 6, the undershoot boundary is 9,860 m. This results in a corridor width of 7820 m. Taking the pass altitude to be the center line between the two boundaries, it turns out to be at 13,770 m, which corresponds to a density of 4.93E-03. This density is used to determine the heating rates on the vehicle as it passes through the atmosphere (see Section III.2.2.3.4).

II.4.1.1.3. Rendezvous

(Seybold)

Once the Waverider reaches Mars, it will have to dock with the supply ship that will already be circling the planet at an altitude of 170 km. Coming out of the aerobrake, the Waverider will fire its thrusters to circularize its orbit at an altitude which is less than the Supply Stage's altitude. Once this orbit has been attained, the code (Appendix C) to perform the rendezvous will be activated at some initial longitudinal distance. For the purposes of our preliminary analysis, the rendezvous will only be considered to be two-dimensional.

To determine the longitudinal and latitudinal velocities at any given time during the rendezvous, a force-free, coplanar form of Hill's equations are used (Kaplan):

$$\dot{y}_o = \frac{[6x_o(nt-\sin nt)-y_o]n\sin nt-2nx_o(4-3\cos nt)(1-\cos nt)}{(4\sin nt-3nt)\sin nt+4(1-\cos nt)^2}$$

$$\dot{x}_o = -\frac{nx_o(4-3\cos nt)+2(1-\cos nt)\dot{y}_o}{\sin nt}$$

Where: x_o= Initial Longitudinal Distance
y_o= Initial Latitudinal Distance
n= 9.988E-04 rad/s for an altitude of 170 km at Mars
t = Time

The code asks for an input of the initial longitudinal and latitudinal distances and computes the above velocities in two minute increments. An example of a velocity profile is in Fig. II.4.1.1.3-1.

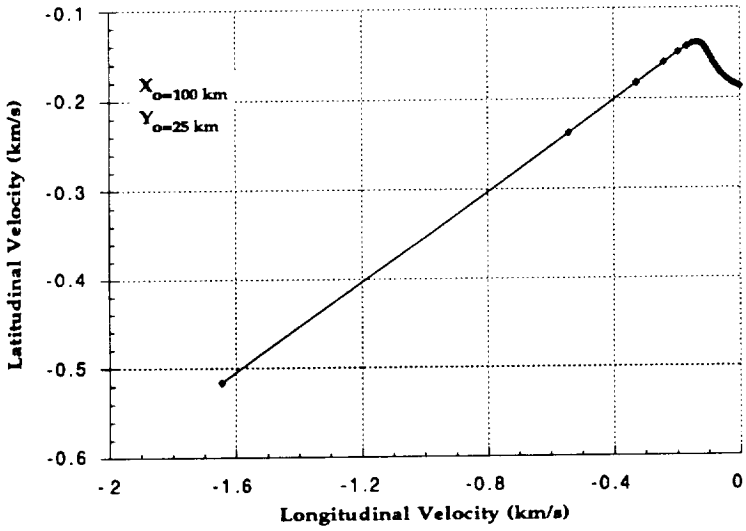

Figure II.4.1.1.3-1: Rendezvous Velocity Profile

Once the velocities are calculated at each time increment, the position is determined by multiplying 170 times the sine or cosine of the angle theta

between the target and the pursuer. Starting from an arbitrary initial value of theta (1.571 rad.), the code recomputes the angle at each time increment until it reaches the value of 0.01 rad, where the code prints out the time required to perform a rendezvous to this distance. Corresponding to the angle, the x and y positions are determined. Since the code only goes until theta reaches 0.01 rad, the final positions of the Waverider and the Supply Stage do not exactly coincide. A more sophisticated code will need to be written to maneuver the Waverider for the last 100 m latitudinally and 5000 m longitudinally. A typical position profile is in Fig. II.4.1.1.3-2.

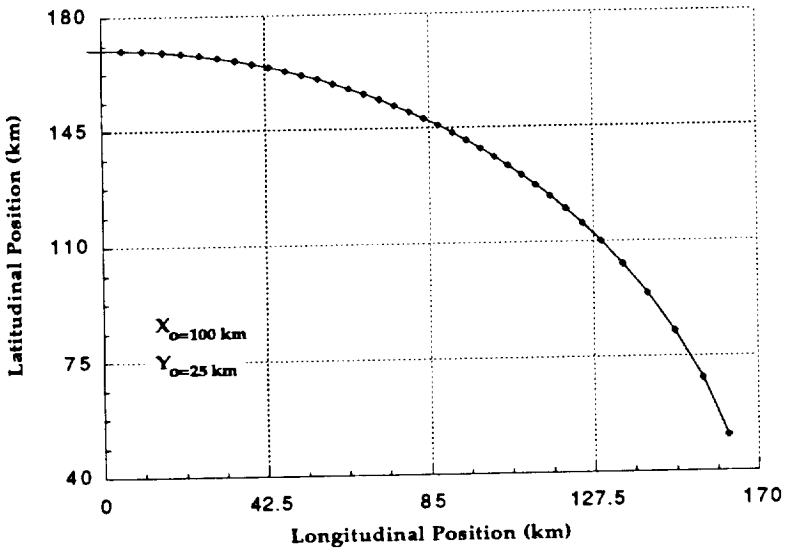

Figure II.4.1.1.3-2: Rendezvous Position Profile

As stated above, the code prints out the time it takes for the rendezvous maneuver to within a theta of 0.01 rad. Assuming that the latitudinal distance to travel will be constant once the Waverider establishes its circular orbit after the aerobrake, several runs were made varying the longitudinal distance. The results of these runs using $y_o = 20$ km and 5 km < x_o < 100 km are in Fig. II.4.1.1.3-3 . It shows that the duration is nearly constant (at about 4500 sec) until the vehicles get to within 20 km; then, the time begins to drop off sharply. At 5 km, the maneuver takes only 400 sec. There is a trade-off between the amount of time it takes to perform the rendezvous at the longer initial distances and the practicality of performing the maneuver at an initial distance of only 5 or 10 km. In the end, the astronauts will probably choose to begin the rendezvous at an initial distance that will give them approximately 2500 to 3500 sec with which to work.

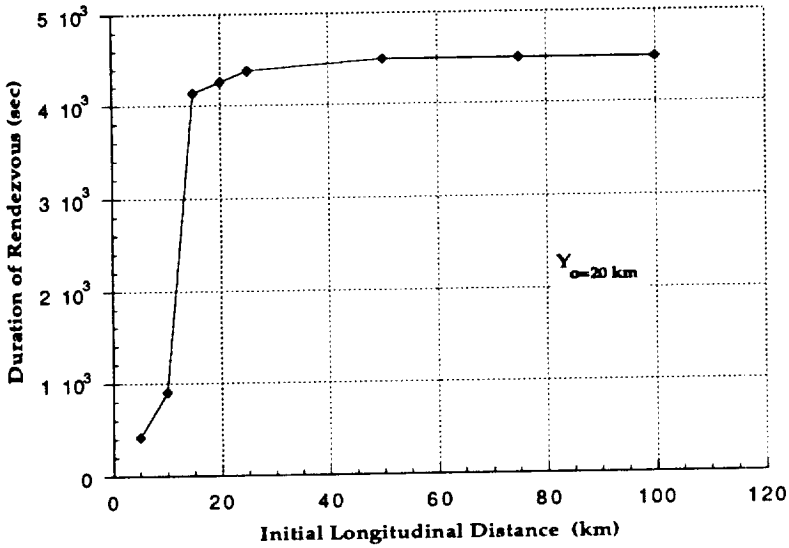

Figure II.4.1.1.3-3: Rendezvous Duration vs Longitudinal Distance

II.4.1.1.4 Transfer from Mars to LEO

(Ryan)

Since a three month stop over at Mars was required for the mission, the launch date for the trajectory from Mars to Earth is now known, given the previously calculated Earth-Mars time of flight. Possible aero-gravity assist or gravity assist maneuvers at Venus were considered for the return trip, but the position of Venus was unfavorable for these maneuvers on the given launch dates. Therefore a straight elliptical transfer orbit was used for the return trip back to Earth.

Again Battin's Universal Formulas were used to obtain the necessary conditions at Mars to place the Waverider on an elliptical transfer orbit back to Earth. The initial conditions and time of flights are listed below:

Mars-Earth Return Trajectory

Date	Time Into Mission	Description
4/02/2027	---	Mars Departure
8/17/2027	137 days	Arrival at Earth

Total Period of Trajectory: 137 days

A schematic of the return trajectory is shown in Figure II.4.1.1-4.

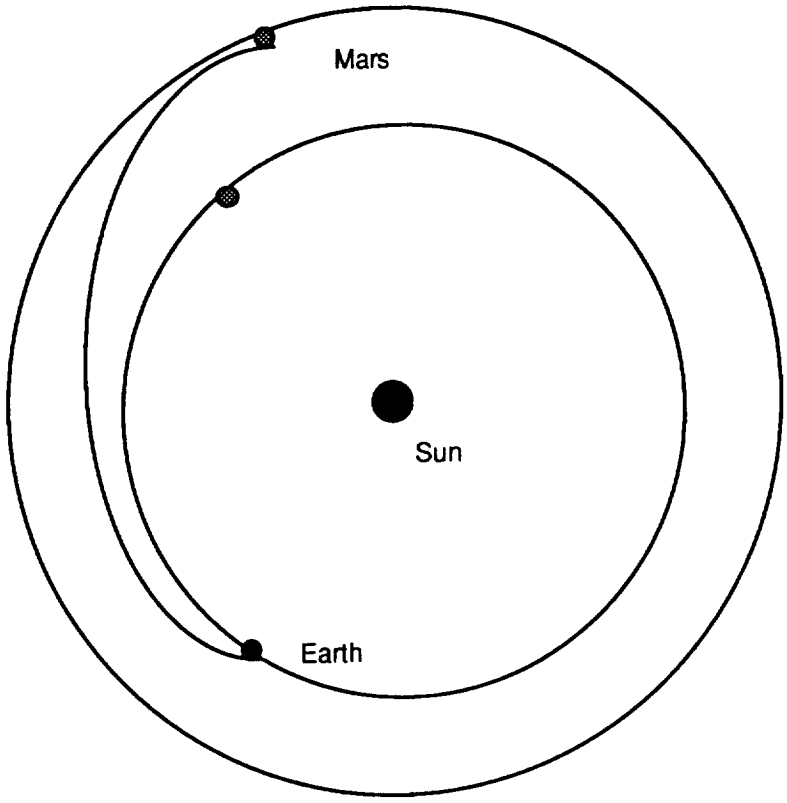

Figure II.4.1.1-4: Waverider Return Trajectory

When using Battin's Universal Formulas, all velocities obtained are in the heliocentric reference frame. In order to obtain these heliocentric velocities, planetary escape and planetary capture sequences must be considered.

The ΔV required from the propulsion systems to place the Waverider on the desired transfer orbit to Venus is obtained in the following way:

Let:
V_r= required heliocentric velocity
V_E= orbital velocity of Earth about the Sun
μ_{earth}= gravitational coefficient of the Earth
r_{earth}= orbital radius of spacecraft about the Earth

$$\Delta V=\sqrt{(V_r-V_{earth})^2+\frac{2\mu_{earth}}{r_{earth}}}-\sqrt{\frac{\mu_{earth}}{r_{earth}}}$$

The required ΔV to be lost by the aerobrake that will place the Waverider in a desired orbit about Mars is obtained in the following way:

Let: V_s= heliocentric velocity of spacecraft
V_{mars}= orbital velocity of Mars about the Sun
μ_{mars}= gravitational coefficient of Mars
r_{mars}=desired orbital radius of spacecraft about Mars

$$\Delta V=\sqrt{(V_s-V_{mars})^2+\frac{2\mu_{mars}}{r_{mars}}}-\sqrt{\frac{\mu_{mars}}{r_{mars}}}$$

The final trajectory was selected by taking into account all of the above considerations. This trajectory meets the requirements of the Request for Proposal, in that it provides the minimum time of flight to Mars within two years of the specified year of 2025. The table below describes the final trajectory for the entire mission duration of the Waverider.

Final Trajectory of Waverider

Launch Date	Planet	V_∞ *	Bend angle
8/22/2026	Earth	6.6 km/sec	---
10/28/2026	Venus	16.0 km/sec	82 degrees
1/02/2027	Mars	-13.2 km/sec **	---
4/02/2027	Mars	6.0 km/sec	---
8/17/2027	Earth	- 5.0 km/sec **	---

* - V_∞ is given as the relative velocity to the corresponding planet.

** - The negative sign indicates the velocity is to be lost at the given planet.

II.4.1.2 LLVM Trajectory
(Ryan)

The Supply Stage (SS) trajectory will consist of placing the vehicle on a Hohmann transfer orbit to Mars, where it will then be placed in a circular orbit about Mars and remain there until it docks with the Waverider.

A Hohmann transfer was selected for the SS because this type of trajectory requires a minimum velocity increment at Earth and also does not require the vehicle to perform AGA maneuvers and aerobrakes. Another reason for using the Hohmann transfer is that launch windows occur about every 26 months, thus giving greater flexibility on launch dates.

Although the time of flight to Mars via a Hohmann transfer is 258 days, the crew of astronauts will not be riding on the SS, so the long time of flight is not a major problem from the crew standpoint. However, the SS cannot be placed in orbit around Mars too far in advance, because fuel and other supplies that are important for the return trip back to Earth may perish during the long wait.

The ΔV required to place the supply ship on the Hohmann transfer orbit is given by the following equation:

Let:
V_p= perihelion velocity of supply ship on transfer orbit
V_E= orbital velocity of Earth about the Sun
μ_{earth}= gravitational coefficient of the Earth
r_{earth}= orbital radius of spacecraft about the Earth

$$\Delta V=\sqrt{(V_p-V_E)^2+\frac{2\mu_{earth}}{r_{earth}}}-\sqrt{\frac{\mu_{earth}}{r_{earth}}}$$

Likewise, the required ΔV to slow the vehicle down and place it into the desired orbit around Mars is given by the following formula:

Let:
V_a= aphelion velocity of supply ship on transfer orbit
V_M= orbital velocity of Mars about the Sun
μ_{mars}= gravitational coefficient of Mars
r_{mars}=desired orbital radius of spacecraft about Mars

$$\Delta V=\sqrt{(V_a-V_M)^2+\frac{2\mu_{earth}}{r_{earth}}}-\sqrt{\frac{\mu_{earth}}{r_{earth}}}$$

The final step in determining the Supply Stage trajectory was to compute possible launch window dates. Since the Hohmann transfer requires that the angle formed between the initial position vector of the Earth and the final position vector of Mars be equal to 180 degrees, the angle between the the initial position vectors had to be found. This angle is called the opportunity angle for the trajectory, and it is found by the following method.

It takes the planet Mars 685 days to "sweep" through an angle of 360 degrees, or one complete revolution about the Sun. It is also known that the period of

the Hohmann transfer orbit is 258 days. Therefore the angle that Mars "sweeps" through in 258 days is determined by the proportion below:

$$\frac{\alpha}{360 \text{ degrees}} = \frac{258 \text{ days}}{685 \text{ days}}$$

where: α= the sweep angle = 136 degrees

The opportunity angle is then simply given as:

opportunity angle = θ = 180 degrees - α= 44 degrees

Therefore, in order for the planets to be in a proper alignment for a Hohmann Transfer, the position vector of Mars has to be 44 degrees to the right of the position vector of Earth at the time of departure.

A schematic of the supply ship trajectory is given in Figure II.4.1.2.

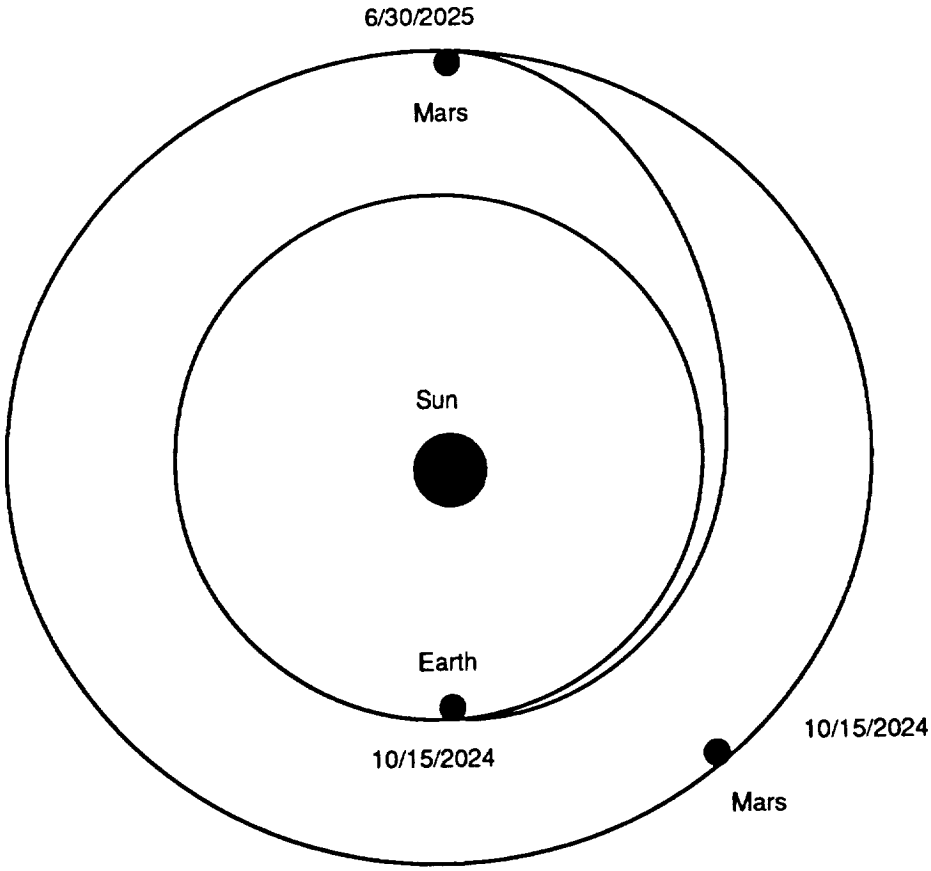

Figure II.4.1.2: Supply Ship Trajectory

The computer code for determining planetary positions for a given date was used again to determine possible launch windows. Various dates were entered into the code until an opportunity angle of 44 degrees was found between the Earth and Mars. A table of an Earth-Mars Hohmann transfer dates are listed below for the years 2018-2029.

Hohmann Transfer Launch Window Dates

Earth Departure	Mars Arrival
5/16/2018	1/29/2019
7/06/2020	3/21/2021
10/15/2024	6/30/2025
12/06/2026	8/21/2027
1/23/2029	10/08/2029

From this data, it can be seen that a launch window for the Hohmann transfer occurs every 26 months.

II.4.1.3 Ascent/Descent

II.4.1.3.1 Landing

II.4.1.3.1.1 Landing Trajectory Design
(Kraft)

The principal drivers in design of the landing trajectory are the reentry velocity and the ballistic coefficient m/C_dA of the vehicle. For manned vehicles, short travel times are required and lead to high approach velocities. These high velocities must be reduced either by maneuvers above the atmosphere and transfer to LMO , with high expenditure of propellant, or reduction of velocity by atmospheric drag, with increased requirements on thermal protection and guidance/control. The manned Waverider trajectory is based on the latter approach; the unmanned LLVM trajectory is based on the former.

Choice of the Lander approach was based on the shape and large size of the Habitat and the need to carry liftoff propellants. The Lander was chosen to be a blunt lifting cone design rather than a high-lift design because of the following considerations:

1. Because long transfer times are not a problem for an unmanned vehicle, LLVM transfer to Mars was chosen as a Hohmann transfer with relatively low Mars approach velocity. Thus the propulsion requirements for capture are relatively low.

2. Because a habitat for eight people must be a large structure, greater efficiencies of space, and therefore mass, could be achieved with a compact shape than with an aerodynamic shape, such as a lifting body or winged blunt body.

3. The blunt nose configuration provides low heating and high drag for velocity reduction with low expenditure of fuel.

The sacrifice required by choosing the blunt lifting cone over a body of higher lift capability is the loss of maneuverability and, therefore, the ability to revise the landing site during the reentry glide. However, parking orbit surveys with accurate instruments and precise reentry guidance can reduce this problem, and the rotation of Mars relative to the parking orbit allows flexibility in choice of a landing site.

II.4.1.3.1.2 Landing Trajectory Analysis

(Kraft)

The first step in descent to the Mars surface is a transfer from the parking orbit (LMO) to the altitude at which thermal and drag considerations are significant. Because the LLVM must remain in LMO for about 6 months during the WOPM transfer from Earth to Mars and during docking with the WOPM for personnel transfer and site survey, the LMO must be chosen at altitudes where drag decay is small. Drag calculations based on the Mars Reference Atmosphere (Reference 55, Figure II.4.1.3.1.2-1) resulted in a choice of 170 km for the docking orbit and 90 km for the entry altitude, the altitude at which thermal control and landing maneuvers begin. At arrival, the LLVM would assume a circular orbit higher than 170 km to allow for decay during the 6-month WOPM transfer. The decay rate is given in m/sec by

$$\frac{\partial r}{\partial t} = -\rho \frac{C_d A}{m} \sqrt{\mu r} \qquad \text{(II.4.1.3-1)}$$

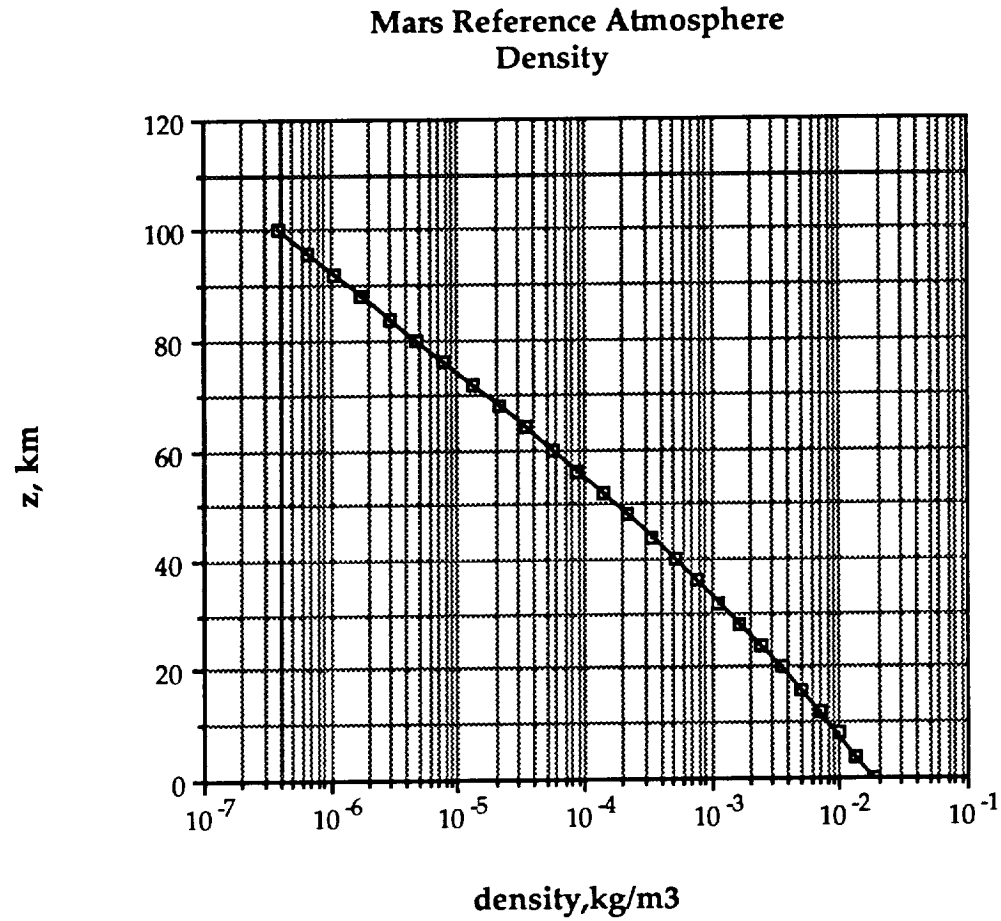

Figure II.4.1.3.1.2-1: Density of Mars Atmosphere

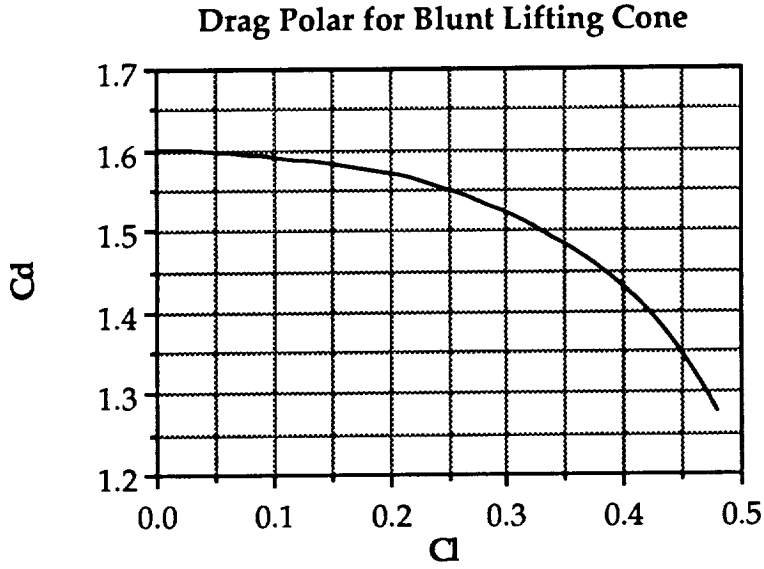

Figure II.4.1.3.1.2-2: Lander Drag Polar

For the Lander, a 70°-half angle blunt lifting cone, the drag polar is given in Figure II.4.1.3.1.2-2 (Reference 18, Cross), and $C_{d0} = 1.6$. Then, for A = 100 m^2 and m = 50,000 kg , the design value of the ballistic coefficient m/C_dA is 312.8 kg/m^2. Then, with the Martian surface radius 3415 km and the gravitational constant $\mu = 45599\ km^3/sec^2$, the following decay rates are determined:

Altitude, km	Decay rate, m/sec	Rate per 3 months, km
100	16.21	26,000
120	0.408	3188
138	0.0408	318
156	0.00408	31.8
174	0.000408	3.18

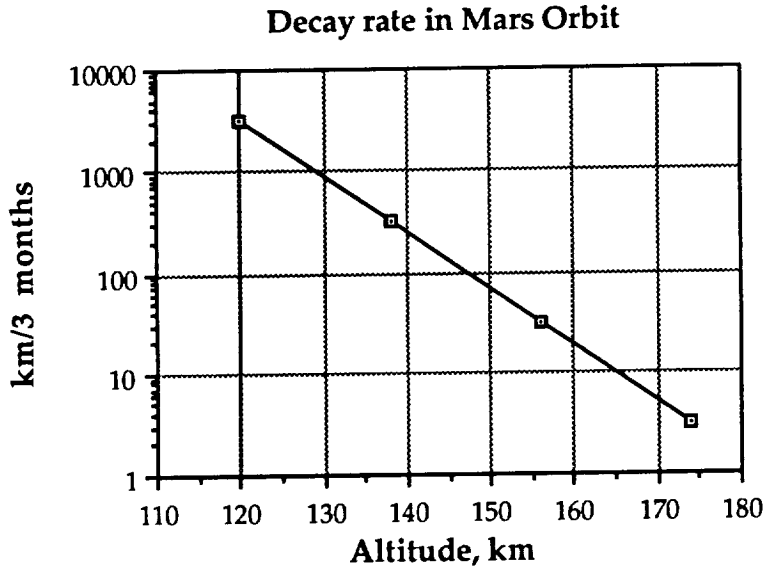

Figure II.4.1.3.1.2-3: Decay Rate for A=100 m^2

Based on an average decay rate (calculated from Figure II.4.1.3.1.2-3) over a three month period (the period of the surface exploration) and final design values (A = 149 m^2), the parking orbit for the LLVM must have an altitude of at least 170 km.

The first phase of the landing will involve a Hohmann transfer from 170 km to 90 km. The small maneuvers required for this transfers are calculated as

$$\Delta V_1 = \sqrt{\frac{\mu}{r_{pk}}} - \sqrt{\frac{2\mu r_e}{r_{pk}(r_e + r_{pk})}} \qquad \text{(II.4.1.3-2)}$$

$$\Delta V_2 = \sqrt{\frac{\mu}{r_e}} - \sqrt{\frac{2\mu r_{pk}}{r_e(r_e + r_{pk})}}$$

where r_e is the radius at entry, and r_{pk} is the parking orbit radius. The associated propellant mass required is given by

$$\Delta V = g_o I_{sp} \ln\left(\frac{m_o}{m_f}\right)$$

(II.4.1.3-3)

where g_o is the Earth sea-level gravity, I_{sp} is the specific impulse, and m_o/m_f is the ratio of initial to final mass.

Reference 42 (Levine) estimates that returning a 4500 kg package to Mars orbit will require an entry weight of 23,000 kg with m/C_dA values of about 630 to 1260 kg/m^2 for lifting capsule designs of low lift to drag ratios (0.5 to 0.75) and about 4100 to 8100 kg/m^2 for large lifting surface designs of high lift to drag ratios (1.5 to 2.0). The large propellant payload causes the ballistic coefficient m/C_dA to be relatively large. Rough estimates of weights can be based on propellant density of about 60 lb/ft^3 (960 kg/m^3). Thermostructural environments are severe for these values of m/C_dA and high entry velocity. The upper limit for Mars entries is about 13.7 km/sec based on a load limit of 6 Earth g's.

The penalties of the high entry velocity approach are heat shield weight and guidance and control system propellant and complexity. The radiation and convective heating rates are proportional to powers of the ballistic coefficient:

$$q_r \propto \left(\frac{m}{C_dA}\right)^{1.85} \qquad \text{(II.4.1.3-4)}$$

$$q_c \propto \sqrt{\frac{m}{C_dA}} \qquad \text{(II.4.1.3-5)}$$

For high velocities the rate of ablation is

$$\frac{dW}{dt} = \frac{q_c}{q_a} \propto \sqrt{\frac{\frac{m}{C_dA}}{1 + \left(\frac{L}{D}\right)^2}} \qquad \text{(II.4.1.3-6)}$$

where q is the thermochemical heat of absorption of the shield material. The strongest effects on ablation rate are the ballistic coefficient and L/D. The

ballistic coefficient of the LLVM in its landing configuration is 210, and its maximum L/D is 0.37.

In addition to heating problems, high entry velocities pose guidance problems. Tauber (Reference 60) also notes that higher speed entries of about 5 km/sec have an acceptable range of entry flight path angle of less than 0.5°, whereas lower speed entries of about 3.5 km/sec permit variations in flight path angle of more than 3°.

Consequently, the design approach for the entry phase of the landing trajectory was chosen for moderate entry velocity and heating alleviation. A shallow flight path at entry is maintained to reduce heating and increase range to permit drag to reduce velocity. Tauber notes that the shallow flight path angle is also ideal because the low decelerations are below one Earth g and, therefore , appropriate for crews which might have been physically weakened during the long voyage to Mars.

A simple Runge-Kutta landing trajectory program was developed to permit parametric studies to support the trajectory design and estimation of propellant requirements (Appendix G). The equations of motion chosen for the integration are as follows:

$$\frac{\partial v}{\partial t} = -\frac{\rho C_d A}{2m} v^2 - \frac{\mu}{r^2} \sin\gamma - g_o I_{sp} \frac{\dot{m}}{m}$$

$$v\frac{\partial \gamma}{\partial t} = \frac{\rho C_L A}{2m} v^2 - \left(\frac{\mu}{r} - v^2\right)\frac{\cos\gamma}{r} \qquad \text{(II.4.1.3-7)}$$

$$\frac{\partial r}{\partial t} = v \sin\gamma$$

$$r\frac{\partial \phi}{\partial t} = v \cos\gamma$$

The state variables (r,ϕ,v,γ) are defined in the following figure:

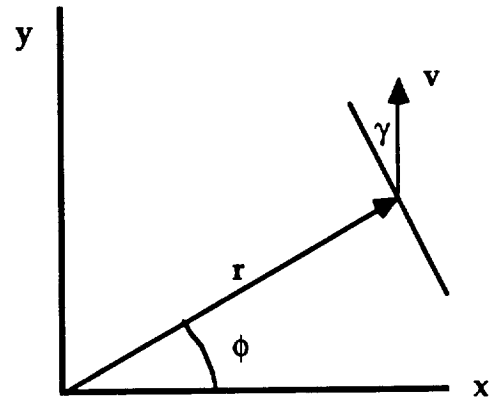

Also, the drag polar was modeled as a least squares fit of the drag polar of Figure II.4.1.3.1.2-2,

$$C_d = C_{do} - 0.22898\, C_l + 1.3015\, C_l^2 - 4.6\, C_l^3 \qquad \text{(II.4.1.3-8)}$$

and the atmospheric density was modeled as an exponential in three segments based on Figure II.4.1.3.1.2-1:

$$\rho = \rho_o\, e^{-\rho_K (h-h_o)} \qquad \text{(II.4.1.3-9)}$$

$\rho_o = 0.0182$ kg/m^3
$h > 60$ km: $\rho_K = 0.100$
$30 < h < 60$ km: $\rho_K = 0.090$
$h < 30$ km: $\rho_K = 0.078$

The parametric landing study assumed reentry from a circular parking orbit with a variety of flight plans. Several methods are available to reduce heating: retro thrust, ablative shields and coatings, insulation, heat sinks, mass-transfer cooling, and aerobrakes. However, selection of a flight plan to minimize heating effects is most important in thermal design. The parametric study is limited in sophistication by the time available and would be extended in a study contract.

A solution for optimum attitude control for maximum range, minimum total heat per unit area, and minimum temperature at the nose stagnation point for lifting vehicles re-entering from a circular orbit has been developed in Reference 14 (Cavoti). In particular, the solution for the case of constant aerodynamic coefficients and small angles of attack with high lift coefficients is

$$\gamma = -\frac{4 g_o \sqrt{K C_{do}}}{V^2 \rho_k} = \text{constant}$$

where:

γ = flight path angle relative to horizontal
g_o = surface gravity of Mars
V = velocity
ρ_k = density scale height factor ($\rho = \rho_o\, e^{-\rho_K \Delta h}$)

and K and C_{do} are aerodynamic constants, the induced drag coefficient and the zero-lift drag coefficient. A control law of this type would be

implemented during the period of high thermal environment to minimize thermostructural impacts. This period can be determined by calculating the convective heat flux at the stagnation point of a three-dimensional nose of radius r_n using the Chapman equation (Reference 59) (Tauber):

$$\dot{q}_c = 1.35 \cdot 10^{-8} \left(\frac{\rho}{r_n}\right)^{.5} V^{3.04}(1 - g_w) \qquad \text{(II.4.1.3-10)}$$

where:

V = orbit velocity at the planet surface
g_w = wall enthalpy/total enthalpy
r_n = .2 meters
V_c = 3.6069 km/sec for entry at 90 km

Heat flux is in Watts/cm^2, and g_w is taken as 0.20, the value for the STS Orbiter. Only convective heating is important because equilibrium shock layer temperatures are too low to produce significant amounts of molecular radiation. Implementation of the thermal control law to maintain low γ was modeled by the trajectory program from 90 km until the limited lift capability of the blunt lifting cone was exceeded. The convective heat flux was calculated by the Runge-Kutta trajectory program using Equation II.4.1.3-10. Also, the dynamic pressure was calculated as

$$q = \tfrac{1}{2}\rho v^2. \qquad \text{(II.4.1.3-11)}$$

Because of the limited lift capability of the blunt lifting cone, significant velocity levels remain to be eliminated at low altitudes by propulsion or other means. As a means of reducing propellant required for landing, use of parachutes was investigated. Reference 46 (McMullen) provides data on parachute drag area vs. mass. Parachutes of existing design may be deployed at Mach numbers of over 2.0. A parametric study was conducted to determine maximum deployment heights which keep loads and deceleration levels to reasonable limits and Mach numbers less than 2.6. The Runge-Kutta trajectory program determined Mach number , a constraint on parachute deployment, as a least squares fit of the speed of sound based on data of Reference 56 (sketch below), the Mars Reference Atmosphere:

$$\text{Mach Number} = v/a \qquad \text{(II.4.1.3-12)}$$

where:

$$a = 0.24641 - 6.7094(10^{-4})\, h - 7.307(10^{-6})\, h^2 + 1.0758(10^{-7})\, h^3$$

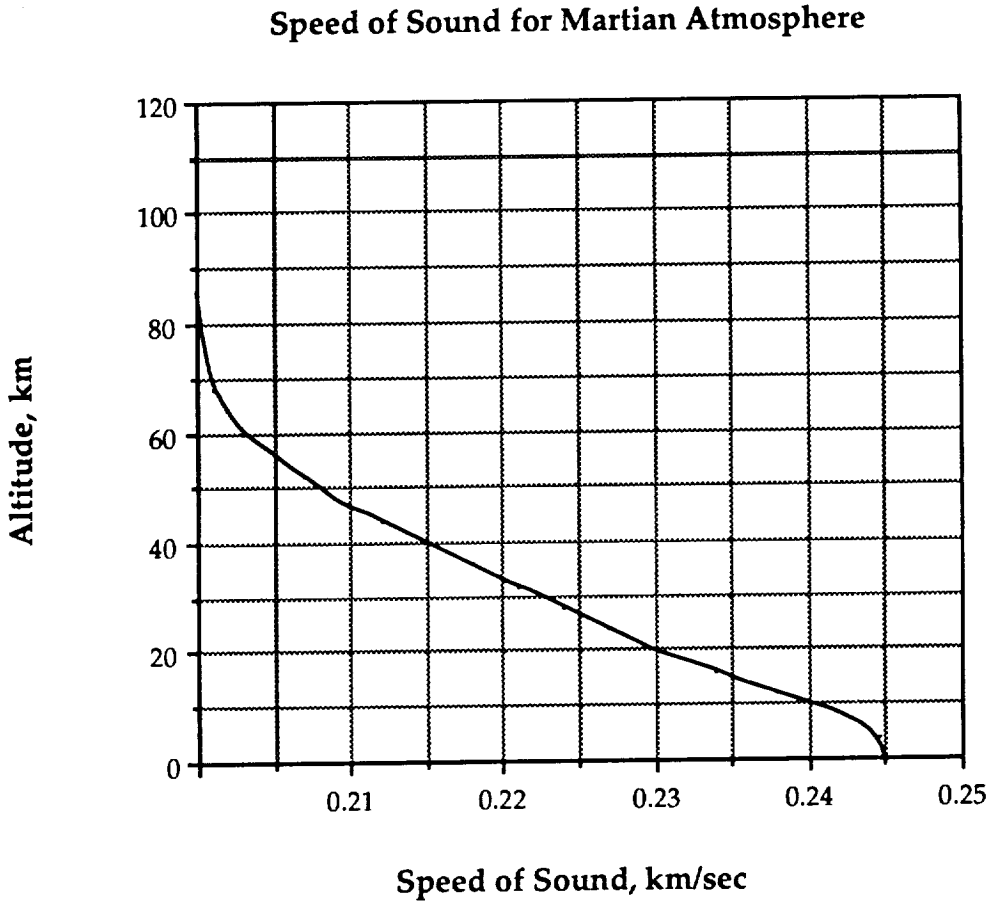

Figure II.4.1.3.1.2-4: Speed of Sound in Martian Atmosphere

Weight of the resulting parachute system was then compared to the weight of propellant required without the parachute system. The parachute approach proved more mass-efficient, with net savings of five to ten percent of Lander weight.

To reduce loads and deceleration, a three-phase plan was adopted. Based on the design criteria of the *Recovery Systems Guide* (USAF Report) and the experience of Reference 46 (McMullen), the choice of systems was as follows, with two parachutes:

Parachute phase 1 - Supersonic of the high-porosity FIST ribbon type, conical equiflo design, with C_dA of 600 square meters.
Parachute phase 2 - Parachute phase 3 in reefed configuration
Parachute phase 3 - Supersonic type, with with C_dA of 4800 square meters.

Initial deployment, by spring ejection, is triggered by radar altimeter in parallel with series-connected g and pressure switches. Deployment of the

second parachute is initiated by a timer, with force provided by the previous parachute on release.

In summary, the final profile chosen involves a moderate entry initiated from a circular parking orbit of 170 km, entry velocity of 3.6069 km/sec at 90 km, guidance for thermal control and velocity reduction from 90 km until conditions are reached to allow parachute deployment, three stage parachute deployment beginning at Mach 2.6, and a final powered flight hover/landing phase initiated at 0.5 km.

II.4.1.3.1.3 Landing Trajectory Program
(Kraft)

The Landing Trajectory Program listing and sample runs are contained in Appendix D. The program has two modes of output: (1) a thermal search mode, useful in designing the lift/drag guidance and control system inputs, and (2) the normal mode, which determines state and environment conditions as a function of time for all phases of the trajectory: Hohmann transfer from parking orbit to entry at 90 km, guided lift/drag control to low altitude, deployment of parachutes, and thrusted landing, including hovering and lateral maneuvering.

The program is first used in the thermal search mode to investigate the effectivity of the lift/drag capability of the blunt lifting cone. Initial studies show capability of lift/drag guidance to maintain low flight path angle for limited periods of time Because of the limited lift/drag capability of the blunt cone configuration, a later sequence of studies maximized lift and investigated heating for various design flight path angles. Trajectories 1 - 5 indicated that convective heating increased rapidly for flight path angles greater than 2°.

Once lift/drag guidance sequences were selected, the trajectory program was used in the normal print mode to select the final trajectory, including possible propulsion corrections and parachute effects. Because lifting capability was limited, the program was modified to include two corrective burns to reduce flight path angle after lift guidance capability was exceeded. Times of the corrective burns were varied. Also, drag characteristics of parachutes were varied within conservative limits.

The parametric studies showed that (1) the blunt lifting cone is an efficient landing system, (2) parachutes, or an equivalent intermediate braking system, are required and efficient for this configuration, and (3) final braking can be reduced to a minimum of hovering and lateral maneuvering to avoid undesirable landing sites.

Data for typical runs is shown in the following table. In particular, the final design trajectory chosen, trajectory 22 of Appendix D, is shown. A mass summary for both the Lander and the Launcher, based on detailed systems studies, is shown in Section II.4.1.3.3.

Mars Lander Trajectory Runs

Traj No.	Initial Mass (kg)	Mass Rate (kg)	Chute Mass/M (kg)/sec)	Parking Orbit (km)	Entry Mass (kg)	Landing Mass (kg)	Hover/ Lateral (kg)	Final Mass (kg)
6	50000	300	0/-	100	82	7247	2033	40638
7	50000	300	851/2.2	100	82	2035	2205	44827
9	50000	300	609/2.2	100	82	2293	2204	44812
10	60000	300	782/2.4	100	105	7971	2631	48511
11	60000	300	782/2.5	100	105	2740	2814	53559
16	53400	200	851/2.4	100	93	1905	2522	48029
17	53400	150	851/2.4	100	93	2017	2521	47918
22	52100	89	920/2.6	100	91	1621	2407	47061

Note: For run 22 the 1450 kg heat shield was dropped at deployment of the second parachute, so that the trajectory printout shows a final mass of 45611 kg.

A comparison of trajectories 6 and 7 from the table shows the importance of the parachute system in the reduction of terminal velocity, with a gain of about ten percent achieved in final mass. The effect of increasing the Mach number at which the first parachute is deployed is shown by trajectories 9 - 11. Trajectories 16 - 22 show the effect of reducing mass flow rate, or thrust (the specific impulse for all runs was 300 seconds). For trajectory 22, the parachute system is not able to totally reduce the terminal velocity in the time available after first deployment. A further iteration to increase thrust slightly or to provide a thrusting period prior to parachute deployment would be required for this trajectory.

II.4.1.3.2 Launch

(Kraft)

The Launcher Submodule is contained within the Launcher/Lander Module and provides the transfer from the Mars surface to a parking orbit where it will rendezvous with the Waverider to transfer personnel and scientific samples for the return to Earth.

A simple Runge-Kutta trajectory program (Appendix E) was developed to allow parametric studies of the launch design. The program assumes gravity turn guidance after an initial period of small constant turn rate to gain altitude. The equations of motion for this program are as follows:

$$\frac{\partial x}{\partial t} = v_x$$
$$\frac{\partial y}{\partial t} = v_y$$
$$\frac{\partial v_x}{\partial t} = g_o I_{sp} \frac{\dot{m}}{m} x_t - \frac{1}{2}\rho \frac{C_d A}{m} v^2 v_x - \frac{\mu x}{r^3} \qquad \text{(II.4.1.3-13)}$$
$$\frac{\partial v_y}{\partial t} = g_o I_{sp} \frac{\dot{m}}{m} y_t - \frac{1}{2}\rho \frac{C_d A}{m} v^2 v_y - \frac{\mu y}{r^3}$$

The x_t and y_t are guidance thrust attitude terms which direct the thrust, initially at a constant rate and, in a subsequent phase, along the velocity vector. The launch program directs powered flight until the osculating apogee equals the target parking orbit altitude. The program then terminates the Runge-Kutta integration and calculates analytically the velocity increment to circularize at the parking orbit altitude.

Appendix E also includes sample trajectories generated in selection of the nominal launch profile. In particular, the final trajectory chosen, trajectory 8 of Appendix E, is shown. A weight summary, based on detailed systems studies, is shown in Section II.4.1.3.3.

Launcher Trajectory Runs

Traj No.	Initial Mass (kg)	Mass Rate (kg/sec)	Turn Time/Rate (sec/°/sec)	Parking Orbit (km)	Dynamic Pressure (N/m^2)	Final Mass (kg)
0	22300	300	4/1.0	100	8105	6744
1	20300	180	4/1.0	170	21164	5670
2	22000	42	240/.35	170	758	5467
3	22000	42	240/.40	170	7443	5505
4	22000	42	240/.45	170	100000	2299
5	22000	42	220/.40	170	4752	5536
6	22000	42	200/.40	170	4320	5540
7	22000	42	180/.40	170	6419	5518
8	22300	42	200/.40	170	9420	5537

Trajectories 0 - 2 show the effect of mass flow rate on final mass in orbit. Sensitivity to the magnitude and duration of the initial pitch rate is shown in trajectories 2 - 4 and 5 - 7, respectively.

Figure II.4.3.3

Lander/Launcher Mass Summary

	Launcher		Lander
Structure	1150		7400
Heat Shield			1450
Life Support	1478		7762
Electrical	600		1800
G&C	422		750
Propulsion	330		402
Science/Equipment			2750
Rovers		800	
Science		1800	
Tools		150	
Parachutes			920
Dry Weight	3980		23234
Contingency (10%)	398		2323
	4378		25557
Propellant	16763		4119
Reserves (2%)	335		82
	21476		29758
Launcher			21476
Total Lander			51234
Crew	800		800
Lander Ignition			52034
Launcher Ignition	22276		

II.4.1.3.3 Ascent/Descent Mass Summary

An overall mass summary, based on the final trajectories for the Lander and Launcher and on the masses provided by systems designers, is given in Figure II.4.3.3. These masses are the result of several iterations between the

propulsion and trajectory analyses. Although the iterations have nearly converged, one further iteration is required to slightly increase Lander thrust to further reduce the small terminal velocity and facilitate hovering. This iteration would reduce slightly the Lander masses of Figure II.4.3.3

III.1 Systems

III.2 WOPM Systems

III.2.1 Propulsion
(Compy)

In order to meet mission requirements, our propulsive system - embodied in a booster - will be capable of a variety of interplanetary missions. By simply changing the amount of fuel, we can use the same booster design for both the SS and the Waverider. This will result in a significant development cost savings.

The propulsion requirements for this mission are primarily safety, reusability, and low development cost. Because we are using nuclear engines, it is extremely important that the mission be safe and successful for the future of space exploration. Accidents tend to slow down progress, as evidenced by the Challenger accident in 1986. Any future missions to Mars will be seriously affected by the results of our mission.

One safety concern is in the construction of our propulsive system. We must develop protection and monitoring systems to ensure that there are no personnel or environmental dangers.

Our second safety concern is a booster operation accident. To prevent one, preliminary testing will be done on the surface, followed by more advanced developmental testing in space.

In this mission, the booster for the supply ship will be reused for the purpose of returning the Waverider to Earth. After it is in Mars orbit, the booster and it's fuel will have to wait at least a year until the Waverider arrives and the crew completes its surface mission before it will be ignited again. It is essential that the engines start when the astronauts push the button. To ensure reliability, we will incorporate appropriate testing into our development phase.

Since the main showcase of this mission will be in the use of the Waverider, it is in this area that development costs will be the highest. To counter-balance this, our propulsion systems emphasize cost and development efficiency over risky technologies.

It is necessary then to do a comparison of different engine types, using several assumptions. The first assumption is that we will be able to build reliable and reusable pumps for the fuel. This is justified by having 30 years of development and improvement (over today's problematic shuttle pumps) before the mission is scheduled for launch. Another assumption is that we have an Advanced Launch System (ALS) capable of lifting 150 tons to Low Earth Orbit (LEO). The figure of 150 tons has been given in the Request For Proposal (RFP) to which we are responding. A third assumption is that there will be a Space Station from which we can accomplish construction and assembly of the vehicles. As a necessary safety precaution, there will be a need for a craft capable of moving the booster/supply ship or booster/Waverider away from the Space Station so that we do not have to fire in its vicinity. The supply ship or the Waverider will have it's own maneuvering thrusters, but to save on fuel it is better for another craft to move the booster/supply ship or booster/Waverider into a higher orbit. For this purpose we propose that we use a space shuttle which carries it's fuel in the cargo bay. The shuttle will use maneuvering thrusters to get away from the space station and then use it's main drive to send the booster/Waverider or booster/supply ship combination into a higher orbit. The shuttle would then use it's remaining fuel to reduce it's orbit back to the space station altitude where it could dock again.

Our final engine choice was a solid core nuclear rocket. We picked that engine type from the following comparison study.

In our comparison study the first engine type that we looked at was a chemical engine . Because this mission occurs in space, we are more concerned with specific impulse (Isp) than thrust. The highest Isp producing chemical engine is the same Hydrogen/Oxygen system that the space shuttle uses. Of course there will be improvements in the engine over a 30 year period. However, using the present Isp value for the space shuttle main engines (460 seconds), we estimate that we could get 480 seconds maximum out of the engines. The amount of delta V is dependent on Isp and fuel, and is determined using the equation:

$$\Delta V = g\ Isp\ \ln(R)$$

where:

g = the gravity constant of earth at sea level
R = the mass fraction

(Hill, Reference 30). If the Isp is low, as with the chemical engine, then more fuel is needed. The amount of fuel is contained in the mass fraction R:

$$R=\frac{(M_0+M_p)}{M_0}$$

where:

Mo = the mass of the structure and the cargo
Mp = the mass of the propellent

(Hill). In Figure III.2.1-1, a comparison of the amount of fuel needed to achieve a given ΔV is shown. For the chemical system, an Isp of 480 seconds was used compared to the nuclear solid core Isp of 1200 seconds. As you can see, the chemical system uses about 4.3 times the amount of fuel at a structure mass (Ms) of 500,000 kg. The value of the structure mass (Ms) includes the mass of the booster. Although chemical engines are typically much lighter than nuclear engines, at large Ms numbers, the added mass of oxidizer and the extra fuel tank mass increase the net booster mass. This balances the large mass of a nuclear booster at large values of Ms. One advantage of a chemical system is the low development cost; it is essentially an existing technology with a few improvements. A disadvantage to this system is the fact that oxidizer as well as fuel must be carried, which increases the amount of mass carried on the booster. Since more fuel is needed than for other engine types, more structure mass is needed to carry the greater amount of fuel. This increases construction costs and transportation costs. With an increase in the amount of launches from earth, there is an increase in the possibility of an accident. Another disadvantage of chemical systems is that they will not help to further space technology for future missions, since current chemical engines are already pushing the limits of this technology. The nuclear solid core booster has the added benefit that future missions will have a new source of propulsion already developed.

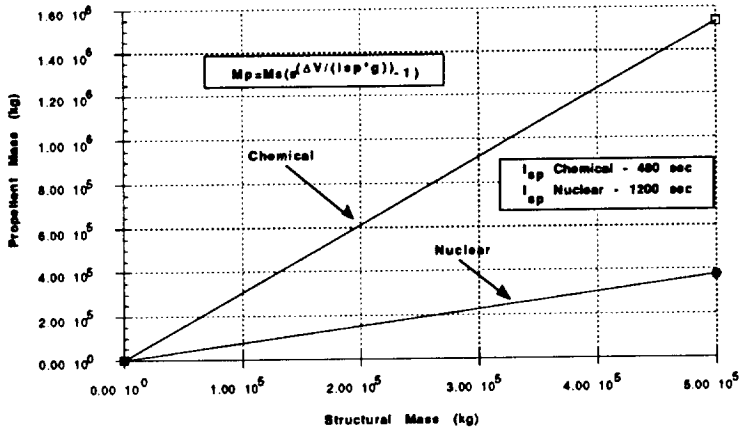

Figure III.2.1-1: Chemical vs. Nuclear System Masses

The next engine type investigated was a nuclear electric engine system. A major disadvantage of this system is that it is not currently being adequately funded, i.e. we would have to absorb the developmental costs. Also, although this system holds great promise for future interplanetary missions, it seems to us to be an unnecessary redundant of the Waverider. The development costs and short flight time indicate that this is an alternate plan to the Waverider and not for use with it.

The third and last type of engine investigated were nuclear engines. There are many nuclear engine types, but we can break them down into two categories - the solid core and gas core. Solid core engines are all monopropellent engines. Hydrogen is usually used because the lower molecular weight, the higher the Isp. This can be shown by

$$Isp=\frac{1}{g}\sqrt{\frac{2\gamma R}{\gamma-1}T_0\left(1-\left(\frac{p_e}{p_o}\right)^{\frac{\gamma-1}{\gamma}}\right)}$$

(Hill, Reference 30). Also, the lower the molecular weight, the larger the value of R. Solid core engines have the disadvantage of being partially developed. They have been studied since the 1950's (Borowski, Reference 8). With improvements in technology we expect an Isp of 1200 seconds. This Isp is more than twice as high as that of chemical engines. Because of the high Isp, there are less structure and transportation costs when compared to chemical engines. We also need the high Isp because we already have a high Ms, and the higher Ms is,

the greater the amount of fuel needed. By once again referring to Figure III.2.1-1, it is obvious that at high Ms values, significant fuel is saved when using the solid core nuclear system. The development costs should not be too high because of all of the prior development that has gone into solid core engines already. Some engines have been built and have worked for long duration periods, proving the concept to be a working system.

The second type of nuclear rocket system considered is a gas core reactor. The benefit of this system is that it is capable of generating Isp's of up to 6000 seconds. At that Isp you could get to Mars much faster than by using the Waverider. It is feasible to get to Mars on a courier mission in just 80 days using this system (Mensing, Reference 49). The problem is that development costs are extreme, as there are many technological problems with the gas core reactor. A gas core reactor uses uranium which is so hot that it is a plasma. Some of the major problems that need to be overcome are computational fluid modeling and development of materials capable of withstanding very high temperatures (Mensing). Development of a nuclear gas core system is similar to the development of the nuclear electric propulsion system. Both propulsion systems are alternatives to the Waverider concept.

In conclusion, it seems that the nuclear solid core system is the best solution. The major safety hazard is from radiation, which is easily shielded by use of a shadow shield (Buden, Reference 11). The shadow shield is a barrier of shield material that is between the reactor and the endangered areas. Using this method you only need to shield in one direction instead of shielding the entire reactor. The radiation does not curve around the shield unless an atmosphere is present.

For construction of the booster we, as previously mentioned, are going to use the space station as a working base. The fuel tanks will be empty space shuttle external tanks which will be brought into orbit instead of being dropped. To hold the fuel tanks and channel the fuel to the reactor, there will be a long, slender truss structure with the necessary equipment. Tank masses and dimensions are provided in Section III.2.1.1. The configuration is shown in Figure III.2.1-2 The amount of tanks will depend on the amount of fuel needed,with the capability of extra tanks to be added around the inner core of tanks. The truss structure will be built in space using pre-fabricated parts that are shipped up by the ALS. The fuel will also be shipped up in several ALS launches. Once launched for Mars, the booster will get added ΔV from momentum transfer by dropping empty fuel tanks.

III.2.1.1 Primary Propulsion System Design
(Compy)

Before the Waverider reaches Venus, our booster will detach from the Waverider and use the remaining fuel in its tanks to put it on a trajectory back to Earth. At Earth the first booster will use its maneuvering thrusters and main engines to put itself into orbit, where it can be recaptured and reused for future missions. At Mars the Waverider will dock with the SS booster and use it to return to Earth. As the SS booster/Waverider approaches Earth it will use its main engines to brake and put the combination into orbit.

The actual fuel tank will be made from the liquid hydrogen tank on board the external fuel tank. The external skin on the external tank will remain on the fuel tank. The oxidizer tank will be cut off from the external tank. A cap will then be placed over that cut. The fuel will need to be cryogenically stored. The reactor will be bimodal to power the cryogenics and to power the other systems on board the booster. By bimodal we mean that the reactor will also act as a power supply as well as an engine. To hold the fuel tanks and channel the fuel to the reactor, there will be a long, slender truss structure with the necessary equipment. The specifications for the Waverider booster are in the table below. The acronym NEBIT refers to Nuclear Engine Booster for Interplanetary Travel, and WR stands for the Waverider.

Waverider Booster Specifications

Booster Length:	40 m	Tank Length:	30 m
Booster Width:	22 m	Truss Length:	35 m
Booster Mass (fueled):	556,440 kg	Miscellaneous Mass:	15,000 kg
Fuel Mass (maximum):	426,440 kg	Reactor Mass:	15,000 kg
Thrust:	2,352,000 N	Tank Mass:	20,000 kg
Specific Impulse:	1,200 sec	Tank Diameter:	8.7 m
Delta V (with WR):	10,523 m/s	Truss Diameter:	4 m
Total Mass (NEBIT + WR):	856,440 kg		

The configuration looks like Figure III.2.1-2 with the capability of extra tanks to be added around the inner core of tanks.

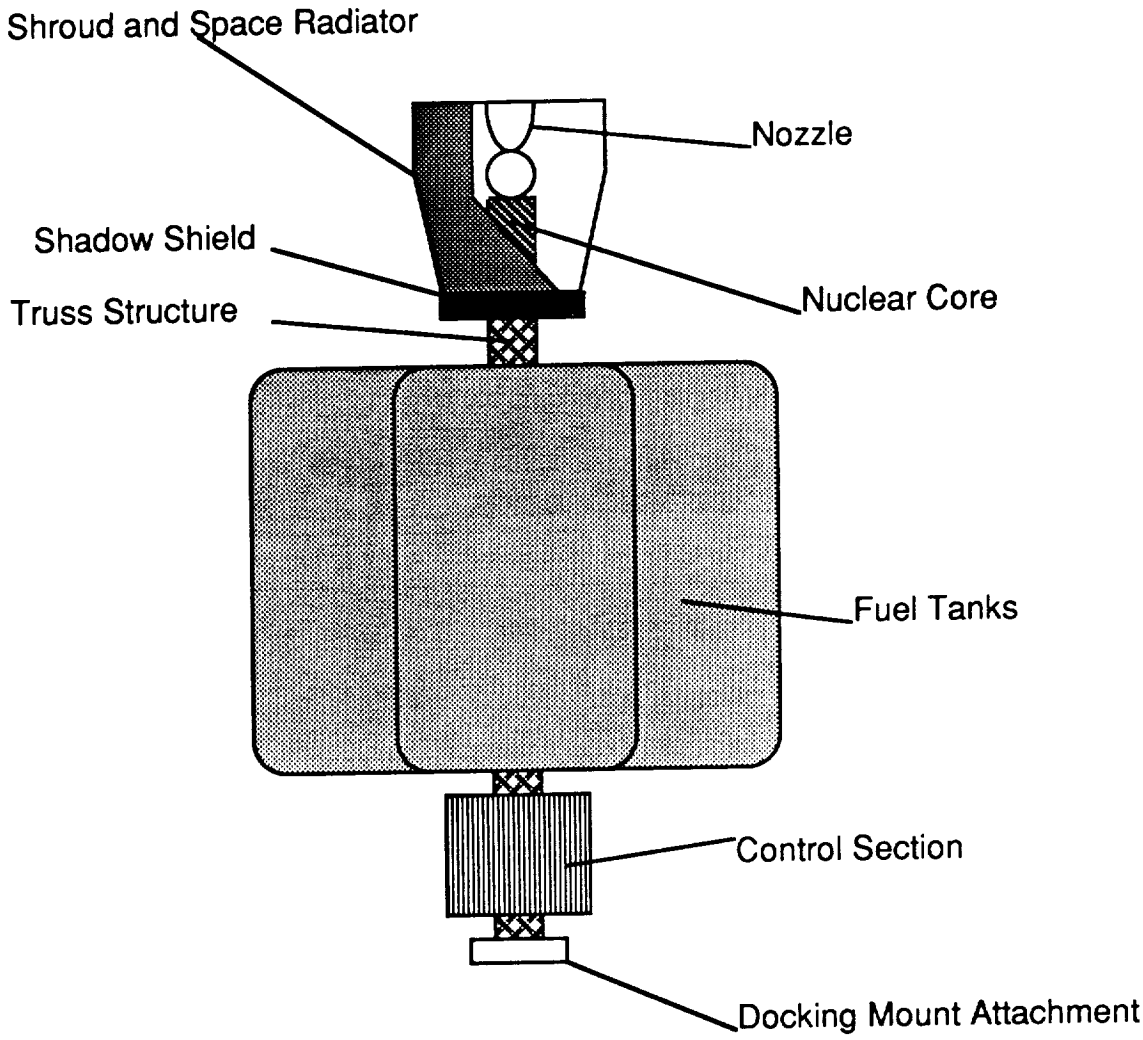

Figure III.2.1-2: WOPM Booster System

The specifications of the LLVM booster system will be discussed in section III.3.1.1. The thrust for both boosters was set to what we desired. The pumps on the space shuttle have a high mass flow rate which is above what we desire for our system. The mass flow relates to Isp and thrust from the following equation.

$$Isp = \frac{T}{g\,\dot{m}}$$

(Hill, Reference 30), where m dot is mass flow. We set a mass flow rate of 200 kg/s for our rocket, which is below the mass flow of the space shuttle. This will make our burn time about 30 minutes for the booster/Waverider combination and about 40 minutes for the

booster/SS combination. We can get any thrust we want by changing the mass flow rate of the pump. Because this is a nuclear rocket, we can also change the heat of the reactor by use of the control rods. The control rods are also what keeps the reactor active or inactive.

Both booster rockets will need a control section to monitor all the subsystems on board as well as to coordinate communications from the booster to any other system attached to the booster. This control center will also guide the Waverider booster on its return trajectory to Earth. For this purpose we propose using two supercomputers of the same type that control the Waverider systems (Section III.2.4). After detachment from the Waverider, the booster section will deploy a small communications array that will handle all the signals coming from Earth.

To radiate excess heat from the reactor, the shroud that covers the reactor will also have a space radiator system built into its skin. This will help improve performance and keep the heat within limits on the reactor.

For guidance and control, the booster will use the same Orbital Maneuvering System (OMS) that the space shuttle uses. For further information on this system see the guidance and control section for the Waverider.

III.2.1.1.1 Core Design
(Iverson)

We now needed to determine what type of solid core reactor to use to meet our objective of attaining an Isp of 1200 seconds and a thrust of 2.2 MN with minimal design costs.

Conceptually, a nuclear solid-core rocket engine is little more than an immense heat reservoir that raises the enthalpy of a given coolant or propellant. As illustrated in Figure III.2.1.1.1-1, this propellant is expanded through a nozzle, thus exerting a force or thrust on the engine.

As shown below, the shadow shield is located above the reactor thus casting a shadow of radiation on the crew and payload. No other shielding is required. The mass of the shield is a function of the thermal power output and the dosage distance. For now, the shield will be approximated to be about 1900 kg.

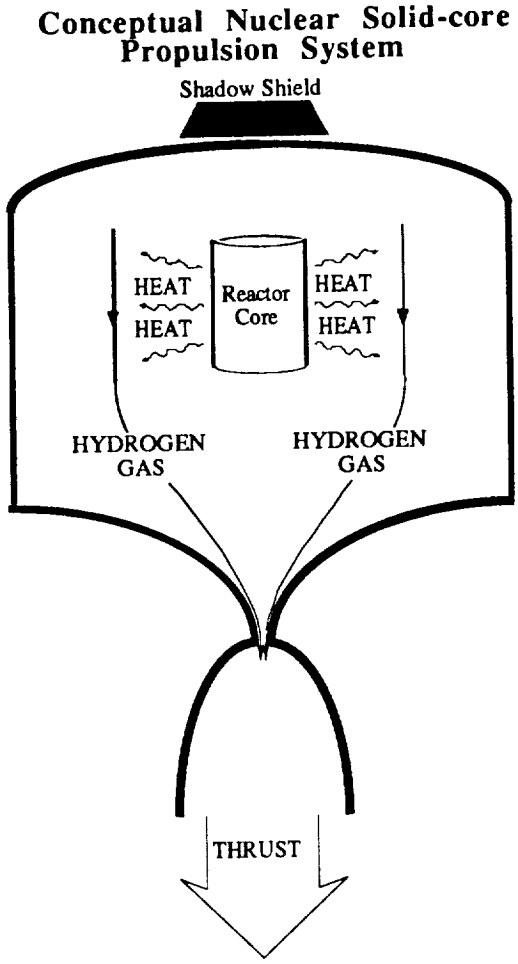

Figure III.2.1.1.1-1: Conceptual Nuclear Solid-Core System

A typical or generic core is made up of several components including: the coolant/propellant tubes, the moderator, the control rods, and the fuel elements. Figure III.2.1.1.1-2 provides a crude model of a typical reactor core.

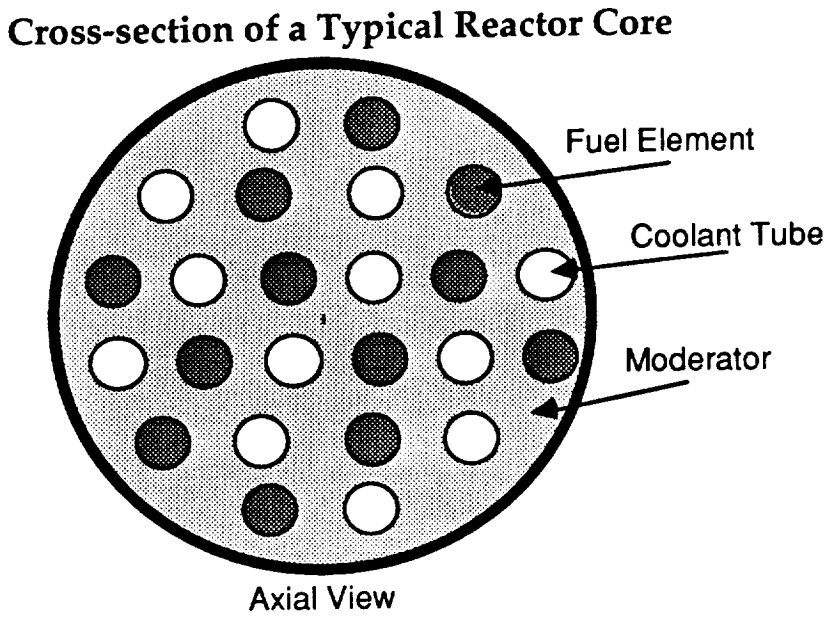

Figure III.2.1.1.1-2: Reactor Core Cross-Section

The moderator (beryllium is often used) has the function of slowing down fast neutrons which would otherwise split atoms/molecules, thereby providing a higher neutron density than is required for sustained fission. The moderator is generally of some material with low atomic/molecular weight. This requirement goes back to simple mechanics where the energy transferred in collision is a function of the relative mass of each body. Little energy is transferred when the difference in mass of the two colliding bodies is large. It is analogous to a ping pong ball bouncing off a bowling ball.

The control rods, as their name implies, control the operation of the core. Their specific function is to absorb neutrons. Control rods are usually made of a boron-carbon material.

The coolant tubes transport the propellant through the core. The tubes are made of a material with high strength, high melting and creep temperature, and high thermal conductivity. Carbon based materials are often used, but suffer from severe corrosion and ablation due to iteration with the hydrogen propellant. This problem can be resolved through the use of special coatings of zirconium carbide or zirconium oxide applied on the coolant tubes of the Waverider.

The fuel elements are of particular interest. The various types of fuel elements will be compared and contrasted in detail later. For now, the fuel elements will be defined as the core component that generates all of the heat energy.

Hydrogen was selected as the propellant because of its low molecular weight and its relatively low heat of dissociation.

Dissociation, in the case of a nuclear solid-core reactor, is considered beneficial, since the reactor core, for all practical purposes, can be thought of as an infinite heat reservoir. Thus, despite the energy lost to dissociation, the abundance of energy provided by the reactor more than makes up for this loss. This can be thought of as an investment into the lowest possible molecular weight available for normal solid-core operation, ionic hydrogen. However, this investment becomes useless if hydrogen ions recombine into hydrogen molecules. The result of recombination is a spontaneous emission or loss of energy. Recombination can be reduced by reducing chamber pressure. Figure III.2.1.1.1-3 shows isobaric plots of specific impulse versus fluid (stagnation) temperature.

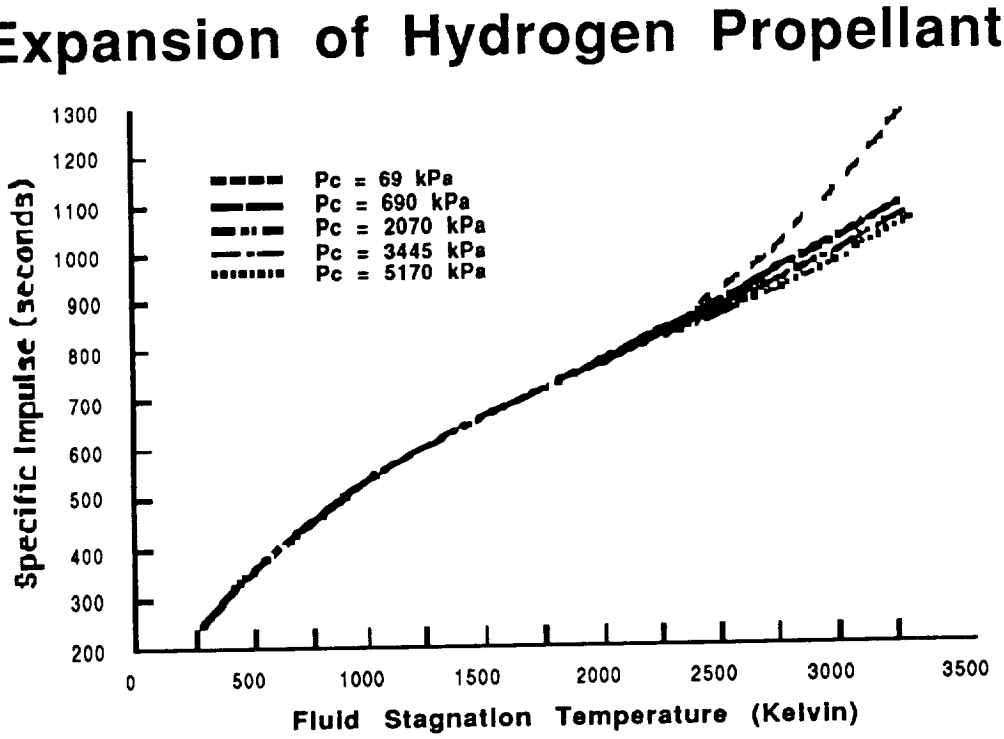

Figure III.2.1.1.1-3: Expansion of Propellant

Notice the Isp for a given temperature increases with decreasing chamber pressure. Therefore, our goal of attaining a specific impulse of 1200 seconds can be attained by encouraging dissociation through a low chamber pressure. For example, 1200 seconds is obtained at a temperature of 3175 K and a chamber pressure of 69 KPa.

Maximizing specific impulse through lowered chamber pressure has a significant trade - off. In order to accommodate the required mass flow rate of

200 kg/s and a chamber pressure of 69 KPa, a throat diameter of about 0.45 meters is required. Figure III.2.1.1.1-4 illustrates this trade-off over different ranges of chamber pressure.

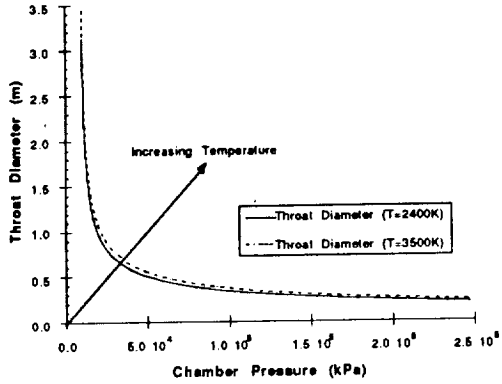

Figure III.2.1.1.1-4: Reactor Core Cross-Section

This has the immediate drawback of requiring a large nozzle. However, with such a low chamber pressure, the pressure vessel container need not be so strong or massive. One concern which requires further study, however, is the effect that such low pressures will have on the heat transfer. Another issue to be considered is the complexity of dissociated/recombining flow with variable vibrational energies. An optimization of pressure and throat diameter (mass), as well as a determination of the nozzle parameters, and, finally, the heat transfers must be examined with a CFD code that utilizes a dissociation/chemistry model. However, it should be noted that higher specific impulses require a significantly larger nozzle than otherwise. Following a thorough analysis, it may be found that a high specific impulse dependent upon dissociation may violate our low development cost objective, whereupon our specific impulse goal would have to be lowered. For the remainder of the paper it will be assumed that no such limitation exists.

Obviously, our objective requires that chamber temperature be maximized. Therefore, a fuel element must be chosen to fit the requirements. There are three general classes of fuel elements: unclad, particle bed, and clad.

The unclad fuel element provides no mechanism for physically confining a molten or gaseous fission fuel. Thus, such a fuel element is limited to the melting temperature of the fission fuel (uranium dioxide) which is just under 3000 K.

The particle bed fuel element is also unclad. However, it differs significantly from the generic core, which uses graphite tubes containing uranium dioxide.

The particle bed fuel element is also unclad. However, it differs significantly from the generic core, which uses graphite tubes containing uranium dioxide. Instead, the particle bed fuel element is made up of spherical fuel beads contained between two concentric, monocoque cylinders. Each fuel bead is coated with a moderator material, which is coated by an anticorrosive coating. The propellant flows in and around the fuel beads, thus providing a much larger effective surface area for a given volume. Therefore, a particle bed fuel element should be considerably smaller and less massive than any other fuel element configuration. The particle bed fuel element violates our low development costs rule since it has not been tested (though SDI tests are rumored to have taken place). Once again, *low development costs are inherent in our overall objective, as the Waverider is to be an alternative to an exotic propulsion system.* One other problem with the particle-bed fuel element is the fact that it is unclad, and is therefore limited to the melting temperature of the fission fuel. A hybrid particle bed-clad fuel element having spheres designed to contain non-solid fission material would be the ultimate in fuel element concepts.

The clad fuel element has been selected for this mission. Note that a clad fuel element physically contains or confines its fission fuel despite its state.

Specifically, we have selected a CerMet (ceramic metal) fuel element. Such an element is composed of a tungsten matrix with uranium dioxide sandwiched inside. The CerMet fuel element is further cladded with a tungsten-molybdenum-rhenium alloy which has a similar thermal expansion coefficient. Tungsten is well suited for this purpose because of its high thermal conductivity, neutronic insensitivity, and the fact that it has a melting point of 3700 K. Furthermore, the CerMet configuration is a fast spectrum, or breeder, reactor. There were many doubts about the feasibility of such a system. A breeder reactor operates without a moderator and exploits the high energy of the fast neutrons by allowing them to collide with the neutronically stable uranium-238. This produces uranium-235 (the desired isotope that fissions spontaneously given critical mass) or more fuel. A breeder reactor can have a significantly longer operating life. Tungsten has a melting temperature of 3700 K, yet the 710 program of the late 60's and early 70's tested a CerMet reactor up to a temperature of only 2740 K. It was mentioned previously that a fluid stagnation temperature of 3175 K was needed to provide for a specific impulse of 1200 s. Consider, though, that the main objective of the 710 program was not to produce the highest specific impulse, which would require much higher operating temperatures, but to simply demonstrate the feasibility of the system. The 710 program eliminated long-standing doubts. Questions of safety, in particular, were laid to rest by immersing the reactor (without control rod and reflectors) in seawater, thus demonstrating that seawater was sufficient enough to moderate, or control, a CerMet reactor in the event of an accident during launch which caused the reactor to be deposited into the ocean. This also implies that that the

hydrogen propellant could be pumped into the reactor to shut down the system - another safety precaution. In conclusion, the CerMet configuration was selected because of its potentially higher operating temperatures, abundant technology base, safety, and its longer operating life.

The mass of the core, pressure vessel, and reflector on the high side, should be approximately 20,000 kg. This figure was estimated from the known masses and thrust capabilities of other reactors. The mass of the nozzle is unknown, pending a computational analysis/optimization.

The CerMet fuel element can be further enhanced. For example, consider a simplified geometry and propellant injection system where the coolant tube is simply a pipe, and the propellant flows through it from one end to the other (reactors do not usually have such a set-up because it leaves one end considerably hotter than the other, and it also induces a very significant thermal gradient and hence a large thermal load). As the flow approaches the exit of the coolant pipe, its temperature has come close to that of the fuel element. With such a low temperature difference, the fuel element at that end is not cooled very much and could suffer severe damage. Since the temperature gradient and thermal loads continuously decrease, the structure need not be as strong on one end as at the other. Therefore, introducing fine grooves into the fuel element would not over-stress the element. By introducing the grooves, the effective surface area is dramatically increased, resulting in greater electromagnetic radiation emission (infrared light, visible light, etc...). This provides a supplemental cooling mechanism for the hot end of the coolant pipe. Furthermore, it transfers or radiates more energy to the propellant. This simplified example applies to reality in that, no matter how well the geometry and coolant injection system is designed, there will always be low thermal gradients and hot spots on the fuel element.

All materials lose their strength, stiffness, and/or elasticity as their temperature approaches the melting point. Therefore, the fuel elements must be "over-cladded" (the cross-section of the elements are increased with the addition of more tungsten) so that structural failure does not occur at operating temperatures near the melting point of tungsten. Despite this added mass, the core of a rocket engine typically accounts for only 10% of the overall mass of the engine. The containment vessel, even with its much lower chamber , accounts for the majority of the engine mass.

The reactor will be of bimodal design; this means that the engine generates electricity as well as thrust, but does not do so simultaneously. Such an output would require 3500 kg of helium (which can be stored in the smaller tanks of the space shuttle external fuel tanks). Helium was chosen for this continuous operation because of its inert properties. Although, hydrogen does not react highly with tungsten or its alloy, over a long operating period it could damage the other components (the control rods are made of

boron/carbon which is corroded by hydrogen if the protective coatings erode over time). The power conversion generator and the heat rejection radiator-manifold have masses of 23,000 kg and 25,000 kg respectively.

In conclusion, our objective of attaining a specific impulse of 1200 s and a thrust of 2.2 MN can be obtained with low development costs by utilizing a CerMet solid-core nuclear propulsion system.

III.2.2 Structures
(McCartney, Martin)

We have chosen to use a Waverider to transport the crew because it will provide for the shortest transit time possible. A Waverider is a vehicle built so that it can create a shock wave that does not separate from the leading edge. The attached shock provides high pressure on the lower surface creating a pressure differential with the freestream pressure on the top. The advantage of this is not allowing for the tremendous pressure drop that occurs across a shock between the freestream and the leading edge of a normal hypersonic vehicle. Because it "rides" on its own shock wave and avoids the usual pressure losses, the vehicle can achieve much better aerodynamic performance for a given high-speed condition.

We intend to use a Waverider for a gravity-assist maneuver around the planet Venus in order to complete the crew's journey as quickly as possible. A standard gravity assist maneuver is usually done to slightly change the direction of the velocity vector of a spacecraft. This is achieved by flying close to a planet and letting the planet's gravity do the work that fuel would normally have to do. For this spacecraft, we intend to enter the atmosphere of the planet to significantly change the velocity vector as well as gain some velocity from the planet's orbital momentum.

If a normal spacecraft were to fly the trajectory we have planned, it would slow down considerably in the atmosphere due to drag, and it would not stay in the atmosphere long enough to change its direction as we have planned to do. The Waverider is special in that it is a lifting body, capable of using the lift produced to keep it inside the atmosphere (by pointing the vector down instead of up) as long as necessary to make the required angular deflection. In other words, the Waverider can "bite off" as much atmosphere and turn as much as it wants in order to get going in the right direction. This type of aero-gravity-assist maneuver will enable the spacecraft to get a large direction change around Venus and arrive at Mars sooner than otherwise possible.

The actual design of the Waverider in terms of size and shape was done by computer generation given several basic parameters. A program was written by University of Maryland graduate student Tom McLaughlin to input the expected flight conditions and certain desired physical characteristics (i.e. length, size

constraints) for a vehicle and output the size, shape, and aerodynamic characteristics of a corresponding Waverider. The program uses an iterative process and designs a vehicle optimizing for a certain parameter such as maximum lift-to-drag ratio (L/D) or maximum volume.

In designing a Waverider, there were a number of considerations to take into account. Shortening the flight time of the crew was a high design criteria and was the driving factor behind our design. In order to accomplish the trip in the shortest possible time, we wanted to have as high an L/D as the Waverider could deliver. The velocity lost due to drag in the atmosphere is not recoverable, so it is imperative to lose as little as possible.

Another consideration was the shape of the vehicle. In order to achieve the required aerodynamic performance necessary for an efficient aero-gravity-assist maneuver, a Waverider must be long and slender. The longer and more slender a Waverider is, the better the performance is, as a general rule. While long and slender gives good aerodynamic characteristics, it makes for poor volume efficiency. From a life support standpoint, the greater the amount of volume inside, the better the mission can be from a number of standpoints, including crew living space, morale, and overall comfort. Hence, it was important to keep the volume of the Waverider high enough for the benefit of the crew without sacrificing too much in the way of vehicle flight performance.

Four preliminary Waveriders were run using computer generation to get an idea as to the shape, size, and characteristics of the vehicle. The Waverider lengths entered were either sixty or seventy meters long and the resulting vehicles had volumes ranging from three thousand to fifteen thousand cubic meters. Some interesting tradeoffs were discovered as a result. The primary concerns for us as a design group have been (L/D) and volume. Waveriders are very thin by nature and while that is helpful for aerodynamic performance, having one too thin could prove useless from the standpoint of the crew and the equipment inside. It was found that, for a given flight condition, optimizing for maximum volume gave a slightly lower L/D but a greatly increased interior volume. From an overall design standpoint, doubling or tripling the volume and taking a five to six percent decrease in L/D is a good trade-off.

Another trade-off found was that of altitude. Because of the temperature drop with altitude, a lower Mach number can be achieved by going lower into the atmosphere. This also tends to increase L/D although the results did not show this effect to a great extent. It seems as though a certain Mach number independence occurs so that for Mach numbers greater than fifty, the characteristics of any given Waverider are fairly similar.

The biggest disappointment after the first runs was that all the L/D's were near four, which is much lower than we needed for an efficient maneuver. At first it was thought that the reason could very well be the high Mach numbers, since no

Waveriders were run at a Mach number below fifty. Without a high L/D, it is not advantageous to go through the atmosphere. Further runs determined that our first design were not slender enough to achieve the desired L/D. This problem was corrected for in the final design. Also, the first runs proved that great increases in volume could come as a result of a small extension of length. Since the majority of volume in a Waverider is at the back, a small increase in length can yield a large increase in volume.

It was determined by the time of our final Waverider design that the optimum atmospheric density for the maneuver was a fixed value based on the lift required to balance the centripetal acceleration. This requirement dictated that the Waverider design be run near eighty-six kilometers. Since the altitude was fixed, the major design consideration at hand was achieving a balance between L/D and interior volume. After a number of design attempts, it could be seen that the smaller the generating cone angle, the greater the L/D and the smaller the volume. At first the optimization was done for L/D, but again it was found that optimizing for volume nearly doubled that parameter while only dropping L/D slightly, so it was decided to alter the optimization. Volume optimizing and designing for an L/D of at least seven was how the final design was completed.

After continuing to lengthen the vehicle at ten meter increments from sixty to eighty, and shortening the cone angle from twelve to below eight, it was determined that the design had reached an optimum balance between length, volume, and L/D. The final design for the Waverider is shown in Figure III.2.2-1.

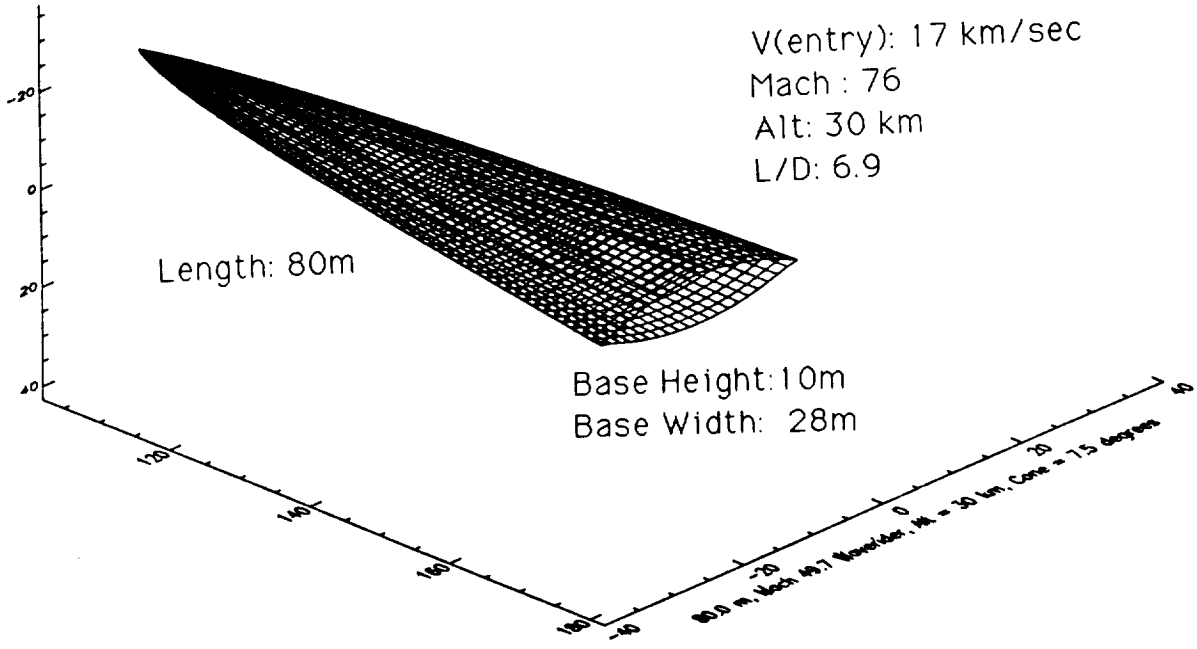

The final design had a L/D of 6.89 and an internal volume of 5,300 m^3.

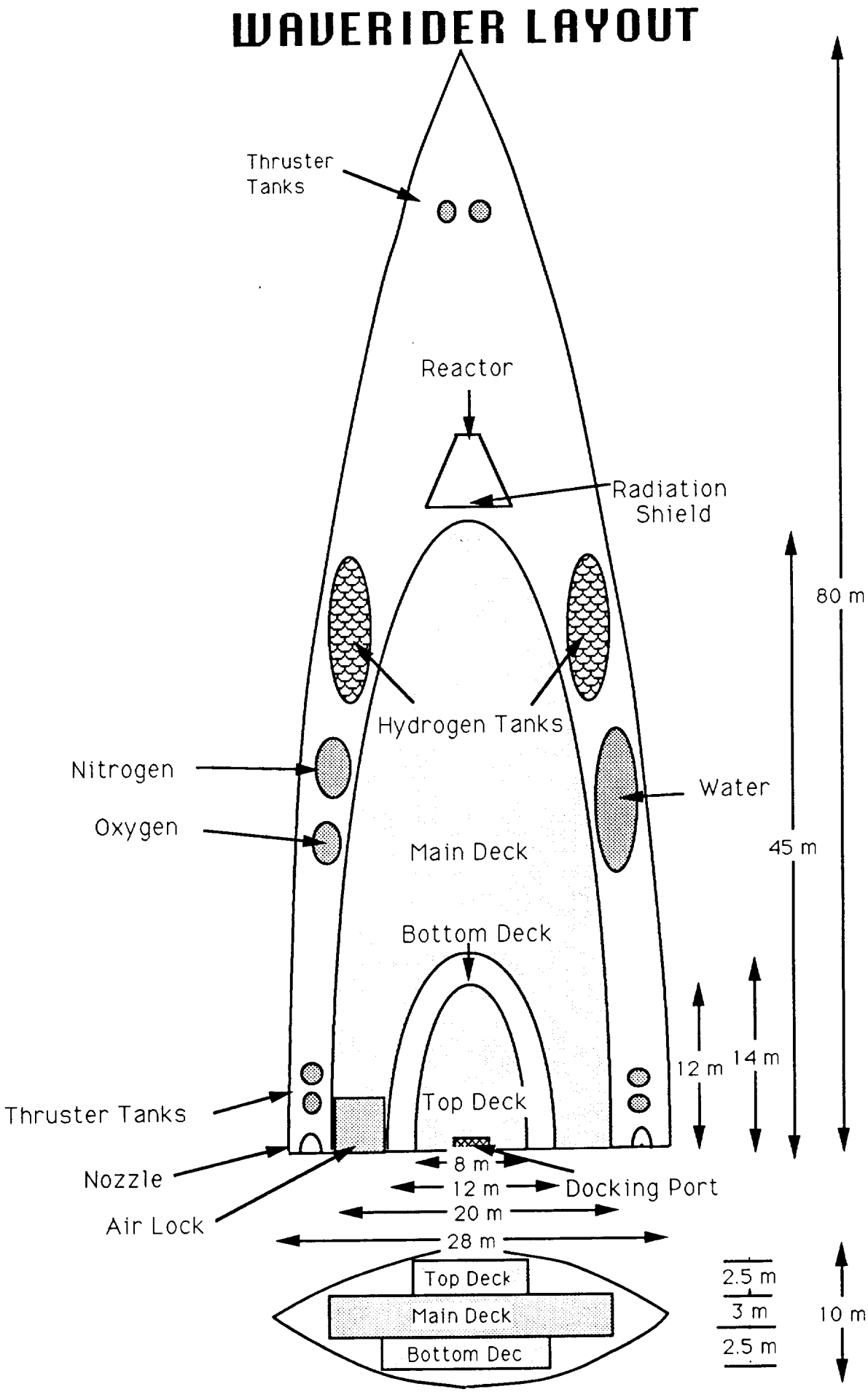

Figure III.2.2-2: Waverider Deck Configuration

A Waverider is extremely volume inefficient by nature. Even though there are 5,300 m^3 in the vehicle, much of it cannot be used effectively. With the most usable volume near the trailing edge, the Waverider was split into three decks of crew living area. (see Figure III.2.2-2). The decks have the following characteristics:

Deck	Floor Area (m^2)	Volume (m^3)
Main	550	1650
Bottom	110	275
Top	65	163
TOTAL	725	2008

This leaves almost 3300 m^3 of space for storage of fuel, cooling fluids, water, food, and equipment. The nuclear reactor will be placed forward of the living spaces to minimize the amount of shielding required. The liquid hydrogen tanks will be placed on the neutral axis so that as they drain, it will not shift the center of gravity. The water tanks will be placed on the right side of the vehicle to counterbalance the oxygen and nitrogen tanks on the left. The rear of the vehicle will be reinforced so that the nuclear booster can be attached.

A first approximation of structural loading was taken by analyzing the major loadings for the point during the trip when maximum loading was expected. That point is during the Venus maneuver when the Waverider experiences an acceleration of 4.5 G's. The approximation was done by assuming the lift force was distributed evenly over the bottom surface. The lift was found using a known lift coefficient for the vehicle and the pressure near eighty kilometers is a given value. A safety factor of 1.5 was included as it is for many aerospace applications. The result of a simple truss structure analysis was a mass of 3,700 kg just for support against compression.

III.2.2.1 Materials
(McCartney, Martin)

III.2.2.1.1 Outer Structure

The Waverider will experience severe heating rates, temperatures, and structural loading when it passes through the atmospheres of Venus, Mars, and Earth. However, these aspects will vary on different parts of the Waverider as shown in Figure III.2.2.1.1-1. The heating on the nose will be quite different than the heating on the upper surface. Therefore, different parts of the Waverider are designed differently.

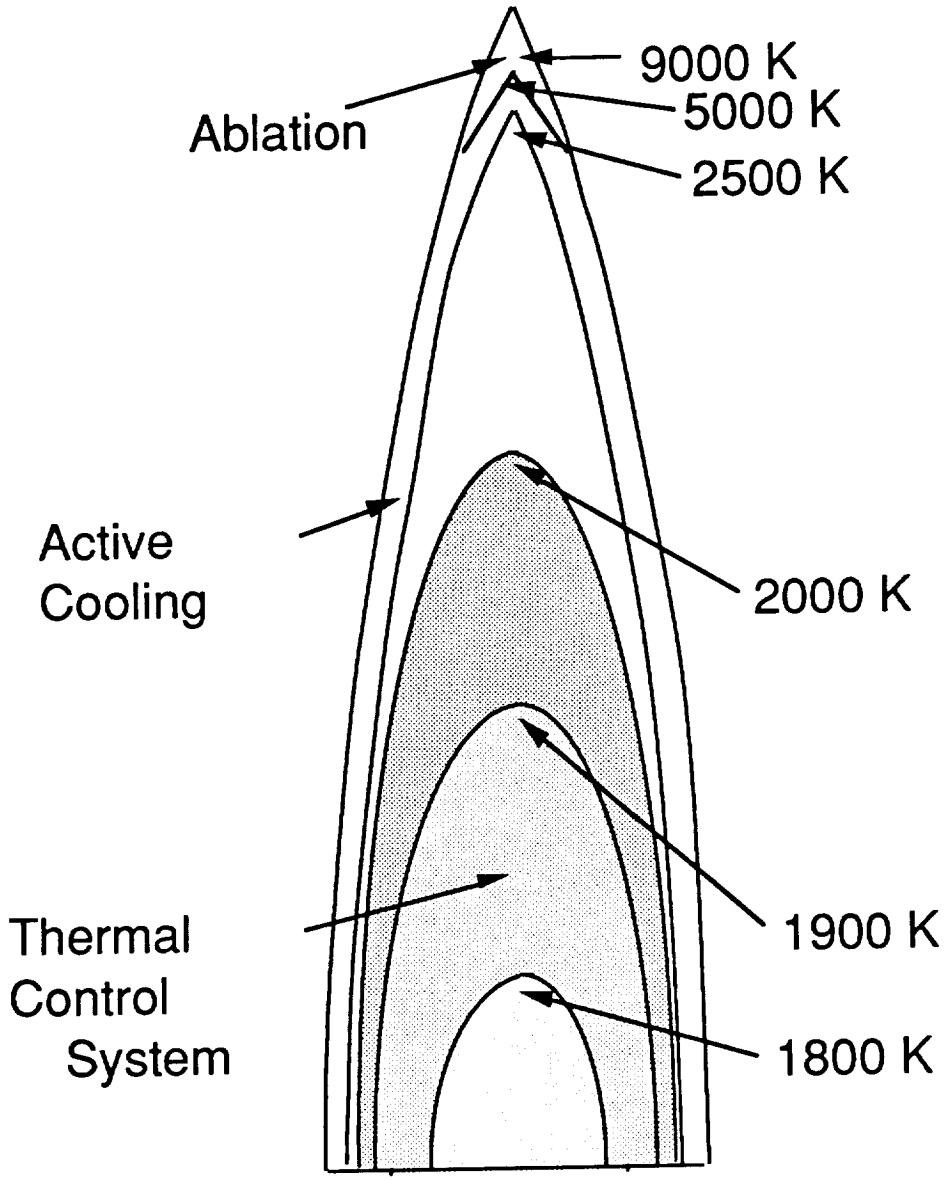

Figure III.2.2.1.1-1: Waverider Heating Distribution

The upper surface of the Waverider will experience relatively low temperatures, since it is parallel to the freestream air flow. It will be protected with a hot structure system (see Figure III.2.2.1.1-2) This structure is the same that is used by the SR-71 Blackbird. The hot structure is composed of a skin supported by corrugated webbing. It can be made with a high temperature alloy like titanium aluminide, which gives the structure high strength up to 1200 K with a significant reduction in weight.

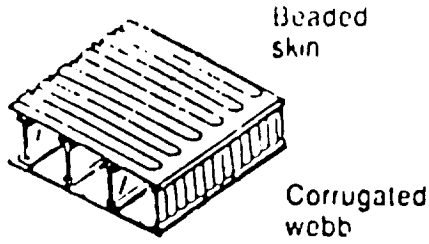

Figure III.2.2.1.1-2: Hot Structure

The lower surface of the Waverider will experience different temperatures and heating rates at different locations. The inner part of the surface that experiences temperatures below 2500 K will be covered with a thermal protection system. This type of structure is used by the Space Shuttle, for which ceramic tiles protect the aluminum primary structure. The thermal protection system consists of a high strength, low weight primary structure which is protected from the heat by a thermally protective material. Since the primary structure is covered by the thermal tiles, it does not have to be smooth. This allows the primary structure to be built with a configuration that maximizes strength while minimizing weight (see Figure III.2.2.1.1-3). For a structure to have the maximum geometric efficiency possible, the principal load bearing area should be symmetric about the neutral axis. It should have curved caps and clamped edges for a high buckling coefficient. Also it should have a low-density web between the caps that support the load. The truss-core web corrugation is the most geometrically efficient configuration. The primary structure will be built with a titanium aluminide for good strength and light weight.

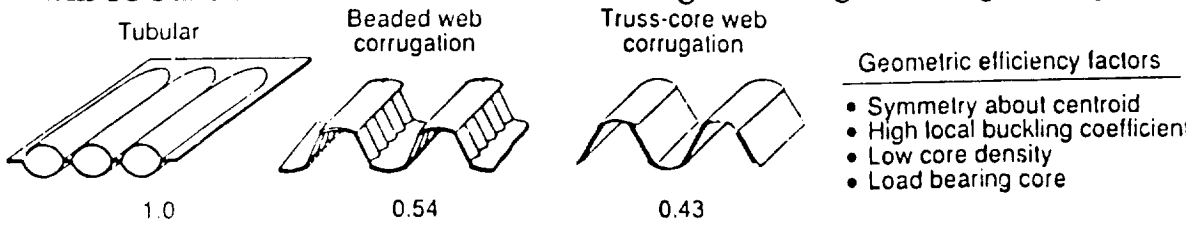

Figure III.2.2.1.1-3: Primary Structure

The thermal tiles will be made of three-dimensional carbon-carbon composites. For temperatures above 1200 K, carbon-carbon composites have the highest specific strength of any structural material. It can withstand temperatures up to 2500 K while maintaining its strength and stiffness. It also has ablative properties, which will give the Waverider extra protection in case it encounters higher heating rates. However, carbon-carbon composites oxidize rapidly in temperatures above 850 K. The carbon-carbon will be coated with silicon carbide, forming a thin layer over the composite and protecting it from oxidation. However, the coating and the carbon-carbon have different rates of thermal expansion, which causes the coating to crack at high temperatures. The carbon-carbon will be protected by a second line of defense consisting of a silicate sealant. As the coating cracks, the sealant will fill the cracks and prevent oxidation.

Since carbon-carbon can only withstand temperatures up to 2500 K, the area behind the nose and leading edges will need an active cooling system. The structure will consist of carbon-carbon composites surrounding refractory metal heat pipes (see Figure III.2.2.1.1-4). Liquid hydrogen will pass through these pipes, absorbing heat from the structure and carrying it to the rear where it can be expanded out of a nozzle to provide a propulsive thrust to help overcome some of the drag. The heat pipes will be composed of tungsten since it has the lowest reaction rate (with carbon) of the refractory metals. It also has very high thermal conductivity and a low rate of thermal expansion. The heat pipes will be spaced and sized so that in the case of system failure, the ablative properties of the carbon-carbon will protect the vehicle. Five-thousand Kg of hydrogen will be needed to protect the structure during the encounter with Venus, and an additional 5,000 kg will be needed for Mars. The hydrogen will be heated to a temperature of 1000 K and expanded through two nozzles at a mass flow rate of 13.89 kg/sec. This will provide an extra 75,000 N of thrust.

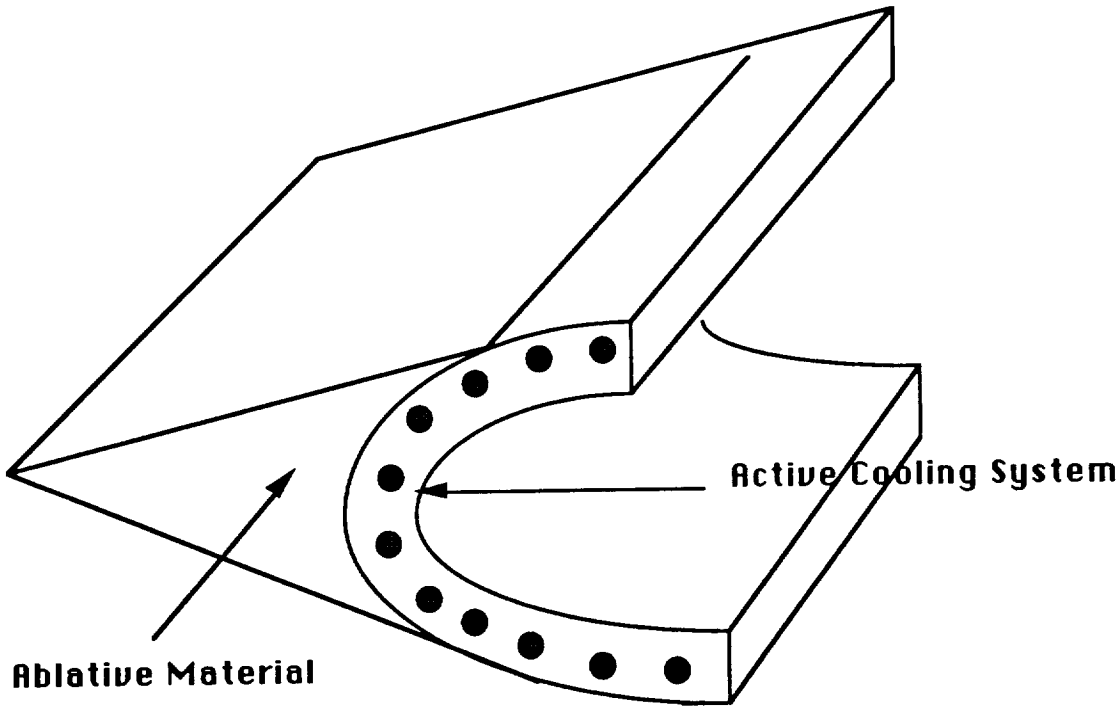

Figure III.2.2.1.1-4: Waverider Cooling System

The nose and the leading edges of the Waverider will experience heating rates of up to 33,500 W/cm2. This corresponds to a temperature of 9000 K, the highest experienced anywhere on the vehicle. No material that exists can withstand this. Therefore, these high-heating areas will be protected by an ablative surface. Carbon phenolic, the ablative material used on the Galileo probe, was selected to protect the

vehicle because it can withstand temperatures over 11,000 K. The ablative edges will be manufactured so that the leading edges of the Waverider remain sharp during the passage through the atmosphere of Venus. It is important that the edges remain sharp so that air does not spill over the edges, reducing the L/D ratio of the vehicle. During the Martian encounter, the last of the ablative material will burn away, exposing the active cooling system. This will reduce the L/D ratio for the Martian aerobrake, which will allow for a quicker reduction in speed.

III.2.2.1.2 Inner Structure

The inner structure will consist of a three dimensional truss network designed to support the outer structure. The beams will be spaced close enough together so that the outer structure doesn't buckle, yet as far apart as possible to cut down on weight.

III.2.2.2 Weights
(McCartney, Martin)

The hot structure making up the upper surface of the Waverider will have a mass of 19.6 kg/m^2. The thermal protection system and active cooling system on the lower surface will have a mass of 34.2 kg/m^2. The total structural mass of the Waverider is as follows:

Upper surface	28,480 kg
Lower surface	48,870 kg
Additional support	3,700 kg
Liquid hydrogen and tanks	12,000 kg
Total structural mass	93,050 kg

III.2.2.3 Environments
(McCartney)

The atmosphere of Venus is very thick and is mostly composed of carbon dioxide. In fact, 97% of the atmosphere is carbon dioxide, so that in general, the other components can be neglected. A complete listing of atmospheric characteristics for altitudes up to 100 kilometers can be found on the following spreadsheet. The temperature of the atmosphere drops significantly with height, making for an increasingly high Mach number for higher altitudes. The orbital velocity (circular) for each altitude is shown giving our absolute minimum speed during transit if we hope to escape from the planet's gravity.

	A	B	C	D	E	F	G	H	I	J	K	L	M	N	O
1	TEMP (K)	ALT. (km)	PRESS (bars)	DENS. (kg/m3)	Gamma (Cp/Cv)	Speed of Sound (m/s)	Spec. Heat p (J/kgK)	kin. visc. (kg/ms)	k (W/mK)	Prandtl No.	Stag. Temp. (K)	Mach No.	Trial velocity (m/s)	mu(kg/sec2)	Circ. Orb. Vel. (km/sec)
2	735.3	0	92.1	64.79	1.193	410	1181	0.0000335	0.0588	0.672849	100799.954	41.4634146	17000	325000	7.328416801
3	696.8	5	65.65	49.87	1.198	400	1159	0.0000221	0.0521	0.49163	88062.34488	42.5	17000	325000	7.325391155
4	658.2	10	47.39	37.72	1.202	389	1138	0.0000208	0.047	0.503626	90759.646611	43.7017995	17000	325000	7.322369253
5	620.8	15	33.04	27.95	1.207	379	1116	0.0000294	0.0432	0.7595	113282.2587	44.8548813	17000	325000	7.319351088
6	580.7	20	22.52	20.39	1.213	367	1091	0.0000278	0.0395	0.767843	116860.2583	46.3215259	17000	325000	7.316336653
7	539.2	25	14.93	14.57	1.22	355	1062	0.0000267	0.0362	0.783298	120917.2514	47.8873239	17000	325000	7.313325938
8	496.9	30	9.581	10.15	1.228	342	1030	0.0000252	0.0336	0.7725	123514.9172	49.7076023	17000	325000	7.310318938
9	455.5	35	5.917	6.831	1.238	329	996	0.0000238	0.0309	0.767146	127214.9358	51.6717325	17000	325000	7.307315643
10	417.6	40	3.501	4.404	1.248	316	964	0.0000225	0.0286	0.758392	130930.2513	53.7974684	17000	325000	7.304316047
11	385.4	45	1.979	2.693	1.257	304	936	0.0000214	0.0264	0.758727	135284.2853	55.9210526	17000	325000	7.301320142
12	350.5	50	1.066	1.594	1.268	292	904	0.0000201	0.0243	0.747753	138009.328	58.2191781	17000	325000	7.29832792
13	302.3	55	0.5314	0.9207	1.287	273	859	0.0000183	0.0223	0.704919	141534.0343	62.2710623	17000	325000	7.295339374
14	262.8	60	0.2357	0.4694	1.304	256	821	0.0000167	0.0204	0.672093	144674.2376	66.40625	17000	325000	7.292354496
15	243.2	65	0.097	0.205							243.2		17000	325000	7.289373279
16	229.8	70	0.0369	0.08393	1.32	241	789	0.0000154	0.017	0.714741	154900.5409	70.5394191	17000	325000	7.286395716
17	215.3	75	0.0136	0.033							215.3		17000	325000	7.283421798
18	197.1	80	0.004476	0.01186	1.338	225	757	0.0000139	0.0139	0.757	165642.2632	75.5555556	17000	325000	7.280451518
19	181	85	0.00138	0.0039							181		17000	325000	7.27748487
20	169.4	90	0.0003736	0.001151	1.353	209	733	0.0000126	0.0125	0.738864	170207.2636	81.3397129	17000	325000	7.274521845
21	168.2	95	0.000315	0.00031							168.2		17000	325000	7.27156243?
22	175.4	100	0.0000789	0.0000789	1.352	213	738	0.0000129	0.0128	0.743766	169764.8938	79.8122066	17000	325000	7.268606637
23															
24	List of other significant val of the atmosphere of Venus														
25	R=191.4 J/KgK														
26	Rm=6051.5 km														

III.2.2.3.1 Thermal
(McCartney)

One of the major problems with Waverider design is heating. Flying at extremely high Mach numbers makes aerodynamic heating a significant problem. A first analysis of stagnation temperature was done using a recovery factor (see the above spreadsheet), but these values were determined to be too high to be accurate. A next step was to examine the chemical reaction that happens to carbon dioxide at high temperature. The results showed that above 4000 K the gas completely dissociates and absorbs energy in the process. However, due to the high speed of the vehicle, complete dissociation will not occur. In examining the heating rates that the Waverider will experience, convective heating rates were calculated both with and without chemistry effects.

III.2.2.3.1.1 Convective Heating Rates (without chemistry)
(Seybold)

In order to obtain a qualitative idea of the convective heating rates we would be facing, we used this general formula to plot stagnation point and laminar flat plate data:

$$\dot{q}=\rho^{n}_{\infty}V^{m}_{\infty}C$$

Stagnation Point: n=0.5, m=3.0, $C=(1.83E\text{-}08)(\sqrt{R})$

Laminar Flat Plate: n=0.5, m=3.2, $C=(2.53E\text{-}09)(\sqrt{\cos\phi})(\sin\phi)(\sqrt{X})$

Where: R=Nose Radius in m

ϕ=Local Body Angle

V=Approaching Velocity in m/s

ρ=Density at Given Altitude in kg/m3

The equation is taken from Anderson's book, Hypersonics and High Temperature Gas Dynamics; it gives reasonable correlations as long as a cold wall is assumed and the boundary layer theory is valid.

III.2.2.3.1.2.1 Stagnation Point

For the stagnation point of the Waverider, we find that the heating rates are high (in the 10000's) and increase significantly with either increasing density (Fig. III.2.2.3.4.2.1-1) or increasing velocity (Fig. III.2.2.3.4.2.1-2). The explanation for the very high heating rates is the small nose radius (0.01 m) that is used in the Waverider configuration. A larger (blunter) nose decreases the heating rate (Fig. III.2.2.3.4.2.1-3).

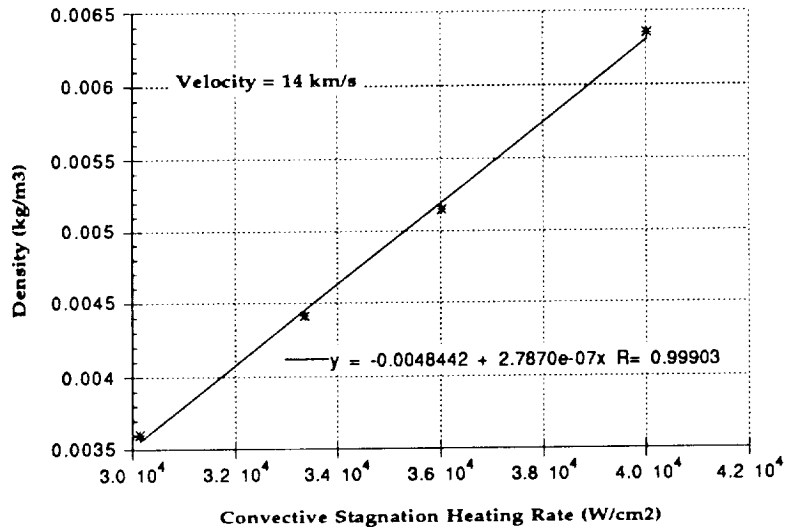

Figure III.2.2.3.4.2.1-1: Density vs. Stagnation Heating Rate

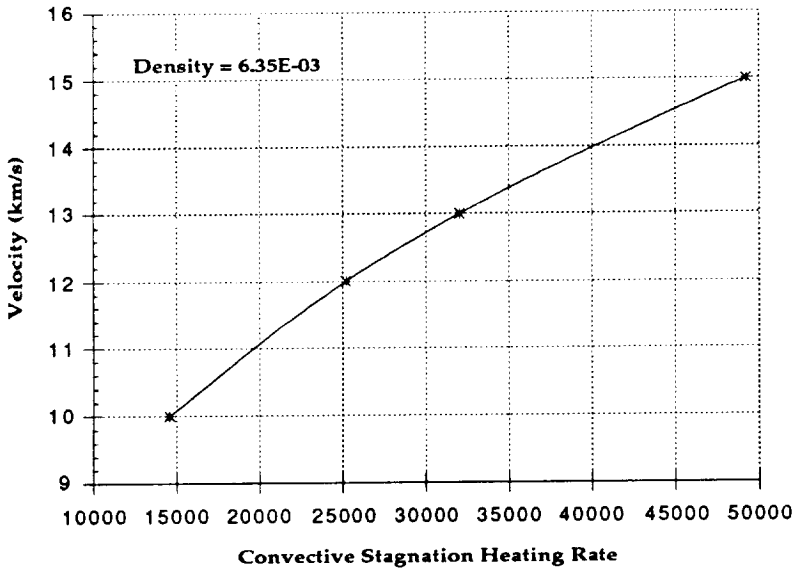

Figure III.2.2.3.4.2.1-2: Velocity vs. Stagnation Heating Rate

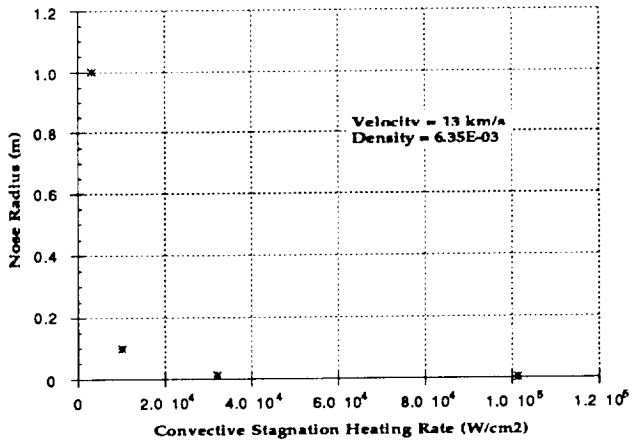

Figure III.2.2.3.4.2.1-3: Nose Radius vs. Stagnation Heating Rate

Using the following relation, we can determine the temperatures that correspond to the stagnation point heating rates:

$$\dot{q}(\text{in(convective)})=\dot{q}(\text{out(radiative)})$$

$$\rho^{n}{}_{\infty}V^{m}{}_{\infty}C=\varepsilon\sigma T^{4}$$

Where: ε=Emissivity of the Material
σ=Stefan-Boltzman Constant
T=Temperature

Corresponding to the high heating rates, the stagnation temperatures reach several thousand degrees Kelvin (Fig. III.2.2.3.4.2.1). These high temperatures stretch the current heat shielding technology and would be nearly unmanageable if they were present over large portions of the Waverider. However, they are only present in the vicinity of the stagnation point, or the circumference of the nose radius, which is at most a few centimeters on a vehicle that is several meters in length. The small size of the affected area allows us to concentrate our shielding so that we can tolerate the high temperatures. Specifically for our Waverider, the stagnation heating rate is 29550 W/cm2; the stagnation temperature is 8730.

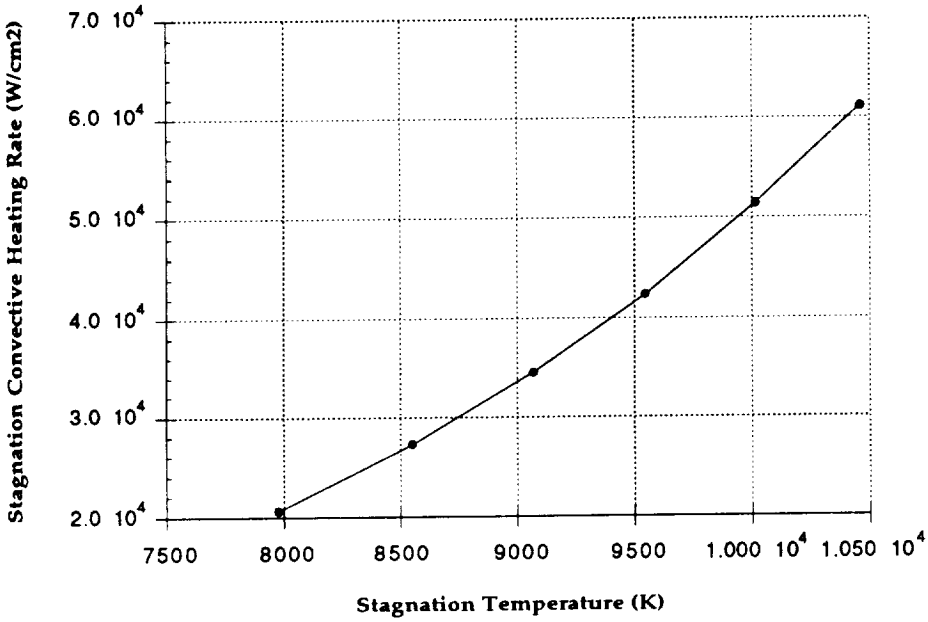

Figure III.2.2.3.4.2.1: Stagnation Convective Heating Rate vs Temperature

III.2.2.3.4.2.2 Laminar Flat Plate

To approximate the heating rates over the under, or "business ", side of the Waverider, the laminar flat plate form of the heating rate equation is used. For our purposes, the Waverider is assumed to be a flat plate because of its relative thinness (a 14 m base height on a 70 m vehicle). Also, because of the thin shock layer around the Waverider, a laminar flow assumption is acceptable. As the velocity increases and/or the vehicle decreases in size, this assumption becomes more accurate.

When the calculations are made, it is shown that the heating rate decreases as the distance from the stagnation point increases. For our Waverider, we determined the body angle from the relation:

$$\frac{1}{\tan \phi_{eff}} = \frac{L}{D}$$

Where: ϕ_{eff} = Effective Body Angle

Since we have an L/D of approximately 6.9, our body angle comes out to be 8.27 deg, or 0.14434 rad. Using this value in our calculations, along with the approaching velocity and appropriate density, the laminar convective heating

value can be determined at any position on the underside of the Waverider. Figure III.2.2.3.4.2.2 is an example of this analysis for the Martian aerobrake.

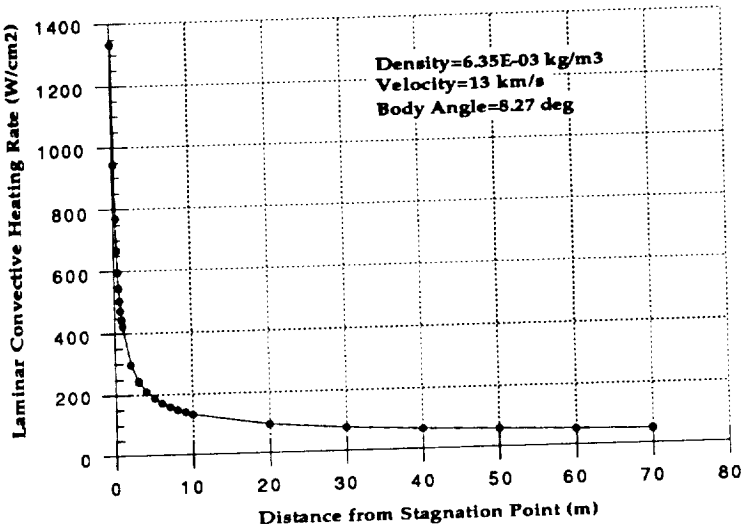

Figure III.2.2.3.4.2.2: Waverider Heating for Martian Aerobrake

III.2.2.3.4.3 Convective Heating Rates (with chemistry)

Because of the personnel shortages, this aspect of aerodynamic heating could not be adequately explored. However, a preliminary analysis was made by a member of the Structures group which indicated that a total reaction would give off more heat than we would be absorbing; this led to the conclusion that the atmospheric gases would not be totally reacting at any point in our journey. We do not know, or have an estimate, of what the actual reaction percentage would be.

III.2.2.3.4.4 Radiative Heating Rates

(McCartney)

The equilibrium temperatures at points on the lifting surface were determined by using the Stefan-Boltzman Law of blackbody radiation. Assuming an emissivity of 0.7, the temperatures were obtained from the relation shown below

$\varepsilon \dot{q} = \sigma T^4$

T=temperature
ε=emissivity
σ=5.67 x 10E-08
q=heating rate

This corresponds to a distribution of temperatures shown in Figure III.2.2.1.1-1. The high heating rates and corresponding temperatures require that some kind of special precautions be taken in terms of materials to prevent the structure from melting or coming apart in the Venus atmosphere.

III.2.3 Electrical

III.2.3.1 Power
(Kamosa)

The requirements for power on extended manned missions are great. Nuclear power is currently a proven means for generation of large amounts of power . Nuclear reactor power generation has several unique characteristics which make it attractive and even singularly enabling for many space applications. The advantages of nuclear power reactor systems are that they can provide a large and continuous supply of electrical power, operate independently of external supplies of fuel or energy, and are relatively invulnerable to environmental hazards of space. In addition, their relatively small size offers certain operational enhancement in reduced spacecraft size and reduced interference with other structures. Nuclear reactor power systems provide a highly reliable direct heat supply and low cost effectiveness despite large initial capital costs (Vaughn). Figure III.2.3.1 shows the various types of power systems available versus mission power requirements and duration. It is obvious from this graph that this mission falls into the nuclear power category, substantiating the use of nuclear power on the Waverider.

Power needs on the Waverider vehicle are large, considering the vast amounts of systems and subsystems and the duration of the mission with a crew of ten. Power needs will include communications, life support areas of lighting, kitchen, bathroom, computer workstations, guidance and control systems, bunking areas, and active heating and cooling, all electrically driven items. Power consumption is in the order of 1MW of power.

The large power requirements will be met by means of a liquid cooled (NaK), UO_2 fuel reactor coupled with 4 free piston stirling engines for power conversion.

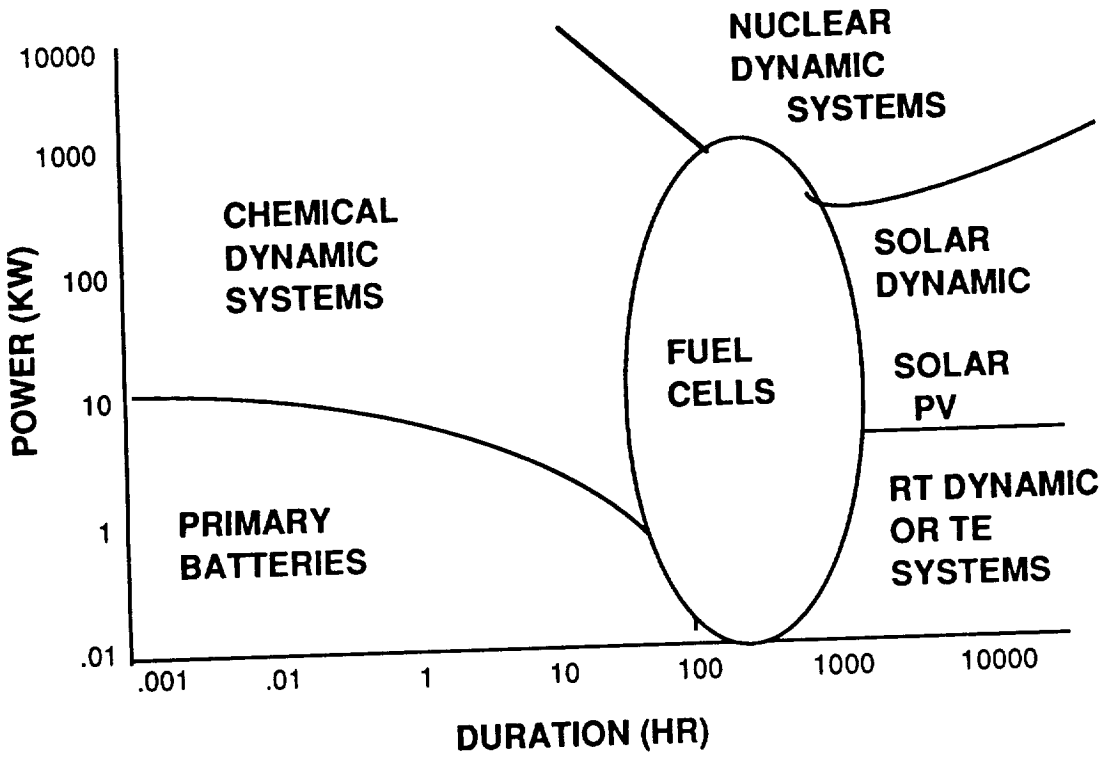

Figure III.2.3.1: Available Power Systems

III.2.3.1.1 Reactor System with Free Piston Stirling Engines

The reactor system represents the main power control area within the Waverider forward section. The power system will be incorporated into the structure and it will have a heat dissipative radiator system integrated into the Waverider top side. Radiation shielding to protect the crew will consist of Tungsten as a shield against gamma radiation and Lithium-Hydride (Natural and Depleted) within a stainless steel matrix as a shield against neutron radiation.

The Waverider's UO_2 reactor coupled with the Free Piston Stirling Engines will nominally have a power output of 1 MW. A drawback of such a system contained within the Waverider will be the means of dissipating the waste heat from the reactor and the various systems associated with it. Waste heat will be transported by a piping system primarily made from molybdenum tubing running from the reactor area to the lower surface area of the outer skin section (Figure III.2.3.1.1-1). These types of heat pipe systems have been tested using a working fluid of sodium to a temperature of 1600 K for periods up to 23,700 hours. Heat pipes used in these tests were from 1.0-1.5 m in length. Excess heat can be utilized for crew heating in the atmospheric control system. An idea for waste elimination would be to use this excess heat diverted to a chamber where waste can be stored, incinerated, then ejected from the Waverider. The expected heat from the reactor and Free

Piston Stirling Engine system is about 1000K. Current heat elimination systems for designed space reactor systems do not have internal means of dissipating waste heat. Further study must be done into areas in which a reactor with power systems can fully utilize such a system on a space vehicle such as the Waverider (Merrigan).

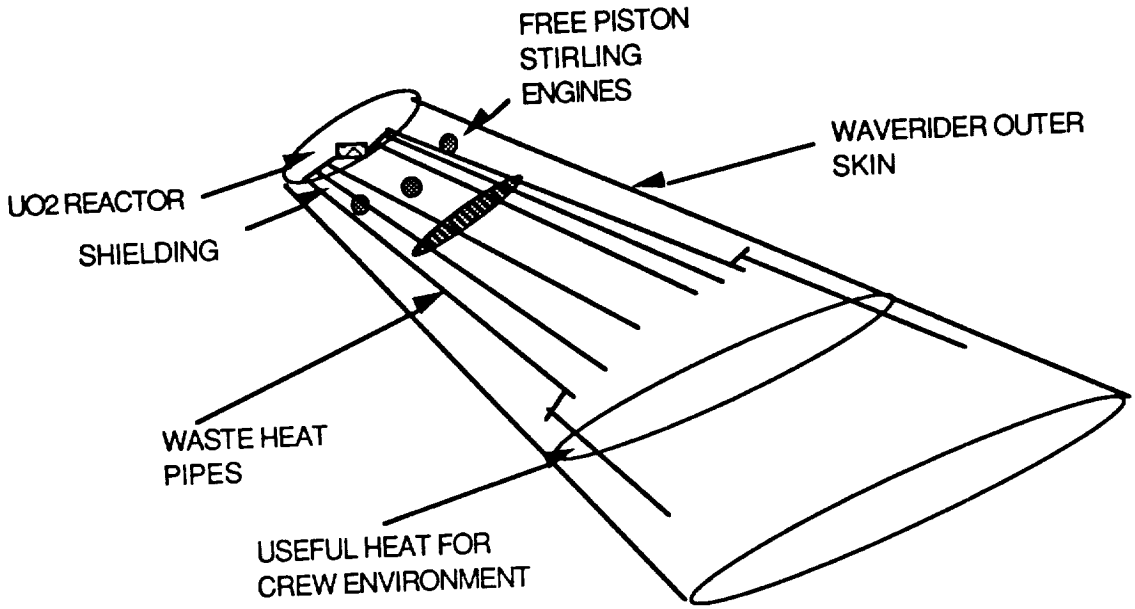

Figure III.2.3.1.1-1: Waste Heat Piping System

To examine radiation shielding and radiation transport, thermal analysis of radiation shielding for a system similar to the SP-100 reactor system was performed using Finite Element codes. These codes were developed at the University of New Mexico and Sandia National Laboratories for fast a reactor operating 1.66 Mw. Shielding consisted of tungsten and lithium hydride pressed into a stainless steel honeycomb matrix as shown in Figure III.2.3.1.1-2. A shield design of graphite, depleted lithium hydride, tungsten and natural lithium hydride was shown to satisfy neutron and gamma fluence requirements. Temperature limits also minimize cracking in the lithium hydride portion of the shield (Barrattino et al, Reference 6).

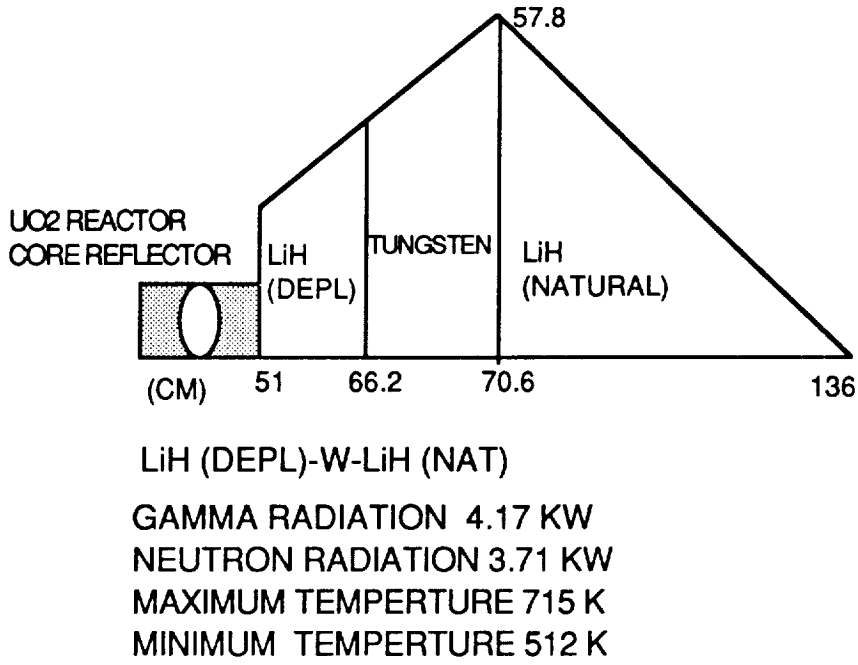

Figure III.2.3.1.1-2: Shielding Configuration for Waverider UO_2 Reactor

The lithium hydride (depleted) with tungsten and lithium (natural) shield appeared to be the best selection when considering both radiation protection and maximum temperature constraints. The importance of the tungsten location is clear from both a radiation transport and thermal transport perspective. Radiation transport optimization required that the tungsten be located 13.4 cm into the shield to minimize effects of secondary gammas emerging from the shield. Heat transfer optimization required the highly conductive material to be located in the front portion of the shield to keep LiH temperatures within tolerable limits (Barattino et al, Reference 6).

III.2.3.1.2 Power Conversion System Comparisons

1. Thermoelectrics

Thermoelectrics is simple heat generation transported by heat pipes. The thermoelectric modules are situated between (hot side) reactor and space side (cold side). A disadvantage is the low conversion rates, which in turn increase the reactor size and thermoelectric modules. This leads to more shielding and heat pipes for dissipation pipes (El-Genk, Reference 22).

2. AMTEC (Alkali Metal Thermoelectric Conversion)

AMTEC uses unique beta alumina electrolyte (BASE) within a closed vessel divided into a high temperature and high pressure region in contact with a heat source and low temperature and low pressure region in contact with a heat sink separated by BASE. Progress has developed significantly in recent years although maintenance on the system is a constant problem. This system was not chosen due to this fact (El-Genk).

3. Rankine Cycle

Rankine engine cycles use a nuclear reactor and heat exchanger to boil working fluid. This working fluid is converted to vapor, which expands through a turbine. The turbine is linked to an alternator, which generates electrical power. The Rankine engine was rejected because (1) turbine/alternator lifetime is not long enough without maintenance, (2) methods are needed to control condensation near turbine exit,
(3) separation of flow occurs in zero-g environment, (4) corrosion of turbine results from the fluid (liquid-metal), and (5) thaw-out of liquid occurs during start-up and restart. (El-Genk)

4. Brayton Cycle

The Brayton Cycle is a closed or open inert gas cycle. Gas is heated in a reactor core directly or through a heat exchanger. High temperature and high pressure gas expands in the turbine/alternator unit. The turbine rotates a compressor, and compressed gas runs an alternator to generate electricity. The cooled gas returns to cycle again. Reasons for rejection of this system are (1) the specific radiator area is large and not suited to the Waverider configuration, (2) material problems are associated with creep in turbine blades, (3) high temperature is required for the working fluid, and (4) the system has low efficiency. (El-Genk)

5. Thermonics

In thermonics a core composed of an emitter or cathode, surrounds a fuel column from which it receives heat and emits electrons. A collector or anode collects the electrons. The collector is cooled by pumped liquid-metal coolant to limit back emission of electrons. Reasons for rejection are (1) low conversion efficiency, (2) high temperature of the core (1800-2000K), (3) material difficulties at high temperatures, (4) premature failure of thermonics fuel elements undergoing irradiation at high temperatures. (El-Genk)

6. Free Piston Stirling Engine

The free piston stirling engine shown in Figures III.2.3.1.2-1 and -2 is a thermal-mechanical-electrical energy conversion system. It uses a linear alternator. By damped oscillation of two opposing pistons, one supplies the

other power. The working fluid is heated and cooled by the heat exchanger, linked to the reactor core coolant and radiator system. Conversion efficiencies have been as high as 30%. Free piston stirling engines do not require a high heat source. A UO2 fueled reactor will be the source of heat, without concern for the.fuel swelling limit of 10%. Free piston stirling engines have the smallest specific mass (29 Kg/KW) of all systems. High performance, long life, and low vibration are due to the design consisting of only two moving parts. A small disadvantage is the extended heat transfer surfaces, although most of the upper surface of the Waverider can be utilized for this process (El-Genk).

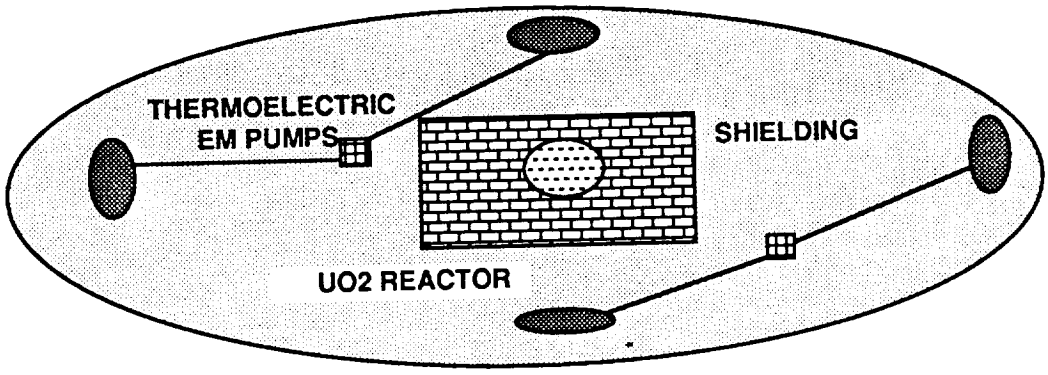

Figure III.2.3.1.2-1: Free-Piston Stirling Engine

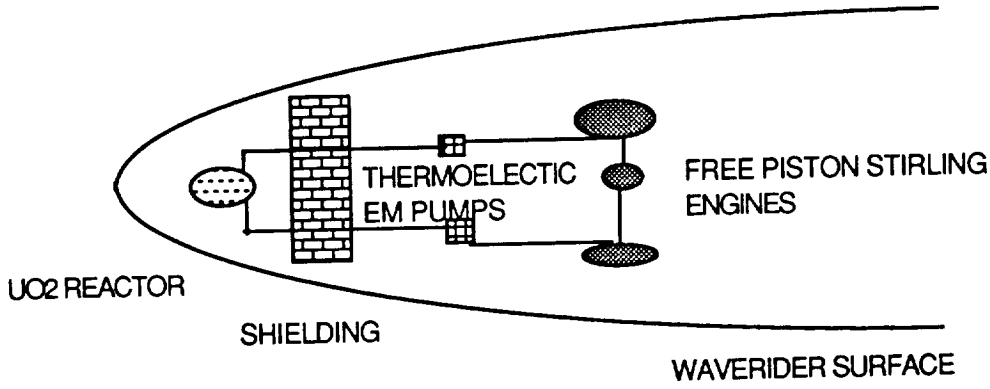

Figure III.2.3.1.2-2: Free-Piston Stirling Engine

A comparison of the above systems is given in Figure III.2.3.1.2-3.

POWER SYSTEMS					
VEHICLE	TYPE OF SYSTEM	POWER OUTPUT	SECONDARY SYSTEM	WEIGHT (Kg)	VOLUME (M3)
WAVERIDER	UO2 REACTOR 4 FREE PISTON STIRLING ENGINES	1000 KW	REGENERATIVE FUEL-CELLS	12000	24
CARGO-SHIP	BI-MODAL POWER FROM BOOSTER ENGINE	50-100 KW	SOLAR PANEL	2000	15
LANDER	REGENERATIVE FUEL-CELLS WITH GaAs SOLAR ARRAY	25-30 KW	Ni-H2 BATTERIES	1200	5
ASCENT	Ni-H2 BATTERIES	5-7KW		300	3

Figure III.2.3.1.2-3: Power Systems

III.2.4 Guidance and Control
(Kraft)

The interfaces of the primary components of the WOPM and LLVM guidance systems are shown in Figure III.2.4-1.

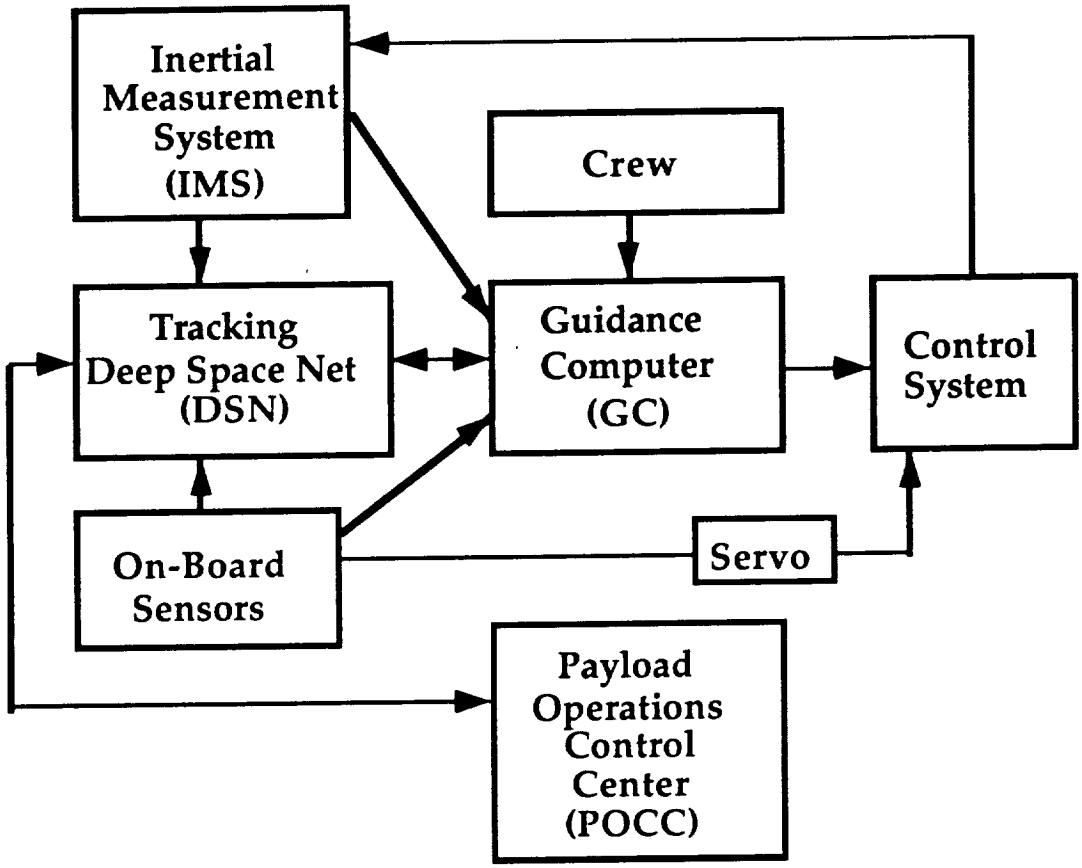

Figure III.2.4-1: Guidance and Control System

(Lander guidance interfaces and components differ somewhat from those of the total LLVM and are discussed in Section III.3.2.4.) This section describes the design of these primary components, the sensors, the Inertial Measurement System (IMS), the Guidance Computer (GC), and the Control System. The design philosophy for the M^3 guidance system has been to select components, where possible, of the latest, most capable version of a proven system, man-rated where necessary, and to be flight proven prior to the next century.

The WOPM Guidance and Control System must operate in a number of different modes. These modes are described in Figure III.2.4-2. The most critical modes, from the guidance and control, are the aeromaneuvers at Venus and Mars and the corrective attitude and velocity maneuvers made for the approaches to the aeromaneuvers. For pure drag capture, i.e. capture without large propulsive maneuvers, the flight path in the entry corridor must be controlled to less than 0.3 degrees (Cross, Reference 18). This accuracy requires precision optical sensors and IMS components.

Waverider Guidance Modes

Mode	Periods	Sensors	Controls
Thrust Vector Control	Burn to Depart LEO	IMS (gyro rates, accel.)	Chemical, ACS Primary
Celestial Cruise	Earth/Mars Transfer Mars Orbit	Sun Star	SGCMG Target Servo
Celestial Guided	Update Guidance Prep. correction	IMS Sun, Star	SGCMG ACS Secondary
Velocity Correction	Midcourse Maneuver	IMS	ACS Primary
Sun/Star Acquistion	Update Guidance	IMS Sun,Star	SGCMG
Aeromaneuver	Venus, Mars, Earth Encounters	IMS Limb, Sun	ACS Primary

Figure III.2.4-2: Waverider Guidance Modes

III.2.4.1 Star , Limb, and Sun Sensors

III.2.4.1.1 Sun Sensors

The sun sensor chosen for this mission is the 4 Pi Steradian Sun Sensor (4ΠSS), a static digital sun sensor which measures the 2-axis position of the sun in the body frame. Measuring 0.08 x 0.08 x 0.02 m per detector and 0.09 x 0.11x 0.03 m for electronics, it weighs 1.6 kg, has a resolution of 0.5°, and requires 0.75 Watts of power for operation. There will be three 4ΠSSs on the WOPM. Each will be a redundant system, and the system will be validated by periodic checks by the GC and the star tracker. These checks are performed by comparing the sun-sensor-measured sun vector with a value propagated via body rate estimates from the last valid sun sensor measurement. If the new value differs significantly from the propagated value, the backup sun-sensor is checked. If the backup measurement is close to the propagated value, it is chosen and the process repeats. If neither measurement is close to the propagated value, both sensors are ignored until the next reading is taken by the primary sensor, and the process continues (Cheng and Tracy, Reference 15).

In addition to the redundancy of the system itself, the sensors will be packaged as orbital replacement units (ORUs), which will allow the LLVM sensors to be removed and kept as spares for the WOPM return voyage.

The 4ΠSS was chosen over other models because it is the most advanced sun sensor currently being developed. It will be flown on the Mars Observer spacecraft in the early 1990's; therefore, it will have been flight tested before use on the M^3 mission.

III.2.4.1.2 Star Sensors

The star sensors chosen for this mission are the ASTROS II sensors. The ASTROS II is an upgrade of the ASTROS I tracker, which was flown on the STS in 1989. The ASTROS II will be flight proven on the Mariner Mark II (MMII) missions during the 1990's. The reasons for the choice of the system (Dennison) are as follows:

1. Capability to track several stars at once for attitude reference
2. Capability to follow rapidly moving, time varying, extended targets during a close flyby or rendezvous
3. Capability to determine the limb position and orientation of a nearby target
4. Capability to develop image data for ground-based target searches during target approach

There will be three star tracker systems on the WOPM. A summary of ASTROS II capabilities is presented in Figure III.5.1.1.

III.2.4.2 Inertial Measurement System

All three vehicles will utilize Inertial Measurement Systems to control fine attitude adjustments. The system for the WOPM will consist of six 64 PMRIGs (Permanent Magnet Rate Integrating Gyros). The 64 PMRIG is a spinning wheel set in a cylindrical case which floats in a viscous fluid in a hollow cylindrical case. An electro magnetic suspension system centers the float axially and radially. This gyro has a single degree of freedom and performs similarly to a conventional strapped-down gyro, which would have mutually orthogonal input, output, and spin axes. Measuring 6.35 cm in diameter x 12.14 cm in length, each 64 PMRIG weighs 4.412 kg, has a resolution of 0.00025 arcsec, a pointing accuracy of 0.007 arcsec, and a mission life of 15 years. It boasts both low noise and low drift in addition to extreme stability. These characteristics make the 64 PMRIG advantageous over ring laser gyros, which have high noise levels and large mass, and over spinning wheels, which have long warm-up times and limited range. Its reliability has been proven through use on the High Energy Astronomical Observatory (HEAO), Hubble Space Telescope (HST), and other classified programs (Lademann, Reference 40).

ASTROS II Capability

Parameter	Attitude Determination	Target Tracking
Target	Stars (5 / field)	Planet, Satellite
Angular size	Point source	Limb if > 100 mrad
Brightness	-3 to +5 mag	0.5-100 W/m^2
Output data	Star centroids/ brightness	Target centroid, size
Resolution	< 4 rad/bit	< 4 rad/bit
Accuracy	40 μrad	100 μ rad
	μ	μ

Physical Properties		
	Mass	11 kg
	Power	15 w - single channel
	Size	Electronics - 28 x 13 x 46 cm
		Sensor head - 18 cm diam x 20 cm long

Figure III.5.1.1: Star Tracker Capability

III.2.4.3 Guidance Computer

As shown in the diagram of Section III.2.4, the guidance computer (GC) is responsible for receiving input from the IMS, sensors, and crew, and relaying this data to the Payload Operations Control Center (POCC) or to the control system. The POCC also receives telemetry data from the IMS, and the sensors via the Deep Space Network (DSN), which it runs through a computer system on the ground and compares to the spacecraft data to be sure that everything is behaving as it should. The POCC can relay instructions to the GC in case of a problem or a change in plans.

The GC for M^3 must be man-rated, and the obvious choice for a proven, man-rated component is the STS Orbiter GC. An upgrade of the current Orbiter GC has been developed and will be flown in the near term. This upgrade, the AP 101S, has been chosen for the M^3 design. A comparison of the current and

upgrade units (McDonnell-Douglas) is shown in Figure III.5.3. The STS system uses five redundant GC units; the M^3 design includes three identical GCs in the WOPM and three in the LLVM. The reduction in number of units per module is possible because of the increase in mean time between failures (MTBF) from 1000 hours to 5000 hours for the new units and the ORU design, which allows changeout of units between the WOPM and the LLVM after the two modules join in LMO. This redundancy assures an accurate computer decision at all times. A computer which provides data which is not close to that of the other two will be disregarded. The crew will also have override capabilities in case of an emergency, as indicated in Figure III.5.3.

Guidance Computer (STS Orbiter)

	Current AP 101B	Upgrade AP 101S
Main Memory (32-Bit Words)	106,496 (128K)	262,144 (286K)
Performance (Instructions/Second)	420,000	1,270,000
Mass (Kg)	55	31
Size (cm)	2 Boxes 49.6 x 25.9 x 19.3	1 Box Same
Volume (m3)	0.049	0.025
Reliability (MTBF-Hr)	1000	5000 (Est.)
Electrical Power (Watts)	650	550
Number of GC units	4 Primary 1 Backup	4 Primary 1 Backup

Figure III.5.3: STS Guidance Computers

III.2.4.4 Attitude Control

The WOPM control modes are shown in Figure III.2.4. During coasting, both the WOPM and the LLVM will use Single-Gimbal Control Moment Gyros (SGCMGs) to make attitude adjustments. During powered flight, however, both vehicles will use chemical thruster systems.

Single-gimbal CMGs were chosen over double-gimbal CMGs or reaction wheels because they are a more effective momentum storage device where large vehicle torques are required. They have the capability of storing 2300 N-m-sec of angular momentum, as well as a peak output torque of ±4600 N-m-sec. DGCMGs are primarily used for moderate momentum exchange and moderate to low output torques, while reaction wheels are used for small amounts of momentum exchange. Both SGCMGs and DGCMGs have similar reliability, having both been flown on various spacecraft over the last 20 years. A trade study performed for the Space Station Freedom project showed that although the DGCMGs require less power than SGCMGs, SGCMGs have less weight and volume, and require less maintenance (Meffe). Therefore, the higher torques and other obvious advantages over DGCMGs prompted the choice of SGCMGs for WOPM and LLVM momentum storage during the M^3 mission.

The chemical thruster system chosen for M^3 is that of the current shuttle orbiter. As the orbiter is very close in weight to the WOPM, this system will provide sufficient thrust for maneuvering, as well as providing reliability due to its many flight hours on the orbiter missions. The thrusters will be located in clusters at the rear of the Waverider in order to provide maximum flexibility in maneuvering without degrading the performance of the working (bottom) surface of the Waverider.

The Orbiter reaction control system has one forward module, with 14 main thrusters, and two vernier thrusters, and two aft subsystems in pods, with 12 main thrusters and two vernier thrusters per pod. The main thrusters have a thrust level of 3870 N, I_{sp} of 289 seconds, and MIB of 88.96 N-sec. The vernier thrusters have a thrust level of 111.2 N, I_{sp} of 228 seconds, and MIB of 3.336 N-sec.

III.2.4.5 Software

As in the Space Shuttle guidance computer software, the M^3 software will be written in separate modules, one for each major phase of the mission. This will limit the amount of memory required to store and run the software.

Software will be independently validated and tested prior to launch. Capability for software to be modified by the crew will be provided.

III.2.5 Life Support
(Rosenberg)

One of the major problems that the astronauts on the Mars mission will have to overcome is the effect that a zero gravity environment will have on the

human body. The effects of prolonged weightlessness on the human body include: decalcification of bones, shrinkage of the heart, decrease in blood volume, and loss of muscle mass. These changes in the body begin to occur as soon as weightlessness is achieved. If the zero gravity environment is maintained with no adaptation measures provided for the body, then some of these problems may become irreversible. For example, after 4 months (approximately), bone decalcification becomes permanent if no means are used to counter the zero gravity environment. There are 3 principal methods for easing the changes occurring in the body: exercise programs, dietary supplements, and the provision of artificial gravity.

Exercise has long been the accepted method for combating the effects of weightlessness on the human body. In fact, exercise will be very effective in stopping three of the four major problems listed above: shrinkage of the heart, decrease in blood volume, and decrease in muscle mass. On Skylab the astronauts were scheduled for approximately 1.5 hours of strenuous exercise per day. This exercise usually came in the form of walking on a treadmill and in riding an exercycle. The exercise is necessary to the body because it replaces the stress placed on the muscles during the constant pull of gravity found on Earth.

One problem of an exercise program is that it is an interactive program. The astronaut has to decide if he is really going to do the exercise, or not. On the extended Russian missions of the 1970's, the Cosmonauts were scheduled to exercise for up to 2 hours per day. The problem is that the Cosmonauts tended not to do the exercise. Exercise is stressful, and basic human psychology shows that people tend to steer away from known stress situations. Another problem with an exercise program is that it does not deal with the complete problem. Over short term flights exercise can be used singly, but for long term flights such as the Mars mission, some provision must be made for the effects on the bones.

Dietary supplements can be used to minimize decalcification of bones. The basic principle is that by adding more calcium to the bones, the bones will absorb more calcium, and then the overall loss will be minimized. However it has been discovered that when calcium alone is added to the diet, the excess calcium is not absorbed, rather it is just flushed from the body as waste. This in turn, can lead to other problems such as kidney stones. There is one way to get the extra calcium absorbed - the use of anabolic steroids. In fact, the steroids will help maintain muscular mass at the proper level. However, it has been shown that large quantities of steroids can cause problems of their own. Heart, liver, and kidney problems have all been linked to steroid use. For this reason, steroids are not being considered for this trip, and therefore dietary supplements are not being considered as a main way to combat zero gravity's effects on the body.

The most complete solution to the problem of zero gravity is to simply eliminate it. By installing an artificial gravity system, the body will behave similarly to its normal patterns in the Earth's gravitational field. Most theorized artificial gravity systems involve the use of centripetal force produced by some form of spinning motion. Spin a cylinder around a fixed point, and an object on an inner surface of the cylinder will experience a gravity like force. Now the Waverider does not exactly lend itself to being spun around an axis. It would be difficult for the Waverider to initiate and maintain a controlled spin. Also, the angular momentum created by this spinning motion would make stability and control during maneuvers difficult to maintain. Finally, the power required to spin the Waverider would be tremendous. So we can see that we will not be able to effectively spin the Waverider; but the idea does not have to be completely abandoned.

As a solution to the problem of the zero gravity environment acting on the astronauts, it is hereby recommended that the crew make use of both an exercise program and an artificial gravity system. This combines an interactive program (exercise), with a passive system (artificial gravity). While the astronaut may chose not to exercise, he has no choice but to gain benefits from the artificial gravity system.

For the exercise program, each astronaut will be scheduled for up to 2 hours of strenuous exercise per day. The familiar treadmill and exercycle will appear on our ship, as well as fluid resistance workout machines. These machines use the viscosity of the fluid in a mass-damper system to provide the needed resistive force. Material stiffness workout devices were also considered, however these devices were discarded due to their tendency to snap back sharply. In the zero gravity environment of space, this snapping action tends to throw the astronaut in the opposite direction.

For the artificial gravity system, the Terrapin Technologies gravity bed system is being planned. This device is essentially a rotating disk to which the astronaut will be strapped while sleeping. An 8 hour sleep shift while strapped to the gravity bed will provide the needed stress on the bones. This stress will be an axial force acting primarily on the long, load bearing members (arm, leg bones & spine). In addition to the bones, the heart and other muscles will gain benefits from feeling the pull of gravity.

The primary design of the gravity bed calls for all parts to be made of aluminum (it is a lightweight, strong metal with properties easily referenced). See Figures III.2.5-1 and III.2.5-2 for the gravity bed dimensions and Figure III.2.5-3 for bed masses.

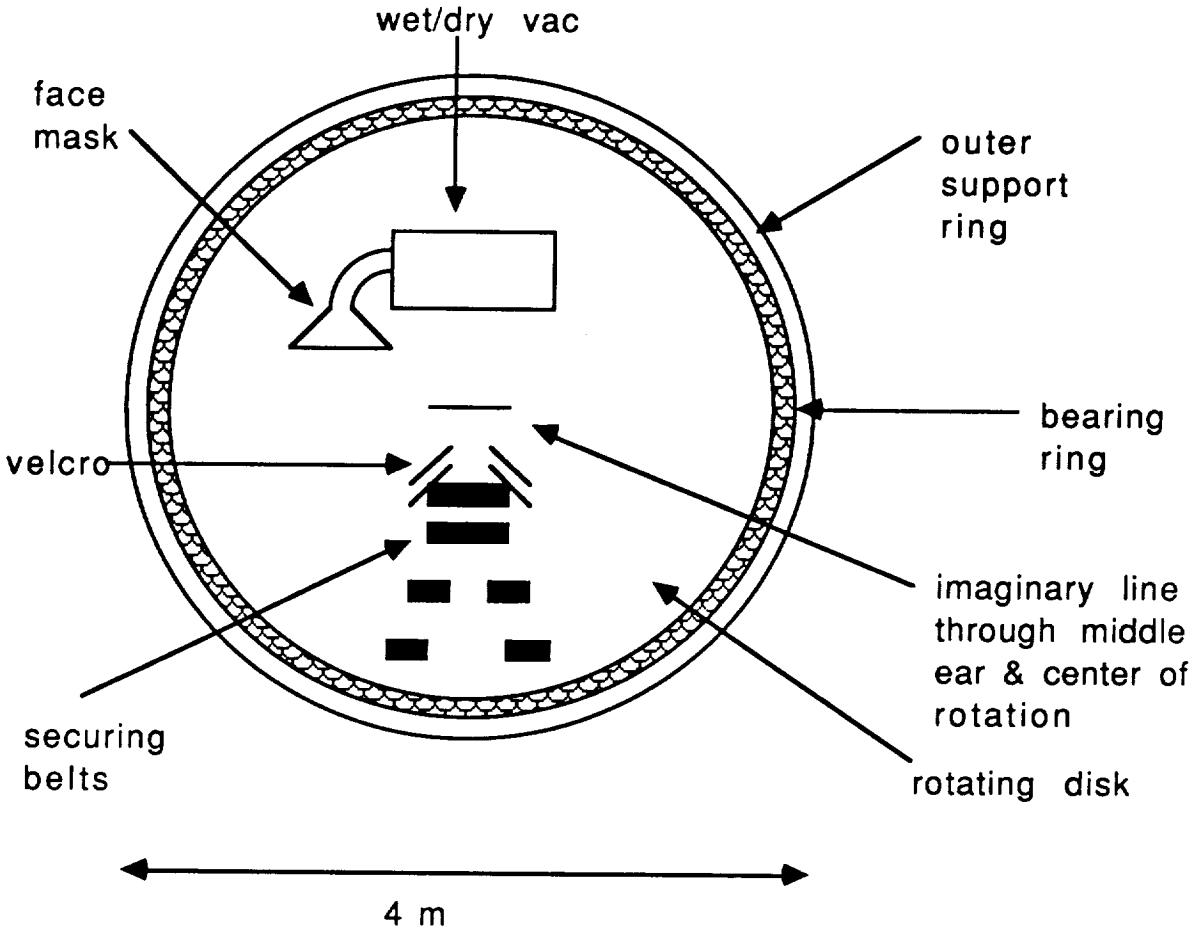

Figure III.2.5-1: Top View - Terrapin Technologies Gravity Bed

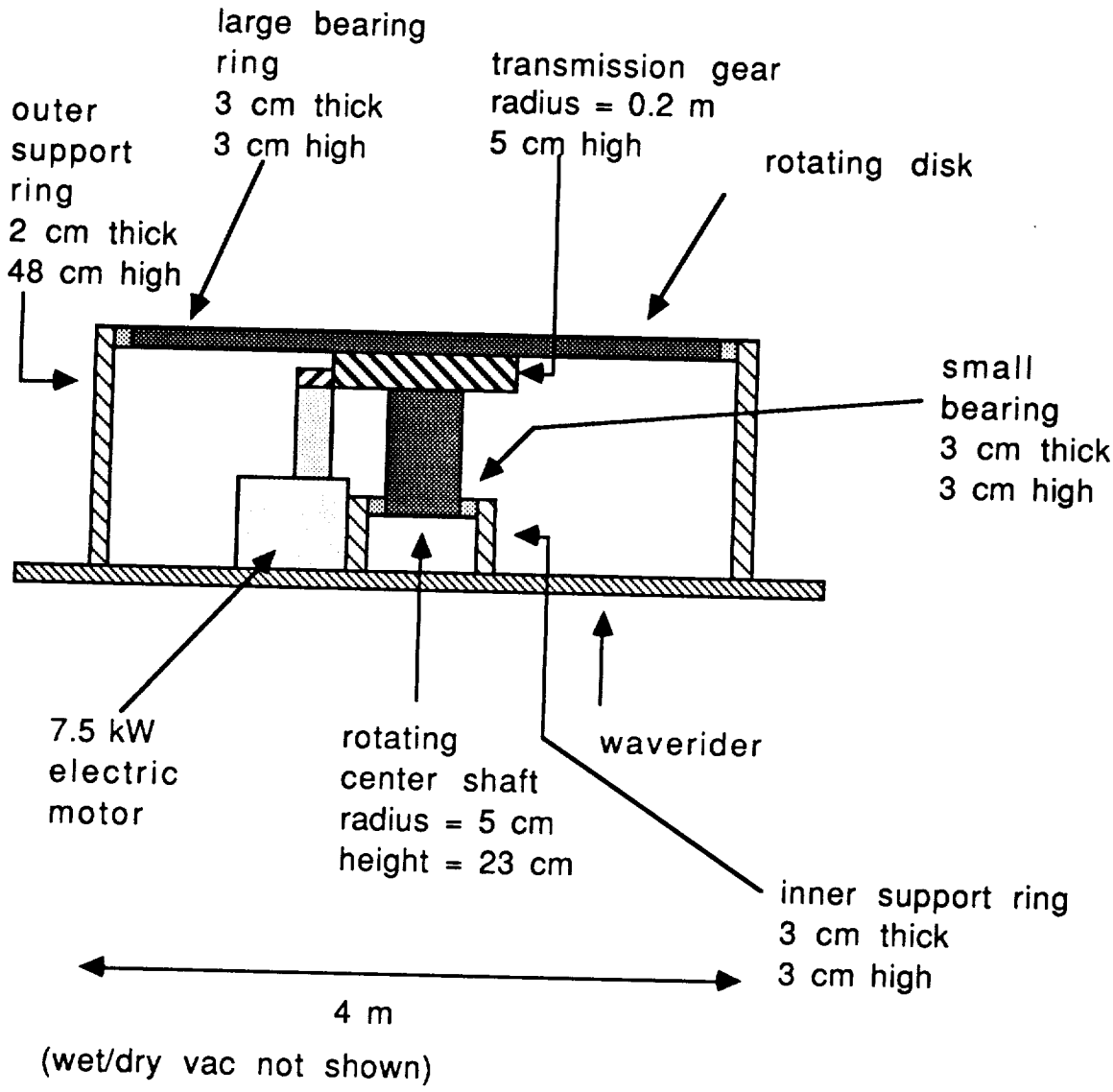

Figure III.2.5-2: Cutaway View

A few notes about the preliminary design of the gravity bed:

All parts made of Aluminum

mass of structure + rotating parts =	1373 kg
mass of padding, velcro, straps =	~ 5 kg
mass of wet/dry vac =	~15 kg
mass of motor =	~100 kg
total mass =	~1493 kg

For the average astronaut to feel an acceleration = 1g at the feet (rotation point at center of line connecting the inner ear)
rotation speed = ~23 rev/min

Figure III.2.5-3: Gravity Bed Design

The design of the gravity bed is such that nausea caused by the spinning motion is minimized. The line connecting the inner ears of the rider goes through the rotation point. This causes the disturbance of the fluid in the inner ear to be minimized. However some people may still become nauseous the first few times they use the bed. For these people, a small wet/dry vacuum has been placed above the bed. The astronaut will be wearing a special sleep suit with velcro on the arms. This velcro will serve to fasten the rider's arms to the bed, just as belts will keep the astronaut's torso and legs fastened. In case the rider feels the need to vomit, the arms can be removed from their fastened position (hence the need for something like velcro), the wet/dry vac can be turned on by removing the face mask from its holder, the face mask will be placed over the face, and the vomiting can now occur. Even though this system is being provided, we hope to be able to acclimate the rider with the rotation before the Waverider is launched. Acclimation to rotation, the low speed of the rotation (23 revs/min), and the positioning of the inner ears should take care of the nausea problem for the gravity beds.

Could the average person sleep on this bed? The only answer is that we hope so. The gravity bed has been slept on before (on Earth) (Diamandis), and hopefully, with acclimation to the system, the astronauts will have no trouble sleeping.

One final note: 4 gravity beds are being planned on the Waverider. This allows the use of 3 sleep shifts, each 8 hours long (The astronauts' day will consist of 8 hours of pure sleep, 8 hours of pure work, and 8 hours of relaxation time). Two of the beds will be rotating opposite to the other two.

This, and the fact that the beds are close together, allows us to effectively assume that the angular momentum caused by the rotation is canceled out (over all the gravity beds). This will be important in the stability and control of the Waverider.

III.2.5.1 Crew Safety
(Rosenberg)

Another of the major problems we will have to deal with is the exposure of the astronauts to radiation. This radiation will come from a few different sources: radiation from the nuclear engines on the ship, radiation due to primary cosmic rays, and radiation due to solar flares. This radiation could be of 4 main types: energetic protons, fast neutrons, x rays, and gamma rays.

The type of shielding needed, as well as the amounts of shielding needed, varies among the 4 types of radiation. The hardest form of radiation to shield against is the energetic protons. There is, however, one method that shields against energetic protons very well - a charged particle field. By placing the charged particles around the spaceship, the incoming protons will either be repulsed or attracted and absorbed by the particle field. But there are several disadvantages to this form of shielding. One prime disadvantage is that the charged particles do not affect the other 3 forms of radiation we will experience. Another disadvantage is that the power required to generate the particle field is huge. Other disadvantages are that the particles can interfere with the ship's computers, and that communication is not possible through the particle field. These disadvantages show that the particle field theory is not the system to use on the Mars mission.

Another form of shielding is the shield-by-blockage method. The most common form of radiation shielding used today, this method relies on placing a high density material in front of the incoming radiation. For x and gamma radiation, the ray's energy is absorbed by the shield material if the shield is thick enough (and the shield heats up). Also, the larger protons and neutrons tend to collide with the nuclei of the atoms in the shield, thus forming smaller particles reflected away from the shield, and energy emitted as x and gamma radiation. The only shield materials for which tables of properties are readily available are air, lead, and water. Air and water shields are generally lighter in weight when compared to a corresponding lead shield; however, there is a large volume penalty paid for the use of a water or air shield instead of a lead shield. The penalty comes in the form of added thickness of the shield, and this penalty is on the order of the water shield being 20 times as thick as the lead shield. To shield against energetic protons we look at lead shields approximately 10-20 m thick (energetic protons require the most shielding, shield against them and x rays, gamma rays, fast neutrons are already shielded). Shield thicknesses of approximately 200-400

m of water are just too large for (present) space applications; therefore, from this point on, lead radiation shielding will be assumed.

For the radiation due to the nuclear engines on the ship, the propulsion group has decided to design the engines so that the shadow shield method may be used. What this means in terms of life support is that the problem of shielding against fast neutrons has already been solved. However, if we were in need of extra shielding, fast neutrons can be shielded by approximately 10 cm of lead (Ohanian). This shielding would essentially need to be a plate covering the back surface of the Waverider.

Cosmic Rays are comprised mostly of energetic protons, along with some background x and gamma radiation. For this problem there are 2 models available.

The first radiation model was created by NASA in the late 1960's (NASA-SP-3006). From their tables, if a 1.5 year space mission is planned, the astronauts will be exposed to a maximum radiation dose of 2415 rads. So for the worst case, according to this model, the astronauts would be absorbing 1610 rads per year. Note that the U. S. government has set the permissible dose for persons occupationally exposed to radiation at 5 rems per year (for energetic protons 5 rems=0.5 rads). According to this model there would have to be shielding on the Waverider, if not on both the Waverider and the lander.

The second radiation model is as recent as 1988 (Fascione). It says that although background cosmic radiation is very penetrating (as far as shielding goes), the flux of the energetic protons is too low to provide a serious health threat. Note that this model is for background cosmic rays and does not include the effects of solar flares (whose effects will be discussed later).

Of the 2 models, we have chosen to accept the latter model. The first model is very old, and does not present a clear picture of the problem. This model gives large expected maximum absorbed doses of radiation (much more than needed to kill), and also very low expected minimum absorbed doses of radiation. The actual absorbed dose of radiation should lie somewhere between the two numbers - a very large range. So the older model is inconclusive.

By choosing the second model, we can save huge amounts of mass from the Waverider. By the second model, no additional shielding is required for the Waverider. This mass can be saved with no compromise to astronaut safety.

The problem of solar flares is slightly more complicated to deal with. Solar flares are essentially a blast of x, gamma, and proton radiation from the sun. As already discussed, if we protect from the energetic protons, we also protect from the gamma and x rays. Basically the only way to protect against this

blast of protons is to put up lots of shield material between the sun and the astronauts. But before we add shielding randomly, notice that we already have a nuclear reactor on board (with its own shielding). If we could orient the Waverider so that the reactor is between the sun and the astronauts, then the total amount of lead shielding needed (between the astronauts and the reactor) would be reduced by a large amount. The basic idea is to create a protective room (or even just one wall) that the astronauts can hide in (behind), during a solar flare.

When energetic protons hit a dense object, the protons go through if their energy is high enough, otherwise the protons will interact with the nuclei of the atoms of the dense material. When this occurs, neutrons and other particles are ejected. But "while each proton produces a variety of particles as it undergoes collisions in the shield, only the neutrons are of biological significance" (Wallace). So we are using the reactor and all of its shielding as our dense object. This will eliminate some of the proton wave, but a large number of neutrons will be produced. By placing another dense object behind the reactor, we can combine the proton shield with the neutron shield needed for the neutrons produced by the reactor. Since medium energy neutrons require 10 cm of lead for shielding (Ohanian), placing a 20 cm thick layer of lead will allow shielding from very energetic neutrons, and also from more of the proton wave. By placing a 10 cm thick plate of lead behind this, we can shield against the neutrons formed from the 20 cm thick plate. This plate should also be all that is required to block the few remaining low energy protons. High energy protons will still make it through the shields, but high energy protons are less biologically damaging than the low energy ones (REA). Placing a second 10 cm thick lead plate behind the first should virtually eliminate neutron radiation reaching the astronauts. Notice in the figure, that there is a 1 cm space between each layer. This is to increase radiation heat transfer from the shield material, and does not effectively change the volume of the radiation shield.

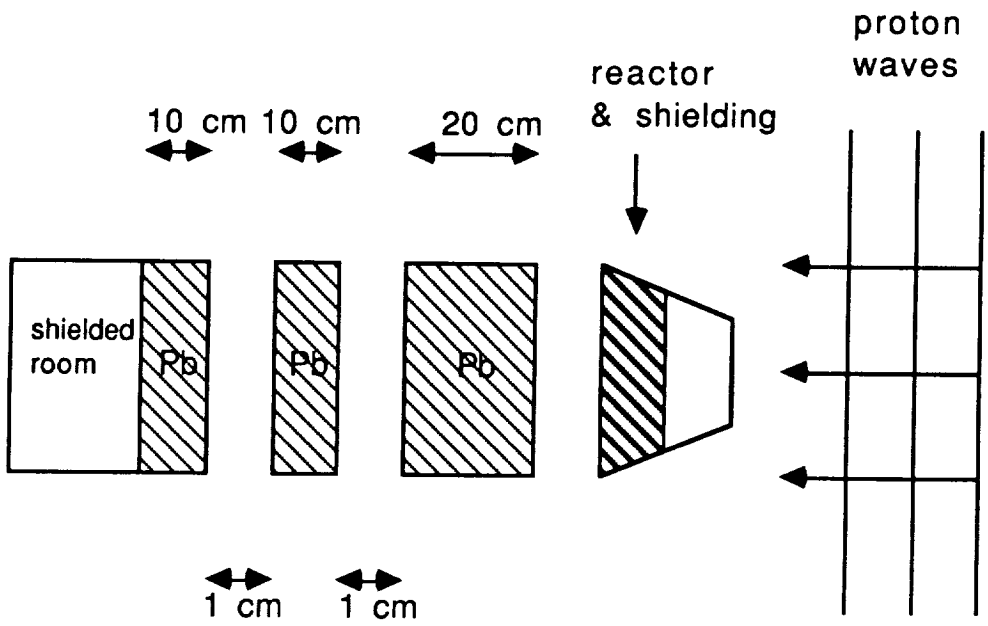

Note:

the shielded room has one 5 m by 3 m wall shielded

so total volume of this shield = (0.4 m)(5 m)(3 m)
+ (2)(.01 m)(5 m)(3 m)
= 6.3 m^3

(volume between shielded room and reactor)

mass of lead = (density of Pb)(vol. of Pb)
= (11340 kg/m^3)(6 m^3)
= 68040 kg

Figure III.2.5.1-1: Waverider Shielding Configuration

III.2.5.2 Air System
(Kamosa)

The Waverider environmental crew life support system (ECLSS) will be comprised of an Air Revitalization System (ARS). This system will be able to generate oxygen, reduce the carbon dioxide in the crew's environment, and maintain the proper mix of oxygen and nitrogen for earth-like conditions. This system will utilize a Sabitier process for CO_2 breakdown, electrolysis process for oxygen generation, and a scrubber system for the concentration of the atmospheric mixes in the Waverider. This system will be of two similar

units capable of handling a maximum of 12 crew members. This over-design is to allow for cabin leakage and minor maintenance during the mission. The ARS will weigh 175 kg each and comprise a total volume of 1.5m3. The ARS will consume about 3.5-4 KW of power during its operation. An advantage of using this type of closed-loop system is the reduction of weight and volume eliminated from the storage of vast amounts of oxygen and nitrogen. ECLSS designs loads are that each astronaut needs .83kg of O_2 and 3.3 Kg of N per day, plus a 2.27 kg per day loss associated with cabin leakage. Therefore each day 8.3kg of O_2 is needed and 30.3 Kg of N is consumed. The ARS system can reclaim up to 95% of this daily expenditure. Over the duration of the mission, a regenerative type system is the best and only choice. Although more research and development must be made in this area in order for manned missions to exist in the future, this current system is being considered for use on the Space Station Freedom. It's operation will no doubt verify a future use on this mission and future similar missions.

III.2.5.3 Habitat design
(Rosenberg)

Just a bit of explanation is needed for the interior plan of the Waverider. First of all, the Waverider will have at least 1 window. Probably the best place to put a window is on the back surface of the Waverider. The logical place for a window is in the rec room; therefore the rec room is located along the back surface of the Waverider. Next, notice that there are 2 entrances along the back surface. One is the docking port at the center of the back surface where the Waverider will dock with the supply ship. This will initially be covered up by the booster attachment as we leave Earth, so a full airlock (with the ability to depressurize - the docking port does not have this capability) has been provided near the edge of the Waverider's back surface. Third, a large amount of space has been designated for experiments and workstations. We do not know what types of scientific data the astronauts will try to obtain while on the Waverider, the idea was merely to provide space for the needed equipment. Last, notice that on the upper deck there is a space reserved for the control center. This area is intended to be the nerve center of the ship. The guidance & control computers and the communications center will be located here. The layout of the Waverider is diagrammed in Figures II.5.3-1 and II.5.3-2.

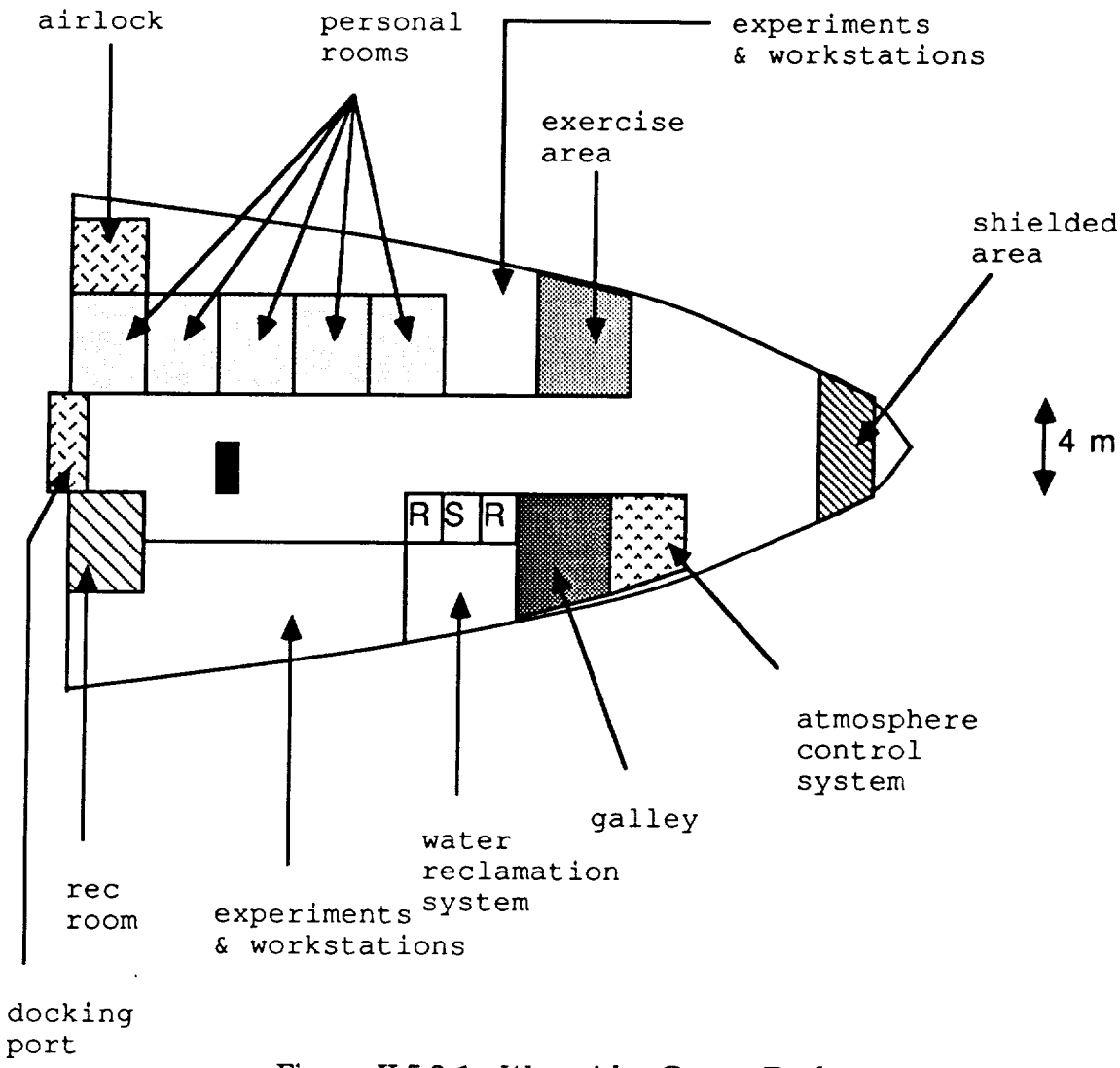

Figure II.5.3-1: Waverider Center Deck

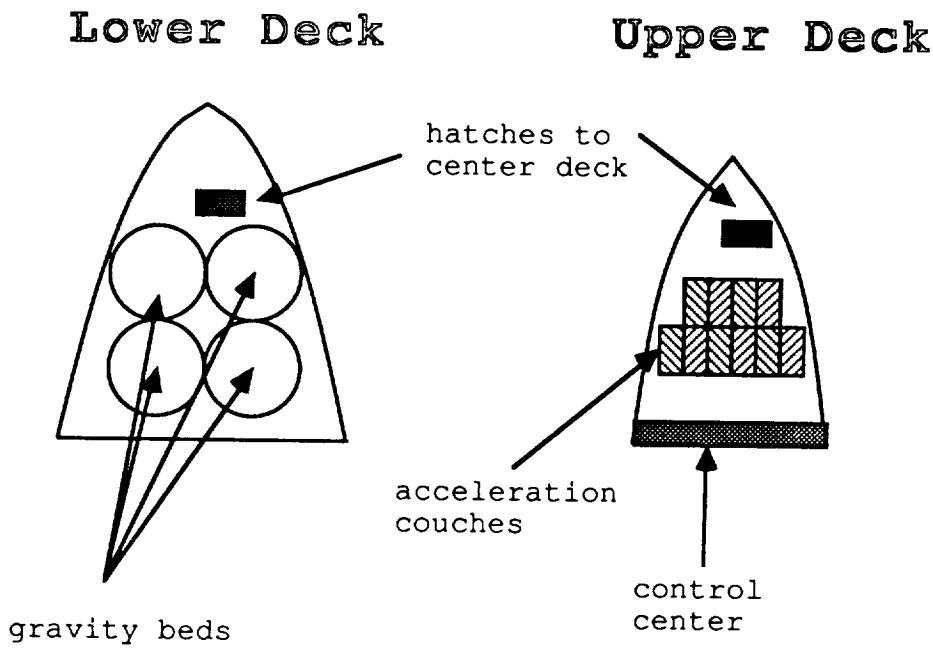

Figure II.5.3-2: Waverider Upper and Lower Decks

III.2.5.3.1 Living Spaces
(Coleman)

The hypersonic Waverider will be divided unto three areas: productive, nonproductive, and support. Nonproductive areas are defined as places where no scientific or technical work is done. This discussion will be mostly limited to the non-productive areas of the spacecraft. The productive areas will encompass laboratories, workstations, and control areas. There are several considerations that should be taken into account as overall design criteria. For example, air vents will tend to collect loose articles and debris (Butler, T. L.). Work stations should not be placed in frequently traveled paths. The nonproductive areas of the spacecraft are of major importance to a mission of this duration, 362 days on the Waverider. For this mission, there will be four classes of nonproductive areas: sleeping, recreation, galley, and private rooms.

The sleeping areas will be provided with gravity beds to stress the skeletal systems for a minimum of eight hours a day. It is of major importance that the equipment used for the gravity beds, and the equipment in the surrounding rooms, generate as little noise as possible. In a space environment, small amounts of noise tend to disturb astronauts when they are attempting to sleep.

The exercise room is one of the most important nonproductive areas of the Waverider because it is the place where the astronauts will physically work

out to overcome the problems associated with weightlessness. Each crew member will be using this area approximately two hours per day. The floor plan of the exercise room should be done in such a way that there is little or no crowding during peak usage periods.

III.2.5.4 Hygiene
(Coleman)

III.2.5.4.1 Space Shower

A special space shower has been designed specifically for use in this mission. The aforementioned shower (Figure III.2.5.4.1-1,-2) contains multiple shower heads that will scatter water mixed with liquid soap on the user. It contains a flow meter/timer unit that will automatically dispense the soap water mixture and plain water for rinsing. The shower will also utilize a series of fans that will blow heated air from top to bottom in order direct the water into a drain equipped with a wet/dry vacuum system. For the most part, the user will be required to stand and use a wash cloth in order to obtain the same level of cleanliness associated with an earth bound shower. After the rinse cycle, the user will then be dried using heated air flowing from top to bottom in the shower and by using a wet/dry vacuum to remove excess water on the skin. Also a hand washing unit will be provided for general hand washing. It will use a design similar to that of the space shower.

III.2.5.4.2 General

General hygiene kits should be issued to each crew member. Obviously there will be marked differences between the kits issued to males and females. The kits should include: safety razors, shaving cream, hand cream, lotion, toothpaste, tooth brushes, combs, brushes, nail clippers, and deodorant (NASA SP-400). The female kits should also contain the necessary feminine hygiene articles.

For general housekeeping, portable vacuum cleaners will be stationed throughout the Waverider to clean up dust and spills. Dry towelettes will be stowed on board for dusting and general cleaning. Wet germicidal towelettes will also be provided for cleaning areas that may contain germs. For example the germicidal towelettes could be used for cleaning in the galley, and for cleaning the space toilet.

Zero Gravity Shower

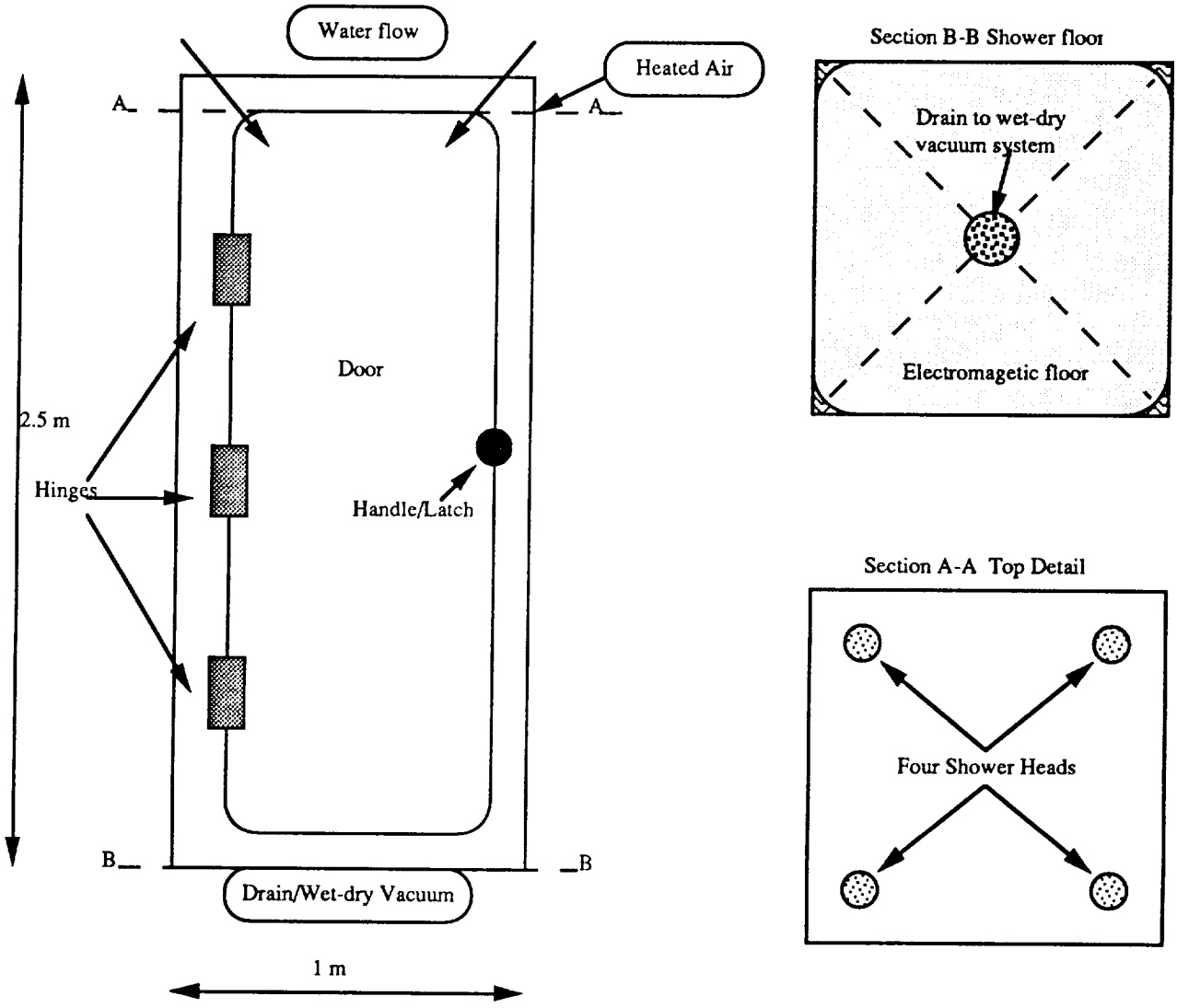

Figure III.2.5.4.1-1 - Space Shower

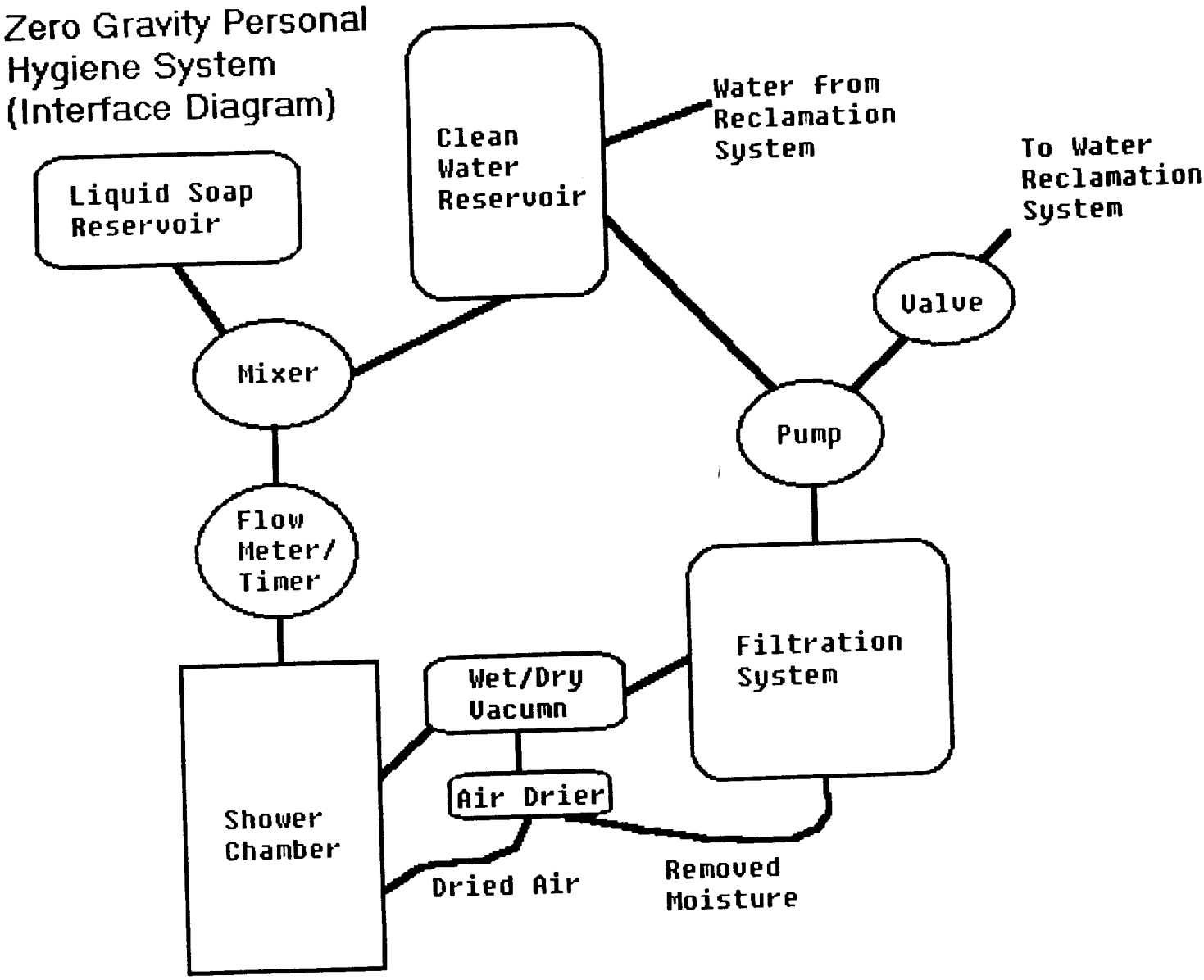

Figure III.2.5.4.1-2 - Space Shower Schematic

C-2

III.2.5.4.3 Waste Elimination

The elimination of waste has been broken into two areas: human waste, and refuse. The elimination of human waste poses more complexity than the elimination of general refuse.

Because the voyage to and from Mars might take slightly longer than a year (worst case scenario given by the trajectory group), a regenerative life support system has been chosen. The major advantage of a regenerative life support system is that the vast majority of body wastes are recovered for later reuse.

A specially designed space toilet will be utilized (Alburn University, June 1989). The toilet will consist of two modules, one for defecation and the other for urination. The toilet will use airflow and water flow to take the place of gravity in space. A provision shall be made for the periodic sampling of human waste material for later laboratory examination (Figure III.2.5.4.3).

On average, a human will expel 1400 grams of urine and 100 grams of feces per day. Of the 1400 grams of urine excreted, only 1200 grams is water; the rest consists primarily of solids, urea, and salts. After the 1200 grams of water is removed from the urine, the remaining solids will be packaged in sealable, removable containers attached to the water reclamation system. When a container is filled to capacity, it will be removed from the system and sealed. It will then be handled in the same fashion as the other waste. The waste obtained from defecation will be packed into diaphragms inside a tube assembly. When the assembly is full, the tube will be emptied, and handled in the same fashion as the solids recovered from urine.

General refuse will be placed into a vacuum chamber that contains a special space garbage bag. First, all air and moisture will be evacuated from the bag and its contents. Then the bag will be sealed. These sealed bags will then be placed into the waste airlock. The static pressure inside the airlock will be lowered to effect a minimal loss of the cabin's atmosphere. Then the other side of the airlock will be opened. The remaining pressure will force the garbage bags out of the airlock, into space.

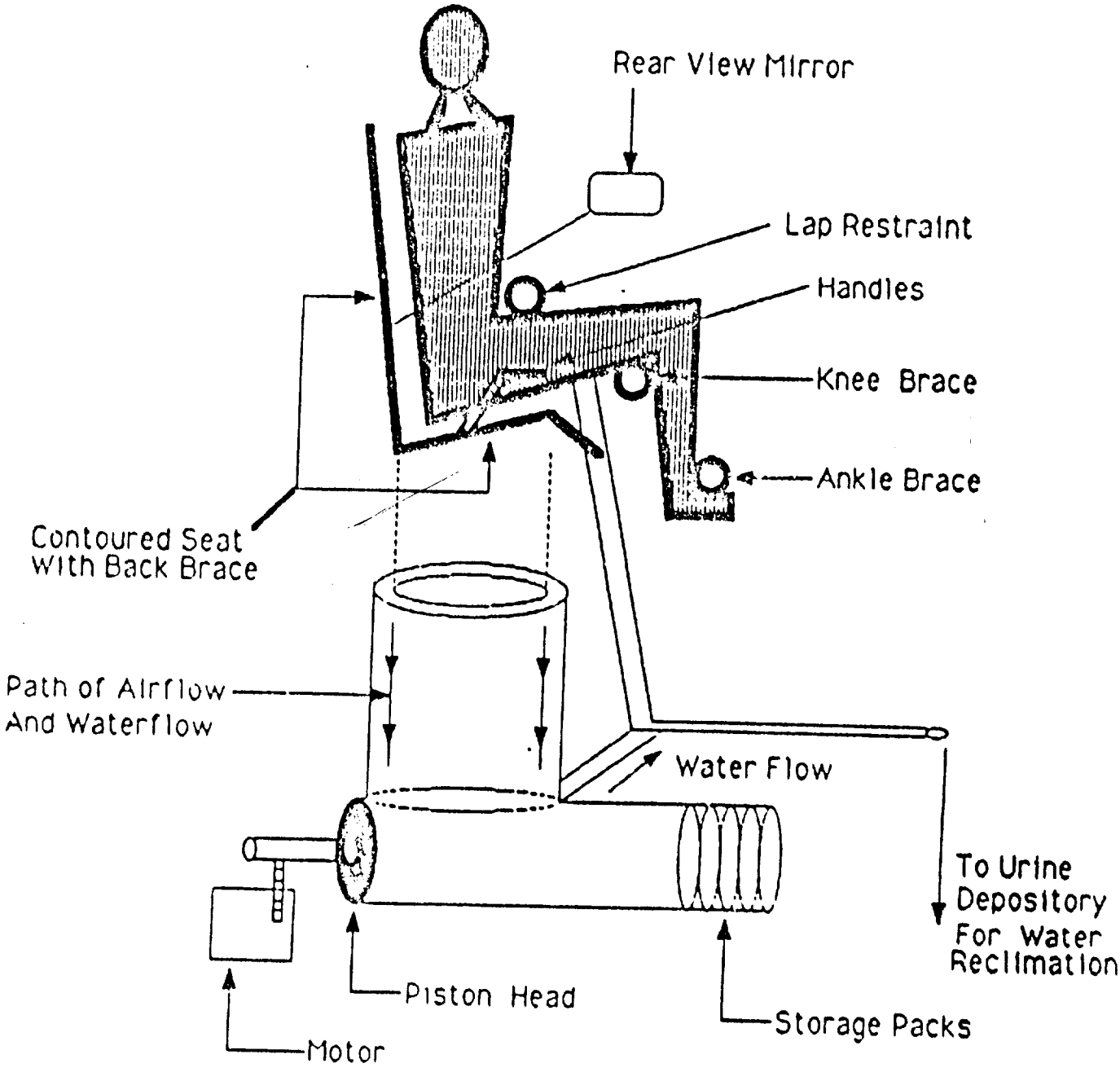

Figure III.2.5.4.3- Space Toilet

III.2.5.5 Crew Logistics
(Coleman)

III.2.5.5.1 Food

The discussion of food will be canvassed by two sections - diet and facilities. There are three forms of food that astronauts can eat while they are traveling through space. Each type offers its advantages and disadvantages. Liquids serve their intended purpose of providing needed water for the body's metabolic functions. For example, they are often needed while the body is experiencing a stressful state like strenuous exercise. This is not shocking because the body is composed primarily of water. Drinking water, beverages, fruit juices, coffee, and tea should be made readily available to the crew. Containers must be specially designed for the storage and consumption of liquids in a microgravity environment. Several types of conventional storage containers used on earth are suitable for use in space. These would include containers that are easy to handle and have spouts that eliminate the possibility of accidental spillage. Containers intended for consumption of liquids should be squeezable. The most important factor to consider is that it is highly undesirable to have globules of liquid floating around in the cabin of the spacecraft. However, when ingested in a microgravity environment, liquids can cause undesirable effects in astronauts. In some reported cases vomiting and nausea have occurred after ingestion. This discomfort was attributed to the usage of seat belts or the external application of abdominal pressure. Because of the possibility of discomfort, the following recommendation is made: only small amounts of liquids should be ingested by the crew at a time (Koelle).

Pastes were successfully used in the Apollo program. An astronaut's meal consisted of foodstuffs rendered into a paste that was packaged into a tube similar to toothpaste. These pastes were utilized for voyages that were of short duration relative to that of a Mars mission. A redeeming quality of paste diets is that they can be lightweight while providing vital nutrients necessary for the continuation of human life. One disadvantage of pastes is that they tend to be bland and unappetizing. It is believed that a diet consisting primarily of pastes would be undesirable. This could lead to at least two problems: low crew morale and undesirable abnormal eating habits. Another disadvantage is that they are prone to thermal problems. For example, storage tubes have ruptured after being stored in an overheated place.

There are several types of solid foods suitable for use in space. The three main types are dehydrated, irradiated, and freeze-dried. Ample technology exists for the preparation and utilization of dehydrated and freeze-dried foods. Irradiated foods are relatively new. For the most part, meats are radiated with electromagnetic radiation that kills off any undesirable organisms present.

The meat is then packaged and stowed in a container using fewer restrictive parameters than those that are required for regular meat purchased in a store.

Because of the aforementioned factors, the diet chosen for the Mars mission will be Space Shuttle foods which are of a dehydrated/freeze-dried type. The following considerations should be taken into account when the menus are selected: high salt and fluid content (Oberg) and plentiful supply of calcium rich foods (Butler). The high salt and fluid content is warranted to boost blood volume which is depleted by the body as a reaction to microgravity. It is hoped that calcium rich foods will help the body retard the loss of bone mass while exposed to microgravity.
For reasons of variety, there should be at least 72 entrees available to the astronauts based on Skylab experience. A sample day's menus should contain the following:

Four vegetable/fruit servings

Two meat/poultry/fish or vegetable protein equivalent servings
Four grain based (cereal), whole grains servings
Two milk or equivalent calcium rich servings

(NASA N88-14856)

Total daily caloric intake should be approximately 3,000 Kcal per day, composed of:

1,600-2,000 Kcal of carbohydrates
630-1,000 Kcal of fat
400-600 Kcal of protein
(Koelle)

The United States Navy serves exotic foods to its sailors stationed on nuclear submarines that are often cut off from contact with civilization for months at a time. Therefore, several of the menu selections should contain exotic dishes. The crew can, at its own discretion, decide to consume the same menu as a group, or it may elect to allow individualism.

A one month supply of military meals-ready-to-eat (MRE's) will be stowed on both the Waverider and the supply ship. In the event of an emergency, the MRE's can be eaten to provide the necessary nutrition until the spacecraft reaches its destination - Earth or Mars.

Much was learned from the experiences of the three Skylab crews about food preparation and dining facilities. For the purpose of a Mars mission, the following has been determined. The effects of microgravity tend to reduce the sensitivity of the taste buds. Because of this, astronauts will use a large

amount of condiments while consuming food. Salt dissolved in water, pepper extract dissolved in vegetable oil, and packets of other condiments will be provided to enhance the food's flavor. The dining table should have several hot/cold water sources for the preparation and rehydration of food. These sources should be easily accessible. Magnetized utensils will be employed. The table should have surfaces that will attract magnetized eating utensils. Also, there should exist a system to retain diners at the table. We have chosen foot holds in which diners can slip their shoes into to stay in one place while eating.

Volume and Mass Estimates (for a ten person crew)
Waverider Outbound Voyage (150 days)

	Volume	Mass
Standard Shuttle Foods	15 m3	2379 Kg
MRE's (30 day supply)	1.19 m3	283 Kg

Supply Ship (260 days)

Standard Shuttle Foods	26.0 m3	4124 Kg
MRE's (30 day supply)	1.19 m3	283 Kg

Note: Although the Waverider will initially carry a smaller amount of supplies to Mars, the capacity to carry the supplies stowed on the supply ship should be the primary design criteria.

III.2.5.5.2 Water Resources

For space travel, there are two strategies for providing water resources to the crew and cabin atmosphere. One is to carry all needed water supplies into space, while not attempting to recycle the expended water. Another approach is to use a regenerative system that reclaims the water expelled from the body.

Nonregenerative water systems have their advantages. Primarily, a nonregenerative water system is ideal for use in a short duration excursion into space. There is no launch weight penalty for this type of system. The United States Space Shuttle program uses this type of system. All required water supplies are stowed on board of the orbiter prior to launch. The crew's voyage is limited to the amount of water stowed on board.

For a voyage to Mars, the amount of water required for one human would be approximately:

Food preparation	.72 Kg/day
Drinking	1.86 Kg/day
Hand washing	1.81 Kg/day
Shower	3.63 Kg/day
Urinal flush	.49 Kg/day
Total	8.51 Kg/day

For ten astronauts on a 362 day mission aboard the Waverider approximately 35,000 Kg of water would be needed. This would increase the payload requirements of the Waverider and its associated propulsion and structural systems by a great deal compared with using a water reclamation system. The calculations below illustrate the weight savings obtainable by using a water reclamation system.

Since the total weight launch penalty for a crew of ten using the above water reclamation system would be approximately 2350 Kg, thus reducing the water supply system by a factor of almost thirteen!

A vacuum distillation system has been selected to perform the task of both urine water and bath water reclamation. The water reclamation system must completely sterilize the water that passes through it (Langton). Also the water reclamation system should produce water that is clear and odorless. Figure III.2.5.5.2 shows the water reclamation system.

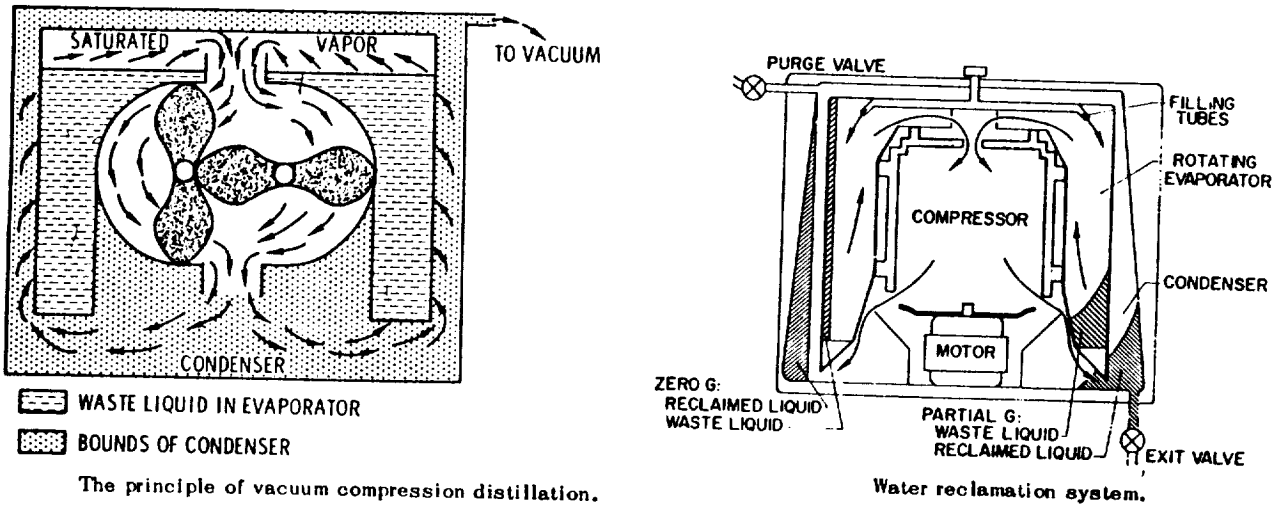

Figure III.2.5.5.2: Water Reclamation System

Launch Weight Penalties (370 day voyage)

Water lost in feces and by the body's metabolism	.113 Kg/person*day
	x 370 days
	x 10 people
	418.1 Kg Lost in feces

1 day reserve H_2O tank includes water for the following:

Food rehydration	25.0 Kg/day
Hand washing	18.1 Kg/day
Shower	36.3 Kg/day
Toilet flush	5.0 Kg/day
Approximate Total	85.0 Kg/day Reserve Tank

Reclamation Loss	2.55 Kg/day (97% system efficiency)
	x 370 days
Total Reclamation Loss	943.5 Kg
Cabin Leakage	2.0 Kg/day (rough estimate)
	x 370 days
Total Cabin Leakage	740.0 Kg
Urine Water Vacuum Compression Distillation system	20.41 Kg/person
Wash water Vacuum Compression Distillation system	3.86 Kg/person
Totals	24.09 Kg/person
	x10 people
	240.9 Kg

Grand total for the regenerative system = 2350 Kg

III.2.5.6 Crew Selection
(Coleman)

There are several factors that can be used to select crew members for this mission. The most important factor for determining the ideal crew for this case is the mission duration. After much thought and careful research, the ideal crew will be composed of five married couples. Each member should hold advanced degrees in areas that would be a direct contribution to the mission. These couples will be enlisted into a rigorous training program in order to ensure their suitability. At least one medical doctor and two other astronauts with extensive emergency medical training should be part of the crew (Oberg). In addition, there should be a pilot/mission commander, a co-pilot, two mission specialists/technicians, and three scientists. Each crew member will be cross-trained. The reasoning for this action is to provide backup crew members if one of the crew members becomes unable to perform his/her function during the mission

To prevent the possibility of a dangerous pregnancy in space, the male astronauts will be required to have a reversible vasectomy. After returning from Mars, the males may have their vasectomy's reversed if they so desire.

The ideal crewmember age has been chosen to be between 45 and 55 (Oberg). This age group was selected because of its mental maturity, stability, and its low susceptibility to motion sickness. However, there is one drawback to using this age group. As humans age, the body's ability to replace bone mass is decreased. It is believed that the proper utilization of a rigorous exercise program in addition to gravity bed usages can overcome this disadvantage.

III.2.5.7 Crew Psychology
(Coleman)

Crew psychology is a soft science compared with the other aspects of this mission. For example, knowing the mass and other parameters of the hypersonic Waverider, one can easily compute the amount of thrust and duration required to achieve desired changes in vehicle trajectory. However, this is the first time in which humans will be placed inside a craft for an extended period of time and expected to cope with daily problems, concerns, and most of all concentrate on their main concern, this mission. Therefore, much thought has been given to considering the psychological effects of a space voyage of this magnitude.

Most importantly, considerations must be made to reduce the crew's stress levels to an absolute minimum. The following recommendations are made. There should be a one hour sleep preconditioning period to allow the astronauts to wind down (Butler). The nonproductive areas of the

Waverider, where the crew is expected to spend most of its free time, should be equipped with a central high-fidelity stereo system.

Each room will contain outlets for portable speakers and jacks for headphones. The portable speakers will be used for group listening. For private listening, each member will have a pair of light-weight, high-quality headphones. The crew members will be allowed to bring with them one dozen compact digital discs that contain their favorite music.

The Waverider's computer system should be equipped with a CD-ROM disk drive. Each private room will be equipped with computer workstations that are networked with the central computer system. This allows the crew access to a plethora of written works that will be available on CD-ROM.

It is recommended that the voice communications system, used to communicate with mission control, have a voice stress detection device attached (Oberg). This device is justified because during past extended spaceflights involving both American and Soviet astronauts/cosmonauts, the crew became hostile towards their respective mission control personnel and acted defiantly. If the mission control personnel possesses a means of detecting stress in the crew, it can adjust its orders in a fashion to lower the crew's work load and other responsibilities. This will bring about a reduction in the crew's stress levels and make them more productive.

While the crew is being trained, the idea that it is a team and not a group of individuals should be continuously stressed. The mission commander should be viewed by his crew not as a superior, but as a colleague. This should eliminate the resentment that can precipitate from a militaristic type of command hierarchy. There should also exist a grievance settling system. This system would allow the crew to settle its own problems in a democratic way. It must be remembered, however, that the mission commander has final say in decisions, because he or she is the one who is most responsible for the mission's success.

III.3 LLVM Systems

III.3.1 Supply Stage/Departure Stage Systems

III.3.1.1 Propulsion

III.3.1.1.1 Primary Propulsion System Design
(Compy)

The booster system for the LLVM will be identical to that of the WOPM except that the LLVM will carry four more tanks than the Waverider booster. These tanks will be fully fueled, which almost doubles the

weight of the booster at launch. The specifications of the supply ship boosters are in the table below. The actual configuration will look like Figure III.2.1-3.

Supply Ship Booster Specifications

Booster Length:	40 m	Tank Length:	30 m
Booster Width:	35 m	Truss Length:	35 m
Booster Mass (fueled):	1,032,880 kg	Miscellaneous Mass:	15,000 kg
Fuel Mass (maximum):	852,880 kg	Reactor Mass:	15,000 kg
Thrust:	2,352,000 N	Tank Mass:	20,000 kg
Specific Impulse:	1,200 sec	Tank Diameter:	8.7 m
Delta V (with SS):	5,621 m/s	Truss Diameter:	4 m
Total Mass (NEBIT + SS):	1,332,880 kg		

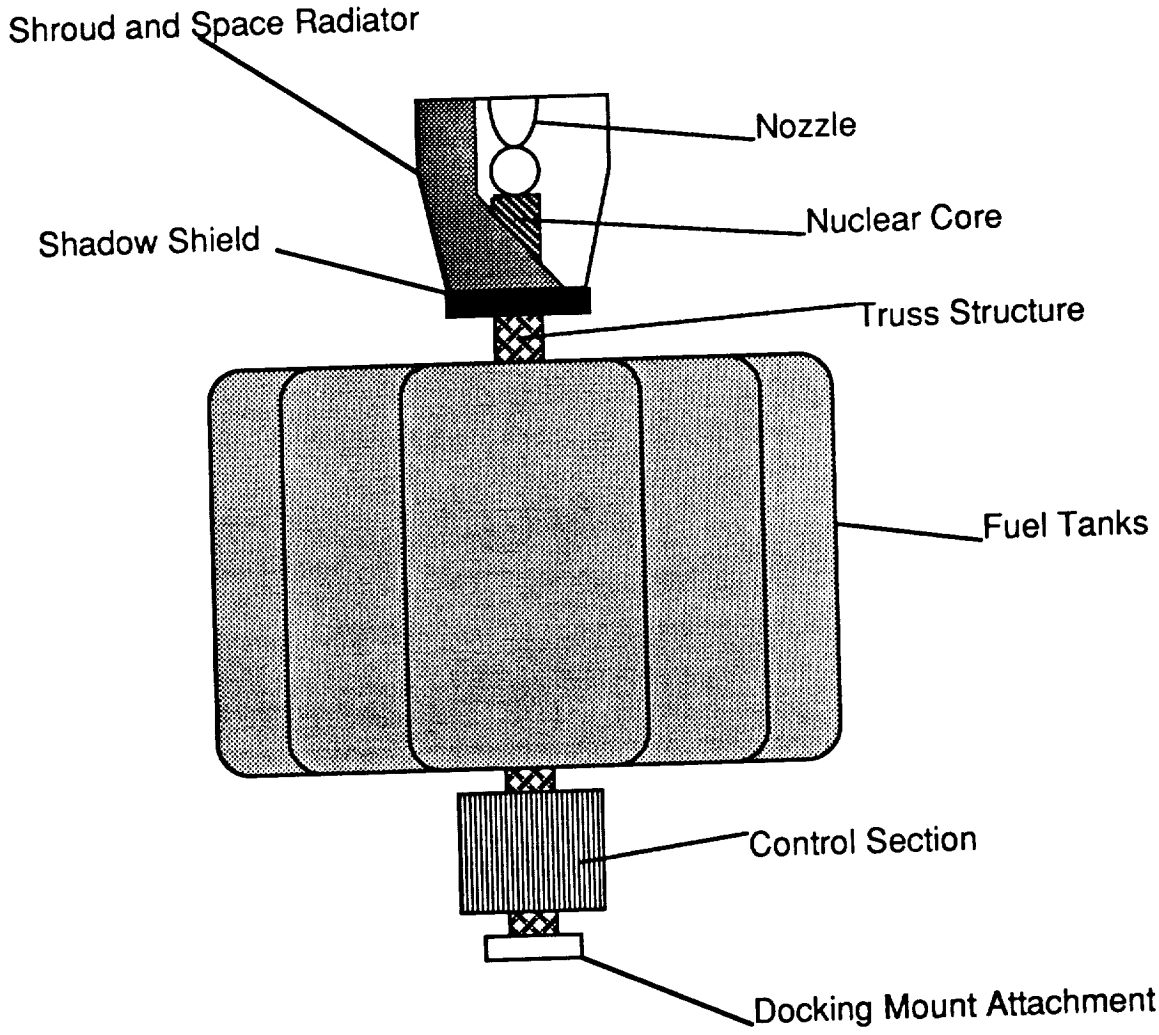

Figure III.2.1-3: LLVM Booster System

The LLVM Departure Stage is equipped with a nuclear propulsion booster. Power can be tapped from this source by means of bimodal power system. A single bimodal reactor can provide both low level continuous power and high level pulse power. The power system has a closed cycle for power conversion with He-Xe as a coolant and an open cycle power conversion for propulsion using H_2 as a fuel as described in section III.3.1.3.2 (Botts et al, Reference 10).

III.3.1.2 Structures
(Miyake)

The volume of the Supply Stage (SS) was based on supply volumes and the need to accommodate the ascent/descent module. However, we designed the supply ship to be as low in volume and weight as possible to facilitate the transport from LEO to LMO and to minimize costs. We have examined two possible configurations for our mission. One is covered by a cone shaped body as shown in Figure III.3.1.2-1, because there needs to be protection from aerodynamic heating if we decided to use aerobraking at Mars. After evaluating fuel trade-offs and considering the large aeroshell needed to prevent heating effects, it was decided not to aerobrake the LLVM. Therefore,the current design is not covered and is of arbitrary shape as in Figures III.3.1.2-2 and -3. Also, the current design is optimized to obtain the most efficient total volume and use of available space.

Since the Waverider must dock with the Waverider in LMO, the configurations of each of the designs were developed in conjunction with the Waverider and booster systems. The cone-shaped version of the supply vehicle is shown in Figure III.3.1.2-4 as it would appear when docked with the Waverider and booster. The non-cone-shaped design is shown in Figure III.3.1.2-5. By comparing these figures, it is apparent that the second (chosen) design is much smaller than the cone-shaped design, since the large volume of the cone-shaped version was necessitated by the need to protect the LLVM from heating effects while aerobraking at Mars. Also, it was decided to jettison the empty supply vehicle before returning to LEO. Therefore, the return configuration is shown in Figure III.3.1.2-6.

The supply ship must be 25 to 30 m long, and the inside diameter of the tunnel must be 5 m so that two astronauts can stand beside each other while transporting supplies. Since nothing large will be brought back from the surface of Mars, it is sufficient that the entrance/exit of the ascent/descent module be 2 m. The tunnel needs to be strong enough to withstand the acceleration of the booster on the trip to LMO.

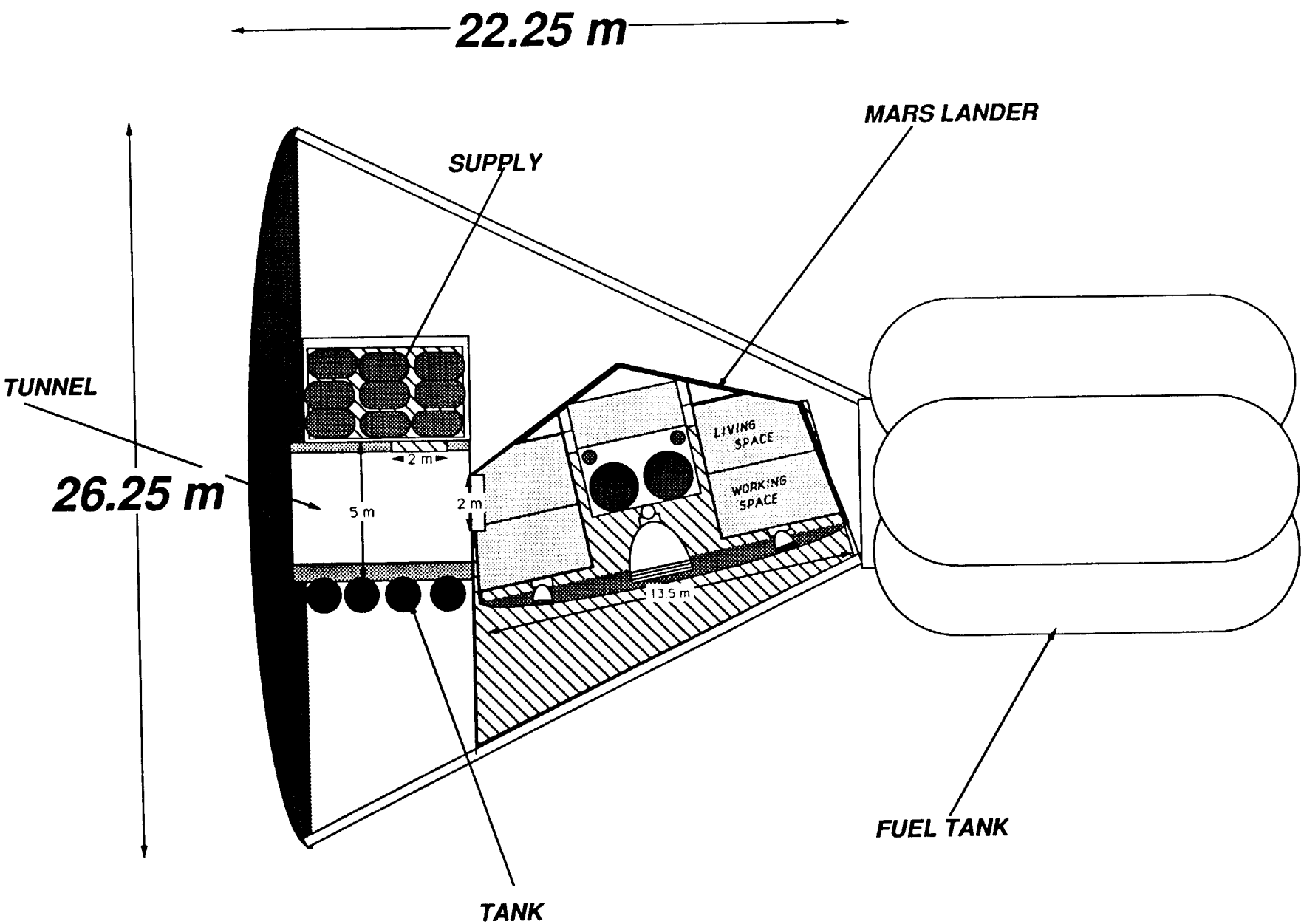

Figure III.3.1.2-1: Cone-shaped supply ship

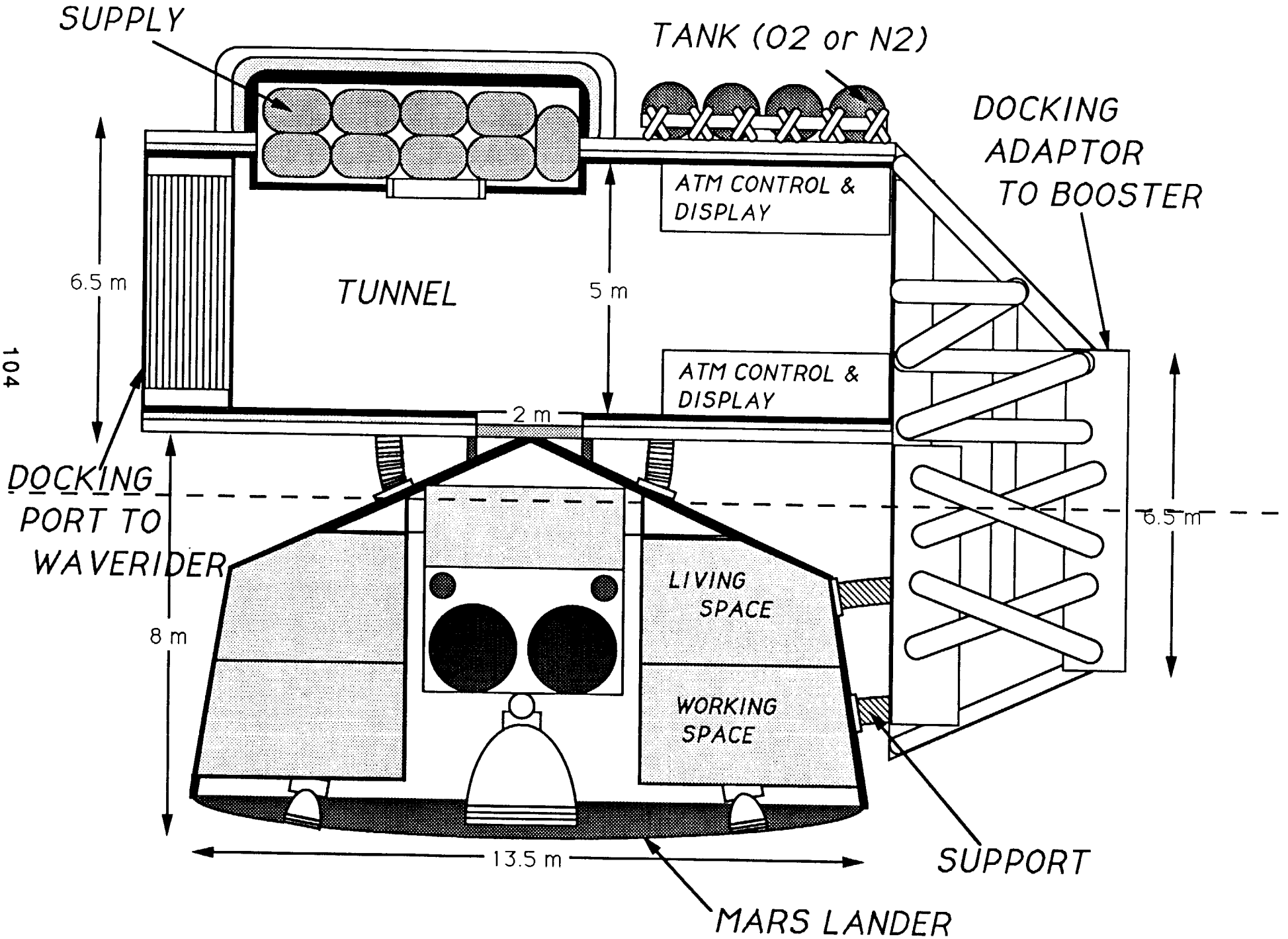

Figure III.3.1.2-2: Normal supply ship

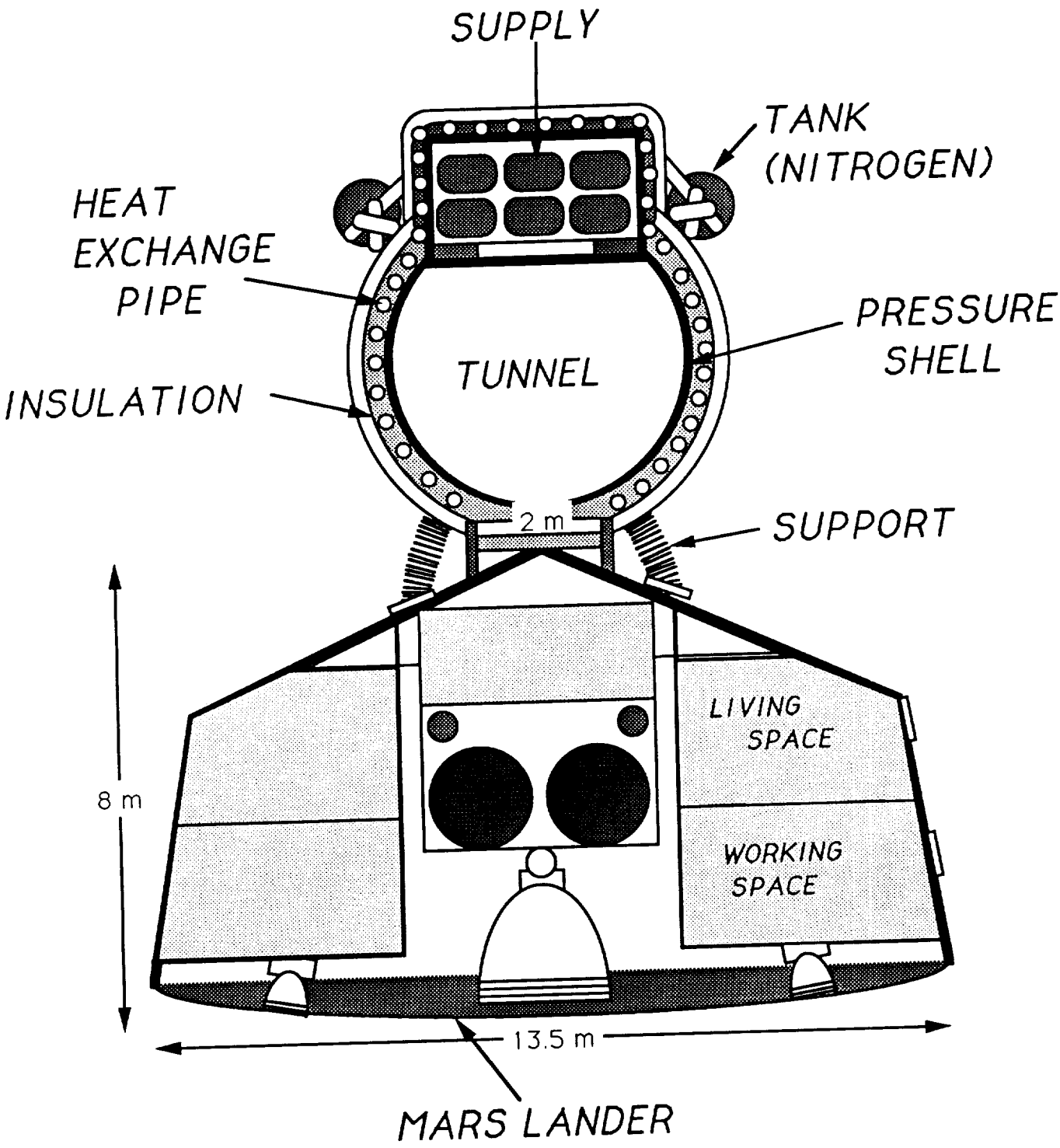

Figure III.3.1.2-3: Normal supply ship-cross section

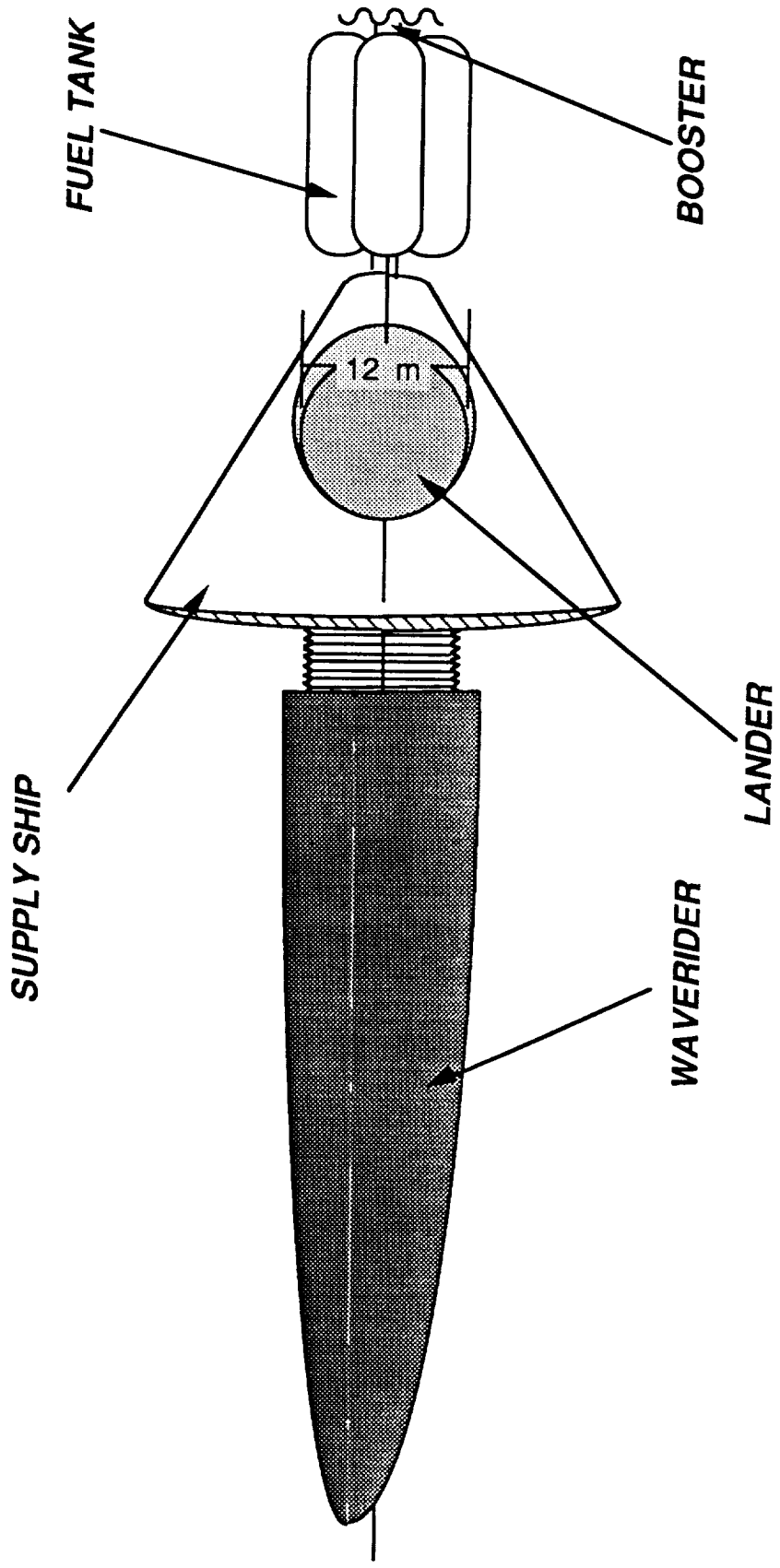

Figure III.3.1.2-4: Cone-shaped Supply Ship in Docked Configuration

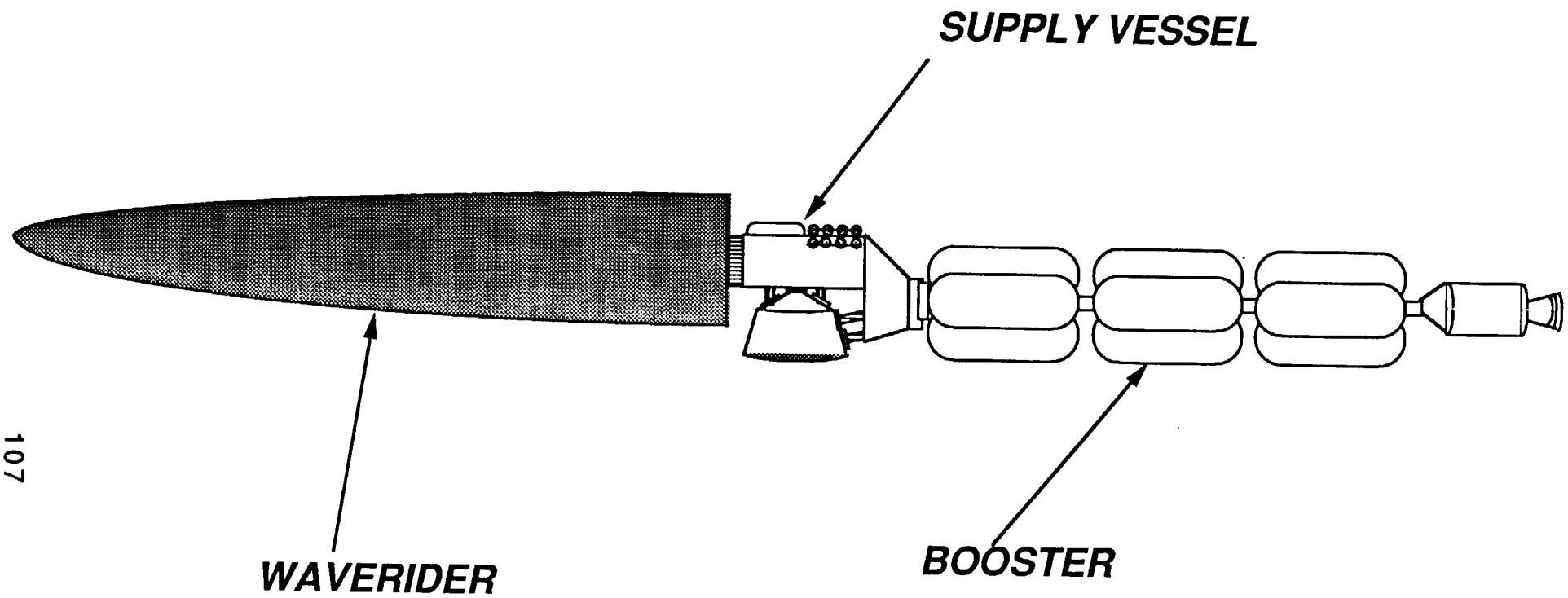

Figure III.3.1.2-5: Waverider , LLVM, and Booster

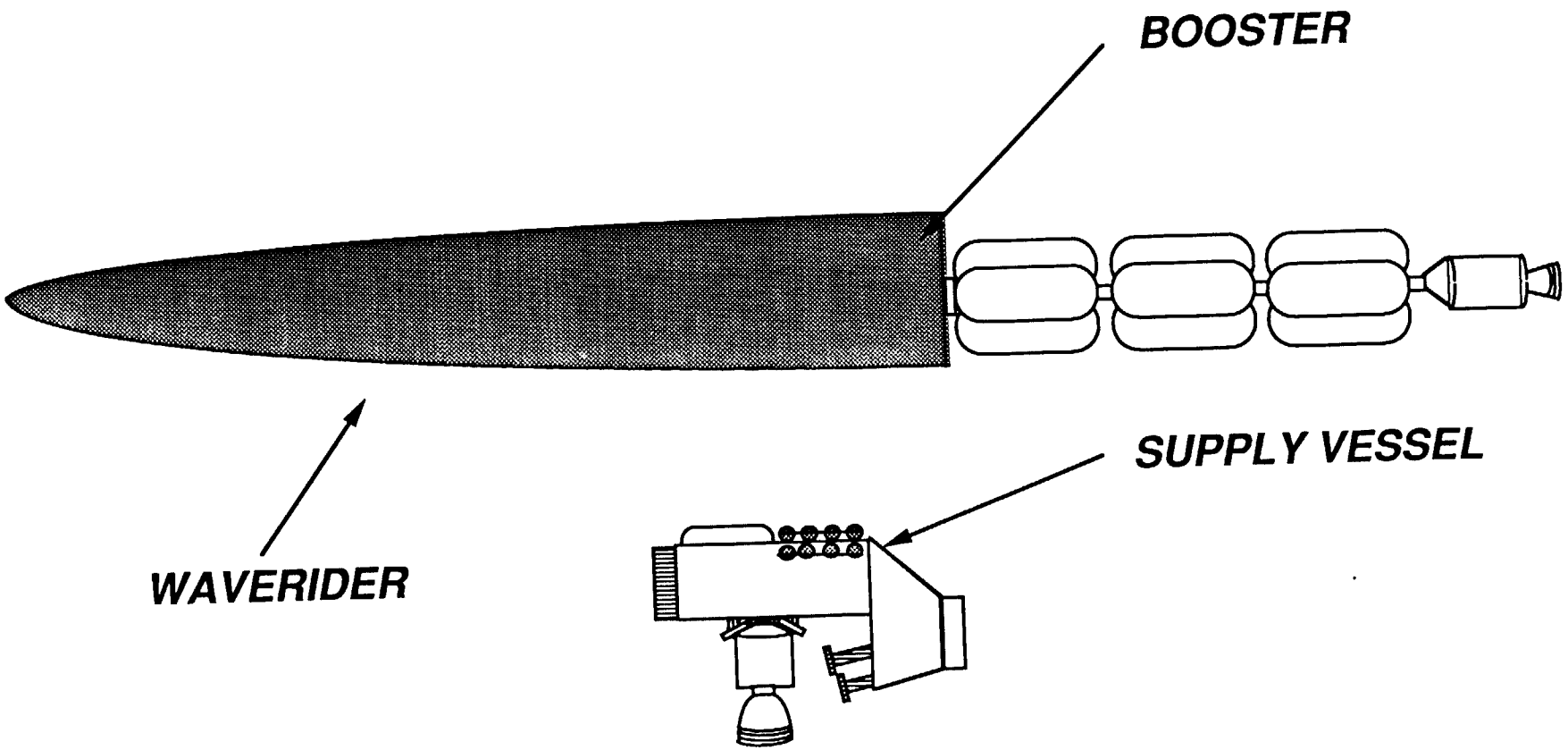

Figure III.3.1.2-6: Jettison of Supply Section

The food and water are contained in aluminium boxes which the astronauts must carry from the SS to the Waverider. The oxygen and nitrogen are contained in cylindrical or spherical tanks in a liquid state. They will be packaged as liquids rather than as gases due to the very high volume necessary to store gases. These tanks are connected outside of the tunnel, and the oxygen and nitrogen are transferred from the tanks of supply ship to those of the Waverider by pipes.

The tunnels of both designs are pressurized and temperature controlled in order to transfer the crew and supplies between the supply ship and the Waverider as safely and effectively as possible. The supply vessel for water and food is also pressurized and temperature controlled. Both the pressure and temperature control systems are maintained by generated power from the booster. There are three hatches inside the supply ship. One is a docking port between the Waverider and the supply ship, and its diameter is four meters. Another one is for an entrance/exit of the ascent/descent module, which is only two meters in diameter. The third one is for the supply vessel and also has a diameter of two meters. The tunnel must have a diameter of five meters so two crew members can stand next to each other and carry supplies effectively. Inside the tunnel, there are ATM controls and control panels.

There are 13 cryogenic tanks for oxygen and nitrogen around the outside of the tunnels. They consist of two oxygen and eleven nitrogen tanks. The diameter of all cryogenic tanks are 1.05 m, since this volume is convenient for holding the required volume of cryogens. Also, it is easy to connect them to the outside of the tunnel if all of the tanks are of the same dimensions.

The dimensions of the supply room are 6 m x 3.5 m x 2 m. The supply room is pressurized and temperature controlled in order to bring water and foods easily. All foods and water are packed into aluminum boxes whose dimensions are 1.25m x 1.25m x 0.8m. Supplies are divided into 22 boxes for foods, 6 boxes for water, and some boxes for spare parts or other supplies.

The adaptor is only needed for the non-cone shaped supply ship because the adaptor is required to align the center of gravity and connect the supply vessel and the Mars lander. Because the center of gravity for the cone-shaped supply ship is the same as that of the booster, an adapter is not needed to align the centers of gravity of the supplies, tanks, and Mars lander.

There exist supporting arms which support the ascent/descent module. The supporting arms must move flexibly and endure high compression and tension. There are eight supporting arms for both supply ship designs. Half of them are used to support the upper side of the ascent/descent module, and the other half are used to support the side of the ascent/descent module.

Both designs of the supply ship are twenty or twenty five meters long. Although the shapes are different, the main purpose and parts are same, with the exception of the outer shell; however, the weights are not the same because the cone shaped supply ship uses a large aero-shell, which increases the total weight of the structure.

The materials used for our supply ship are presently very expensive. By 2020, our technology will have been developed sufficiently to produce these materials cheaply. Furthermore, the total weight may be reduced to two thirds of the current weight if human beings can develop new materials which cost the same as current materials. If the total weight is reduced, the fuel consumption would be less than the current estimation of fuel consumption; therefore, the total cost will decrease.

III.3.1.2.1 Materials

The tunnel of Figure III.3.1.2.1-1 consists of four major parts - the pressure shell, insulation, heat exchange pipe, and outer shell. The pressure shell is made from 7075 - T6 Al because it is very high in compression yield strength, and its weight is very light. The heat exchange pipe is also made from aluminum. The outer shell is made from composite material in order to reduce the weight of the structure. Composite materials are very expensive right now; however, by 2020, we anticipate that the price of composites will be reduced. A comparison of material properties is shown in Figure III.3.1.2.1-2.

The outer shell of the cryogenic tanks is composed of graphite/epoxy. The specific weight of graphite/epoxy is 40 % less than that of aluminum; however, the strength is three or four times that of aluminum as seen in Figure III.3.1.2.1-3.

The adaptor consists of many support rods and circular rings. Graphite epoxy is used for the support rods, and kevlar is used for the circular ring. Kevlar is about six times stronger than aluminum, yet its specific gravity is half that of aluminum. Using composites instead of aluminum cuts the weight of the adaptor in half.

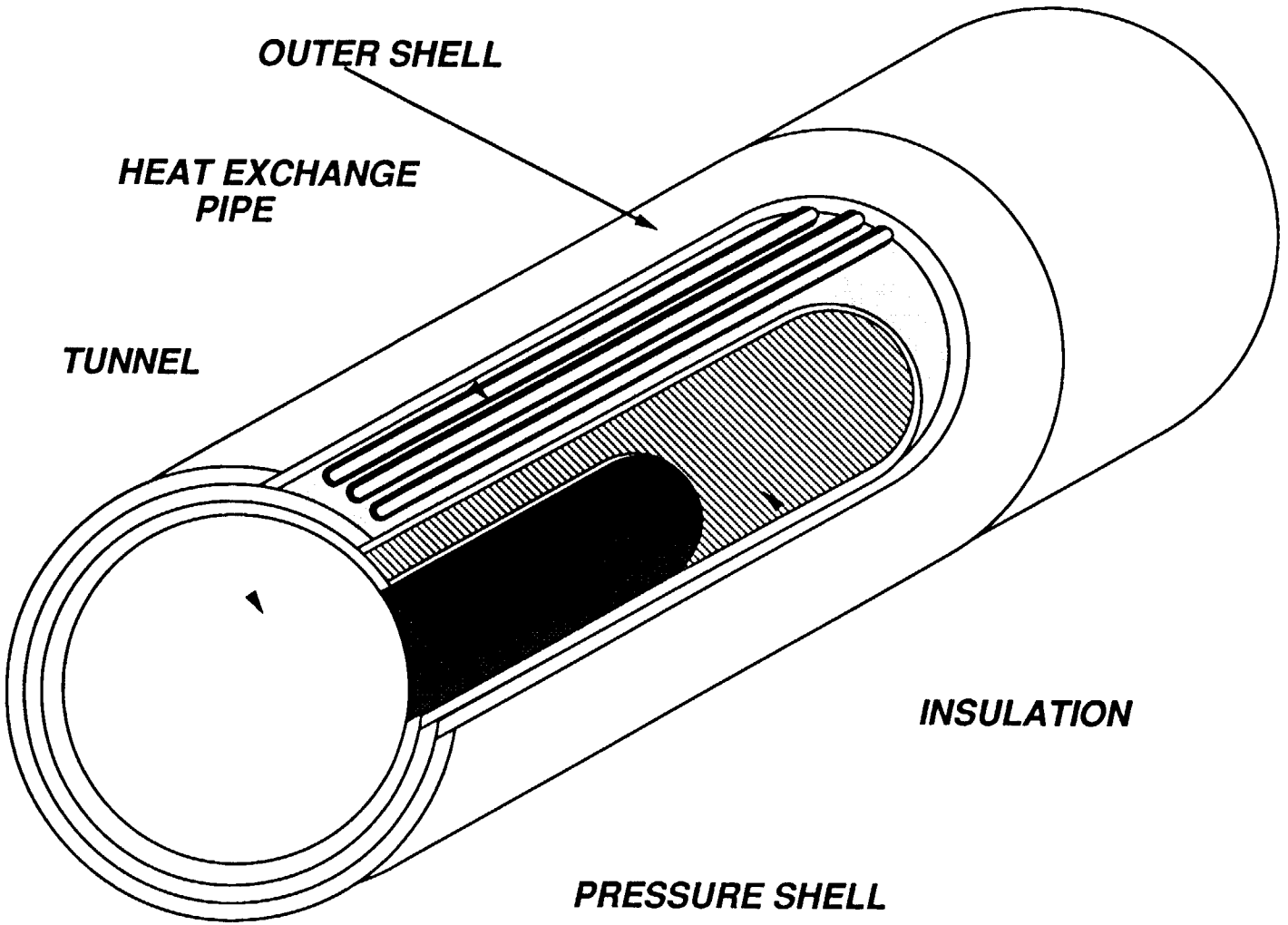

Figure III.3.1.2-7: Tunnel Cut-away View

COMPARISON OF METAL ALLOYS					
MATERIAL DESIGNATION	Tensile Ultimate, MPa	Comp. Yield, MPa	Modulus, GPa	Specific Gravity	Specific Modulus
2024-T3 Al	462	290	74	2.77	27
7075-T3 Al	586	531	72	2.80	26
7175-T73 Al	504	436	70	2.80	25
Ti6 A l-4V	923	909	110	4.43	25
300M Steel	1931	1703	200	7.84	25
GRAPHITE/ EPOXY	1661	1698	130	1.61	81

Figure III.3.1.2.1-2: Materials Comparison Table

PROPERTIES OF FIBERS			
FILAMENT	Specific Gravity	Tensile Ultimate MPA	Modulus, GPa
E-Glass	2.52	3400	72
S-Glass	2.49	4500	86
Boron	2.60	3400	400
Fiber	1.74	1900	190
HMS (High Modulus)	1.94	2100	380
HTS (High Tensile)	1.80	2400	250
Kevlar	1.44	3600	130

Figure III.3.1.2.1-3: Composite Properties Table

III.3.1.2.2 Weights

In order to make the Waverider as light as possible for its aero-gravity assist maneuver at Venus, we have decided to carry all supplies for the return voyage including food, water, and spare parts, as well as the landing module, on the LLVM. Since the SS carries only supplies, life support is not a major criterion, and radiation shielding and whole vehicle pressurization are not required.

The table below describes the supply and structure weights of each of the supply ship designs considered. Both supply ships have the same supply and structure, except having outer shell for only the cone shaped supply ship. Although the cone shaped supply ship does not need an adaptor, the weight of the cone shaped supply ship is still heavier than the non-cone shaped one, due to the large weight of the outer shell - about 27,000 kg. Therefore, the total weight difference between the cone shaped supply ship and the non-cone shaped one is about 20,000 kg. This confirms the decision to keep the non-cone shaped design.

The LLS must have the capability to connect to the WOPM when it arrives in LMO. Therefore, the SS design includes a tunnel which will connect the WOPM to the LLS to transfer astronauts both before descent and after ascent. The tunnel is also used for bringing supplies from the SS to the WOPM for both the return trip to Earth and for use by the two crew members remaining in orbit. In order to transfer astronauts and supplies as safely and effectively as possible, we plan to pressurize the tunnel and to connect the tunnel and docking port. The tunnel will be retractable to accommodate the difference in size between the lander and liftoff portions of the LLS, which must both dock in the same area.

There is no need to transport the added weight of the empty SS back to earth. Therefore, the SS must be able to separate from the booster so that the WOPM can dock with the booster for the return voyage. Thus, when the ascent module comes back from Mars, it and the SS are jettisoned, and the booster is connected to the Waverider directly. By eliminating the transport of unnecessary weight back to earth, this configuration allows the WOPM to return to earth in a minimum of time - a critical concern for the astronauts.

ESTIMATION OF SUPPLY SHIP WEIGHT

SUPPLY WEIGHT		*STRUCTURE WEIGHT*	
m_{O_2}	1,300 kg	$m_{TANK\ SYSTEM}$	5,000 kg
m_{N_2}	5,200 kg	$m_{PRESSURE\ SHELL}$	7,500 kg
m_{WATER}	4,410 kg	$m_{INSULATION\ \&\ HEAT\ EXCHAGE\ PIPE}$	2,000 kg
m_{FOOD}	1,900 kg	$m_{COMPOSITE\ SHELL}$	5,700 kg
		$m_{SUPPLY\ BOX}$	70 kg
		$m_{ADAPTOR}$	6,800 kg
		$m_{8\ ARMS}$	10,000 kg
m_{SUPPLY}	12,810 kg	$m_{STRUCTURE}$	37,070 kg
m_{TOTAL} =		49,880 kg	

NOTE 1: NOT INCLUDING THE WEIGHT OF SPARE PARTS
NOTE 2: NOT INCLUDING THE WEIGHT OF COMPUTER SYSTEM & OTHER STAFF
NOTE 3: NOT INCLUDING THE WEIGHT OF THE MARS LANDER

III.3.1.2.3 Environments
(Miyake)

III.3.1.2.3.1 Thermal

Since the connecting tunnel for the LLS as well as the food and water aboard the SS must be thermally controlled, there are heating and cooling pipes which are operated on power generated by the booster to keep the tunnel at constant temperature. These pipes are located around the tunnel and the food and water supply vessels. In addition, these areas must be pressurized; therefore, this system is also maintained by the booster.

III.3.1.2.4 Mechanical

III.3.1.2.4.1 Separation Systems

There are three main hatches inside the supply ship. One is the docking port between the Waverider and the LLVM, another one is the entrance/exit for the LLS, and the third one is for the booster and the SS.

III.3.1.3 Electrical

III.3.1.3.1 Power

III.3.1.3.2 Electronics
(Kamosa)

The cargo-ship is equipped with a nuclear propulsion engine. Electric power can be tapped from this source by means of a bimodal power system that can provide both low level continuous power and high level pulse power. This system is diagrammed in Figure III.3.1.3.2. The power system has a closed cycle for power conversion with He-Xe as a coolant. An open cycle power conversion for propulsion using H_2 as a fuel is used in both operations (Botts T.E. et al).

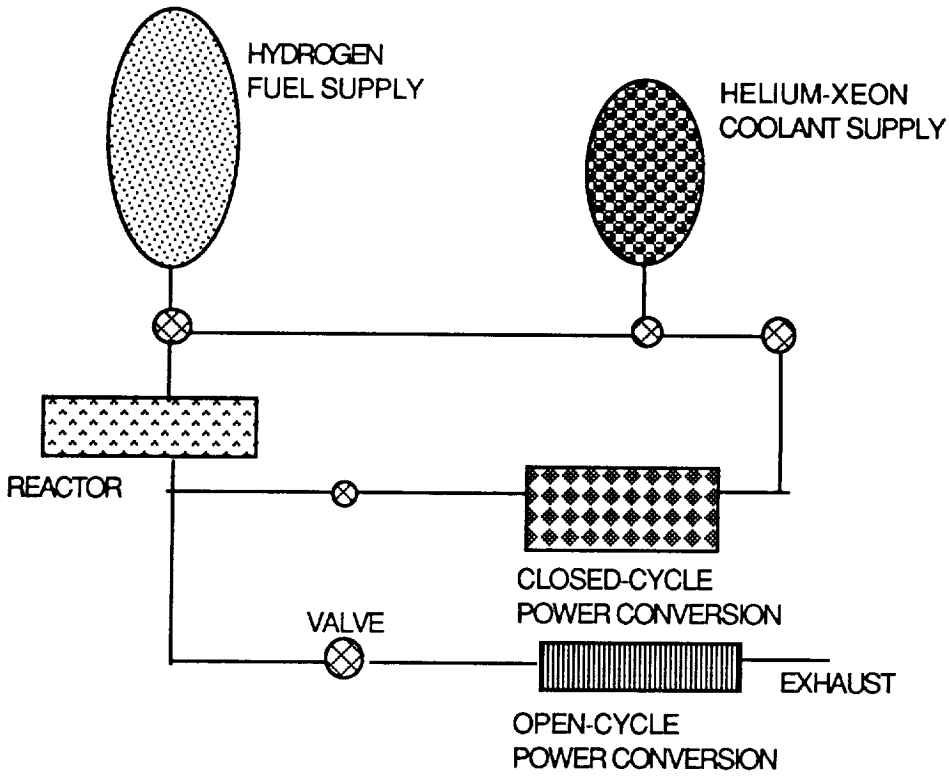

Figure III.3.1.3.2: Bimodal Power System

III.3.1.4 Guidance and Control
(Kraft)

The interfaces of the primary components of the LLVM guidance systems are very similar to those of the WOPM guidance and control (G&C) system. This section describes the similarities and differences between the two systems. The G&C modes of the WOPM are shown in Figure III.2.4. The modes of the LLVM are similar to those of the WOPM, except that the LLVM does not require an aeromaneuver mode.

III.3.1.4.1 Star , Limb, and Sun Sensors

There will be three 4ΠSSs on the Supply Stage (SS). As in the WOPM, each will be a redundant system, and the system will be validated by periodic checks by the GC and the star tracker. Since they have similar tracking and attitude requirements, the WOPM and the LLVM will use the same star tracker equipment. There will be three ASTROS II star trackers located strategically on the LLVM.

III.3.1.4.2 Inertial Measurement System

The inertial measurement system (IMS) of the LLVM SS is identical to that of the WOPM (see section III.2.4.2). It will use the 64 PMRIGs for attitude data determination, which will be placed as necessary and mechanically convenient for control.

III.3.1.4.3 Guidance Computer

The GC for the LLVM will be located in the Lander/Launcher Submodule portion of the vehicle, so that it may be used to guide the LLVM from LEO to LMO and support landing and launching operations. Once the LLVM docks with the WOPM in LMO, the GC of the LLVM will no longer be needed by the LLVM SS; therefore it is free to be used to control the LLS during its phase of the journey.

III.3.1.4.4 Attitude Control

Attitude control of the LLVM SS is accomplished by the same means used on the WOPM. The thrusters are located at strategic locations along the length of the LLVM SS. Also, SGCMGs are used to store momentum and provide attitude control during coast modes.

III.3.1.4.5 Software

Since the LLVM uses the same GC as the WOPM, it will also require similar software for mission control. The LLVM software will be oriented for the LLVM trajectories, and must be responsible of autonomously operating the LLVM systems while the LLVM is in LMO awaiting a rendezvous with the WOPM. The LLVM GC software must also contain information for the LLS to use in its trip to the Martian surface and back, as the LLVM GC is located in the LLS, as stated above. The WOPM software will be capable of operating the SS systems after docking.

III.3.2 Lander/Launcher Systems

III.3.2.1 Propulsion

(Amato)

The primary design goal of the ascent and descent module propulsion systems is reliability. If the descent propulsion system fails, the descent module will hit the surface too rapidly and crash. If the ascent propulsion

system fails, we watch as 8 people die on the surface of Mars. In propulsion systems, the pumps are the most common and likely failure - the 'weak link'- because they are the only moving parts besides valves. The weak link can be eliminated by using a blowdown system, a diagram of which is shown in Figure III.3.2.1-1. Although the pump weight is thereby eliminated, the necessary pressurant and pressurant tanks cancel this gain by adding weight to the system. Yet blowdown rockets are often lighter than pump rockets built for the same job. As shown in Figure III.3.2.1-1, regulators keep the pressure to the tanks constant (at 3.1×10^6 N/m^2 for the engines in this paper) during blowdown. The heat exchangers replace heat the pressurant losses during expansion. This reduces the amount of pressurant, which is stored at 5 to 8 times the tank operating pressure, needed for the job. One disadvantage of a blowdown system is that the combustion pressure is limited to what the pressurant can blow down to at the end of firing after expanding into the fuel and oxidizer tanks. Pump rockets often have a combustion pressure around 2 x 10^7 N/m^2; blowdown systems often have combustion pressures of around 2 x10^6 N/m^2. Higher combustion pressures give us a little higher To and limit dissociation; however, the higher the desired combustion pressure, the more pressurant you need and, therefore, bigger and heavier pressurant tanks are required.

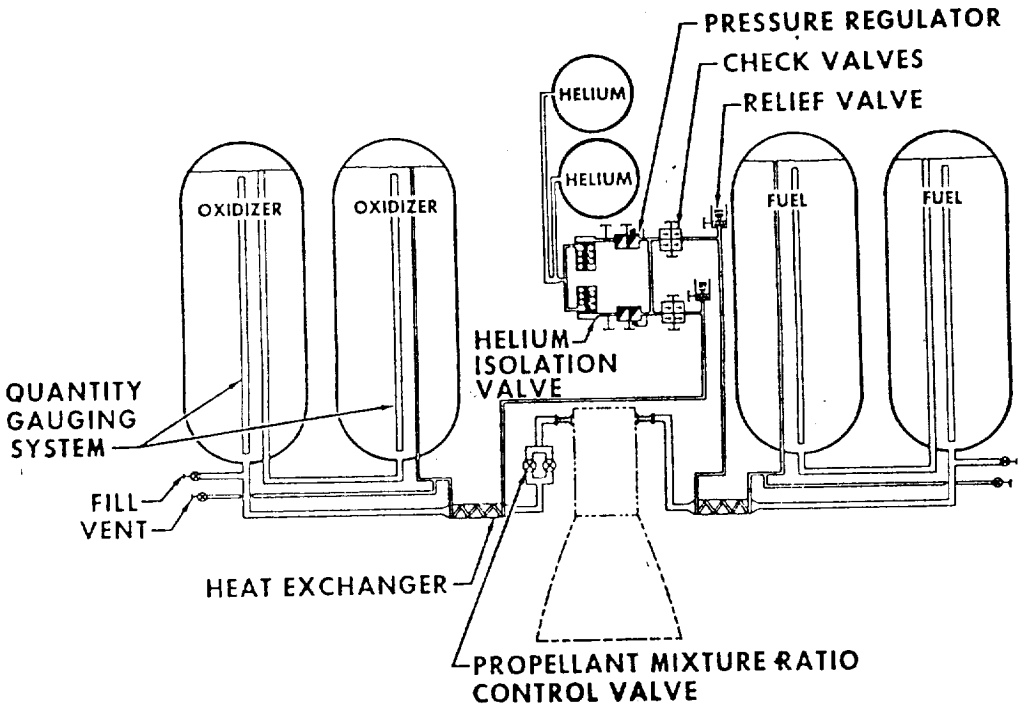

FIGURE III.3.2.1-1: Blowdown system

Nuclear propulsion for the ascent/descent module was ruled out because of their heavy weights, possible exposure difficulties if problems arose, and start up shut down problems (if cooling over a three month period is not necessary, it should not be done). The use of nuclear propulsion with hydrogen during descent and carbon dioxide pumped from the Martian atmosphere for ascent also is not the best idea for the following reasons. The ΔV needed for descent is much smaller than that for ascent; therefore, descent requires less fuel. Using hydrogen with nuclear engines gives high Isp values also greatly reduces fuel needs for descent. For ascent much more fuel is required for the much larger ΔV (especially if the whole descent module is also used for ascent) and if you use CO_2 fuel with the same nuclear engine, the Isp is 313 s - close to the same Isp if 50-50 aerozene and NO_4 is used with much lighter engines. Using CO_2 would increase ascent fuel needs even more (3 to 4 times). This results in about 8 times the fuel needed for ascent than for descent. Therefore, using CO_2 for ascent instead of H_2 would require an 8 fold increase in the amount of ascent tanks. These extra tanks would have to be carried on the lander as dead weight until the Martian surface was reached, when they would be filled with the CO_2 obtained from the Martian environment. In addition, extra pumps would be required to accumulate this needed CO_2. A disadvantage of the planetary hop configuration is the need for extra pumps, tanks, and power. This equipment must also be compatible with both CO_2 and H_2 in order to provide the thrust required by the mission profile.

The lander and ascent module will be aboard the supply ship for up to a year and a half before being used. One thing that is immediately apparent is that the successful storage of cryogenic fuels in a space environment would be difficult, requiring elaborate cooling and pressure systems along with backup systems. The solution is to use storable fuels like hydrazine or it's derivatives: unsymmetrical dimethylhydrazine (UDMH) and monomethylhydrazine (MMH). A 50-50 mix of UDMH and hydrazine (50-50 aerozene) gives the highest specific impulse (Isp=300 s compared to 277 s for MMH) and is less toxic than MMH. However, MMH has a larger temperature range (- 52.4 to 87.5 °C compared to - 57.2 to 63.3 °C for 50-50 aerozene). Nitrogen Tetroxide (N_2O_4) as an oxidizer with the 50-50 aerozene gives the highest Isp of all the storable oxidizers usable with this fuel (hydrogen peroxide Isp=274 s, red fuming nitric acid Isp=272 s). It's temperature range is from -11.6 to 21.2 °C. Because of it's relatively high freezing point, the oxidizer tanks will have to be temperature controlled by a heater/thermal blanket shown in Figure III.3.2.1-2. This system heats more uniformly than heating coils placed in the tank and also insulates the tank.

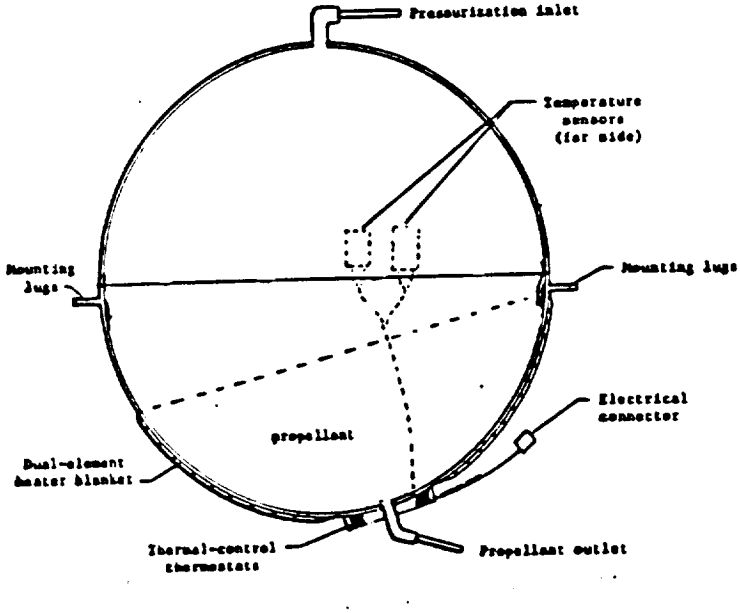

Figure III.3.2.1-2: Tank with Heating Insulating Blanket

Another benefit from using 50-50 aerozene and N_2O_4 is that they are hypergolic - they ignite on contact. This eliminates the need for an ignition system which could fail. However, since full ignition relies on proper mixing of the fuels, care must be taken to design the injectors so that the fuel and oxidizer mix early and well. Therefore, an unlike stream impingement design was chosen for the injector, with special attention paid to injection velocities for proper mixing.

The penalty paid for this extra reliability is performance. Cryogenic fuels like liquid oxygen and liquid hydrogen can give an Isp of 540 s in a vacuum. Figure III.3.2.1-3 compares cryogenic fuel Isp's to storable fuel Isp's.

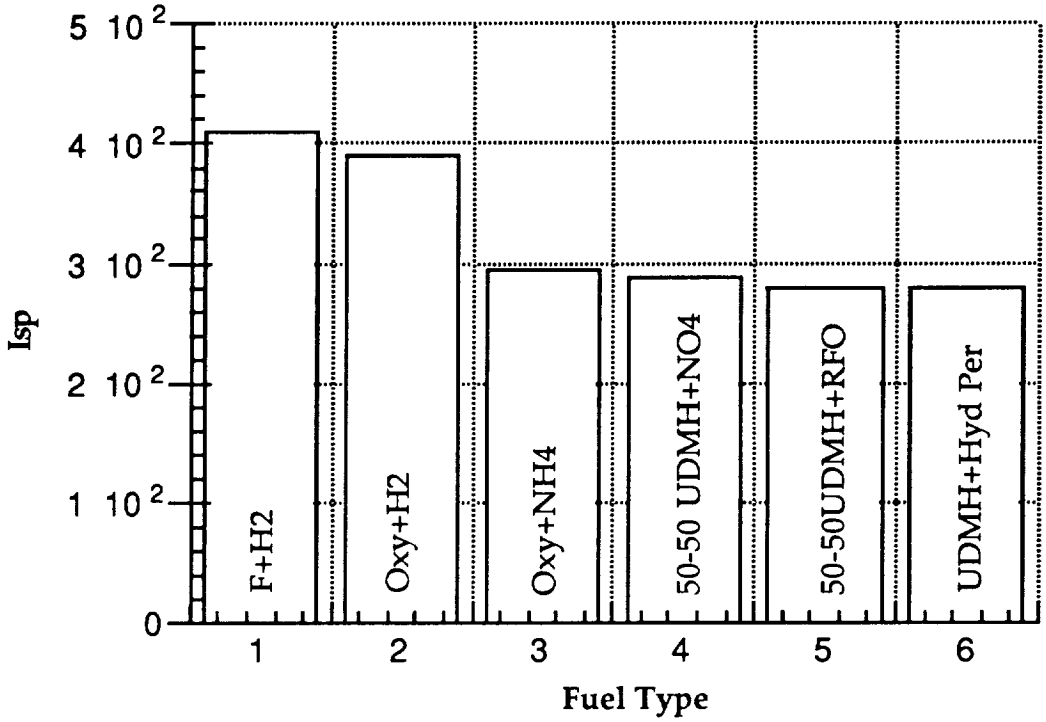

Figure III.3.2.1-3: Specific Impulse of Different Fuels

The original plan called for 3 descent engines because parachutes will not be sufficient in the thin Martian atmosphere. This configuration included 3 descent engines (for stability) and one ascent engine as shown in Figure III.3.2.1-4. However, the size of these descent engines can be cut in half by utilizing the ascent engine during descent. The resulting configuration is shown in Figure III.3.2.1-5. All four of these engines are gimballed for the ascent. The ascent engine will utilize two oxidizer tanks and two fuel tanks stored on the descent module during descent. The ascent engine will be disconnected from this fuel source and connected to fuel tanks on the ascent stage for ascent.

For a destination circular orbit of 170 Km, a ΔV of 3488 m/s is needed - not including drag. From the rocket equation, the weight of fuel needed can be figured out if you know payload and structure weight (approximately 5178 Kg total). So $M_f = e^{1.18 \times 5178 - 5178} = 11740$ Kg. A trajectory program (Section II.4.1.3.1.2) calculates that an additional 2061 Kg of fuel will be needed to overcome the atmospheric drag, producing a total fuel needed of 14082 Kg. Therefore the total payload weight is about 19260 Kg, allowing 281 Kg (or 2%) of reserve fuel. To insure the ascent module has sufficient acceleration to lift off, a thrust to weight ratio of at least 1.3 is needed. Using a safer ratio of 1.5

means the engine must be capable of producing a thrust of 1.5x19260 Kg x 4 m/s^2 = 115563 N. The descent module will weigh about 48000 Kg including the ascent module weight and fuel and 4157 Kg of descent fuel which is enough to get rid of the 70 m/s left after using one supersonic parachute and 3 low speed parachutes all with drag coefficients of approximately 0.8. This includes sufficient fuel to hover and navigate for over 30 seconds to the best landing sight.

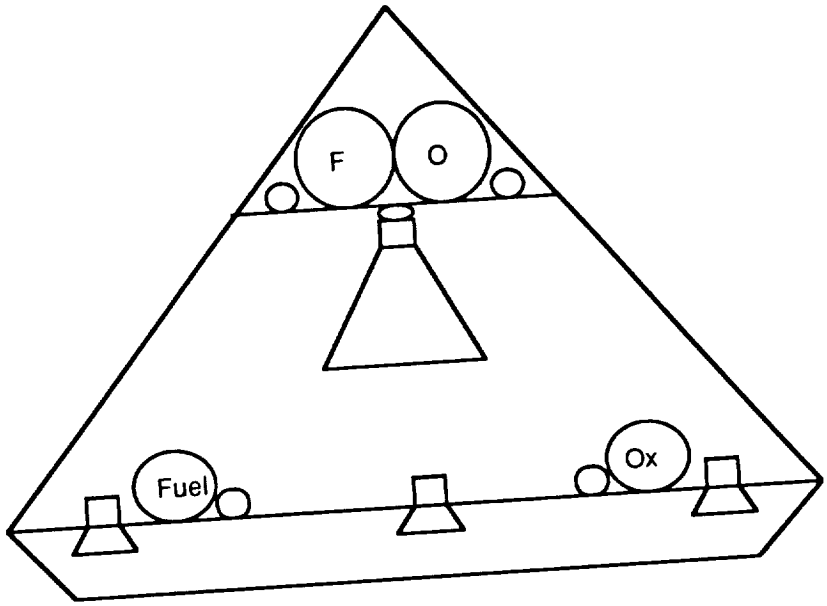

Figure III.3.2.1-4 : Original Ascent/Descent Module Configuration

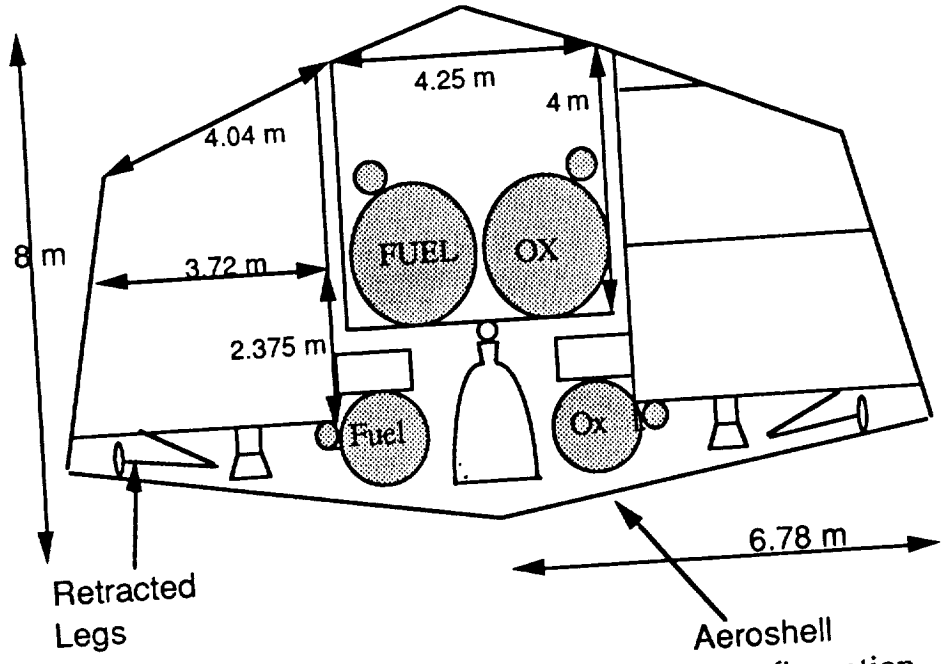

Figure III.3.2.1-5: Single Ascent/Descent Engine Configuration

The optimum oxidizer to fuel ratio for the chosen fuel is 1.62 by weight. Therefore, ascent requires 8707 Kg of oxidizer. At a density of 1445.6 kg/m^3, this requires 2 tanks of volume 6.2 m^3 weighing about 34 Kg each (if made of Ti-6Al-4B with an operating pressure of 3.1 x 106 N/m^2. Two tanks of 6.9 m^3 in volume are required to store the 5374 Kg of fuel is required at 820.4 kg/m^3. These would weigh about 36 Kg a piece for the same material and pressures. Three pressurant tanks weighing about 29 Kg with a storage pressure of 2.07 x 10^7 N/m^2 each are also required. The third tank is a backup tank capable of performing the task of either of the main pressurant tanks or some tasks of each. A similar configuration is used for the descent tanks, which are about 0.625 the size and weight of the ascent tanks and operate at the same pressures.

Using a combustion pressure of $2.07x10^6$ N/M^2 to minimize pressurant tank weights, it was attempted to expand to a middle atmospheric pressure so that the engine was never far from optimum performance. This required a nozzle that was too large, given the low Martian atmospheric pressures. Even expanding to Martian surface pressures of 537 N/m^2 required a nozzle 14 m wide and 25 m long. Expanding to only 48794 N/m^2 kept the penalty paid for not expanding completely (because the 48794 N/m^2 - 3806 N/m^2 term now introduced in the thrust coefficient equation is small). Therefore,the throat area increased (for the same thrust), but the exit area and length are 12 times smaller, greatly reducing size and weight. Appendix G shows the code used to calculate engine parameters and shows important parameter choices and justifications.

A diagram of ascent and descent engine parameters is shown in Figures III.3.2.1-6 and -7.

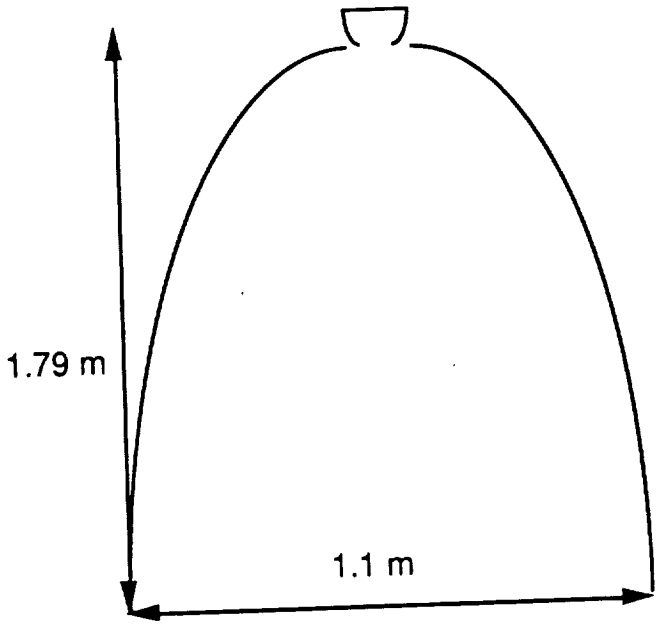

Thrust = 115563 N (26000 lb)

Combustion Temp = 2871 °C (5200 °F)

Throat area =327.1 cm2 (50.7")
Throat diameter = 0.20 m (8.03")

Exit area= 7849.65 cm2 Exit diameter= 1.0 m

Chamber area=2908 cm2/ Chamb vol=49882cm3

Mass flow= 41.9 Kg/s weight=30.1 Kg carbon-carbon composites

Burn time ascent=5 min 50 s ascent

Carbon-carbon dens=1.99 g/cm3 Max stress for multi directional at high temp = 400 MPa

Figure III.3.2.1-6 : Ascent Engine Parameters

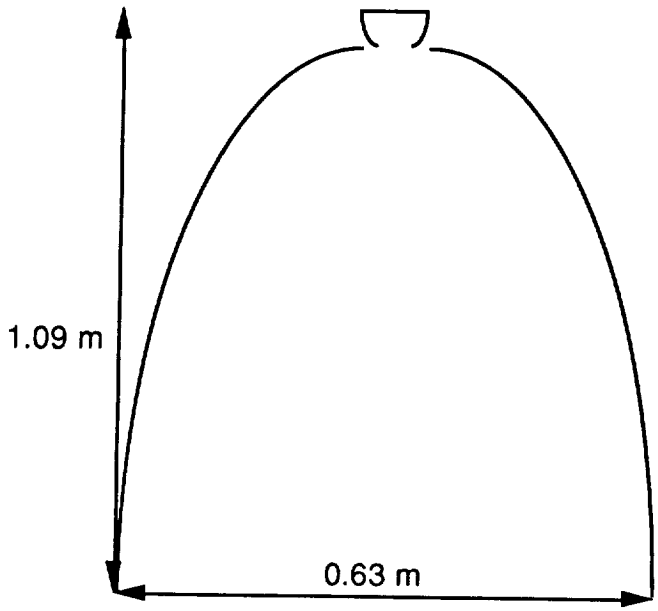

Thrust = 42045.4 N

Combustion Temp = 2871 °C

Throat diameter = .12 m (4.9")

Exit area= 2916.1 cm2 Exit diameter= .624 m

Chamber area=1080cm2/ Chamb vol=18517cm3

Mass flow= 15.5 Kg/s weight=5.41 Kg carbon-carbon composites

Throat area = 121.5 cm2 (18.84 in2)

Carbon-carbon density =1.99 g/cm3 Max stress for multi directional at high temp = 400 MPa

Figure III.3.2.1-7 : Descent Engine Parameters

The nozzle and combustion chamber will be made of carbon-carbon composites. Carbon-carbon maintains its strength through 2482.2 °C and can handle temperatures of up to 4000 °C. This material not only saves considerable weight, but also the combustion temperature is around 2871.1 °C. This means the nozzle and combustion chamber will not have to be regeneratively cooled, thus saving even more weight and eliminating pressure losses that would have occurred in the cooling coils. Although using the fuel for cooling the nozzle and combustion chamber can add some performance, it was decided that the small Isp increase was not worth the extra weight savings and simplicity gained by not cooling the engine. Carbon-carbon is not as brittle as other composites, but baffles and acoustical absorbers

will be needed to control vibrations. Metal supports might be added to critical areas like the throat to add strength.

Since we are using this engine for descent deceleration also, some maneuvering to adjust the landing sight might be desirable. This requires variable thrust capabilities. Arguably, the easiest way to do this is to vary the flow rate; however, variable flow rates could have a negative effect on proper fuel oxidizer mixing (on which the combustion relies when using hypergolic fuels). The solution is to vary the fuel rate by cutting off a certain number of injectors. This would not effect the injection speeds, but would lower the mass flow rate, lowering thrust as desired.

Thrusters will be in four three thruster clusters all at 90 degrees to each other with the nozzles cut to fit the contour of the vehicle. To save weight and space, it was decided to use hydrazine with a catalyst bed (see Figure III.3.2.1-8). This gives a little less performance (Isp=270 s) but requires no oxidizer or oxidizer tanks. Each cluster will have one tank (with the pressurant in the same tank) separated from the fuel by a diaphragm. They will have a heater/thermal blanket shown in Figure III.3.2.1-9 like the main engine oxidizer tanks (hydrazine freezes at 0.5 °C). There will be one extra tank for each two clusters capable of doing one clusters' job. These thrusters will be used to separate from the supply ship for entry into Mars' atmosphere, and will be used to stabilize and maneuver the descent module during reentry and deceleration. The thrusters will be uncooled carbon-carbon like the main engine.

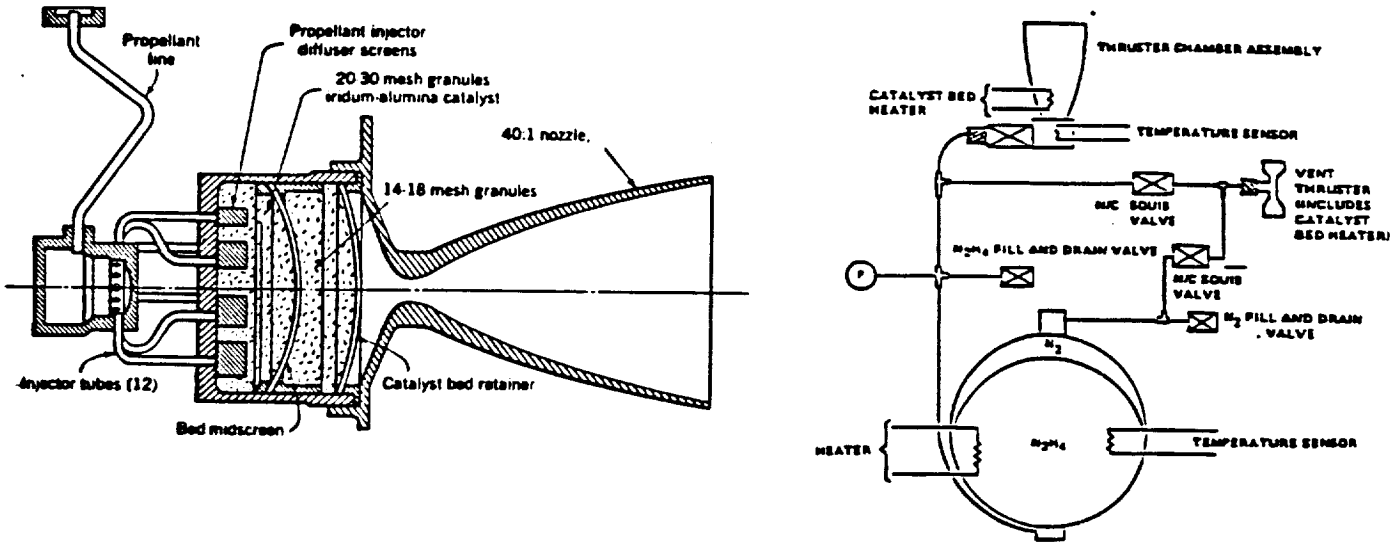

Figure III.3.2.1-8: Hydrazine Monopropelant Thruster

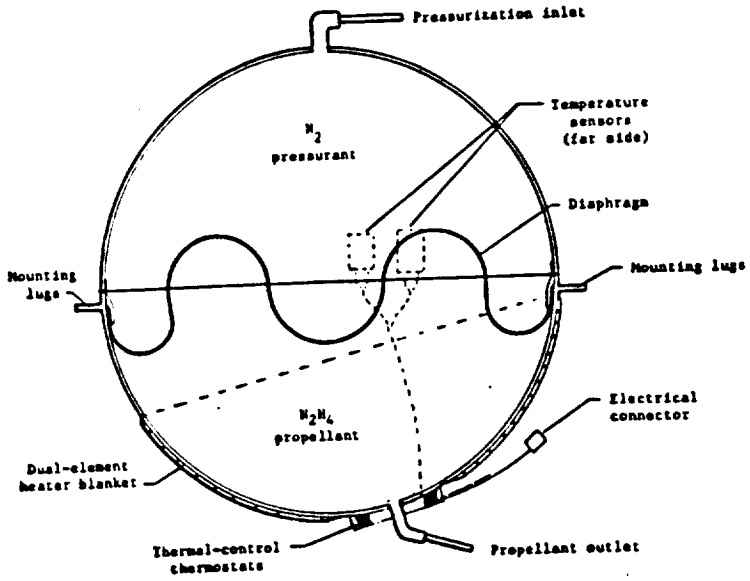

Figure III.3.2.1-9: Hydrazine Tank with Pressurant & Heater/Thermal Blanket

III.3.2.2 Structures
(Crouse)

During the planning phase of the landing segment of the mission, the decision was made to perform only one landing. This decision was based on the need to keep all the supplies centrally located on the planet surface and the desire to reduce the total complexity of the mission. Additionally, the probability of finding one smooth landing site is much greater than finding several that are relatively close together. We want our astronauts to be able to begin research shortly after landing. We do not want them to have to take time to set up a base made of many components.

A low structure mass is desired since the lander must be transported to Mars. Fuel requirements and overall cost scale with mass. Therefore, composite materials will be used to reduce mass. The cost of composites will decrease over the next thirty years as the technology is improved. The mass savings and the subsequent cost savings will outweigh the higher cost of composite materials in comparison to metals such as aluminum alloys.

Atmospheric entry at hypersonic speeds will produce high heating due to the viscous effects of atmospheric molecules interacting with the surface of the vehicle. An aeroshell similar to that used on the Viking spacecraft (Holmberg, Reference 33) will be employed to protect the lander from the heat loads. The lander will encounter a maximum heating rate of $8 W/cm^2$. This will produce a stagnation point temperature on the order of 1200 K. Carbon-carbon composites can withstand temperatures up to 4000 K, and therefore it will be the

material chosen for the composition of the aeroshell. The choice of carbon-carbon eliminates the need for an ablative material. The aeroshell will be designed as a lifting body that will decelerate the lander until parachutes can be used to further slow the descent. After the parachutes are deployed, the aeroshell will be jettisoned using explosive bolts which will expose the descent nozzle and landing gear. Once the parachutes are separated from the craft, the descent engine will fire and the legs will fold out in order to complete the soft landing onto the Martian surface.

There will be four legs evenly spaced around the base of the lander. Each leg will consist of a primary strut, two secondary struts and a footpad. The struts will be of piston-cylinder construction with an aluminum honeycomb that will crush on landing and absorb the force of impact (Figure III.3.2.2-1). The force will be minimal since we are using a propulsive descent. The primary strut will provide support in the vertical direction and the secondary struts will provide additional stability in the horizontal direction in the event of a landing with some horizontal velocity. The legs will be made of aluminum alloy to provide the added flexibility that composites lack. The footpad will be relatively large to help displace the landing force and to add stability by reducing sliding. A low center of gravity is a major criteria for the design of the lander vehicle, since the lower the c.g. the more stable the craft will be upon landing.

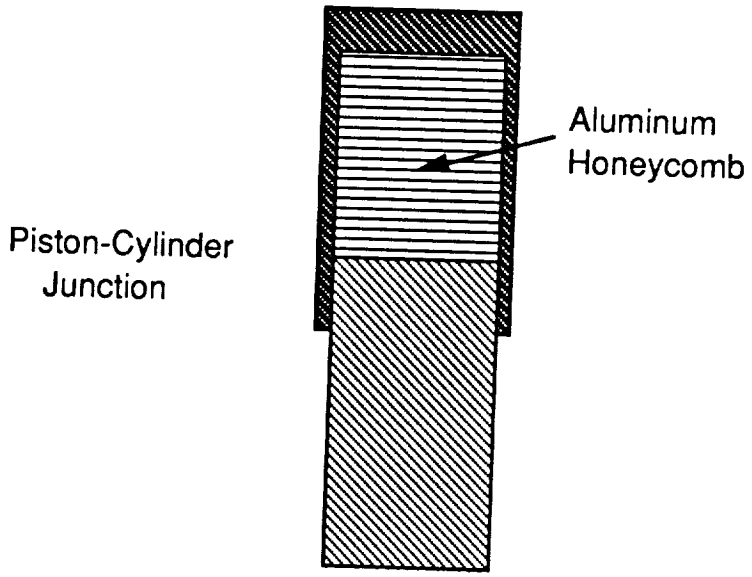

Figure III.3.2.2-1: Strut Design

A single atmospheric entry dictates the need for the lander to contain an ascent module as well as the supplies for the three month stay and

the necessary living and working space within the habitat. Initially, the lander was designed to provide the minimum volume needed for living space. The additional space required for research experiments was to be provided by erecting inflatable tents. This design is shown in Figure III.3.2.2-2. The ascent module for this design was considered to be aerodynamically inefficient due to the relatively large base diameter. A second design is shown in Figure III.3.2.2-3 which features a more aerodynamic and lighter ascent module. The fuel tanks for the ascent module are placed above the combustion chamber and nozzle. The increased height provided the volume to create more living space on the upper level. The increased size of this design is offset by the elimination of the need for tents and the equipment necessary to pressurize, heat and support them.

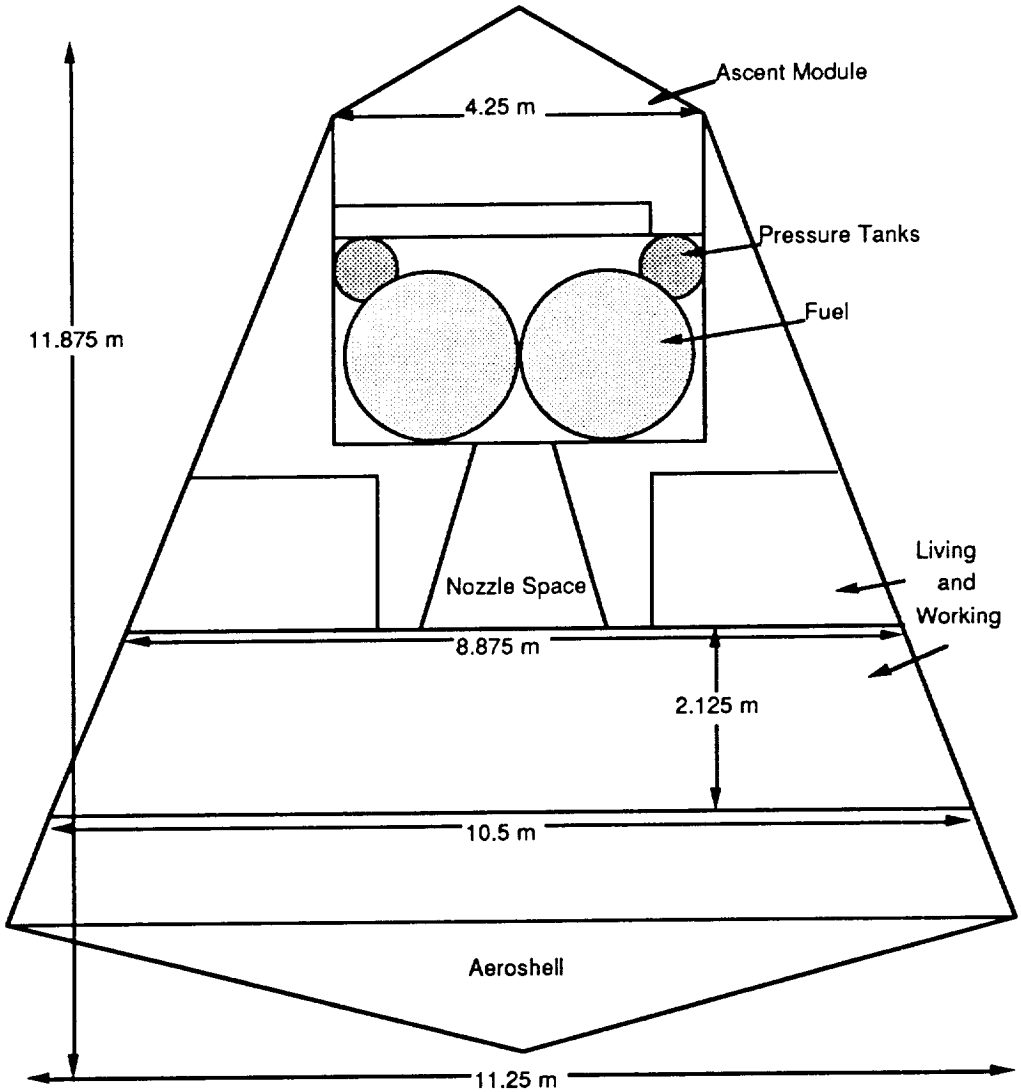

Figure III.3.2.2-2: Initial Lander Design

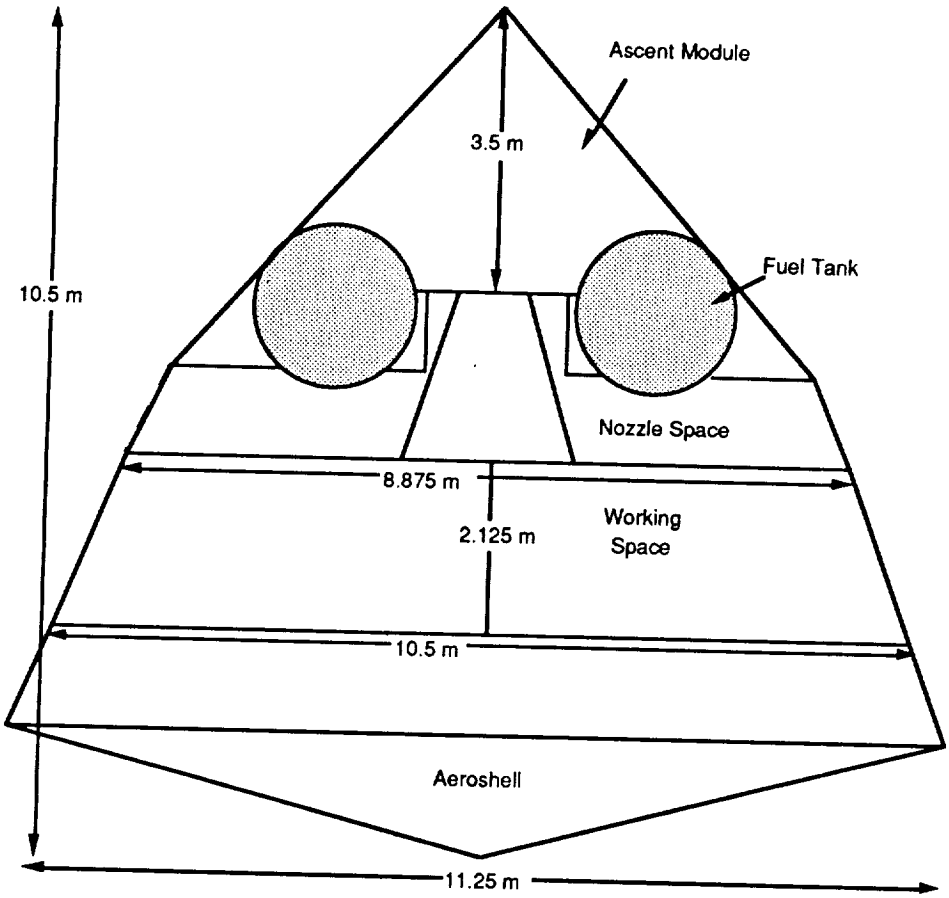

Figure III.3.2.2-3: Second Lander Design

Both of the two previous designs use one engine for ascent only and three engines for descent only. A third design employs the ascent engine during the descent phase of the mission (Figure III.3.2.2-4). In order to supply the necessary volume for living space, the diameter of the lander was increased to compensate for the volume lost to the ascent stage. Since the living and working space on both levels has an annular cross-section, compensations had to be made to provide an amount of useful space. This dictated the need for the new design to actually have more volume than the previous two designs. The volume in this lander's habitat module is about 450 m^3, while in the other two it was about 225 m^3. This design is more volume efficient than the second design, as is illustrated by the figures, and eliminates the second skin on the upper portion of the second design. Due to the increased volume efficiency, this design provides twice the volume as the second design, but has essentially the same structure mass of approximately 8550 kg. The ascent portion of the lander will be connected to the rest of the craft by support beams. When the time comes to return to the supply ship, the ascent module will separate

from the rest of the lander by means of explosive bolts and exit the lander similar to a missile from a silo.

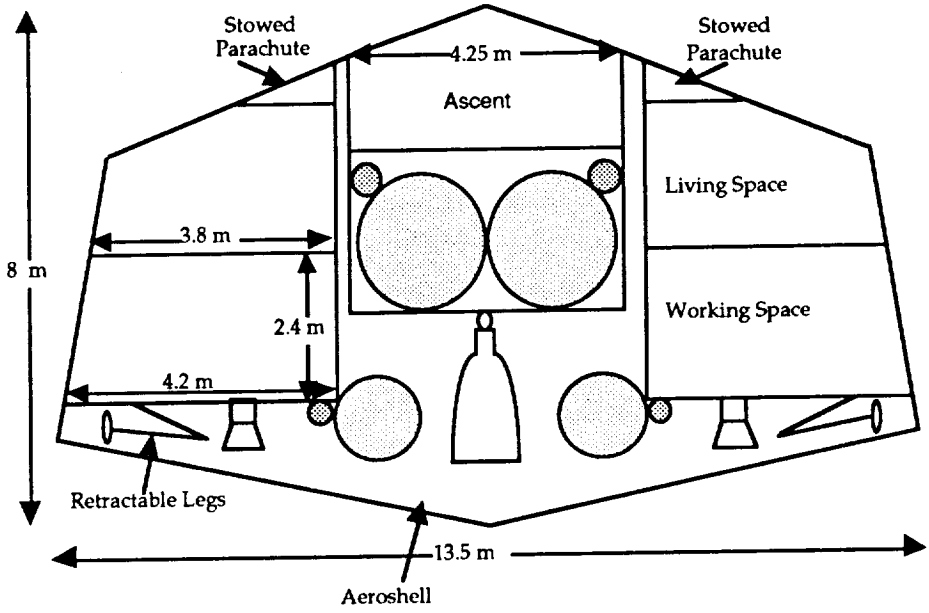

Figure III.3.2.2-4: Third (Final) Lander Design

The first design was removed from consideration due to its requirement that a habitat needed to be constructed on the surface of the planet. A secondary reason for the dismissal of this design is the design of its ascent stage. It is a heavier design than that of the second configuration's ascent module. This alternative design is employed in both of the remaining configurations to be decided between. By bringing the fuel tanks as close together as possible, the base area of the ascent module was minimized. Therefore the drag encountered during its passage from the surface of the planet will also be minimized. This reduction in drag, in addition to the fact that this second design is lighter, made the second design superior to the first. The ascent stage has a mass of about 1150 kg. While the astronauts may be cramped, they will be able to fit into this module for the duration of its flights. The radius of the module is 2.1 m. The astronauts will either lie or be placed in a sitting position on their backs such that they will radiate from the center of the craft like spokes on a wheel.

The third design is the configuration chosen for this mission. The increased volume efficiency, the lower center of gravity which produces a more stable craft during landing, and the ability to use the ascent engine during descent formed the basis for this decision. The use of the ascent engine during descent not only allows for the descent

engines to be smaller and thus lighter, but it also provides a margin for safety in the event of a loss of one of those engines during landing.

The habitat section of the lander will pressurized to one Earth atmosphere. This does not present a problem structurally, as we can see by approximating the craft as a thin-walled cylinder. A radius of 6 meters and a wall thickness of 1mm will not produce a stress that exceeds the tensile strength of Graphite/Epoxy, which is 1660 MPa. We are using a wall thickness of 5 mm to provide structural integrity. The design of the lander must be able to support the weight of the payload and withstand the stresses of entry and, for the ascent module, launch. The support structure for the skin of the lander will be comprised of lightweight hat sections running in the longitudinal direction and intersecting with similar supports that form the circular cross-section of the craft. The fuel and pressure tanks will be supported by a structure that will encompass these tanks and prevent them from damaging themselves due to movement.

III.3.2.2.1 Materials

A low structure mass is desired since the lander must be transported to Mars. Fuel requirements and overall cost increase with mass. Therefore, composite materials will be used to reduce mass. The cost of composites will decrease over the next thirty years as the technology is improved. Thus, the mass savings and the subsequent cost savings will outweigh the higher cost of composite materials in comparison to metals such as aluminum-alloys.

III.3.2.2.2 Weights

The lander/Launcher weight summary is listed in the table below. The weights are based on structure and life support weights, as well as mass iterations between the trajectory code and the propulsion code.

III.3.2.2.3. Deployments

III.3.2.2.3.1 Parachutes

As in the Viking mission, the drag on the parachutes will provide the primary force required to separate the parachute from the lander (Holmberg, Reference 33).

III.3.2.2.3.2 Landing Gear

Landing gear will be stowed under the aeroshell to protect it from reentry heating effects, as well as to avoid the drag effects they would produce if not stowed.

Lander/Launcher Mass Summary

		Launcher		Lander
Structure		1150		7400
Heat Shield				1450
Life Support		1478		7762
Electrical		600		1800
Battery	300		1200	
Harnesses, Dist.	50		400	
Controls	100		100	
TM	50		100	
G&C		422		750
GC's (2)	62			
Aux, Elect.	20			
Controls	60		200	
Propellant	200		400	
Tanks	60		100	
Sensors	20		50	
Propulsion		330		402
Tanks				
Engines				
Science/Surface Eq.				2750
Rovers			800	
Science			1800	
Tools			150	
Braking				920
Parachutes				
Dry Weight		3980		23234
Contingency (10%)		398		2323
		4378		25557
Propellant		16763		4119
Reserves (2%)		335		82
		21476		29758
Launcher				21476
Total Lander				51234
Crew				800
Lander Ignition				52034

III.3.2.3 Electrical
(Kamosa)

III.3.2.3.1 Power

An electrical power source is required for the ascent portion of the lander during the ascent and descent stages of the mission. A critical factor is the power source levels for their trip back to the cargo-ship and Waverider. The minimum trip duration is expected to be 45 minutes. For emergencies, the power will need to last at least 2.5-3 hours. Of the systems available, rechargeable Ni-H2 batteries as shown in Figure III.3.2.3.1-1 (Perez) are the best choice. Ni-H2 batteries are currently used on many long duration satellites. Other battery systems that were candidates for this mission profile were Ni-Cd at a specific energy of 28 W/Kg and 80% efficiencies, and Na-S, which has 120W/Kg specific energy and 85% and efficiency. An Ag-Zn system was also explored. This system attains a 90 W/Kg specific energy and 85% efficiency. The current system on the ascent vehicle will weigh 100Kg and comprise $2m^3$. This system will supply power for the life support system, control, communication, and engine systems (O'Donnell).

The lander vehicle will be utilized as the crew's living quarters for the 3 month stay on the surface of Mars. Power demands can be met by a small nuclear reactor; but due to safety and Martian environmental disposal problems, an alternative set of systems will be utilized. The power system will consist of Ga-As solar arrays during daylight hours in tandem with regenerative fuel cells and Ni-H_2 batteries at night and during dust storm periods. The regenerative fuel cells will be used primarily due to their flexibility with different systems,weight and low cost factors. The solar array system as shown in Figure III.3.2.3.1-2 will be comprised of two 10m by 10m solar panels. Each panel is divided into subpanels 2 m long and 0.5 m wide. The subpanels will consist of 20 of the panel strips. Each subpanel strip will be installed on the structure open to full length and secured. If and when a dust storm approaches, the solar array can be secured if each subpanel is rotated and closed in an accordion like fashion. The system will be similar to Venetian blinds. Each subpanel can be secured easily and quickly. The structure will be comprised of modular pieces of PVC like material. Each array can be assembled easily by two crewmen in a minimal time period. The arrays will then be secured into the Martian soil by means of half-hoop stakes. The entire system will weigh 196.5 Kg and, when stowed on the lander vehicle before deployment, will comprise $4m^3$ of volume. These are critical factors for the lander vehicle.

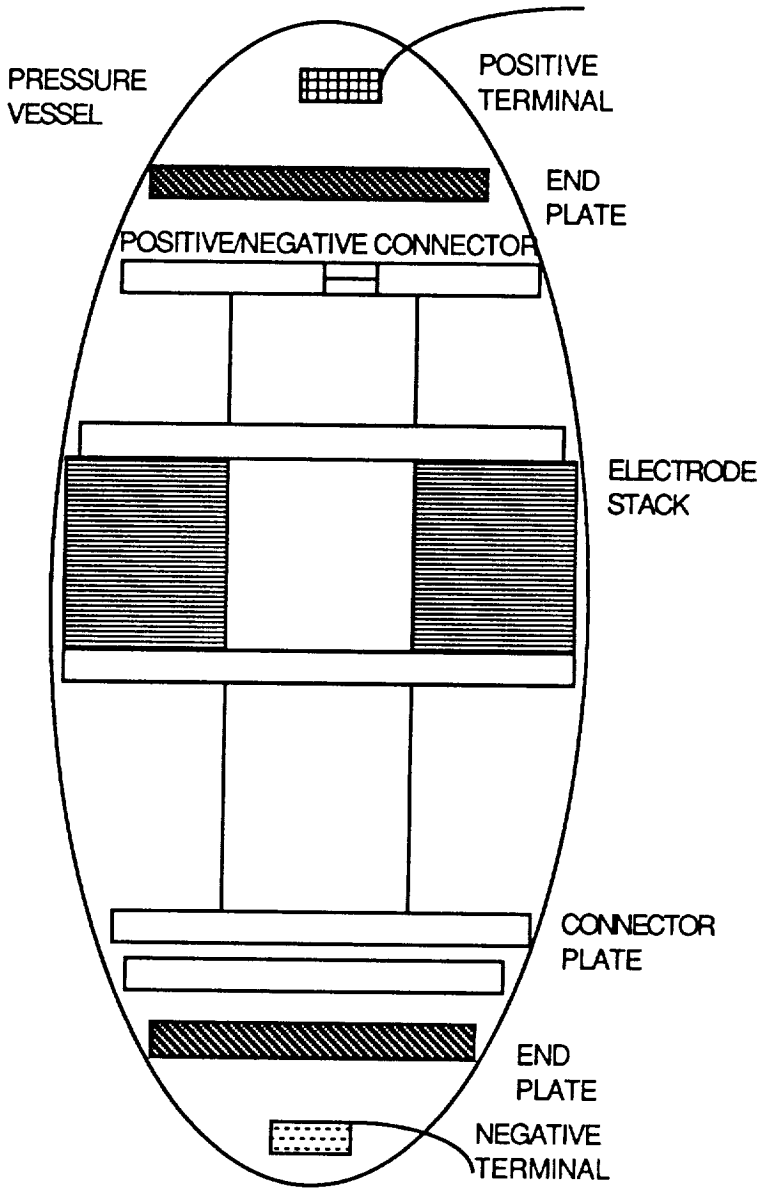

Figure III.3.2.3.1-1: Nickel-Hydrogen Common Pressure Vessel

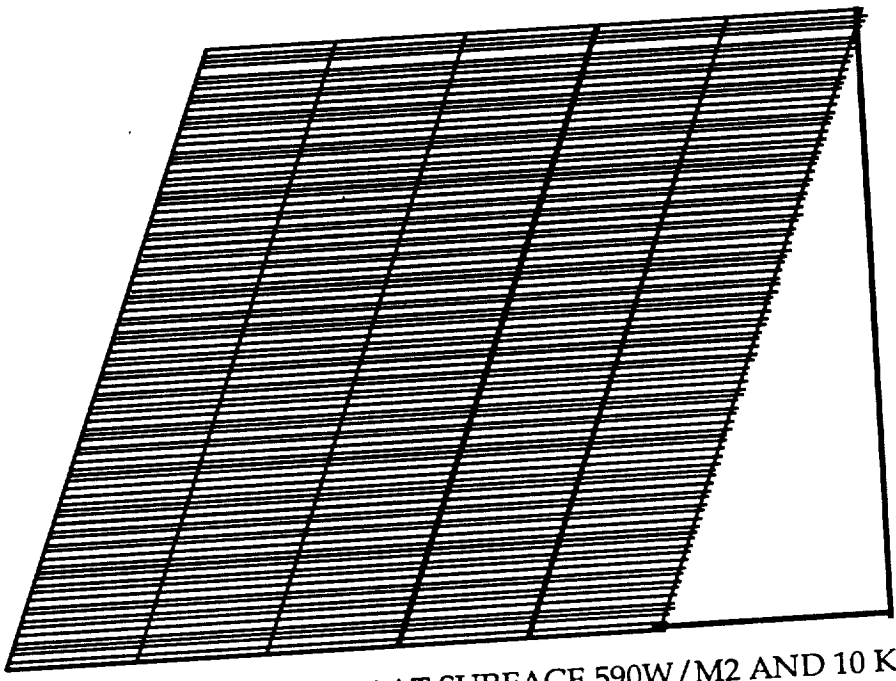

*AVERAGE POWER DENSITY AT SURFACE 590W/M2 AND 10 Kg/KW
*EACH ARRAY 10M*10M SURFACE AREA
*ARRAY RETRACKABLE AND STOWABLE DUING DUST STORMS
*STRUCTURE QUICK AND EASY TO ASSEMBLE

*STRUCTURE WEIGHTS
PANELS+EXTRAS----------126.5 Kg
STOWABLE CONTROL--------20.0 Kg
RIGID STRUCTURE---------- 50.0 Kg
TOTAL----------196.5 Kg

* POWER OUTPUT----------14.75 KW @25.0% EFFICIENCY

Figure III.3.2.3.1-2: Gallium Arsenide Solar Array

At times when the solar arrays can not be used, power will be supplied by regenerative fuel cells (Figure III.3.2.3.1-3) (Roy). The regenerative fuel cells can be categorized into two main areas; the fuel cells and the electrolyzer units. Within these categories, they can be either acid or alkaline electrolyzer systems. Our system will utilize an alkaline fuel cell. The alkaline fuel cell has been shown to be a reliable, lightweight, efficient power source for space and to have: 1) Low specific energy and power (W/Kg and W/Kg), 2) Low energy and power density, and 3) Low reliability forkaline fuel cell. These

items are of primary concern when faced with the mission profiles of the manned Mars mission.

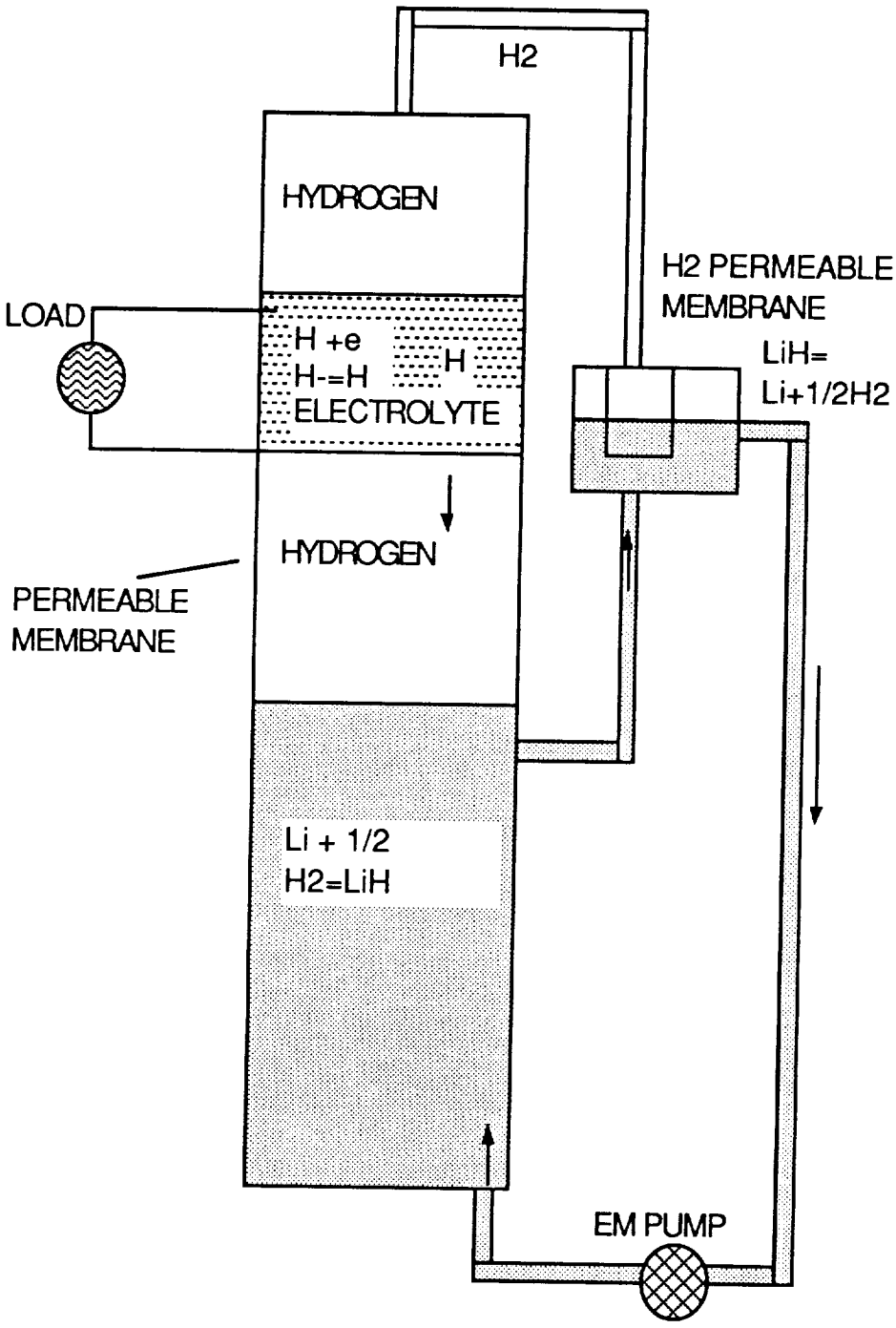

Figure III.3.2.3.1-3: Regenerative Fuel Cell

The basic set-up for this fuel cell system is that the cell consists of two H_2 permeable metallic membranes which contain the hydride transporting

molten electrolyte. The H_2 gas released from the high temperature decomposition of the LiH enters the high pressure side of the cell, and is transported across the membranes and electrolyte. It then reacts with liquid lithium to form LiH in the low pressure side of the cell. The H_2 gas diffusing through the first membrane combines with the electrons to form hydrogen ions. The hydrogen ions are then transported through the electrolyte under the potential gradient and release electrons at the second membrane. The hydrogen atoms diffuse through the metal electrode to react with the liquid lithium. The electrons released at the anode are transported through the load circuit to the cathode electrode to complete the cycle (Roy).

A table of the properties of each of the above power supplies is given in Figure III.3.2.3.1-4 below.

POWER SYSTEMS

VEHICLE	TYPE OF SYSTEM	POWER OUTPUT	SECONDARY SYSTEM	WEIGHT (Kg)	VOLUME (M3)
WAVERIDER	UO2 REACTOR 4 FREE PISTON STIRLING ENGINES	1000 KW	REGENERATIVE FUEL-CELLS	12000	24
CARGO-SHIP	BI-MODAL POWER FROM BOOSTER ENGINE	50-100 KW	SOLAR PANEL	2000	15
LANDER	REGENERATIVE FUEL-CELLS WITH GaAs SOLAR ARRAY	25-30 KW	Ni-H2 BATTERIES	1200	5
ASCENT	Ni-H2 BATTERIES	5-7KW		300	3

Figure III.3.2.3.1-4: Power Systems

III.3.2.4 Guidance and Control
(Kraft)

III.3.2.4.1 Sensors

Special sensors for the landing and launch phases include redundant laser radar (LADAR) altimeters, pressure switches, and g switches. The altimeter is in parallel with a series circuit of the g and pressure switches to provide for actuating parachute deployment at a specified minimum altitude even if pressure and g switch activation is retarded due to environment uncertainties or trajectory variations (McMullen).

The LADAR was chosen over radar altimeter systems due to its high accuracy and its flight proven reliability. The LADAR system will include an aperture on the aeroshell for use before aeroshell ejection and an aperture under the

aeroshell for use after aeroshell ejection. The LADAR data will be used to periodically update and validate the gyro data. LADAR searches will be divided into several altitude modes to prevent false tracking of the ejected parachutes or the ejected aeroshell.

III.3.2.4.2 Inertial Measurement System

The IMS of the LLVM is contained in the Lander/Launcher (LL) and supports the landing and launching phases. The gyros and accelerometers will be located in the ascent portion of the module in order that they may be used on both the ascent and descent portions of the mission. Gyro accuracy was discussed in the WOPM IMS section of this report. The accelerometers will have short term bias stability less than 5×10^{-5}g (Holmberg). The entire IMS should be thermally controlled in order to keep the instruments operating properly and prevent thermal stress failures.

III.3.2.4.3 Guidance Computer

The GC for the LLS will be the same as the one used by the LLVM in its trip from LEO to LMO. It will be located in the ascent module so that it may be used in all phases of the mission. LLVM SS functions will be carried out by the WOPM GC after LLS departure. As is the case for the WOPM and LLVM, the LLS crew can override the GC at any time.

III.3.2.4.4 Attitude Control

The LLS will use an entirely different system than that used by the SS. Four sets of thrusters will be located around the bottom of both the ascent and descent portions of the vehicle. These chemical thrusters will be used in the powered flight phases of the LLS trajectory for docking and attitude control maneuvers. As mentioned in section III.3.2.2.4.2.1, the parachutes are designed such that no interference with the LLS roll capability provided by the thrusters will occur.

III.3.2.4.5 Software

The LLS GC will require software capable of controlling both the ascent and descent trajectories, as well as all functions of the habitat environment during the three month stay on the Martian surface. These functions include data collection, storage, transmission and receipt of data (downlinks and uplinks) by the communications system, and power distribution to various subsystem components by interface with the power subsystem (Holmberg, Vol. I).

III.3.2.5 Life Support
(Crunkleton)

Life Support concerns for the Mars lander are simplified due to the 0.38 g's that the planet has to offer. The procedure will be that four of the married couples will go to the Martian surface while the fifth couple remains in orbit. Even though the duration of the visit to the surface will be short, an emphasis on regenerative systems is still critical. In particular, water must be recovered whenever possible. These and other requirements were considered in developing a life support system to accommodate the needs of the crew.

III.3.2.5.1 Crew Safety

III.3.2.5.1.1 Radiation Shielding
(Crunkleton, Rosenberg)

Two types of radiation are present on the surface of Mars: ultraviolet and ionizing. Since the astronauts will never be exposed directly to the atmosphere, ultraviolet radiation is not a major concern. However, ionizing radiation in the form of solar flares is a major problem(Applebaum). The prediction and warning of threatening solar activity cannot be performed from earth because it will be located on the opposite side of the sun during much of the mission. Therefore, equipment should be placed on the Waverider to constantly monitor the sun, or else a continuous communications network should be provided between lander, Waverider, and Earth.

The solution to solar flare exposure discussed in section III.2.5.1 is fine for use in the Waverider, but it is impractical for the lander. Mars has a weak electromagnetic field and a thin atmosphere, so most of the incident radiation due to a solar flare will make it to the surface. Essentially, there is no practical way to shield the lander. Shielding to protect against solar flares would make the lander too heavy to fly (and land safely). The only reasonable solution seems to be to abort the mission in case of a solar flare that would affect the lander. Remember that 50% of the time while on Mars will be spent in night, so the planet will be between the sun and the lander. Astronomers on Earth can predict a solar flare a few hours before it actually occurs. This means that there would be time for an emergency boost to orbit of the lander. The lander would then dock with the Waverider, and the Waverider would then orient in the safety configuration described earlier (reactor between sun and astronauts). For this abort situation we must accept the fact that some astronauts may be left behind on Mars. Astronomers using computers can predict solar flares approximately 3 hours ahead of time. If the rover is far from the lander, it may not be possible to wait for those astronauts return. However, we see that all the astronauts on the surface

will die from the radiation due to the solar flare. Any of the astronauts that can be saved in this situation must be saved at all costs, even if that means leaving some on the surface (to die in the flare).

III.3.2.5.2 Air System
(Kamosa)

The lander vehicle will employ the same ECLSS system as used on the Waverider vehicle. This system will have one module for a crew of 6 and the other for a crew of 3. This combination allows for cabin leakage and extra oxygen diverted to the EVA suits. This system, when coupled with the algae feed that produces oxygen from the available CO_2 on the Martian atmosphere (Section III.3.2.5.2.1), will enable the astronauts to live and work while on the Martian surface. The weight for the total system will be about 300 kg and comprise 3.0 m^3 of volume. The power consumption will be on the order of 2.5-3 KW. The waste heat from this system will also be utilized for the cabin heating. This system will also supply oxygen for the ascent part of the vehicle during it's ascent and descent phase. Each astronaut will be in their own suit hooked to the cryogenic system on board the ascent vehicle. This part of the vehicle must have a separate system during the ascent phase due to the fact that it will not be connected to the lander part. This system will weigh approximately 75 kg and comprise about 0.4m^3 of volume. While on the surface of Mars, the lander vehicle will keep the ascent vehicle's cryogen tanks operational in case an emergency ascent is required. The amount of oxygen needed for each 8 hour EVA period is 0.55kg of O_2.

III.3.2.5.2.1 Oxygen Supply
(Crunkleton)

The oxygen supply for the crew will be provided by a pressurized atmosphere in the lander itself. An airlock will be provided for exit from the lander to the Martian surface.

Microorganisms may also play a role for the lander due to the ability of the algae spirulina to produce oxygen. A scheme for using algae to produce oxygen has been suggested in which carbon dioxide is forced through an airless closed algae culture. Here, the algae is fermented, and the residue is recycled (Pirt). Oxygen comprises 80% of the gas output of this system, and the yield of algal biomass to oxygen is 1:2. Growing this culture will require a leak proof chamber and a carbon source, namely carbon dioxide recovered from the cabin spaces. Spirulina requires a 0.2 to 0.05 molar sodium bicarbonate mineral medium at pH of 8-11. A regular fluorescent bulb may serve as the necessary light source. The culture should be kept at about 35°C (Gant). Note that this system will only provide a supplemental oxygen supply. The intention is to have a source that can replace the amount of oxygen that escapes through cabin leaks. The main worry about this system is

in keeping an axenic (unicellular) environment. If the culture were to be contaminated by some other organism, the system would be in competition and start to consume oxygen instead of producing it. An incubator has been devised that weighs about 36kg that can grow this algae. Based on the systems ability to produce 2.5kg of oxygen per day, the total lander weight could be reduced by 189kg for the three month mission (Zinc).

III.3.2.5.3 Habitat Design
(Crunkleton)

The lander will have two levels. The upper deck will be the private quarters and contain the bathroom; the lower deck will have work stations and the galley. The diagram for the upper level shows the four double beds for the four couples (Figure III.3.2.5.3a). The beds will be hinged so that more work space can be created during the day. Initially the plan was to have two bathrooms aboard the lander, but due to weight constraints and lack of space we settled for one. Figure III.3.2.5.3b diagrams the lower level, including a galley unit which will contain a washer, dryer, microwave oven, sink, trash compactor, refridgerator, freezer, and storage space. This level will contain the airlock for outside excursions as well as work space, an exercise area and storage space for the EVA suits.

Life Support Weights For The Mars Lander

	Total Weight (kg)
Food (solids)	712
Water*	2000
Bathroom (sink,toilet,shower)	102
4 Double Beds	180
Galley Unit (see Lower Level)	500
Astronauts (4 men, 4 women)	410
	3904

*Based on a regenerative water processing system where 1500kgs can not be recovered due to evaporation, urine, feces.

While on Mars, the astronauts will collect rock and soil samples from different depths in order to determine composition and water content. Our trip to Mars will most likely be a precursor to a permanent base, and this mission will have to show us how well people can adapt to the environment. Therefore, the need to assess Mars' resource potential is the most critical for this mission.

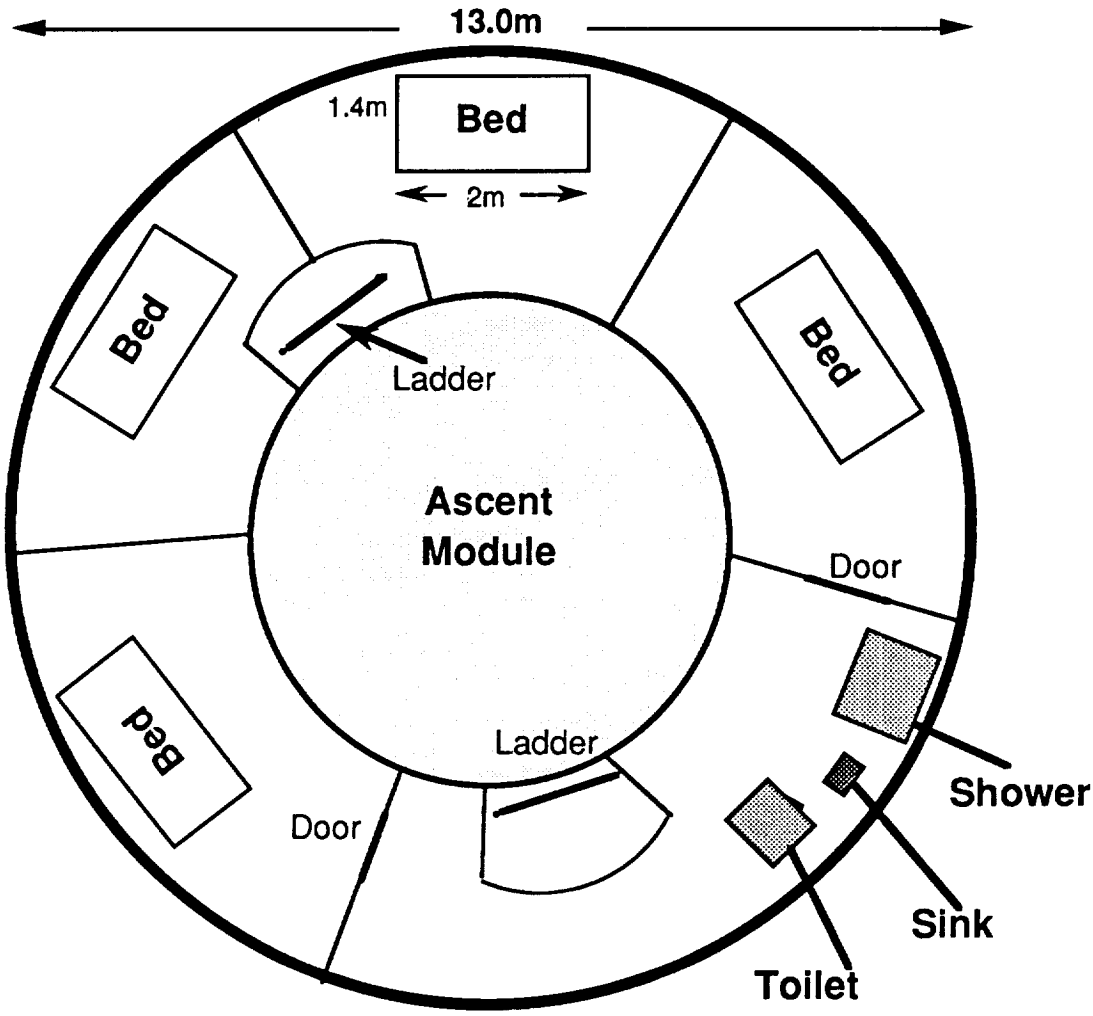

Figure III.3.2.5.3a Upper Level Layout

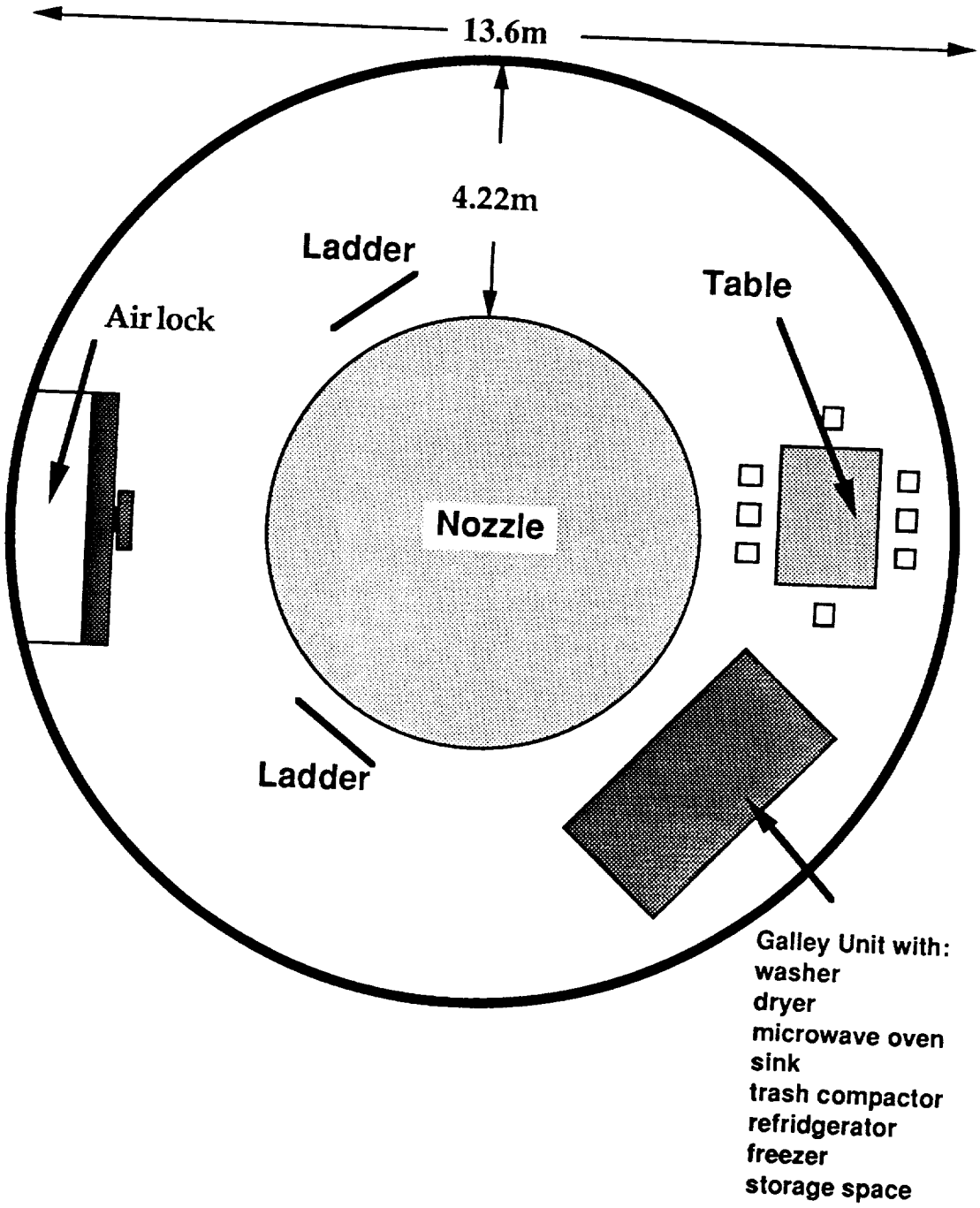

Figure III.3.2.5.3b Lower Level Layout

III.3.2.5.4 Pressure Suits
(Rosenberg)

There is much research presently being done to advance the state-of-the-art in pressure suit design. We are currently estimating a weight of 23 kg per suit for our mission. These suits should be extremely flexible to allow the astronauts to work quickly and efficiently in the Martian environment.

III.3.2.5.5 Water Requirements
(Crunkleton)

The water supply for the lander needs to be connected to a regenerative system in order to reduce the overall weight of the water and necessary equipment. When determining the amount of water required, the water that cannot be recovered must be taken into account. This includes water that will escape through evaporation and from cabin leakage. Also, the water from human waste, such as feces, will not be recycled.

The water processing will occur by a static-feed electrolysis system. The electrolysis package will be kept at 340K by active thermal control. Electrical energy should be supplied at the rate of 17 MJ/kg of water electrolyzed. The fluid pressure of 1240 kPa for this system is the highest water pressure in the life support system (Cullingford). All fixtures in the bathroom and the galley will be connected to this system. Also, the toilet, sink and shower will have a slight vacuum in order to help with recovery. Even though there is some gravity to help with the plumbing, water should be vacuumed from the pipes in order to cut down on bacterial growth.

Water for hygiene will cause the biggest strain on the system, so conservation should be stressed. The astronauts will be allowed to shower five out of six days. The sixth day will be designated as laundry day. A continuous flow rate of 1.3 kg/hr can be expected with the system, and these measures should not interrupt this flow.

III.3.2.5.6 Food Requirements
(Crunkleton)

When determining the amount of food that will be needed for the three months on Mars, one needs to take into account that a human requires about 3000 kcal of releasable energy per day. These calories come from 14.6% protein, 31.0% fat, 54.4% carbohydrates, and essential vitamins and minerals (such as calcium, sodium, potassium, iron, magnesium, copper, and zinc) (Stadler, et. al.). The diet for the astronauts on Mars will not change from that on the Waverider.

The food will be onboard the supply ship for about 265 days before the lander descends to Mars so packaging the food for safe arrival is a critical concern. There are many forms of packaged food available for space travel, such as dehydrated (having water removed), freeze dried (vacuum drying in a frozen state), thermostabilized (cooked at moderate temperatures and sealed in cans), irradiated (preserved by exposure to ionizing radiation), intermediate moisture process (removing part of the water), and natural (food in its natural form) (Andrews, et. al).

Food in its natural form would not be a viable solution due to the length of the mission. However, consideration was given to having the astronauts grow and harvest their own food. Since the lander does not have much free space, large plants are out of the question, but microorganisms, namely algae, could be grown with minimal space. This form of food production is called Single Cell Protein (SCP) or using microorganisms as a source of protein (Boston). The advantage of the SCP system lies in the fact that a single culture can proliferate in a very short time (several hours) and, once partially removed, the culture will continue to grow. In addition, the starter cultures can be purchased cheaply and only require refrigeration for storage. The disadvantages are that part of the organisms are not digestible, nor are they very palatable. Therefore, something would have to be done to the collected protein to make it edible. Even though growing their own food may be a morale booster for the astronauts, the disadvantages outweigh the advantages and we will not choose SCP as a source of food.

IV.1 Communications
(Hurtado)

Terp Tech's philosophy relative to communications is to keep the ground crew in contact with the flight crew as long as possible. The LLVM will be directed by Mission Control and thus needs to be in contact with Earth at all times. Communications with the Waverider must be lost during the AGA at Venus and during aerobraking at Mars. However, the AGA is estimated to take only 10 minutes, and the aerobrake will take 15 minutes at most. Thus, for a year-long mission the only known blackout time is 25 minutes. At this time, no means of communicating with vehicles entering the atmosphere is known.

LLVM The LLVM must carry a sophisticated communications system. It will be used as a platform to do in-depth studies of Mars' geology, meteorology, and atmosphere before the Waverider arrives. It is essential that this information be transmitted back to Earth in a quick and quality manner. When the Lander is on the surface, the Supply Stage will act as a relay station and as an advance warning system for changes in Martian meteorology and solar flares.

Waverider Communications, as the only link of the crew to Earth, will be fundamental to completing the mission. Should there be a problem with communications, crew morale will suffer. Especially before the critical maneuvers - AGA and aerobrake - the crew will compare instrument readings with Ground Control. Here, lag time is a significant problem. The maximum lag time will be 20 minutes, but the combination of lag and AGA blackout time will result in longer periods without communication.

The M^3 system must be light, low in power consumption, able to handle large amounts of data, transmit with minimal error, and be reliable. With recent progress in electronics, these goals can be met.

V. Cost
(Kraft)

Cost for the Manned Mars Mission was estimated primarily from Reference 31 (Hoffman), which provides costs for a Mars mission similar to M^3 with similar hardware complexity. Reference 58 (Stuart) provides costs of delivery of payload to Mars by a number of launch vehicle/stage combinations.

Figure V-1 presents the cost estimates of Reference 31, except that costs have been adjusted for inflation from 1984 dollars to 1990 dollars (inflation of 1.282 based on the NASA Inflation Index). This figure serves as a reference for certain of the M^3 costs shown in Figure V-2 and determined as follows (all costs in 1990 dollars):

Waverider The Waverider is similar in complexity and function to the STS Orbiter, which had a development cost of $21.8 Billion The Waverider cost was determined by scaling the Orbiter development cost by mass. The production cost is taken as the cost of the outbound vehicle of Figure V-1.

Other Hardware Costs of the LLVM and the WOPM Departure Stage were determined by scaling costs from Figure V-1 by mass. With the exception of certain life support systems, hardware is assumed to be developed prior to the M^3 flight.

Launch Performance to low Earth orbit and vehicle cost data are shown in Figure V-3 for a number of expendable launch vehicles. The WOPM and LLVM would be launched into LEO by a large expendable vehicle. Reference 58 selected STS/Centaur G' as most cost effective, but STS costs were subsidized at the time the paper was written, and NASA policy has changed to utilize expendable vehicles unless crew participation is essential.

On-Orbit Assembly and Test Cost is taken from Figure V-1.

Operations Cost from Figure V-1 was scaled for operation time.

Management Cost was taken as ten percent as in Figure V-1.

In summary, the total program cost, shown in Figure V-2, is $105 Billion. This compares to $96 Bilion development cost for the Apollo Program.

Figure V-1

Reference 31 Cost Estimate
Manned Mars Mission (Crew of Four)

	Mass, kg	Cost, $B
Outbound Vehicle	38546	4.62
Orbiter/Rendezvous Vehicle	19545	2.69
Mars Lander Vehicle	54141	7.69
Earth Return Vehicle	38175	3.08
Launch Adapters (2)	676	0.26
STS (18 launches)		2.56
Upper Stages		4.10
On-Orbit Assembly and Test		8.97
Operations (3 years)		10.90
Management (10%)		4.49
Total		49.36

Figure V-2

M^3 Cost

	Mass, kg	Cost, $B
Waverider Development		21.79
Waverider Production	300,000	36.00
Supply Stage	49,880	6.87
Lander/Launcher/Habitat	52,100	7.40
Booster (2 required)*	26,000	3.08
Launch Adapters	1014	0.39
Launch Vehicles (454994 kg @ $9000/kg)		4.09
On-Orbit Assembly and Test		8.97
Operations (2 years)		7.27
Management (10%)		9.56
Total		105.15

* Dry booster weight (each booster) is 130,000, and fueled mass is 556,440 kg. However, tanks are salvaged STS external tanks, so that only ten percent of mass is assumed for cost. For launch vehicle mass-to-orbit requirements, a total of 1,112,880 kg was assumed for two fueled boosters (Section II.2.1.1)

Figure V-3

Cost and Performance of Expendable Launch Vehicles

Vehicle	Performance to LEO, kg	Est.Cost, $M	$/kg
Delta II	5035	45	8900
Atlas IIA	7000	85	12100
Titan IIIT	15000	150	10000
Titan IV	22200	200	9000

VII Summary
(Hurtado)

In summary, Terrapin Technologies has met the requirements of the RFP as demonstrated by the following key features of the proposed design:

Minimum Time of Crew Flight The Waverider trajectory selected allows the crew to reach Mars in 135 days, 125 days earlier than the arrival time for a Hohmann trajectory.

Minimum Cost The boosters for both the LLVM and WOPM vehicles are of the same design, and both return to Earth so that they may be reused in future missions. The dual flight design, with the WOPM and LLVM flying separately to Mars, allows reduction in the size and volume of the more complex manned Waverider. Regenerative life support systems reduce the amount of life support supplies needed on the mission. Terp Tech is certain that the country will be willing and able to support such a mission fiscally and spiritually.

Feasibility in the Time Scale Proposed The mission has been planned as if it were the *first* Manned Mars Mission. A nuclear engine will be proven technology in the early twenty-first century. Composites will be sufficiently advanced and affordable for these types of missions.

Journey Compatible with Humans The guiding principle behind the *entire* mission design is the safety and comfort of the crew. Sleeping, eating, resting, and working habits of the crew were considered carefully. The design focuses on the facts that this is a manned mission and that it is crucial that the crew return safely.

Stretching the Technology Envelope Terrapin Technologies has proven that a Waverider can be built, flown, and equipped for a crew and that solid reactor rockets can be used to explore the inner solar system. With these two technologies, the exploration of the planets lies within our grasp.

VI References

1. Alburn University Aerospace Engineering Department, "Proposal for a Zero-Gravity Toilet Facility for the Space Station", June 1989.

2. Anderson, John D., Hypersonic and High Temperature Gas Dynamics,New York: McGraw-Hill, Inc., 1989, pp. 291.

3. Anderson, J., Lewis, M., and Kothari, A., "Hypersonic Waveriders for Planetary Atmospheres", AIAA Paper No. 90-0538, 1990.

4. Andrews and Kirschenbaum, Living in Space: Book Two, 1987.

5. Applebaum, Joseph and Flood, Dennis, Solar Radion on Mars. NASA Technical Memorandum, August 1989.

6. Barattino, William J et al, "A Coupled Radiation Transport-Thermal Analysis of the Radiation Shield for an SP-100 Type Reactor", Space Nuclear Power Systems 1985, Vol IV, pg 287-302.

7. Boltax A. et al, "SP-100 Fuel Pin Performance Analysis", Space Nuclear Power Systems 1985, Vol III, pg 81.

8. Borowski, Stanley K., *Nuclear Thermal Rockets: Next Step To Space*, "Aerospace America", pg. 16, June 1989.

9. Boston and Penelope, Critical Life Sciences Issues for a Mars Base.

10. Botts T.E. et al "A Biomodal Reactor for High and Low Space Power", Space Nuclear Power Systems 1985, Vol III, pg 257-263.

11. Buden, David, "Mars Mission Safety", Aerospace America, pg. 22, June 1989.

12. Butler, George V., Working in Space, American Institute of Aeronautics and Astronautics, New York, NY, 1981.

13. Cullingford, Hatice S, "Method and Apparatus for Bioregenerative Life Support Systems" NASA Johnson Space Center, July 1989.

14. Cavoti, C. R., "On Range and Aerodynamic Heating Optimality for Lifting Planetary Entry in a Class of Hypervelocity Orbits", Dynamics of Manned Lifting Planetary Entry, Wiley & Sons, p 408, 1963.

15. Cheng, G.J., and T.G. Tracy, "The Mars Observer: Attitude and Articulation Control System", Guidance and Control 1988, *Advances in*

the Aeronautical Sciences, Vol. 66, American Astronautical Society, San Diego, CA, p 13, 1988.

16. Compton, W. David, Charles D. Benson., Living and Working in Space, The NASA History Series, 1983.

17. Crocker, M.J. , P.K Raju, E. Christensen, et al, "Structural Vibrations of Space Station Power Systems," Space Structures Power Conditioning, Vol. 871, 1988.

18. Cross, D.B., and Butts, A.J., "Manned Mars Mission Landing and Departure Systems", The Case for Mars, AAS Science and Technology Series, Volume 57, 1981, pp 75-81.

19. Cullingford, Hatice S., "Method and Apparatus for Bioregenerative Life Support Systems", NASA Johnson Space Center, July 1989.

20. Dennison, E.W., Stanton, R.H., and Shimada, K., "The Development of a Charge-Coupled Device Tracker for Spacecraft", Advances in Astronautical Sciences, Volume 63, AAS 87-007, pp 117-137.

21. Dotts, R.L. , H.H.Battely, J.T.Hughes, W.E. Neuenschwander., "Shuttle Orbiter Reusable Surface Insulation," Progress in Astronautics and Aeronautics, Vol.85, 1982.

22. El-Genk, Mohamad S et al, "Trends and Limits in Upgrading of SP-100 Baseline Design of Nuclear Powered Space Systems", Space Nuclear Power Systems 1985, Vol IV, pp 273-284.

23. Elikan, Leonard (editor), Aerospace Life Support, American Institute of Chemical Engineers, New York, NY, 1966, pp 1-9.

24. Fraser, Wilson M. Jr., "Space Shuttle Mission Extension Capability," Space Systems Technology, Sp-593, 1984.

25. Fredrickson, A.R., D.B.Cotts, J.A.Wall, F.L.Bouquet., "Spacecraft Dielectric Material Properties and Spacecraft Charging," Progress in Astronautics and Aeronautics, Vol.107, 1986.

26. Gant, Elizabeth, Professor at the University of Maryland Botany Department. From a phone conversation, 17 April 1990.

27. Greger, Gottfried, "Spacelab Mission Plans," Advances in the Astronautical Sciences, Vol. 37, 1978.

28. Grey, Jerry, Beachheads in Space: A Blueprint for the Future, Macmillan, 1983.

29. Haffner, James W. , " Radiation and Shielding in Space," Nuclear Science and Technology, 1967.

30. Hill, Philip G. and Peterson, Carl R., Mechanics and Thermodynamics of Propulsion, Addison-Wesley Publishing Company: Reading, Mass., 3rd printing, 1970.

31. Hoffman, Stephen J., and Soldner, John K., Concepts for the Early Realization of a Manned Mission to Mars, The Case for Mars II, AAS Science and Technology Series, Vol. 62, 1984, pp.377-390.

32. Hoffmann, Hans E. W., "Eugen Sanger Memorial Lecture," Advances in the Astronautical Sciences, Vol. 56, 1984.

33. Holmberg, Neil A., Robert P. Faust, and H. Milton Holt, Viking '75 Spacecraft Design and Test Summary: Volume I - Lander Design, NASA Langley Research Center, Hampton, VA, 1980, p 84-101.

34. Hunten, D.M., L. Colin, T.M. Donahue and V.I. Moroz, ed. Venus. Tuscon: University of Arizona Press, 1983.

35. Kaplan, Marshall H., Modern Spacecraft Dynamics and Control, New York: John Wiley & Sons, Inc., 1976, pp. 109-115.

36. Kaplan, Marshall H., Space Shuttle: America's Wings To The Future., Aero Publishers, Inc., Fallbrook, CA, 2nd edition, 1983.

37. Koelle, Heinz H.(editor), Handbook of Astronautical Engineering, McGraw-Hill, New York, 1961, Chapter 26.

38. Keathley, W. C. , "Apollo Telescope Mount Experiments," Skylab and Pioneer Report, Science and Technology Series, Vol. 46, 1974.

39. Kerry, Mark Joels, Gregory P. Kennedy., " The Space Shuttle Operator's Manual," Ballantine Books,1988.

40. Lademann, Ernest E.,"Gyro Technology", Guidance and Control 1988, *Advances in the Aeronautical Sciences*, Vol. 66, American Astronautical Society, San Diego, CA, p 221-31, 1988.

41. Langton, N. H., The Space Environment, University of London Press Ltd., London.

42. Levine, Philip, "The Dynamics and Flight Environment of Lifting Vehicles Entering the Atmospheres of Earth, Mars, and Venus," Dynamics of Manned Lifting Planetary Entry, Wiley & Sons, p 349, 1963.

43. Lewis, M.J. and A.P. Kothari. "The Use of Hypersonic Waveriders for Planetary Exploration." August 1989.

44. Loftus, Joseph P. Jr, "Space Station Initiates Permanent Space Facilitiy Development" Space Nuclear Power Systems 1985 Vol III, pg 23.

45. Lyndon B. Johnson Space Center, Space Shuttle., Scientific and Technical Information Office, NASA, Washington DC, 1976.

46. McMullen, J.C., and Smith, A.M., "Martian Entry Capsule: Design Considerations for Terminal Deceleration", Dynamics of Manned Lifting Planetary Entry, Wiley & Sons, p 349, 1963.

47. McDonnell Douglas Company presentation, March, 1990.

48. Meffe, Marc,"Control Moment Gyroscope Configurations for the Space Station", Guidance and Control 1988, *Advances in the Aeronautical Sciences*, Vol. 66, American Astronautical Society, San Diego, CA, p 271-6, 1988.

49. Mensing, Arthur E., "Gas-Core Technology", Aerospace America, pg. 25, June 1989.

50. Merigan M.A. "Heat Pipe Technology Issues", Space Nuclear Power Systems, 1985, Vol I, pg 419.

51. National Aeronautics and Space Administration Technical Reports: NASA N88-14856, NASA SP-400, NASA SP-483.

52. Oberg, James E., Mission to Mars: Plans and Concepts for the First Manned Landing, Stackpole Books, Harrisburg, PA, 1982.

53. Perez F.A. et al, "Design Considerations Related to Nickel Hydrogen Common Pressure Vessel Battery Modules", 21st Intersociety Energy Conversion Engineering Conference, Vol III, pg 1554-9.

54. Pirt, S. J., Microbial Photosynthesis as a Route to Renewable Sources of Energy, Food and Carbon Material, Presented at IUPAC Conference, 1979.

55. Roy P. et al, "HYTEC- Hydrogen Thermo-Electrical Chemical Converter", 23rd Intersociety Energy Conversion Engineering Conference, Vol II, pg 287.

56. Seiff, A., "Post-Viking Models for the Structure of the Summer Atmosphere of Mars", [Kliore, A. (editor)], The Mars Reference Atmosphere, *Advances in Space Research, the Official Journal of the Committee on Space Research (COSPAR)*, v. 2, n.2, Pergamon Press, 1982, pp. 3-17.

57. Stadler, Rapp, Bourland, and Foley, Space Shuttle Food Systems Summary, December 1988.

58. Stuart, James R., and Coffey, Randall E., "Analysis of Delivery Capabilities and Costs to Low Mars Orbits Applying Current Technology Launch/Retro Propulsion Systems, The Case for Mars II, AAS Science and Technology Series, Vol. 62, 1984, pp.391-417.

59. Tauber, M. and Yang, L., "The Heating Environment During Martian Atmospheric Descent", AIAA Paper No. 88-2671, 1988.

60. Tauber, M., Bowles, J., and Yang, L., "Atmospheric Maneuvering During Martian Entry", 88-4345-CP, 1988.

61. Tauber, M., Bowles, J., and Yang, L., "The Use of Atmospheric Braking During Mars Missions", AIAA Paper No. 89-1730, 1989.

60. Vaughn, James W. Jr , "Nuclear Power Applications in Future Space Activities", Space Nuclear Power Systems 1985, Vol III, pg 13.

61. Wilkerson, Thomas D. , Michel Lauviente, Gerald W. Sharp., "Space Shuttle Environment," 1984.

62. Zinc, "Incubator for Cell Culturing Under Microgravity", 1989.

Acronyms

ACS	Attitude Control System
ALS	Advanced Launch System
DGCMG	Double Gimbal Control Moment Gyro
DSN	Deep Space Net
GC	Guidance Computer
IMS	Inertial Measurement System
LEO	Low Earth Orbit
LL	Lander/Launcher
LMO	Low Mars Orbit
LLVM	Lander/Launcher Vehicle Module
MMII	Mariner Mark II
MTBF	Mean Time Between Failures
ORU	Orbital Replacement Unit
PMRIG	Permanent Magnet Rate Integrating Gyro
POCC	Payload Operations Control Center
REA	Research and Education Association
RFP	Request for Proposal
SGCMG	Single-Gimbal Control Moment Gyro
WOPM	Waverider Orbital Personnel Module
4πSS	Four Pi Steradian Sun Sensor

Appendix A

Aerogravity Assist Code

(Bryant)

```
C
C     ANALYSIS OF AER0-GRAVITY ASSIST MANEUVER
C
C     HEATHER  BRYANT
C
C
C     DEFINITION OF VARIABLES
C
      INTEGER I,J
      REAL LD, VIN, AREA, THETA, CL, MASS, DELTA
      REAL RHO, LIFT, NU, RADIUS, DELTA1, DELTA2, VINF1
      REAL VCIRC, VOUT, G, MV, ALT, DTHETA, VNORM, DALT
      REAL NUM, TALT, TTHETA, VESC, VINF2
      G=6.67E-11
      MV=4.88E+24
C
C     CALCULATION OF LIFT
      WRITE (*,*) 'INPUT THE WAVERIDER MASS IN KGS'
      WRITE (5,*) 'INPUT THE WAVERIDER MASS IN KGS'
      READ (*,*)  MASS
      WRITE (5,*) MASS
      WRITE (*,*)  'INPUT INCOMING VELOCITY IN KM/SEC'
      WRITE (5,*)  'INPUT INCOMING VELOCITY IN KM/SEC'
      READ (*,*) VIN
      WRITE (5,*) VIN
      VIN=VIN*1000.0
      NU=G*MV
      ALT= 0.0
      WRITE (*,*) 'INPUT AREA OF WAVERIDER IN SQUARE METERS.'
      WRITE (5,*) 'INPUT AREA OF WAVERIDER IN SQUARE METERS.'
      READ (*,*) AREA
      WRITE (5,*) AREA
      WRITE (*,*) 'INPUT LIFT COEFFICIENT FOR THE WAVERIDER.'
      WRITE (5,*) 'INPUT LIFT COEFFICIENT FOR THE WAVERIDER.'
      READ (*,*) CL
      WRITE (5,*) CL
      I=0
      J=0
5     RADIUS=6.161E+6 + ALT
      TALT=ALT
      LIFT=MASS*((VIN**2/RADIUS)-(NU/RADIUS**2))
C     CALCULATION OF DENSITY
      RHO=(2*LIFT)/(VIN**2*AREA*CL)
C     CALCULATION OF ALTITUDE FROM  DENSITY VALUE
      IF (RHO .GT. 151 .OR. RHO .LT. 5.32E-08) THEN
      WRITE (*,*) 'VALUE OF DENSITY IS TOO HIGH OR TOO LOW.'
```

```
      WRITE (5,*) 'VALUE OF DENSITY IS TOO HIGH OR TOO LOW.'
      GO TO 35
      ENDIF
      ALT=(57.629-10.158*LOG10(RHO))*1000.0
      DALT=ABS(ALT-TALT)
      I=I+1
      IF(DALT.GE.10.0) GO TO 5
      WRITE(*,8) I
      WRITE(5,8) I
    8 FORMAT (/,'I= ',I2,'  (NO. OF ITERATIONS FOR ALTITUDE)',
     ~/)
      WRITE (*,10) LIFT
      WRITE (5,10) LIFT
   10 FORMAT ('LIFT =', F12.3,'  NEWTONS',/)
      WRITE (*,15)  RHO
      WRITE (5,15)  RHO
   15 FORMAT ('DENSITY =',F12.8,'  KGS PER CUBIC METER',/)
      ALT=ALT/1000.0
      WRITE (*,20)  ALT
      WRITE (5,20)  ALT
   20 FORMAT('ALTITUDE=',F7.3, '  KM',/)
      RADIUS=6.161E+6 + ALT*1000.0
C     CALCULATION OF FINAL VELOCITY
      WRITE (*,*) 'INPUT TOTAL DEFLECTION ANGLE IN DEGREES'
      WRITE (5,*) 'INPUT TOTAL DEFLECTION ANGLE IN DEGREES'
      READ (*,*) DELTA
      WRITE (5,*) DELTA
      DELTA=DELTA*3.1415926/180.0
      WRITE(*,*) 'INPUT WAVERIDER LIFT-TO-DRAG RATIO'
      WRITE(5,*) 'INPUT WAVERIDER LIFT-TO-DRAG RATIO'
      READ(*,*) LD
      WRITE (5,*) LD
      VINF1= ((VIN**2 - 2.0*NU/RADIUS)**0.5)/1000.0
      WRITE (*,22) VINF1
      WRITE (5,22) VINF1
   22 FORMAT ('VINF1 = ',F12.7,'KM/SEC',/)
      VINF1 = VINF1*1000.0
      VCIRC=(NU/RADIUS)**0.5
      VESC=((2.0)**.5)*VCIRC
      VNORM=VINF1/VCIRC
      DELTA1=ASIN(1.0/(1.0+VNORM**2))
      THETA = DELTA - 2.0*DELTA1
   25 DELTA2=ASIN(EXP(2.0*THETA/LD)/(1.0+VNORM**2))
      TTHETA=THETA
      THETA=DELTA-(DELTA1+DELTA2)
      WRITE (*,*) 'THETA',THETA
```

```
      DTHETA=ABS(THETA-TTHETA)
      J=J+1
      IF(DTHETA.GE.0.0087266) GO TO 25
      WRITE(*,27) J
      WRITE(5,27) J
27    FORMAT ('J= ',I2,'  (NO. OF ITERATIONS FOR THETA)',/)
      NUM=EXP(-2.0*THETA/LD)
      VOUT=((((NUM*VIN**2)-(NUM-1.0)*NU/RADIUS))**0.5)
     ~/1000.0
      VINF2= (((VOUT*1000.0)**2 - 2.0*NU/RADIUS)**0.5)/1000.0
      VCIRC=VCIRC/1000.0
      VESC=VESC/1000.0
      THETA=THETA*180.0/3.1415926
      DELTA1=DELTA1*180.0/3.1415926
      DELTA2=DELTA2*180.0/3.1415926
      WRITE(*,28) THETA,DELTA1,DELTA2
      WRITE(5,28) THETA,DELTA1,DELTA2
28    FORMAT('THETA= ',F6.2,' DEGREES',/,'DELTA1=',F6.2,' DEGREES',
     & /,'DELTA2= ',F6.2,' DEGREES',/)
      WRITE (*,29) VCIRC, VESC
      WRITE (5,29) VCIRC, VESC
29    FORMAT ('VCIRC =',F6.3,' KM/SEC',/,'VESC =',F6.3,' KM/SEC',/)
      WRITE (*,30) VOUT
      WRITE (5,30) VOUT
30    FORMAT ('FINAL VELOCITY =', F6.3,'  KM/SEC',/)
      WRITE (*,32) VINF2
C     WRITE (5,32) VINF2
      WRITE (5,*)' FINAL VINF=',VINF2
32    FORMAT ('FINAL VINF =',F6.3,' KM/SEC')
      VINF1=VINF1/1000.
      WRITE(*,*)' VINF1=',VINF1,' VINF2=',VINF2,' DELTA=',DELTA
      DV=((VINF1)**2.0+VINF2**2.0-
     &    (2.0*VINF1*VINF2*COS(DELTA)))**0.5
      WRITE (*,*) 'DELTA V = ', DV
      WRITE (5,*) 'DELTA V = ', DV
35    STOP
      END
```

Appendix B

Mars Aerocapture Code

(Seybold)

```
C
C  CALINA'S PROGRAM 1
C
C  DETERMINE THE AEROBRAKE CORRIDOR FOR THE MARTIAN ATM
C
C  DEFINITION OF VARIABLES
C
      REAL ALT, MASS, AREA, VEL, VELCIR, CL, CD, DECEL, GEES
      REAL LOVRD
      REAL RADIUS, RHOEST, RHOOVR, RHOUND, HIALT, LOWALT
      REAL N, M, CORIDR, A, AVE, RHOFLY, FLYAT
C
C  OVERSHOOT BOUNDARY
C
      WRITE (*,*) 'INPUT AN ALTITUDE IN KM'
      WRITE (5,*) 'INPUT AN ALTITUDE IN KM'
      READ (*,*) ALT
      WRITE (5,*) ALT
      N=1
      WRITE (*,*) 'INPUT THE MASS OF THE WAVERIDER IN KG'
      WRITE (5,*) 'INPUT THE MASS OF THE WAVERIDER IN KG'
      READ (*,*) MASS
      WRITE (5,*) MASS
      WRITE (*,*) 'INPUT THE AREA OF THE WAVERIDER IN M2'
      WRITE (5,*) 'INPUT THE AREA OF THE WAVERIDER IN M2'
      READ (*,*) AREA
      WRITE (5,*) AREA
      WRITE (*,*) 'INPUT THE APPROACHING VELOCITY IN M/S'
      WRITE (5,*) 'INPUT THE APPROACHING VELOCITY IN M/S'
      READ (*,*) VEL
      WRITE (5,*) VEL
      WRITE (*,*) 'INPUT THE RADIUS OF MARS IN M'
      WRITE (5,*) 'INPUT THE RADIUS OF MARS IN M'
      READ (*,*) RADIUS
      WRITE (5,*) RADIUS
      WRITE (*,*) 'INPUT THE CIRCULAR VELOCITY OF MARS IN M/S'
      WRITE (5,*) 'INPUT THE CIRCULAR VELOCITY OF MARS IN M/S'
      READ (*,*) VELCIR
      WRITE (5,*) VELCIR
      WRITE (*,*) 'INPUT A NEGATIVE LIFT COEFFICIENT'
      WRITE (5,*) 'INPUT A NEGATIVE LIFT COEFFICIENT'
      READ (*,*) CL
      WRITE (5,*) CL
```

```
      RHOOVR=((2*MASS)/(RADIUS*CL*AREA))*(((VELCIR/VEL)**2)-
     1)
   10 IF (ALT.GT.36) THEN
            RHOEST=0.03933*(EXP(-0.0001181*ALT*1000))
      ELSE IF (ALT.GE.9) THEN
            RHOEST=0.01901*(EXP(-0.00009804*ALT*1000))
      ELSE IF (ALT.LT.9) THEN
            RHOEST=0.01501*(EXP(-0.00007124*ALT*1000))
      ENDIF
      WRITE (*,*) 'RHOEST = ', RHOEST, ' AND RHOOVR = ', RHOOVR
      WRITE (5,*) 'RHOEST = ', RHOEST, ' AND RHOOVR = ', RHOOVR
      IF (RHOOVR.LT.0.000557) THEN
            HIALT=(ALOG(RHOOVR/0.03933))/(-0.0001181)
      ELSE IF (RHOOVR.GE.0.000557.AND.RHOOVR.LE.0.007866) THEN
            HIALT=(ALOG(RHOOVR/0.01901))/(-0.00009804)
      ELSE
            HIALT=(ALOG(RHOOVR/0.01501))/(-0.00007124)
      ENDIF
      IF (ABS(RHOEST-RHOOVR).LE.0.0003) THEN
            WRITE (*,*) 'HIGH ALTITUDE IS ', HIALT, ' M'
            WRITE (5,*) 'HIGH ALTITUDE IS ', HIALT, ' M'
      ELSE IF (N.EQ.25) THEN
            WRITE (*,*) 'NOT IN RANGE; TRY AGAIN'
            WRITE (5,*) 'NOT IN RANGE; TRY AGAIN'
      ELSE
            N=N+1
            ALT=ALT+1
            GOTO 10
      ENDIF
C
C THE UNDERSHOOT BOUNDARY
C
      WRITE (*,*) 'INPUT A LIFT-TO-DRAG RATIO'
      WRITE (5,*) 'INPUT A LIFT-TO-DRAG RATIO'
      READ (*,*) LOVRD
      WRITE (5,*) LOVRD
      CD=-((1/LOVRD)*CL)
      WRITE (*,*) 'CD =', CD
      WRITE (5,*) 'CD =', CD
      WRITE (*,*) 'INPUT THE DECELERATION MULTIPLE'
      WRITE (5,*) 'INPUT THE DECELERATION MULTIPLE'
      READ (*,*) GEES
      WRITE (5,*) GEES
```

```
      DECEL=3.73*GEES
      WRITE (*,*) 'DECEL = ', DECEL
      WRITE (5,*) 'DECEL = ', DECEL
       A=(1/3.73)*DECEL
      RHOUND=((2*MASS)/(RADIUS*CD*AREA))*((VELCIR/VEL)**2)*A
      ALT=ALT+1
   20 IF (ALT.GT.36) THEN
            RHOEST=0.03933*(EXP(-0.0001181*ALT*1000))
      ELSE IF (ALT.GE.9) THEN
            RHOEST=0.01901*(EXP(-0.00009804*ALT*1000))
      ELSE
            RHOEST=0.01501*(EXP(-0.00007124*ALT*1000))
      ENDIF
      WRITE (*,*) 'RHOEST = ', RHOEST, ' AND RHOUND = ', RHOUND
      WRITE (5,*) 'RHOEST = ', RHOEST, ' AND RHOUND = ', RHOUND
      IF (RHOUND.LT.0.000557) THEN
            LOWALT=(ALOG(RHOUND/0.03933))/(-0.0001181)
      ELSE IF (RHOUND.LE.0.007866) THEN
            LOWALT=(ALOG(RHOUND/0.01901))/(-0.00009804)
      ELSE
            LOWALT=(ALOG(RHOUND/0.01501))/(-0.00007124)
      ENDIF
      IF (ABS(RHOEST-RHOUND).LE.0.0003) THEN
            WRITE (*,*) 'LOW ALTITUDE IS ', LOWALT, ' M'
            WRITE (5,*) 'LOW ALTITUDE IS ', LOWALT, ' M'
      ELSE IF (M.EQ.25) THEN
            WRITE (*,*) 'NOT IN RANGE;TRY AGAIN'
            WRITE (5,*) 'NOT IN RANGE; TRY AGAIN'
      ELSE
            M=M+1
            ALT=ALT-1
            GOTO 20
      ENDIF
C
C THE CORRIDOR
C
      IF (HIALT.GT.LOWALT) THEN
            CORIDR=HIALT-LOWALT
            WRITE (*,*) 'THE CORRIDOR IS ', CORIDR, ' M'
            WRITE (5,*) 'THE CORRIDOR IS', CORIDR, ' M'
      ELSE
            WRITE (*,*) 'COULD NOT EVALUATE'
            WRITE (5,*) 'COULD NOT EVALUATE'
```

```
 ENDIF
 AVE=CORIDR/2
 FLYAT=LOWALT+AVE
 FLYAT=FLYAT/1000
 IF (FLYAT.GT.36) THEN
       RHOFLY=0.03933*(EXP(-0.0001181*FLYAT*1000))
 ELSE IF (FLYAT.GE.9) THEN
       RHOFLY=0.01901*(EXP(-0.00009804*FLYAT*1000))
 ELSE
       RHOFLY=0.01501*(EXP(-0.00007124*FLYAT
& *1000))
 ENDIF
 WRITE (*,*) 'THE PASS ALTITUDE SHOULD BE ', FLYAT, ' KM'
 WRITE (5,*) 'THE PASS ALTITUDE SHOULD BE ', FLYAT, ' KM'
 WRITE (*,*) 'THE DENSITY HERE IS ', RHOFLY, ' KG/M3'
 WRITE (5,*) 'THE DENSITY HERE IS ', RHOFLY, ' KG/M3'
 STOP
 END
```

Appendix C

Waverider/Supply Stage Rendezvous Code

(Seybold)

```
C
C CALINA'S PROGRAM 3
C
C RENDEZVOUS AT MARS
C
      REAL N, TIME, VELY, VELX, A, B, C, D, E, F, G, D2
      REAL H, I, J, K, L, M, O, X, Y, DUMMY, POSITY, POSITX
      REAL ANGLE, ARCTAN
      N=9.988E-04
      WRITE (*,*) 'INPUT INITIAL LONGITUDINAL DISTANCE IN KM'
      WRITE (5,*) 'INPUT INITIAL LONGITUDINAL DISTANCE IN KM'
      READ (*,*) X
      WRITE (5,*) X
      WRITE (*,*) 'INPUT INITIAL LATITUDINAL DISTANCE IN KM'
      WRITE (5,*) 'INPUT INITIAL LATITUDINAL DISTANCE IN KM'
      READ (*,*) Y
      WRITE (5,*) Y
C
C DETERMINE THE VELOCITIES
C
      ANGLE=1.571
      DUMMY=60
 5    IF (ANGLE.GT.0.01) THEN
           A=(6*X*((N*DUMMY)-(SIN(N*DUMMY)))-Y)
           B=2*N*X*(4-(3*(COS(N*DUMMY))))
           C=1-(COS(N*DUMMY))
           D=((4*(SIN(N*DUMMY)))-(3*N*DUMMY))
           D2=SIN(N*DUMMY)
           E=4*((1-(COS(N*DUMMY)))**2)
           VELY=((A*N*(SIN(N*DUMMY)))-(B*C))/((D*D2)+E)
      WRITE (*,*) 'THE LATITUDINAL VELOCITY IS ', VELY, ' KM/S'
      WRITE (5,*) 'THE LATITUDINAL VELOCITY IS ', VELY, ' KM/S'
           F=N*X*(4-(3*(COS(N*DUMMY))))
           G=2*(1-(COS(N*DUMMY)))*VELY
           VELX=-((F+G)/(SIN(N*DUMMY)))
      WRITE (*,*) 'THE LONGITUDINAL VELOCITY IS ', VELX, ' KM/S'
      WRITE (5,*) 'THE LONGITUDINAL VELOCITY IS ', VELX, ' KM/S'
C
C DETERMINE THE POSITION
C
           ANGLE=ATAN((VELX*DUMMY)/(VELY*DUMMY))
           POSITX=170*SIN(ANGLE)
      WRITE (*,*) 'THE LONGITUDINAL POSITION IS ', POSITX, ' KM'
      WRITE (5,*) 'THE LONGITUDINAL POSITION IS ', POSITX, ' KM'
           POSITY=170*COS(ANGLE)
      WRITE (*,*) 'THE LATITUDINAL POSITION IS ', POSITY, ' KM'
```

```
      WRITE (5,*) 'THE LATITUDINAL POSITION IS ', POSITY, ' KM'
            DUMMY=DUMMY+120
            WRITE (*,*)
            WRITE (5,*)
            GOTO 5
      ELSE IF (ANGLE.LE.0.01) THEN
            GOTO 10
      ENDIF
10    WRITE (*,*) 'THE TIME IS ', DUMMY, ' SEC'
      WRITE (5,*) 'THE TIME IS ', DUMMY, ' SEC'
      STOP
      END
```

Appendix D

Lander Trajectory Program and Key Runs

(Kraft)

```
00010 REM planar Mars lander - blunt lifting cone trajectory
00020 REM fourth order Runge-Kutta integration
00030 REM Hohmann transfer from parking orbit altitude ALTP to pullup
altitude, ALTST
00040 REM  Beginning at ALTST, maintain flight path angle, allow drag to
reduce velocity
00050 REM  Coast to first parachute deployment at altitude ALTCH1 if
ZMACH < ZMACHCH
00060 REM  Option to apply small thrusts to extend range, allow longer drag
time
00070 REM          Deploy second parachute at altitude ALTCH2 and third at
ALTCH3
00080 REM  Drop last parachute at ALTCHF, start landing burn at ALTBRN
00090 REM  Calculate landing velocity + hover propellant + lateral
maneuver
00100 DEFDBL A-H, O-Z : DEFINT I-N
00110 BREAK ON
00120 DIM
QQ(4,4),TIME(1000),ALT(1000),PHI(1000),VEL(1000),GAM(1000),ZMACHP(100
0),ZMPR(1000),VF(1000),FNC(4),QCC(1000),QPP(1000),CDP(1000),CLP(1000)
00130 G0=0.00980665 : CMU=45599. : RHOZ=.0182 : RMARS=3415. : TT=0.
00140 RHOK1=0.1 : RHOK2=0.09 : RHOK3=0.078 : GW=.2 : VROTM90=.24787
00150 REM RHOK1 for altitude > 60 km; RHOK2 for 30 < alt < 60; RHOK3 for
alt < 30
00160 RAD= 57.2957795 : ICOUNT=0 : IPP=0 : MBURN=0 : CD0=1.60
00170 REM G0 = Earth surface gravity, CMU = Mars gravitational constant
00180 REM RHO = Density = RHOZ*exp(-RHOK*(r-RMARS), RMARS = Mars
radius
00190 REM VROTM90 = Velocity of rotation at 90 KM altitude in km/sec
00200 PI=ATN(1)<<2 : PHIX=0.
00210 DEF FN FCD(CLF)=CD0-.22898*CLF+1.3015*CLF*CLF-4.6*CLF^3
00220 DEF FN ARCCOS(Q)=ATN(1)*2-ATN(Q/SQR(1-Q*Q))
00230 DEF FN ARCSIN(Q)=ATN(Q/SQR(1-Q*Q))
00240 DEF FN DRDT(VVF,GGF)=VVF*SIN(GGF)
00250 DEF FN DPDT(RRF,VVF,GGF)=VVF*COS(GGF)/RRF
00260 LONG FN DVDT(TTF,RRF,VVF,GGF)
00270 IF MBURN=0 THEN ZMDOTX=0.
00280 IF MBURN=1 THEN ZMDOTX=ZMDOT AND ZM=ZMASS0-
ZMDOT*(TTF-TBURNST)
00290 IF RRF-RMARS > 60 THEN RHOK=RHOK1
00300 IF RRF-RMARS <= 60 THEN RHOK=RHOK2
00310 IF RRF-RMARS < 30 THEN RHOK=RHOK3
00320 RHO=RHOZ*EXP(-RHOK*(RR-RMARS))
00330 END FN =-G0*ZISP*ZMDOTX/ZM-
500.*RHO*VVF*VVF*CD*AREA/ZM-CMU*SIN(GGF)/RR^2
```

```
00340 DEF FN DVDTM(TTF,RRF,VVF,GGF)=-G0*ZISP*ZMDOT/ZM-
500.*RHOZ*VVF*VVF*CD*AREA/ZM-CMU*SIN(GGF)/RR^2
00350 LONG FN DGDT(TTF,RRF,VVF,GGF)
00360 IF RRF-RMARS > 60 THEN RHOK=RHOK1
00370 IF RRF-RMARS <= 60 THEN RHOK=RHOK2
00380 IF RRF-RMARS < 30 THEN RHOK=RHOK3
00390 RHO=RHOZ*EXP(-RHOK*(RR-RMARS))
00400 END FN =500.*RHO*VVF*CL*AREA/ZM-(CMU/(RRF*VVF)-
VVF)*COS(GGF)/RRF
00410 PRINT "Mars Landing Trajectory"
00420 PRINT "Enter 0 for thermal search for flight path gamma; 1 normal
print" : INPUT ISEARCH
00430 REM Search prints every step of thermal glide, then stops
00440 PRINT "Enter 0 to run from stored file; 1 to enter all inputs with
prompts" : INPUT IINP
00450 IF IINP = 0 THEN GOTO 750
00460 PRINT "Enter initial mass, kg" : INPUT ZMASS0
00470 PRINT "Enter mass flow rate, kg/sec" : INPUT ZMDOT
00480 PRINT "Enter specific impulse, sec" : INPUT ZISP
00490 PRINT "Enter forward surface area, sq meters" : INPUT AREA
00500 PRINT "Enter nose radius, cm" : INPUT RN
00510 PRINT "Enter nominal flight path angle during thermal control, deg" :
INPUT GMAX
00520 PRINT "Enter initial lift coefficient" : INPUT CL
00530 PRINT "Enter step in lift coefficient for glide angle control" : INPUT
STPCL
00540 PRINT "Enter integration step during burn, sec" : INPUT DTB
00550 PRINT "Enter integration step during coast, sec" : INPUT DTC
00560 PRINT "Enter integration step during parachute glide, sec" : INPUT
DTCH
00570 PRINT "Enter N to print every Nth step" : INPUT IPRINT
00580 PRINT "Enter parking orbit altitude, km" : INPUT ALTP
00590 PRINT "Enter pullup altitude, km" : INPUT ALTST
00600 PRINT "Enter 0 for two thrusted flight path corrections, 2 for none" :
INPUT ITH
00610 PRINT "Enter Mach number limit for first deployment" : INPUT
ZMACHH
00620 PRINT "Enter altitude of first parachute deployment, km" : INPUT
ALTCH1
00630 PRINT "Enter CdA for first parachute, meter sq" : INPUT CDA1
00640 PRINT "Enter mass of heat shield to be dropped at second parachute
deployment, kg" : INPUT HTSH
00650 PRINT "Enter altitude of second parachute deployment, km" : INPUT
ALTCH2
00660 PRINT "Enter CdA for second parachute, meter sq" : INPUT CDA2
```

```
00670 PRINT "Enter altitude of third parachute deployment, km" : INPUT
ALTCH3
00680 PRINT "Enter CdA for third parachute, meter sq" : INPUT CDA3
00690 PRINT "Enter altitude to drop last parachute, km" : INPUT ALTCHF
00700 PRINT "Enter starting altitude of landing burn, km" : INPUT ALTBRN
00710 PRINT "Enter hover time, sec" : INPUT THOVER
00720 PRINT "Enter inclination of parking orbit, deg" : INPUT AINC
00730 PRINT "Enter lateral maneuver distance, km" : INPUT XLAT
00740 GOTO 810
00750 ZMASS0=52100. : ZMDOT=88.7. : ZISP=300. : AREA=99.93 : RN=100.
00760 GMAX=0. : DTB=.2 : DTC=10. : IPRINT=5 : ALTP=100. : ALTST=90.
00770 ZMACHH=2.8 : ALTCH1=5.6 : CDA1=600. : STPCL=.05 : ITRAJ=22
00780 ALTCH2=4.3 : CDA2=600. : ALTCH3=4. : CDA3=4800. : ZMACHCH=2.6
00790 ALTCHF=.5 : ALTBRN=ALTCHF : THOVER=30. : DTCH=.2 :
HTSH=1450.
00800 AINC=0. : XLAT=1. : ITH=2
00810 ZMCHUTE1=CDA1*.1505 : ZMCHUTE3=CDA3*.1729
00820 REM Chute 2 is reefed chute 3
00830 CL=.48 : CD=FN FCD(ABS(CL)) : VVTH1=1.6 : VVTH2=1.1
00840 REM XVF is Mars rotation speed at landing latitude
00850 CLS : LPRINT "     MARS LANDING TRAJECTORY FOR A BLUNT
LIFTING CONE  -  Trajectory no. ";ITRAJ
00860 REM Set initial conditions
00870 RR=RMARS+ALTP : PP=0. : VP=SQR(CMU/RR) : GG=0. :
RST=RMARS+ALTST
00880 VV=SQR(2.*CMU*RST/RR/(RR+RST)) : GGMAX=GMAX/RAD
00890 REM Hohmann transfer to surface+ALTST km;calculate Δv from
circular velocity
00900 REM Burn at parking orbit is calculated from Δv=g*Isp*ln(Mo/Mf)
00910 DELTVP=VP-VV
00920 ZM=ZMASS0/(EXP(DELTVP/G0/ZISP)) : DELTMP=ZMASS0-ZM
00930 TBURNP=DELTMP/ZMDOT
00940  TTRANS=PI*RR*SQR(RR/CMU)  :  TSTART=TBURNP+TTRANS
00950 ZMDOTX=0. : DT=DTC
00960 LPRINT USING "       De-Orbit Burn at ###.# km:";ALTP
00970 LPRINT USING "        ΔV = ##.### km/sec";DELTVP;USING "   Mass
Consumed = ####.# kg";DELTMP
00980 REM Calc Hohmann perigee velocity, Δv to start thermal phase
00990  VPST=SQR(2.*CMU*RR/RST/(RR+RST))  :  VVI=SQR(CMU/RST)
01000 GG=0. : DELTVST=VPST-VVI
01010 ZMST=ZM/(EXP(DELTVST/G0/ZISP)) : DELTMST=ZM-ZMST
01020 LPRINT USING "       Thermal Phase Burn at ###.#
km";ALTST;USING " at time #####.# sec";TSTART
01030 LPRINT USING "        ΔV = ##.### km/sec";DELTVST;USING "   Mass
Consumed = ####.# kg";DELTMST
01040  TBURNST=DELTMST/ZMDOT :TT=TSTART+TBURNST
```

```
01050 ZM=ZMST : RR=RST : PP=0. : ZMASS0=ZM
01060  VV=SQR(VVI*VVI+VROTM90*VROTM90-
2.*VVI*VROTM90*COS(AINC/RAD))
01070 REM Print initial conditions
01080 LPRINT : LPRINT : LPRINT "    CONDITIONS AT ENTRY:" : LPRINT
01090 LPRINT "      MDOT   MASS0   ISP   AREA   ALTP   ALTST
XLAT   INCP   STEPC"
01100 LPRINT "      (KG/S)  (KG)   (SEC)  (M SQ)  (KM)   (KM)   (KM)
(DEG)  (SEC)"
01110 LPRINT USING "      ####.#";ZMDOT;USING "
######.#";ZMASS0;USING "    ####.#";ZISP;USING "
###.#";AREA;USING "  ####.#";ALTP;USING "    ####.#";ALTST;USING "
#.##";XLAT;USING "  ###.##";AINC;USING "      ###.#";DTC
01120 LPRINT
01130 LPRINT "      CD0   CDA1   CDA2   CDA3   CL    ALTC1   ALTC2
ALTC3   STEPB"
01140 LPRINT "            (SQ M)  (SQ M)  (SQ M)        (KM)    (KM)    (KM)
(SEC)"
01150 LPRINT USING "       #.##";CD0;USING "  ####.#";CDA1;USING "
####.#";CDA2;USING "   ####.#";CDA3;USING "      ##.##";CL;USING "
####.#";ALTCH1;USING "    ####.#";ALTCH2;USING "
####.#";ALTCH3;USING "     ##.#";DTB
01160 LPRINT
01170 LPRINT "     Mach number limit to leave pullup = ";ZMACHH
01180 LPRINT "     Design flight path angle = ";GMAX; " deg"
01190 IF ITH = 0 THEN LPRINT "     Flight path correction thrusts of 1 sec at
velocity ";VVTH1;" AND ";VVTH2
01200 LPRINT "     Mach number limit for first parachute deployment =
";ZMACHCH
01210 LPRINT "     Altitude to drop last parachute = km";ALTCHF
01220 LPRINT "     Altitude to start landing burn = km";ALTBRN : LPRINT
01230 REM Begin integration for coast to pullup altitude (IPHASE=1)
01240 IPHASE=1
01250 MBURN=0 : ICC=1
01260 IF ISEARCH=0 THEN LPRINT "THERMAL SEARCH MODE"
01270 GOSUB "RUNGE-KUTTA"
01280 XALT=RR-RMARS : QP=.5*RHO*VV*VV*1.E6 : QC=1.35E-
8*SQR(RHO*100./RN)*(VV*1000)^3.04*(1.-GW)
01290 XALT=RR-RMARS : AA=.24641-6.7094E-4*XALT-7.3074E-
6*XALT*XALT+1.0758E-7*XALT^3
01300 IF XALT > 60. THEN AA=.200
01310 ZMACH=VV/AA
01320 LONG IF ISEARCH=0
01330 GGDEG=GG*RAD
01340 IF ICC MOD 5 = 0 THEN LPRINT USING "    ALT =
###.##";XALT;USING "  a = #.###";AA;USING "  Qp= #####.#";QP;USING
```

```
" Qc= ####.#";QC;USING " g°= ####.#";GGDEG;USING " MachNo=
#####.#";ZMACH
01350 ICC=ICC+1
01360 IF ICC > 300 OR XALT < 0. THEN GOTO 2080
01370 END IF
01380 LONG IF ICOUNT MOD IPRINT =0
01390 IPP=IPP+1
01400 TIME(IPP)=TT : ALT(IPP)=XALT : PHI(IPP)=PP*RAD : VEL(IPP)=VV :
CDP(IPP)=CD : CLP(IPP)=CL
01410 GAM(IPP)=GG*RAD : ZMPR(IPP)=ZM : QCC(IPP)=QC : QPP(IPP)=QP :
ZMACHP(IPP)=ZMACH
01420 END IF
01430 IF IPP >= 999 THEN GOTO 1830
01440 ON IPHASE GOTO 1450,1620,1690,1750,1800
01450 LONG IF XALT > ALTCH1 OR ZMACH > ZMACHH
01460 IF ZMACH < ZMACHCH+0.25 AND ZMACH > ZMACHCH-1. THEN
DT=DTCH
01470 IF GG > GGMAX AND GG < GGMAX+.0035 THEN GOTO 1270
01480 IF GG < GGMAX THEN CL=CL+STPCL
01490 IF GG > GGMAX+.0035 THEN CL=CL-STPCL
01500 IF ABS(CL) > .48 THEN CL=SGN(CL)*.48
01510 CD=FN FCD(ABS(CL))
01520 IF CL > -.48 AND ISEARCH = 0 THEN LPRINT USING " CL =
##.###";CL;USING " CD = ##.###";CD
01530 IF VV < VVTH1 AND ITH = 0 THEN GOSUB "THRUST"
01540 IF VV < VVTH2 AND ITH = 1 THEN GOSUB "THRUST"
01550 GOTO 1270
01560 END IF
01570 IF ZMACH > ZMACHCH OR XALT > ALTCH1 THEN GOTO 1270
01580 IPHASE=2 : CD=CD0+CDA1/AREA : TT1=TT
01590 IF ZMACH < ZMACHCH-1. THEN DT=DTC
01600 LPRINT USING " Deploy parachute 1 at #####.# sec";TT;USING "
Altitude = #.## km";XALT;USING " Mach no = ##.#";ZMACH
01610 GOTO 1270
01620 REM Begin Phase 2 (parachute 1 deployed)
01630 IF XALT > ALTCH2 THEN GOTO 1270
01640 IF TT < TT1+3. THEN GOTO 1270
01650 IPHASE=3 : CD=CD0+CDA2/AREA : ZM=ZM-ZMCHUTE1-HTSH
01660 LPRINT USING " Deploy parachute 2 at #####.# sec";TT;USING "
Altitude = #.## km";XALT;USING " Mach no = #.##";ZMACH
01670 LPRINT USING " Heat shield dropped, mass ####.#
kg";HTSH;USING " Total mass = #####.# kg";ZM
01680 GOTO 1270
01690 REM Begin Phase 3 (parachute 2 deployed)
01700 IF XALT > ALTCH3 THEN GOTO 1270
01710 IF TT < TT1+5. THEN GOTO 1270
```

```
01720 IPHASE=4 : CD=CD0+CDA3/AREA
01730 LPRINT USING "    Deploy parachute 3 at #####.# sec";TT;USING "
Altitude = #.## km";XALT;USING "  Mach no = ##.#";ZMACH
01740 GOTO 1270
01750 REM Begin Phase 4 (parachute 3 deployed)
01760 IF XALT > ALTCHF THEN GOTO 1270
01770 IPHASE=5 : CD=CD0 : ZM=ZM-ZMCHUTE3 : TBURNST=TT :
MBURN=1 : ZMASS0=ZM
01780 LPRINT USING "    Parachute 3 dropped at #####.# sec";TT;USING "
Altitude = #.## km";XALT;USING "  Mass = #####.";ZM
01790 GOTO 1270
01800 REM Begin Phase 5 (final burn)
01810 IF XALT > 0. AND VV > 0. THEN GOTO 1270
01820 A$="  ###.#" : B$=" ##.##"
01830 LPRINT
01840 LPRINT : LPRINT
01850 LPRINT "    T    ALT   PHI   GAM   VEL    MACH CD    CL    QP
      QC     MASS"
01860 LPRINT "    (SEC)  (KM)   (DEG)  (DEG)  (KM/S)              (N/M2)
(W/CM2)  (KG)"
01870 LPRINT
01880 FOR I = 1 TO IPP STEP IPRINT
01890 LPRINT USING "   #####.#";TIME(I);USING B$;ALT(I);USING
A$;PHI(I);USING A$;GAM(I);USING "  ##.####";VEL(I);USING "
##.###";ZMACHP(I);USING B$;CDP(I);USING B$;CLP(I);USING "
####.#";QPP(I);USING "  ####.#";QCC(I);USING " ######.#";ZMPR(I)
01900 NEXT I
01910 REM Calculate lateral maneuver
01920 DELTVLAT=XLAT/THOVER : ZMLF=ZM/EXP(DELTVLAT/G0/ZISP)
01930 DELTMLAT=ZM-ZMLF : ZM=ZMLF
01940 LPRINT "    Lateral range of ";XLAT;" km requires ";DELTMLAT;" kg"
01950 REM Calculate landing maneuver
01960 ZMFIN=ZM/(EXP(VV/G0/ZISP)) : DELTMLAND=ZM-ZMFIN :
TLAND=DELTMLAND/ZMDOT
01970 LPRINT USING "  Landing ΔV = ##.### km/sec";VV; USING "  ΔM =
####.# kg";DELTMLAND
01980 REM Calculate mass to hover
01990
DELTMHOV=ZMFIN*LOG(1.+THOVER/(G0*ZISP*RMARS*RMARS/CMU)
) : ZMLAND=ZMFIN-DELTMHOV
02000  TFINAL=TT+TLAND+THOVER
02010 LPRINT USING "    Hover for ##.# sec";THOVER;USING " ΔM =
####.## kg";DELTMHOV; USING "  Final Mass = ######.# kg";ZMLAND
02020 LPRINT USING "    Land at ######.# SEC"; TFINAL
02030 GOTO 2080
02040 LPRINT : LPRINT "FINAL VALUES"
```

```
02050 LPRINT USING "   ###.#";TT;USING "  ###.#";XX-RMARS;USING "
####.#";PHIX;USING "  ######.#";GG
02060 IF XALT < 0. OR VFF < 0. GOTO 2080
02070 BREAK OFF
02080 END
02090 :
02100 "RUNGE-KUTTA"
02110 FNC(1)=FN DRDT(VV,GG)
02120 FNC(2)=FN DPDT(RR,VV,GG)
02130 IF MBURN=0 THEN FNC(3)=FN DVDT(TT,RR,VV,GG) ELSE
FNC(3)=FN DVDTM(TT,RR,VV,GG)
02140 FNC(4)=FN DGDT(TT,RR,VV,GG)
02150 FOR I = 1 TO 4
02160 QQ(I,1)=DT*FNC(I)
02170 NEXT I
02180 FNC(1)=FN DRDT(VV+.5*QQ(3,1),GG+.5*QQ(4,1))
02190 FNC(2)=FN DPDT(RR+.5*QQ(1,1),VV+.5*QQ(3,1),GG+.5*QQ(4,1))
02200 IF MBURN=0 THEN FNC(3)=FN
DVDT(TT+.5*DT,RR+.5*QQ(1,1),VV+.5*QQ(3,1),GG+.5*QQ(4,1)) ELSE
FNC(3)=FN
DVDTM(TT+.5*DT,RR+.5*QQ(1,1),VV+.5*QQ(3,1),GG+.5*QQ(4,1))
02210 FNC(4)=FN
DGDT(TT+.5*DT,RR+.5*QQ(1,1),VV+.5*QQ(3,1),GG+.5*QQ(4,1))
02220 FOR I = 1 TO 4
02230 QQ(I,2)=DT*FNC(I)
02240 NEXT I
02250 FNC(1)=FN DRDT(VV+.5*QQ(3,2),GG+.5*QQ(4,2))
02260 FNC(2)=FN DPDT(RR+.5*QQ(1,2),VV+.5*QQ(3,2),GG+.5*QQ(4,2))
02270 IF MBURN=0 THEN FNC(3)=FN
DVDT(TT+.5*DT,RR+.5*QQ(1,2),VV+.5*QQ(3,2),GG+.5*QQ(4,2)) ELSE
FNC(3)=FN
DVDTM(TT+.5*DT,RR+.5*QQ(1,2),VV+.5*QQ(3,2),GG+.5*QQ(4,2))
02280 FNC(4)=FN
DGDT(TT+.5*DT,RR+.5*QQ(1,2),VV+.5*QQ(3,2),GG+.5*QQ(4,2))
02290 FOR I = 1 TO 4
02300 QQ(I,3)=DT*FNC(I)
02310 NEXT I
02320 FNC(1)=FN DRDT(VV+QQ(3,3),GG+QQ(4,3))
02330 FNC(2)=FN DPDT(RR+QQ(1,3),VV+QQ(3,3),GG+QQ(4,3))
02340 IF MBURN=0 THEN FNC(3)=FN
DVDT(TT+DT,RR+QQ(1,3),VV+QQ(3,3),GG+QQ(4,3)) ELSE FNC(3)=FN
DVDTM(TT+DT,RR+QQ(1,3),VV+QQ(3,3),GG+QQ(4,3))
02350 FNC(4)=FN DGDT(TT+DT,RR+QQ(1,3),VV+QQ(3,3),GG+QQ(4,3))
02360 FOR I = 1 TO 4
02370 QQ(I,4)=DT*FNC(I)
02380 NEXT I
```

```
02390 TT=TT+DT
02400 RR=RR+(QQ(1,1)+2.*QQ(1,2)+2.*QQ(1,3)+QQ(1,4))/6.
02410 PP=PP+(QQ(2,1)+2.*QQ(2,2)+2.*QQ(2,3)+QQ(2,4))/6.
02420 VV=VV+(QQ(3,1)+2.*QQ(3,2)+2.*QQ(3,3)+QQ(3,4))/6.
02430 GG=GG+(QQ(4,1)+2.*QQ(4,2)+2.*QQ(4,3)+QQ(4,4))/6.
02440 IF MBURN=1 THEN ZM=ZM-DT*ZMDOT
02450 RETURN
02460 :
02470 "THRUST"
02480 REM One second burn to change gamma only
02490 GG=GG+2.* FN ARCSIN(G0*ZISP*LOG(ZM/(ZM-ZMDOT))/(2*VV))
02500 ZM=ZM-ZMDOT : TT=TT+1. : ITH=ITH+1
02510 RETURN
```

MARS LANDING TRAJECTORY FOR A BLUNT LIFTING CONE - Trajectory no. 16

De Orbit Burn at 100.0 km:
ΔV = .003 km/sec Mass Consumed = 46.6 kg
Thermal Phase Burn at 90.0 km at time 3066.1 sec
ΔV = .003 km/sec Mass Consumed = 46.6 kg

CONDITIONS AT ENTRY:

MDOT (KG/S)	MASSO (KG)	ISP (SEC)	AREA (M SQ)	ALTP (KM)	ALTST (KM)	XLAT (KM)	INCP (DEG)	STEPC (SEC)
200.0	53306.9	300.0	99.9	100.0	90.0	1.00	.00	10.0

CDO	CDA1 (SQ M)	CDA2 (SQ M)	CDA3 (SQ M)	CL	ALTC1 (KM)	ALTC2 (KM)	ALTC3 (KM)	STEPB (SEC)
1.60	600.0	600.0	4400.0	.48	5.6	4.3	4.0	.2

Mach number limit to leave pullup = 2.6
Design flight path angle = 0 deg
Mach number limit for first parachute deployment = 2.4
Altitude to drop last parachute = km .5
Altitude to start landing burn = km .5

Deploy parachute 1 at 3978.4 sec Altitude = 2.80 km Mach no = 2.4
Deploy parachute 2 at 3981.4 sec Altitude = 2.31 km Mach no = 2.03
Deploy parachute 3 at 3983.4 sec Altitude = 2.01 km Mach no = 1.8
Parachute 3 dropped at 4007.4 sec Altitude = .45 km Mass = 52456.

T (SEC)	ALT (KM)	PHI (DEG)	GAM (DEG)	VEL (KM/S)	MACH	CD	CL	QP (N/M2)	QC (W/CM2)	MASS (KG)
3076.4	89.98	.5	-.1	3.3587	16.794	1.28	.48	12.7	.8	53306.9
3126.4	89.13	3.3	-.5	3.3581	16.791	1.28	.48	13.4	.9	53306.9
3176.4	87.08	6.0	-.9	3.3586	16.793	1.28	.48	16.1	1.0	53306.9
3226.4	83.83	8.8	-1.3	3.3599	16.799	1.28	.48	21.8	1.1	53306.9
3276.4	79.37	11.5	-1.7	3.3615	16.807	1.28	.48	33.3	1.4	53306.9
3326.4	73.75	14.3	-2.1	3.3622	16.811	1.28	.48	57.1	1.8	53306.9
3376.4	67.01	17.1	-2.5	3.3595	16.797	1.28	.48	109.5	2.5	53306.9
3426.4	59.25	19.8	-2.8	3.3465	16.454	1.28	.48	425.5	4.9	53306.9
3476.4	51.08	22.6	-2.8	3.2763	15.796	1.28	.48	851.4	6.6	53306.9
3526.4	43.50	25.2	-2.5	3.1326	14.759	1.28	.48	1567.9	8.2	53306.9
3576.4	37.64	27.7	-1.9	2.8893	13.343	1.28	.48	2349.5	8.5	53306.9
3626.4	34.12	30.0	-1.1	2.5756	11.745	1.28	.48	2670.5	7.2	53306.9
3676.4	32.21	32.0	-.8	2.2601	10.235	1.28	.48	2486.3	5.3	53306.9
3726.4	30.34	33.7	-1.4	1.9771	8.893	1.28	.48	2227.4	3.8	53306.9
3776.4	27.85	35.2	-1.9	1.6398	7.308	1.28	.48	2677.6	2.9	53306.9
3826.4	24.43	36.5	-3.7	1.3457	5.923	1.28	.48	2297.9	1.8	53306.9
3876.4	19.03	37.5	-6.9	1.0847	4.681	1.28	.48	2200.7	1.1	53306.9
3926.4	11.68	38.3	-11.2	.8333	3.505	1.28	.48	2243.2	.7	53306.9
3976.4	3.16	38.9	-17.3	.5944	2.434	1.28	.48	2191.6	.3	53306.9
3981.4	2.31	38.9	-18.1	.4964	2.027	7.60	.48	1849.6	.2	53306.9
3986.4	1.69	38.9	-20.2	.2382	.971	45.63	.48	449.3	.0	53216.6
3991.4	1.36	38.9	-25.8	.1354	.552	45.63	.48	149.4	.0	53216.6
3996.4	1.07	39.0	-34.1	.0985	.401	45.63	.48	80.8	.0	53216.6
4001.4	.80	39.0	-43.7	.0819	.333	45.63	.48	57.1	.0	53216.6
4006.4	.51	39.0	-53.1	.0743	.302	45.63	.48	48.0	.0	53216.6
4011.4	.25	39.0	-63.0	.0412	.167	1.60	.48	15.1	.0	51655.8
4016.4	.15	39.0	-84.1	.0021	.009	1.60	.48	.0	.0	50655.8

Lateral range of 1 km requires 568.447 kg
Landing ΔV = -.006 km/sec ΔM = -95.8 kg
Hover for 30.0 sec ΔM = 1954.16 kg Final Mass = 48029.0 kg
Land at 4046.9 SEC

MARS LANDING TRAJECTORY FOR A BLUNT LIFTING CONE - Trajectory no. 17

De Orbit Burn at 100.0 km:
ΔV = .003 km/sec Mass Consumed = 46.6 kg
Thermal Phase Burn at 90.0 km at time 3066.1 sec
ΔV = .003 km/sec Mass Consumed = 46.6 kg

CONDITIONS AT ENTRY:

MDOT (KG/S)	MASSO (KG)	ISP (SEC)	AREA (M SQ)	ALTP (KM)	ALTST (KM)	XLAT (KM)	INCP (DEG)	STEPC (SEC)
200.0	53306.9	300.0	99.9	100.0	90.0	1.00	.00	10.0

CDO	CDA1 (SQ M)	CDA2 (SQ M)	CDA3 (SQ M)	CL	ALTC1 (KM)	ALTC2 (KM)	ALTC3 (KM)	STEPB (SEC)
1.60	600.0	600.0	4400.0	.00	5.6	4.3	4.0	.2

Mach number limit to leave pullup = 2.6
Design flight path angle = 0 deg
Mach number limit for first parachute deployment = 2.4
Altitude to drop last parachute = km .5
Altitude to start landing burn = km .5

Deploy parachute 1 at 3976.4 sec Altitude = 2.79 km Mach no = 2.4
Deploy parachute 2 at 3979.4 sec Altitude = 2.30 km Mach no = 2.02
Deploy parachute 3 at 3981.4 sec Altitude = 2.00 km Mach no = 1.8
Parachute 3 dropped at 4004.4 sec Altitude = .50 km Mass = 52456.

T (SEC)	ALT (KM)	PHI (DEG)	GAM (DEG)	VEL (KM/S)	MACH	CD	CL	QP (N/M2)	QC (W/CM2)	MASS (KG)
3076.4	89.98	.5	-.1	3.3587	16.793	1.60	.00	12.7	.8	53306.9
3126.4	89.11	3.3	-.5	3.3577	16.789	1.55	.25	13.5	.9	53306.9
3176.4	87.03	6.0	-.9	3.3580	16.790	1.28	.48	16.2	1.0	53306.9
3226.4	83.74	8.8	-1.3	3.3594	16.797	1.28	.48	22.0	1.1	53306.9
3276.4	79.25	11.5	-1.7	3.3609	16.805	1.28	.48	33.7	1.4	53306.9
3326.4	73.59	14.3	-2.1	3.3616	16.808	1.28	.48	58.0	1.8	53306.9
3376.4	66.80	17.1	-2.5	3.3588	16.794	1.28	.48	111.6	2.5	53306.9
3426.4	59.01	19.8	-2.8	3.3422	16.425	1.28	.48	433.6	4.9	53306.9
3476.4	50.87	22.5	-2.8	3.2706	15.760	1.28	.48	864.9	6.6	53306.9
3526.4	43.33	25.2	-2.5	3.1248	14.714	1.28	.48	1585.3	8.2	53306.9
3576.4	37.51	27.7	-1.9	2.8797	13.293	1.28	.48	2361.8	8.5	53306.9
3626.4	34.02	29.9	-1.1	2.5652	11.694	1.28	.48	2672.1	7.1	53306.9
3676.4	32.11	31.9	-.8	2.2498	10.185	1.28	.48	2484.5	5.2	53306.9
3726.4	30.21	33.7	-1.4	1.9669	8.842	1.28	.48	2229.2	3.8	53306.9
3776.4	27.85	35.2	-1.9	1.6201	7.220	1.28	.48	2615.5	2.8	53306.9
3826.4	24.41	36.4	-3.8	1.3329	5.865	1.28	.48	2255.2	1.7	53306.9
3876.4	18.87	37.4	-7.1	1.0757	4.639	1.28	.48	2186.6	1.1	53306.9
3926.4	11.38	38.2	-11.5	.8252	3.467	1.28	.48	2248.3	.6	53306.9
3967.4	4.37	38.7	-16.3	.6268	2.576	1.28	.48	2508.1	.4	53306.9
3972.4	3.49	38.7	-16.9	.6022	2.468	1.28	.48	2479.5	.4	53306.9
3977.4	2.62	38.8	-17.6	.5506	2.251	7.60	.48	2219.8	.3	53306.9
3982.4	1.88	38.8	-18.9	.3465	1.413	45.63	.48	934.4	.1	53216.6
3987.4	1.47	38.8	-23.2	.1626	.662	45.63	.48	213.4	.0	53216.6
3992.4	1.18	38.8	-30.5	.1095	.446	45.63	.48	99.2	.0	53216.6
3997.4	.90	38.8	-39.8	.0870	.354	45.63	.48	63.9	.0	53216.6
4002.4	.62	38.8	-49.4	.0766	.311	45.63	.48	50.6	.0	53216.6
4007.4	.35	38.9	-59.1	.0498	.202	1.60	.48	21.9	.0	51855.8
4012.4	.21	38.9	-75.6	.0103	.042	1.60	.48	1.0	.0	50855.8

Lateral range of 1 km requires 568.447 kg
Landing ΔV = -.005 km/sec ΔM = -89.5 kg
Hover for 30.0 sec ΔM = 1953.91 kg Final Mass = 48023.0 kg
Land at 4043.9 SEC

MARS LANDING TRAJECTORY FOR A BLUNT LIFTING CONE - Trajectory no. 18

De Orbit Burn at 100.0 km:
ΔV = .003 km/sec Mass Consumed = 46.6 kg
Thermal Phase Burn at 90.0 km at time 3066.2 sec
ΔV = .003 km/sec Mass Consumed = 46.6 kg

CONDITIONS AT ENTRY:

MDOT (KG/S)	MASS0 (KG)	ISP (SEC)	AREA (M SQ)	ALTP (KM)	ALTST (KM)	XLAT (KM)	INCP (DEG)	STEPC (SEC)
175.0	53306.9	300.0	99.9	100.0	90.0	1.00	.00	10.0

CD0	CDA1 (SQ M)	CDA2 (SQ M)	CDA3 (SQ M)	CL	ALTC1 (KM)	ALTC2 (KM)	ALTC3 (KM)	STEPB (SEC)
1.60	600.0	600.0	4400.0	.48	5.6	4.3	4.0	.2

Mach number limit to leave pullup = 2.6
Design flight path angle = 0 deg
Mach number limit for first parachute deployment = 2.4
Altitude to drop last parachute = km .5
Altitude to start landing burn = km .5

Deploy parachute 1 at 3978.4 sec Altitude = 2.80 km Mach no = 2.4
Deploy parachute 2 at 3981.4 sec Altitude = 2.31 km Mach no = 2.03
Deploy parachute 3 at 3983.4 sec Altitude = 2.01 km Mach no = 1.8
Parachute 3 dropped at 4007.4 sec Altitude = .45 km Mass = 52456.

T (SEC)	ALT (KM)	PHI (DEG)	GAM (DEG)	VEL (KM/S)	MACH	CD	CL	QP (N/M2)	QC (W/CM2)	MASS (KG)
3076.4	89.98	.5	-.1	3.3587	16.794	1.28	.48	12.7	.8	53306.9
3126.4	89.13	3.3	-.5	3.3581	16.791	1.28	.48	13.4	.9	53306.9
3176.4	87.08	6.0	-.9	3.3586	16.793	1.28	.48	16.1	1.0	53306.9
3226.4	83.83	8.8	-1.3	3.3599	16.799	1.28	.48	21.8	1.1	53306.9
3276.4	79.37	11.5	-1.7	3.3615	16.807	1.28	.48	33.3	1.4	53306.9
3326.4	73.75	14.3	-2.1	3.3622	16.811	1.28	.48	57.1	1.8	53306.9
3376.4	67.01	17.1	-2.5	3.3595	16.797	1.28	.48	109.5	2.5	53306.9
3426.4	59.25	19.8	-2.8	3.3465	16.454	1.28	.48	425.5	4.9	53306.9
3476.4	51.08	22.6	-2.8	3.2763	15.796	1.28	.48	851.4	6.6	53306.9
3526.4	43.50	25.2	-2.5	3.1326	14.759	1.28	.48	1567.9	8.2	53306.9
3576.4	37.64	27.7	-1.9	2.8893	13.343	1.28	.48	2349.5	8.5	53306.9
3626.4	34.12	30.0	-1.1	2.5756	11.745	1.28	.48	2670.5	7.2	53306.9
3676.4	32.21	32.0	-.8	2.2601	10.235	1.28	.48	2486.3	5.3	53306.9
3726.4	30.34	33.7	-1.4	1.9771	8.893	1.28	.48	2227.4	3.8	53306.9
3776.4	27.85	35.2	-1.9	1.6398	7.308	1.28	.48	2677.6	2.9	53306.9
3826.4	24.43	36.5	-3.7	1.3457	5.923	1.28	.48	2297.9	1.8	53306.9
3876.4	19.03	37.5	-6.9	1.0847	4.681	1.28	.48	2200.7	1.1	53306.9
3926.4	11.68	38.3	-11.2	.8333	3.505	1.28	.48	2243.2	.7	53306.9
3976.4	3.16	38.9	-17.3	.5944	2.434	1.28	.48	2191.6	.3	53306.9
3981.4	2.31	38.9	-18.1	.4964	2.027	7.60	.48	1849.6	.2	53306.9
3986.4	1.69	38.9	-20.2	.2382	.971	45.63	.48	449.3	.0	53216.6
3991.4	1.36	38.9	-25.8	.1354	.552	45.63	.48	149.4	.0	53216.6
3996.4	1.07	39.0	-34.1	.0985	.401	45.63	.48	80.8	.0	53216.6
4001.4	.80	39.0	-43.7	.0819	.333	45.63	.48	57.1	.0	53216.6
4006.4	.51	39.0	-53.1	.0743	.302	45.63	.48	48.0	.0	53216.6
4011.4	.24	39.0	-62.6	.0468	.190	1.60	.48	19.5	.0	51755.8
4016.4	.10	39.0	-76.2	.0148	.060	1.60	.48	2.0	.0	50880.8

Lateral range of 1 km requires 567.321 kg
Landing ΔV = -.004 km/sec ΔM = -70.3 kg
Hover for 30.0 sec ΔM = 1949.30 kg Final Mass = 47909.5 kg
Land at 4049.0 SEC

MARS LANDING TRAJECTORY FOR A BLUNT LIFTING CONE - Trajectory no. 19

De Orbit Burn at 100.0 km:
ΔV = .003 km/sec Mass Consumed = 46.6 kg
Thermal Phase Burn at 90.0 km at time 3066.2 sec
ΔV = .003 km/sec Mass Consumed = 46.6 kg

CONDITIONS AT ENTRY:

MDOT (KG/S)	MASSO (KG)	ISP (SEC)	AREA (M SQ)	ALTP (KM)	ALTST (KM)	XLAT (KM)	INCP (DEG)	STEPC (SEC)
150.0	53306.9	300.0	99.9	100.0	90.0	1.00	.00	10.0

CDO	CDA1 (SQ M)	CDA2 (SQ M)	CDA3 (SQ M)	CL	ALTC1 (KM)	ALTC2 (KM)	ALTC3 (KM)	STEPB (SEC)
1.60	600.0	600.0	4400.0	.48	5.6	4.3	4.0	.2

Mach number limit to leave pullup = 2.6
Design flight path angle = 0 deg
Mach number limit for first parachute deployment = 2.4
Altitude to drop last parachute = km .5
Altitude to start landing burn = km .5

Deploy parachute 1 at 3978.5 sec Altitude = 2.80 km Mach no = 2.4
Deploy parachute 2 at 3981.5 sec Altitude = 2.31 km Mach no = 2.03
Deploy parachute 3 at 3983.5 sec Altitude = 2.01 km Mach no = 1.8
Parachute 3 dropped at 4007.5 sec Altitude = .45 km Mass = 52456.

T (SEC)	ALT (KM)	PHI (DEG)	GAM (DEG)	VEL (KM/S)	MACH	CD	CL	QP (N/M2)	QC (W/CM2)	MASS (KG)
3076.5	89.98	.5	-.1	3.3587	16.794	1.28	.48	12.7	.8	53306.9
3126.5	89.13	3.3	-.5	3.3581	16.791	1.28	.48	13.4	.9	53306.9
3176.5	87.08	6.0	-.9	3.3586	16.793	1.28	.48	16.1	1.0	53306.9
3226.5	83.83	8.8	-1.3	3.3599	16.799	1.28	.48	21.8	1.1	53306.9
3276.5	79.37	11.5	-1.7	3.3615	16.807	1.28	.48	33.3	1.4	53306.9
3326.5	73.75	14.3	-2.1	3.3622	16.811	1.28	.48	57.1	1.8	53306.9
3376.5	67.01	17.1	-2.5	3.3595	16.797	1.28	.48	109.5	2.5	53306.9
3426.5	59.25	19.8	-2.8	3.3465	16.454	1.28	.48	425.5	4.9	53306.9
3476.5	51.08	22.6	-2.8	3.2763	15.796	1.28	.48	851.4	6.6	53306.9
3526.5	43.50	25.2	-2.5	3.1326	14.759	1.28	.48	1567.9	8.2	53306.9
3576.5	37.64	27.7	-1.9	2.8893	13.343	1.28	.48	2349.5	8.5	53306.9
3626.5	34.12	30.0	-1.1	2.5756	11.745	1.28	.48	2670.5	7.2	53306.9
3676.5	32.21	32.0	-.8	2.2601	10.235	1.28	.48	2486.3	5.3	53306.9
3726.5	30.34	33.7	-1.4	1.9771	8.893	1.28	.48	2227.4	3.8	53306.9
3776.5	27.85	35.2	-1.9	1.6398	7.308	1.28	.48	2677.6	2.9	53306.9
3826.5	24.43	36.5	-3.7	1.3457	5.923	1.28	.48	2297.9	1.8	53306.9
3876.5	19.03	37.5	-6.9	1.0847	4.681	1.28	.48	2200.7	1.1	53306.9
3926.5	11.68	38.3	-11.2	.8333	3.505	1.28	.48	2243.2	.7	53306.9
3976.5	3.16	38.9	-17.3	.5944	2.434	1.28	.48	2191.6	.3	53306.9
3981.5	2.31	38.9	-18.1	.4964	2.027	7.60	.48	1849.6	.2	53306.9
3986.5	1.69	38.9	-20.2	.2382	.971	45.63	.48	449.3	.0	53216.6
3991.5	1.36	38.9	-25.8	.1354	.552	45.63	.48	149.4	.0	53216.6
3996.5	1.07	39.0	-34.1	.0985	.401	45.63	.48	80.8	.0	53216.6
4001.5	.80	39.0	-43.7	.0819	.333	45.63	.48	57.1	.0	53216.6
4006.5	.51	39.0	-53.1	.0743	.302	45.63	.48	48.0	.0	53216.6
4011.5	.23	39.0	-62.2	.0524	.213	1.60	.48	24.5	.0	51855.8
4016.5	.05	39.0	-73.0	.0274	.111	1.60	.48	6.8	.0	51105.8

Lateral range of 1 km requires 570.7 kg
Landing ΔV = .013 km/sec ΔM = 217.5 kg
Hover for 30.0 sec ΔM = 1949.64 kg Final Mass = 47918.0 kg
Land at 4051.0 SEC

MARS LANDING TRAJECTORY FOR A BLUNT LIFTING CONE - Trajectory no. 20

De Orbit Burn at 100.0 km:
ΔV = .003 km/sec Mass Consumed = 46.6 kg
Thermal Phase Burn at 90.0 km at time 3066.3 sec
ΔV = .003 km/sec Mass Consumed = 46.6 kg

CONDITIONS AT ENTRY:

MDOT (KG/S)	MASSO (KG)	ISP (SEC)	AREA (M SQ)	ALTP (KM)	ALTST (KM)	XLAT (KM)	INCP (DEG)	STEPC (SEC)
125.0	53306.9	300.0	99.9	100.0	90.0	1.00	.00	10.0

CDO	CDA1 (SQ M)	CDA2 (SQ M)	CDA3 (SQ M)	CL	ALTC1 (KM)	ALTC2 (KM)	ALTC3 (KM)	STEPB (SEC)
1.60	600.0	600.0	4400.0	.48	5.6	4.3	4.0	.2

Mach number limit to leave pullup = 2.6
Design flight path angle = 0 deg
Mach number limit for first parachute deployment = 2.4
Altitude to drop last parachute = km .5
Altitude to start landing burn = km .5

Deploy parachute 1 at 3978.7 sec Altitude = 2.80 km Mach no = 2.4
Deploy parachute 2 at 3981.7 sec Altitude = 2.31 km Mach no = 2.03
Deploy parachute 3 at 3983.7 sec Altitude = 2.01 km Mach no = 1.8
Parachute 3 dropped at 4007.7 sec Altitude = .45 km Mass = 52456.

T (SEC)	ALT (KM)	PHI (DEG)	GAM (DEG)	VEL (KM/S)	MACH	CD	CL	QP (N/M2)	QC (W/CM2)	MASS (KG)
3076.7	89.98	.5	-.1	3.3587	16.794	1.28	.48	12.7	.8	53306.9
3126.7	89.13	3.3	-.5	3.3581	16.791	1.28	.48	13.4	.9	53306.9
3176.7	87.08	6.0	-.9	3.3586	16.793	1.28	.48	16.1	1.0	53306.9
3226.7	83.83	8.8	-1.3	3.3599	16.799	1.28	.48	21.8	1.1	53306.9
3276.7	79.37	11.5	-1.7	3.3615	16.807	1.28	.48	33.3	1.4	53306.9
3326.7	73.75	14.3	-2.1	3.3622	16.811	1.28	.48	57.1	1.8	53306.9
3376.7	67.01	17.1	-2.5	3.3595	16.797	1.28	.48	109.5	2.5	53306.9
3426.7	59.25	19.8	-2.8	3.3465	16.454	1.28	.48	425.5	4.9	53306.9
3476.7	51.08	22.6	-2.8	3.2763	15.796	1.28	.48	851.4	6.6	53306.9
3526.7	43.50	25.2	-2.5	3.1326	14.759	1.28	.48	1567.9	8.2	53306.9
3576.7	37.64	27.7	-1.9	2.8893	13.343	1.28	.48	2349.5	8.5	53306.9
3626.7	34.12	30.0	-1.1	2.5756	11.745	1.28	.48	2670.5	7.2	53306.9
3676.7	32.21	32.0	-.8	2.2601	10.235	1.28	.48	2486.3	5.3	53306.9
3726.7	30.34	33.7	-1.4	1.9771	8.893	1.28	.48	2227.4	3.8	53306.9
3776.7	27.85	35.2	-1.9	1.6398	7.308	1.28	.48	2677.6	2.9	53306.9
3826.7	24.43	36.5	-3.7	1.3457	5.923	1.28	.48	2297.9	1.8	53306.9
3876.7	19.03	37.5	-6.9	1.0847	4.681	1.28	.48	2200.7	1.1	53306.9
3926.7	11.68	38.3	-11.2	.8333	3.505	1.28	.48	2243.2	.7	53306.9
3976.7	3.16	38.9	-17.3	.5944	2.434	1.28	.48	2191.6	.3	53306.9
3981.7	2.31	38.9	-18.1	.4964	2.027	7.60	.48	1849.6	.2	53306.9
3986.7	1.69	38.9	-20.2	.2382	.971	45.63	.48	449.3	.0	53216.6
3991.7	1.36	38.9	-25.8	.1354	.552	45.63	.48	149.4	.0	53216.6
3996.7	1.07	39.0	-34.1	.0985	.401	45.63	.48	80.8	.0	53216.6
4001.7	.80	39.0	-43.7	.0819	.333	45.63	.48	57.1	.0	53216.6
4006.7	.51	39.0	-53.1	.0743	.302	45.63	.48	48.0	.0	53216.6
4011.7	.22	39.0	-61.9	.0580	.236	1.60	.48	30.0	.0	51955.8
4016.7	.00	39.0	-70.9	.0400	.162	1.60	.48	14.5	.0	51330.8

Lateral range of 1 km requires 576.897 kg
Landing ΔV = .037 km/sec ΔM = 624.6 kg
Hover for 30.0 sec ΔM = 1954.99 kg Final Mass = 48049.3 kg
Land at 4052.7 SEC

MARS LANDING TRAJECTORY FOR A BLUNT LIFTING CONE - Trajectory no. 21

De Orbit Burn at 100.0 km:
ΔV = .003 km/sec Mass Consumed = 46.6 kg
Thermal Phase Burn at 90.0 km at time 3066.4 sec
ΔV = .003 km/sec Mass Consumed = 46.6 kg

CONDITIONS AT ENTRY:

MDOT (KG/S)	MASSO (KG)	ISP (SEC)	AREA (M SQ)	ALTP (KM)	ALTST (KM)	XLAT (KM)	INCP (DEG)	STEPC (SEC)
88.7	53306.9	300.0	99.9	100.0	90.0	1.00	.00	10.0

CDO	CDA1 (SQ M)	CDA2 (SQ M)	CDA3 (SQ M)	CL	ALTC1 (KM)	ALTC2 (KM)	ALTC3 (KM)	STEPB (SEC)
1.60	600.0	600.0	4400.0	.48	5.6	4.3	4.0	.2

Mach number limit to leave pullup = 2.6
Design flight path angle = 0 deg
Mach number limit for first parachute deployment = 2.4
Altitude to drop last parachute = km .5
Altitude to start landing burn = km .5

Deploy parachute 1 at 3979.0 sec Altitude = 2.80 km Mach no = 2.4
Deploy parachute 2 at 3982.0 sec Altitude = 2.31 km Mach no = 2.03
Deploy parachute 3 at 3984.0 sec Altitude = 2.01 km Mach no = 1.8
Parachute 3 dropped at 4008.0 sec Altitude = .45 km Mass = 52456.

T (SEC)	ALT (KM)	PHI (DEG)	GAM (DEG)	VEL (KM/S)	MACH	CD	CL	QP (N/M2)	QC (W/CM2)	MASS (KG)
3077.0	89.98	.5	-.1	3.3587	16.794	1.28	.48	12.7	.8	53306.9
3127.0	89.13	3.3	-.5	3.3581	16.791	1.28	.48	13.4	.9	53306.9
3177.0	87.08	6.0	-.9	3.3586	16.793	1.28	.48	16.1	1.0	53306.9
3227.0	83.83	8.8	-1.3	3.3599	16.799	1.28	.48	21.8	1.1	53306.9
3277.0	79.37	11.5	-1.7	3.3615	16.807	1.28	.48	33.3	1.4	53306.9
3327.0	73.75	14.3	-2.1	3.3622	16.811	1.28	.48	57.1	1.8	53306.9
3377.0	67.01	17.1	-2.5	3.3595	16.797	1.28	.48	109.5	2.5	53306.9
3427.0	59.25	19.8	-2.8	3.3465	16.454	1.28	.48	425.5	4.9	53306.9
3477.0	51.08	22.6	-2.8	3.2763	15.796	1.28	.48	851.4	6.6	53306.9
3527.0	43.50	25.2	-2.5	3.1326	14.759	1.28	.48	1567.9	8.2	53306.9
3577.0	37.64	27.7	-1.9	2.8893	13.343	1.28	.48	2349.5	8.5	53306.9
3627.0	34.12	30.0	-1.1	2.5756	11.745	1.28	.48	2670.5	7.2	53306.9
3677.0	32.21	32.0	-.8	2.2601	10.235	1.28	.48	2486.3	5.3	53306.9
3727.0	30.34	33.7	-1.4	1.9771	8.893	1.28	.48	2227.4	3.8	53306.9
3777.0	27.85	35.2	-1.9	1.6398	7.308	1.28	.48	2677.6	2.9	53306.9
3827.0	24.43	36.5	-3.7	1.3457	5.923	1.28	.48	2297.9	1.8	53306.9
3877.0	19.03	37.5	-6.9	1.0847	4.681	1.28	.48	2200.7	1.1	53306.9
3927.0	11.68	38.3	-11.2	.8333	3.505	1.28	.48	2243.2	.7	53306.9
3977.0	3.16	38.9	-17.3	.5944	2.434	1.28	.48	2191.6	.3	53306.9
3982.0	2.31	38.9	-18.1	.4964	2.027	7.60	.48	1849.6	.2	53306.9
3987.0	1.69	38.9	-20.2	.2382	.971	45.63	.48	449.3	.0	53216.6
3992.0	1.36	38.9	-25.8	.1354	.552	45.63	.48	149.4	.0	53216.6
3997.0	1.07	39.0	-34.1	.0985	.401	45.63	.48	80.8	.0	53216.6
4002.0	.80	39.0	-43.7	.0819	.333	45.63	.48	57.1	.0	53216.6
4007.0	.51	39.0	-53.1	.0743	.302	45.63	.48	48.0	.0	53216.6
4012.0	.21	39.0	-61.5	.0661	.269	1.60	.48	39.0	.0	52101.0

Lateral range of 1 km requires 582.985 kg
Landing ΔV = .060 km/sec ΔM = 1028.1 kg
Hover for 30.0 sec ΔM = 1960.10 kg Final Mass = 48175.0 kg
Land at 4057.6 SEC

MARS LANDING TRAJECTORY FOR A BLUNT LIFTING CONE - Trajectory no. 22

De Orbit Burn at 100.0 km:
ΔV = .003 km/sec Mass Consumed = 45.4 kg
Thermal Phase Burn at 90.0 km at time 3066.4 sec
ΔV = .003 km/sec Mass Consumed = 45.4 kg

CONDITIONS AT ENTRY:

MDOT (KG/S)	MASSO (KG)	ISP (SEC)	AREA (M SQ)	ALTP (KM)	ALTST (KM)	XLAT (KM)	INCP (DEG)	STEPC (SEC)
88.7	52009.2	300.0	99.9	100.0	90.0	1.00	.00	10.0

CDO	CDA1 (SQ M)	CDA2 (SQ M)	CDA3 (SQ M)	CL	ALTC1 (KM)	ALTC2 (KM)	ALTC3 (KM)	STEPB (SEC)
1.60	600.0	600.0	4800.0	.48	5.6	4.3	4.0	.2

Mach number limit to leave pullup = 2.8
Design flight path angle = 0 deg
Mach number limit for first parachute deployment = 2.6
Altitude to drop last parachute = km .5
Altitude to start landing burn = km .5

Deploy parachute 1 at 3966.7 sec Altitude = 5.11 km Mach no = 2.6
Deploy parachute 2 at 3972.1 sec Altitude = 4.27 km Mach no = 1.99
Heat shield dropped, mass 1450.0 kg Total mass = 50468.9 kg
Deploy parachute 3 at 3974.3 sec Altitude = 3.97 km Mach no = 1.8
Parachute 3 dropped at 4028.3 sec Altitude = .49 km Mass = 49639.

T (SEC)	ALT (KM)	PHI (DEG)	GAM (DEG)	VEL (KM/S)	MACH	CD	CL	QF (N/M2)	QC (W/CM2)	MASS (KG)
3076.9	89.98	.5	-.1	3.3587	16.794	1.28	.48	12.7	.8	52009.2
3126.9	89.13	3.3	-.5	3.3581	16.790	1.28	.48	13.4	.9	52009.2
3176.9	87.08	6.0	-.9	3.3585	16.793	1.28	.48	16.1	1.0	52009.2
3226.9	83.83	8.8	-1.3	3.3597	16.799	1.28	.48	21.8	1.1	52009.2
3276.9	79.38	11.5	-1.7	3.3612	16.806	1.28	.48	33.3	1.4	52009.2
3326.9	73.76	14.3	-2.1	3.3618	16.809	1.28	.48	57.0	1.8	52009.2
3376.9	67.02	17.1	-2.5	3.3589	16.794	1.28	.48	109.3	2.5	52009.2
3426.9	59.28	19.8	-2.8	3.3453	16.450	1.28	.48	424.4	4.9	52009.2
3476.9	51.12	22.5	-2.8	3.2735	15.785	1.28	.48	846.8	6.6	52009.2
3526.9	43.60	25.2	-2.5	3.1273	14.739	1.28	.48	1550.2	8.1	52009.2
3576.9	37.82	27.7	-1.8	2.8819	13.317	1.28	.48	2303.2	8.4	52009.2
3626.9	34.36	30.0	-1.1	2.5681	11.721	1.28	.48	2599.2	7.0	52009.2
3676.9	32.47	32.0	-.8	2.2539	10.217	1.28	.48	2414.5	5.2	52009.2
3726.9	30.58	33.7	-1.4	1.9720	8.878	1.28	.48	2167.3	3.7	52009.2
3776.9	27.96	35.2	-1.9	1.6395	7.310	1.28	.48	2649.1	2.8	52009.2
3826.9	24.49	36.5	-3.7	1.3411	5.903	1.28	.48	2270.9	1.7	52009.2
3876.9	19.12	37.5	-6.9	1.0775	4.651	1.28	.48	2158.3	1.1	52009.2
3926.9	11.82	38.2	-11.3	.8259	3.475	1.28	.48	2182.3	.6	52009.2
3957.3	6.73	38.6	-14.7	.6764	2.806	1.28	.48	2470.2	.5	52009.2
3958.3	6.56	38.6	-14.8	.6733	2.785	1.28	.48	2466.2	.4	52009.2
3959.3	6.39	38.6	-15.0	.6682	2.763	1.28	.48	2462.1	.4	52009.2
3960.3	6.22	38.6	-15.1	.6632	2.741	1.28	.48	2457.8	.4	52009.2
3961.3	6.04	38.7	-15.2	.6581	2.718	1.28	.48	2453.4	.4	52009.2
3962.3	5.87	38.7	-15.3	.6531	2.696	1.28	.48	2448.9	.4	52009.2
3963.3	5.70	38.7	-15.4	.6481	2.674	1.28	.48	2444.2	.4	52009.2
3964.3	5.53	38.7	-15.6	.6431	2.652	1.28	.48	2439.4	.4	52009.2
3965.3	5.35	38.7	-15.7	.6382	2.630	1.28	.48	2434.5	.4	52009.2
3966.3	5.18	38.7	-15.8	.6332	2.609	1.28	.48	2429.4	.4	52009.2
3967.3	5.01	38.7	-15.9	.6112	2.517	7.60	.48	2293.8	.4	52009.2
3968.3	4.85	38.7	-16.1	.5802	2.388	7.60	.48	2094.0	.3	52009.2
3969.3	4.69	38.7	-16.3	.5520	2.270	7.60	.48	1918.8	.3	52009.2
3970.3	4.54	38.7	-16.5	.5262	2.163	7.60	.48	1764.4	.2	52009.2
3971.3	4.39	38.8	-16.7	.5025	2.065	7.60	.48	1627.9	.2	52009.2
3972.3	4.25	38.8	-17.0	.4806	1.974	7.60	.48	1505.8	.2	50468.9

3973.3	4.11	38.8	-17.3	.4599	1.888	7.60	.48	1394.0	.2	50468.9
3974.3	3.97	38.8	-17.6	.4408	1.809	7.60	.48	1294.3	.1	50468.9
3975.3	3.86	38.8	-18.0	.3426	1.406	49.63	.48	789.3	.1	50468.9
3976.3	3.76	38.8	-18.5	.2801	1.149	49.63	.48	531.8	.0	50468.9
3977.3	3.68	38.8	-19.3	.2370	.972	49.63	.48	383.2	.0	50468.9
3978.3	3.60	38.8	-20.1	.2055	.843	49.63	.48	289.9	.0	50468.9
3979.3	3.53	38.8	-21.1	.1816	.745	49.63	.48	227.7	.0	50468.9
3980.3	3.47	38.8	-22.3	.1630	.668	49.63	.48	184.2	.0	50468.9
3981.3	3.41	38.8	-23.5	.1480	.606	49.63	.48	152.6	.0	50468.9
3982.3	3.35	38.8	-24.9	.1358	.556	49.63	.48	129.1	.0	50468.9
3983.3	3.29	38.8	-26.4	.1257	.515	49.63	.48	111.1	.0	50468.9
3984.3	3.24	38.8	-28.0	.1173	.480	49.63	.48	97.2	.0	50468.9
3985.3	3.18	38.8	-29.7	.1102	.451	49.63	.48	86.1	.0	50468.9
3986.3	3.13	38.8	-31.4	.1042	.426	49.63	.48	77.3	.0	50468.9
3987.3	3.08	38.8	-33.3	.0990	.405	49.63	.48	70.1	.0	50468.9
3988.3	3.02	38.8	-35.1	.0946	.387	49.63	.48	64.3	.0	50468.9
3989.3	2.97	38.8	-37.1	.0908	.372	49.63	.48	59.5	.0	50468.9
3990.3	2.91	38.8	-39.0	.0876	.358	49.63	.48	55.6	.0	50468.9
3991.3	2.86	38.8	-40.9	.0848	.347	49.63	.48	52.3	.0	50468.9
3992.3	2.80	38.8	-42.9	.0824	.337	49.63	.48	49.6	.0	50468.9
3993.3	2.74	38.8	-44.9	.0803	.329	49.63	.48	47.4	.0	50468.9
3994.3	2.69	38.8	-46.8	.0786	.321	49.63	.48	45.5	.0	50468.9
3995.3	2.63	38.8	-48.7	.0771	.315	49.63	.48	44.0	.0	50468.9
3996.3	2.57	38.8	-50.5	.0758	.310	49.63	.48	42.7	.0	50468.9
3997.3	2.51	38.8	-52.4	.0747	.305	49.63	.48	41.7	.0	50468.9
3998.3	2.45	38.8	-54.1	.0738	.301	49.63	.48	40.8	.0	50468.9
3999.3	2.39	38.8	-55.9	.0730	.298	49.63	.48	40.2	.0	50468.9
4000.3	2.33	38.8	-57.5	.0723	.295	49.63	.48	39.6	.0	50468.9
4001.3	2.27	38.8	-59.1	.0718	.293	49.63	.48	39.2	.0	50468.9
4002.3	2.21	38.8	-60.7	.0713	.291	49.63	.48	38.9	.0	50468.9
4003.3	2.15	38.8	-62.1	.0709	.290	49.63	.48	38.7	.0	50468.9
4004.3	2.08	38.8	-63.5	.0706	.288	49.63	.48	38.5	.0	50468.9
4005.3	2.02	38.8	-64.9	.0703	.287	49.63	.48	38.4	.0	50468.9
4006.3	1.96	38.8	-66.2	.0701	.286	49.63	.48	38.4	.0	50468.9
4007.3	1.89	38.8	-67.4	.0699	.285	49.63	.48	38.4	.0	50468.9
4008.3	1.83	38.8	-68.6	.0698	.285	49.63	.48	38.4	.0	50468.9
4009.3	1.76	38.8	-69.7	.0697	.284	49.63	.48	38.4	.0	50468.9
4010.3	1.70	38.8	-70.8	.0695	.284	49.63	.48	38.5	.0	50468.9
4011.3	1.63	38.8	-71.8	.0695	.283	49.63	.48	38.6	.0	50468.9
4012.3	1.56	38.8	-72.7	.0694	.283	49.63	.48	38.7	.0	50468.9
4013.3	1.50	38.8	-73.6	.0693	.282	49.63	.48	38.8	.0	50468.9
4014.3	1.43	38.8	-74.5	.0692	.282	49.63	.48	39.0	.0	50468.9
4015.3	1.36	38.8	-75.3	.0692	.282	49.63	.48	39.1	.0	50468.9
4016.3	1.30	38.8	-76.1	.0691	.281	49.63	.48	39.2	.0	50468.9
4017.3	1.23	38.8	-76.8	.0690	.281	49.63	.48	39.4	.0	50468.9
4018.3	1.16	38.8	-77.5	.0690	.281	49.63	.48	39.5	.0	50468.9
4019.3	1.10	38.8	-78.1	.0689	.280	49.63	.48	39.6	.0	50468.9
4020.3	1.03	38.8	-78.8	.0688	.280	49.63	.48	39.7	.0	50468.9
4021.3	.96	38.8	-79.3	.0687	.280	49.63	.48	39.9	.0	50468.9
4022.3	.89	38.8	-79.9	.0687	.279	49.63	.48	40.0	.0	50468.9
4023.3	.83	38.8	-80.4	.0686	.279	49.63	.48	40.1	.0	50468.9
4024.3	.76	38.8	-80.9	.0685	.279	49.63	.48	40.2	.0	50468.9
4025.3	.69	38.8	-81.4	.0684	.278	49.63	.48	40.3	.0	50468.9
4026.3	.62	38.8	-81.8	.0683	.278	49.63	.48	40.4	.0	50468.9
4027.3	.56	38.8	-82.3	.0682	.277	49.63	.48	40.5	.0	50468.9
4028.3	.49	38.8	-82.7	.0681	.277	49.63	.48	40.6	.0	50468.9
4029.3	.42	38.8	-83.0	.0666	.270	1.60	.48	39.0	.0	49550.2
4030.3	.36	38.8	-83.4	.0650	.264	1.60	.48	37.4	.0	49461.5
4031.3	.29	38.8	-83.8	.0635	.258	1.60	.48	35.9	.0	49372.8
4032.3	.23	38.8	-84.1	.0620	.252	1.60	.48	34.3	.0	49284.1
4033.3	.17	38.8	-84.4	.0605	.246	1.60	.48	32.8	.0	49195.4
4034.3	.11	38.8	-84.8	.0590	.239	1.60	.48	31.3	.0	49106.7
4035.3	.05	38.8	-85.1	.0574	.233	1.60	.48	29.9	.0	49018.0
[illegible]		[illegible]	[illegible]	0559	227	1.60	.48	28.4	.0	48929.3

Lateral range of 1 km requires 551.249 kg
Landing ΔV = .056 km/sec ΔM = 910.9 kg
Hover for 30.0 sec ΔM = 1855.79 kg Final Mass = 45611.4 kg
Land at 4076.6 SEC

Appendix E

Launcher Trajectory Program and Key Runs

(Kraft)

```
00010 REM planar, single-stage mars launch trajectory
00020 REM fourth order Runge-Kutta integration
00030 REM For liftoff , pitch over at PRATE deg/sec until TTURN
00040 REM   Burn until apogee > parking orbit altitude, calculate circularization ΔV and Δm
      by Keplerian elements
00050 DEFDBL A-H, O-Z : DEFINT I-N
00060 DIM QQ(4,4),TIME(2000),ALT(2000),PHI(2000),VEL(2000),GAM(2000),APO(2000),ZMPR(2000),Q
      P(2000),FNC(4)
00070 G0=0.00980665 : CMU=45599. : RHOZ=.0182 : RHOK=0.1 :RMARS=3415. : TT=0.
00080 VROTMARS=.24206 : RAD= 57.2957795 : ICOUNT=0 : IPP=0
00090 REM G0 = Earth surface gravity, CMU = Mars gravitational constant
00100 REM RHO = Density = RHOZ*exp(-RHOK*(r-RMARS), RMARS = Mars radius
00110 REM VROTMARS = Velocity of rotation at Mars equator in km/sec
00120 PI=ATN(1)<<2 : PHIX=0.
00130 DEF FN ARCCOS(Q)=ATN(1)*2-ATN(Q/SQR(1-Q*Q))
00140 DEF FN DXDT(VXF)=VXF
00150 DEF FN DYDT(VYF)=VYF
00160 LONG FN DVXDT(TTF,XXF,YYF,VXF,VYF)
00170   ZM=ZMASS0-ZMDOT*TTF
00180   VV=SQR(VXF*VXF+VYF*VYF)
00190   RR=SQR(XXF*XXF+YYF*YYF)
00200   CD=.1
00210   RHO=RHOZ*EXP(-RHOK*(RR-RMARS))
00220 END FN =(G0*ZISP*ZMDOTX)*XT/ZM-500.*RHO*VV*VV*CD*AREA*VXF/VV/ZM-CMU*XXF/RR^3
00230 LONG FN DVYDT(TTF,XXF,YYF,VXF,VYF)
00240   ZM=ZMASS0-ZMDOT*TTF
00250   VV=SQR(VXF*VXF+VYF*VYF)
00260   RR=SQR(XXF*XXF+YYF*YYF)
00270   CD=.1
00280   RHO=RHOZ*EXP(-RHOK*(RR-RMARS))
00290 END FN =(G0*ZISP*ZMDOTX)*YT/ZM-500.*RHO*VV*VV*CD*AREA*VYF/VV/ZM-CMU*YYF/RR^3
00300 PRINT "Mars Launch Trajectory"
00310 REM Burn at parking orbit is calculated from Δv=g*Isp*ln(Mo/Mf)
00320 PRINT "Enter initial mass, kg" : INPUT ZMASS0
00330 PRINT "Enter mass flow rate, kg/sec" : INPUT ZMDOT
00340 PRINT "Enter specific impulse, sec" : INPUT ZISP
00350 PRINT "Enter forward surface area, sq meters" : INPUT AREA
00360 PRINT "Enter integration step, sec" : INPUT DT
00370 PRINT "Enter 0 for single trajectory, 1 for search" : INPUT ISEARCH
00380 PRINT "Enter N to print every Nth step" : INPUT IPRINT
00390 PRINT "Enter parking orbit altitude, km" : INPUT ALTP
00400 PRINT "Enter duration of initial pitch rate" : INPUT TTURN
00410 PRINT "Enter magnitude of initial pitch rate, deg/sec" : INPUT PRATE
00420 PRINT "Enter launch azimuth, deg" : INPUT AZIM
00430 PRINT "Enter trajectory number" : INPUT ITRAJ
00440 VY=COS(PI/2.-AZIM/RAD)*VROTMARS
00450 CLS : LPRINT "MARS LAUNCH TRAJECTORY  -  Trajectory Number";ITRAJ
00460 REM Set initial conditions
00470 XX=RMARS
00480 YY=0.
00490 REM VY set from Mars rotation adjusted for launch azimuth
00500 ZETA=0. : XT=1. : YT=0.
00510 ZMDOTX=ZMDOT
00520 REM Print initial conditions
00530 LPRINT : LPRINT : LPRINT "INITIAL CONDITIONS" : LPRINT
00540 LPRINT "   TTURN    PRATE    MDOT    MASS0     ISP     AREA     ALTP     L-AZ     INC
      P     STEP"
00550 LPRINT "   (SEC)    (DEG/S)  (KG/S)   (KG)     (SEC)    (M SQ)     (KM)     (DEG)     (DEG
      )     (SEC)"
00560 LPRINT USING "   ###.#";TTURN;USING "    #.##";PRATE;USING "   ####.#";ZMDOT;USING "
       ######.#";ZMASS0;USING "  ####.#";ZISP;USING "   ###.#";AREA;USING "    ####.#";ALTP
      ;USING "  ####.##";AZIM;USING "  ###.##";AINC;USING "    ##.#";DT
00570 REM Begin integration
00580 GOSUB "RUNGE-KUTTA"
00590 RR=SQR(XX*XX+YY*YY) : VV=SQR(VX*VX+VY*VY) : XALT=RR-RMARS
00600 GGG=(XX*VX+YY*VY)/RR/VV : GG=ATN(GGG/SQR(1.-GGG*GGG))
```

```
00610 CPHI=XX/RR : PHIX=FN ARCCOS(CPHI) : RHO=RHOZ*EXP(-RHOK*(RR-RMARS))
00620 RVG=RR*VV*COS(GG) : QPP=.5*RHO*VV*VV*1.E6
00630 AAA=(2./RR-VV*VV/CMU) : EE=SQR(1.-RVG*RVG*AAA/CMU)
00640 VAP=CMU/RVG*(1.-EE) : XAP=(1.+EE)/AAA-RMARS : VFF=SQR(CMU/(ALTP+RMARS))-VAP
00650 REM XAP is instantaneous apocenter altitude
00660 LONG IF ICOUNT MOD IPRINT =0
00670   IPP=IPP+1
00680   TIME(IPP)=TT : ALT(IPP)=XALT : PHI(IPP)=PHIX*RAD : VEL(IPP)=VV
00690   GAM(IPP)=GG*RAD : ZMPR(IPP)=ZM : QP(IPP)=QPP
00700   APO(IPP)=XAP
00710 END IF
00720 IF IPP >= 1999 THEN GOTO 850
00730 LONG IF TT < TTURN
00740   ZETA=ZETA+DT*PRATE/RAD : XT=COS(ZETA) : YT=SIN(ZETA)
00750   GOTO 800
00760 END IF
00770 LONG IF TT >= TTURN
00780   XT=VX/VV : YT=VY/VV
00790 END IF
00800 IF XAP >= ALTP AND ISEARCH = 0 THEN GOTO 850
00810 GOTO 580
00820 IF ISEARCH = 0 THEN GOTO 850
00830 TTURN=TTURN+1.
00840 IPP=0 : ICOUNT=0 : ISEARCH=ISEARCH+1 : GOTO 850
00850 LPRINT
00860 LPRINT : LPRINT
00870 LPRINT "   T      ALT      PHI        GAM       VEL       APO       q          MASS"
00880 LPRINT " (SEC)    (KM)     (DEG)      (DEG)     (KM/S)    (KM)      (N/M2)      (KG)"
00890 LPRINT
00900 LONG IF ISEARCH = 0
00910   FOR I = 1 TO IPP STEP IPRINT
00920     LPRINT  USING " ###.#";TIME(I);USING "  ###.#";ALT(I);USING "    ###.###";PHI(I);
          USING "    ####.##";GAM(I);USING "    ##.####";VEL(I);USING "    ###.#";APO(I);US
          ING "   #####.#";QP(I);USING "   ######.##";ZMPR(I)
00930   NEXT
00940   LPRINT : LPRINT "Final Values"
00950   LPRINT  USING " ###.#";TT;USING "  ###.#";XALT;USING "    ###.###";PHIX*RAD;USING "
          ####.##";GG*RAD;USING "    ##.####";VV;USING "    ###.#";XAP;USING "   #####.#"
        ;QPP;USING "   ######.##";ZM
00960   REM Calculate circularization Δv at apocenter
00970   DELTV=SQR(CMU/(XAP+RMARS))-VAP : ZMFIN=ZM/(EXP(DELTV/G0/ZISP))
00980   LPRINT USING "  Circularization ΔV = ##.#### km/sec";DELTV;USING "     Final Mass =
         ######.#  kg";ZMFIN
00990   GOTO 1050
01000 END IF
01010 LPRINT : LPRINT "FINAL VALUES"
01020 LPRINT USING "   ###.#";TT;USING "  ###.#";XX-RMARS;USING "  ####.#";PHIX;USING "  ##
      ####.#";GG
01030 IF XALT < 0. OR VFF < 0. GOTO 1050
01040 IF ISEARCH < 10 THEN GOTO 470
01050 END
01060 :
01070 "RUNGE-KUTTA"
01080 FNC(1)=FN DXDT(VX)
01090 FNC(2)=FN DYDT(VY)
01100 FNC(3)=FN DVXDT(TT,XX,YY,VX,VY)
01110 FNC(4)=FN DVYDT(TT,XX,YY,VX,VY)
01120 FOR I = 1 TO 4
01130   QQ(I,1)=DT*FNC(I)
01140 NEXT I
01150 FNC(1)=FN DXDT(VX+.5*QQ(3,1))
01160 FNC(2)=FN DYDT(VY+.5*QQ(4,1))
01170 FNC(3)=FN DVXDT(TT+.5*DT,XX+.5*QQ(1,1),YY+.5*QQ(2,1),VX+.5*QQ(3,1),VY+.5*QQ(4,1))
01180 FNC(4)=FN DVYDT(TT+.5*DT,XX+.5*QQ(1,1),YY+.5*QQ(2,1),VX+.5*QQ(3,1),VY+.5*QQ(4,1))
01190 FOR I = 1 TO 4
01200   QQ(I,2)=DT*FNC(I)
```

```
01210 NEXT I
01220 FNC(1)=FN DXDT(VX+.5*QQ(3,2))
01230 FNC(2)=FN DYDT(VY+.5*QQ(4,2))
01240 FNC(3)=FN DVXDT(TT+.5*DT,XX+.5*QQ(1,2),YY+.5*QQ(2,2),VX+.5*QQ(3,2),VY+.5*QQ(4,2))
01250 FNC(4)=FN DVYDT(TT+.5*DT,XX+.5*QQ(1,2),YY+.5*QQ(2,2),VX+.5*QQ(3,2),VY+.5*QQ(4,2))
01260 FOR I = 1 TO 4
01270   QQ(I,3)=DT*FNC(I)
01280 NEXT I
01290 FNC(1)=FN DXDT(VX+QQ(3,3))
01300 FNC(2)=FN DYDT(VY+QQ(4,3))
01310 FNC(3)=FN DVXDT(TT+DT,XX+QQ(1,3),YY+QQ(2,3),VX+QQ(3,3),VY+QQ(4,3))
01320 FNC(4)=FN DVYDT(TT+DT,XX+QQ(1,3),YY+QQ(2,3),VX+QQ(3,3),VY+QQ(4,3))
01330 FOR I = 1 TO 4
01340   QQ(I,4)=DT*FNC(I)
01350 NEXT I
01360 TT=TT+DT
01370 XX=XX+(QQ(1,1)+2.*QQ(1,2)+2.*QQ(1,3)+QQ(1,4))/6.
01380 YY=YY+(QQ(2,1)+2.*QQ(2,2)+2.*QQ(2,3)+QQ(2,4))/6.
01390 VX=VX+(QQ(3,1)+2.*QQ(3,2)+2.*QQ(3,3)+QQ(3,4))/6.
01400 VY=VY+(QQ(4,1)+2.*QQ(4,2)+2.*QQ(4,3)+QQ(4,4))/6.
01410 RETURN
```

MARS LAUNCH TRAJECTORY - Trajectory Number 1

INITIAL CONDITIONS

TTURN (SEC)	PRATE (DEG/S)	MDOT (KG/S)	MASS0 (KG)	ISP (SEC)	AREA (M SQ)	ALTP (KM)	L-AZ (DEG)	INCP (DEG)	STEP (SEC)
4.0	1.00	180.0	20300.0	300.0	14.9	170.0	90.00	.00	.2

T (SEC)	ALT (KM)	PHI (DEG)	GAM (DEG)	VEL (KM/S)	APO (KM)	q (N/M2)	MASS (KG)
.2	.0	-.000	1.05	.2421	.0	533.3	20264.00
2.2	.1	-.000	11.49	.2479	.4	556.4	19904.00
4.2	.2	.013	20.10	.2667	1.3	634.7	19544.00
6.2	.4	.024	18.67	.3187	1.7	888.8	19184.00
8.2	.6	.036	17.46	.3719	2.2	1184.4	18824.00
10.2	.8	.050	16.40	.4262	2.7	1520.0	18464.00
12.2	1.1	.065	15.47	.4817	3.2	1894.0	18104.00
14.2	1.4	.081	14.65	.5384	3.8	2304.4	17744.00
16.2	1.6	.100	13.90	.5963	4.3	2749.2	17384.00
18.2	1.9	.120	13.23	.6556	4.9	3226.3	17024.00
20.2	2.2	.143	12.62	.7161	5.5	3733.2	16664.00
22.2	2.5	.167	12.06	.7779	6.1	4267.8	16304.00
24.2	2.9	.194	11.55	.8412	6.7	4827.5	15944.00
26.2	3.2	.222	11.08	.9059	7.4	5409.9	15584.00
28.2	3.6	.253	10.64	.9721	8.0	6012.9	15224.00
30.2	3.9	.286	10.24	1.0398	8.7	6633.9	14864.00
32.2	4.3	.322	9.87	1.1092	9.4	7270.6	14504.00
34.2	4.7	.360	9.52	1.1802	10.1	7920.9	14144.00
36.2	5.1	.400	9.20	1.2530	10.9	8582.2	13784.00
38.2	5.5	.443	8.90	1.3277	11.7	9252.5	13424.00
40.2	5.9	.488	8.62	1.4043	12.6	9929.7	13064.00
42.2	6.3	.536	8.37	1.4830	13.5	10611.1	12704.00
44.2	6.8	.586	8.13	1.5639	14.5	11295.2	12344.00
46.2	7.2	.639	7.91	1.6470	15.5	11979.7	11984.00
48.2	7.7	.695	7.70	1.7326	16.6	12662.4	11624.00
50.2	8.2	.754	7.51	1.8207	17.8	13341.2	11264.00
52.2	8.6	.816	7.34	1.9116	19.2	14013.9	10904.00
54.2	9.1	.881	7.18	2.0054	20.7	14678.6	10544.00
56.2	9.6	.950	7.03	2.1023	22.3	15332.9	10184.00
58.2	10.2	1.021	6.90	2.2026	24.3	15974.7	9824.00
60.2	10.7	1.096	6.78	2.3065	26.5	16601.8	9464.00
62.2	11.3	1.174	6.67	2.4142	29.1	17211.9	9104.00
64.2	11.8	1.256	6.57	2.5262	32.3	17802.2	8744.00
66.2	12.4	1.342	6.49	2.6427	36.3	18370.4	8384.00
68.2	13.0	1.432	6.41	2.7642	41.5	18914.0	8024.00
70.2	13.6	1.526	6.35	2.8911	48.5	19430.1	7664.00
72.2	14.3	1.624	6.30	3.0239	58.6	19916.1	7304.00
74.2	15.0	1.727	6.26	3.1633	74.5	20369.1	6944.00
76.2	15.7	1.834	6.23	3.3100	103.1	20785.7	6584.00
78.2	16.4	1.947	6.21	3.4649	167.0	21163.6	6224.00
Final Values							
78.4	16.5	1.958	6.21	3.4808	177.6	21199.0	6188.00

Circularization ΔV = .2575 km/sec Final Mass = 5669.5 kg

MARS LAUNCH TRAJECTORY - Trajectory Number 2

INITIAL CONDITIONS

TTURN (SEC)	PRATE (DEG/S)	MDOT (KG/S)	MASSO (KG)	ISP (SEC)	AREA (M SQ)	ALTP (KM)	L-AZ (DEG)	INCP (DEG)	STEP (SEC)
240.0	.35	42.2	22000.0	300.0	14.9	170.0	90.00	.00	.2

T (SEC)	ALT (KM)	PHI (DEG)	GAM (DEG)	VEL (KM/S)	APO (KM)	q (N/M2)	MASS (KG)
.2	.0	-.000	.08	.2421	.0	533.2	21991.56
10.2	.1	.041	4.32	.2441	.1	537.4	21569.56
20.2	.4	.082	8.54	.2511	.5	553.0	21147.56
30.2	.8	.125	12.50	.2631	1.3	579.1	20725.56
40.2	1.5	.169	15.99	.2800	2.3	613.2	20303.56
50.2	2.4	.215	18.90	.3015	3.6	651.6	19881.56
60.2	3.5	.265	21.19	.3274	5.3	689.8	19459.56
70.2	4.8	.318	22.89	.3574	7.3	722.9	19037.56
80.2	6.2	.375	24.04	.3914	9.5	746.7	18615.56
90.2	7.9	.438	24.72	.4291	12.1	757.6	18193.56
100.2	9.8	.506	24.99	.4705	15.0	753.7	17771.56
110.2	11.9	.581	24.93	.5154	18.1	734.6	17349.56
120.2	14.2	.663	24.59	.5639	21.4	701.4	16927.56
130.2	16.6	.753	24.02	.6159	24.9	656.3	16505.56
140.2	19.2	.851	23.27	.6714	28.6	602.6	16083.56
150.2	21.9	.959	22.37	.7306	32.3	543.7	15661.56
160.2	24.7	1.076	21.34	.7934	36.1	482.9	15239.56
170.2	27.7	1.205	20.22	.8599	39.8	423.1	14817.56
180.2	30.7	1.345	19.02	.9302	43.4	366.6	14395.56
190.2	33.7	1.498	17.76	1.0044	46.9	315.0	13973.56
200.2	36.8	1.663	16.45	1.0825	50.2	269.3	13551.56
210.2	39.8	1.843	15.10	1.1646	53.2	229.7	13129.56
220.2	42.8	2.036	13.72	1.2509	55.9	196.3	12707.56
230.2	45.8	2.246	12.31	1.3415	58.2	168.6	12285.56
240.2	48.5	2.471	10.89	1.4364	60.0	146.3	11863.56
250.2	51.2	2.712	9.69	1.5360	61.9	128.3	11441.56
260.2	53.7	2.971	8.60	1.6404	63.7	113.8	11019.56
270.2	56.1	3.249	7.61	1.7498	65.3	102.0	10597.56
280.2	58.4	3.544	6.71	1.8645	66.9	92.5	10175.56
290.2	60.5	3.860	5.91	1.9848	68.3	84.8	9753.56
300.2	62.4	4.196	5.20	2.1112	69.8	78.8	9331.56
310.2	64.3	4.553	4.57	2.2440	71.1	74.0	8909.56
320.2	66.0	4.933	4.02	2.3838	72.5	70.2	8487.56
330.2	67.6	5.336	3.54	2.5313	74.0	67.4	8065.56
340.2	69.1	5.764	3.15	2.6871	75.6	65.2	7643.56
350.2	70.6	6.219	2.83	2.8521	77.5	63.6	7221.56
360.2	72.0	6.701	2.58	3.0273	80.2	62.4	6799.56
370.2	73.3	7.213	2.40	3.2140	84.8	61.5	6377.56
380.2	74.7	7.757	2.30	3.4138	97.1	60.6	5955.56

Final Values

388.4	75.8	8.228	2.27	3.5885	171.8	59.7	5609.52

Circularization ΔV = .0758 km/sec Final Mass = 5466.9 kg

MARS LAUNCH TRAJECTORY - Trajectory Number 3

INITIAL CONDITIONS

TTURN (SEC)	PRATE (DEG/S)	MDOT (KG/S)	MASSO (KG)	ISP (SEC)	AREA (M SQ)	ALTP (KM)	L-AZ (DEG)	INCP (DEG)	STEP (SEC)
240.0	.40	42.2	22000.0	300.0	14.9	170.0	90.00	.00	.2

T (SEC)	ALT (KM)	PHI (DEG)	GAM (DEG)	VEL (KM/S)	APO (KM)	q (N/M2)	MASS (KG)
.2	.0	-.000	.08	.2421	.0	533.2	21991.56
10.2	.1	.041	4.31	.2444	.1	538.5	21569.56
20.2	.4	.082	8.49	.2521	.5	557.4	21147.56
30.2	.8	.125	12.33	.2653	1.3	588.8	20725.56
40.2	1.5	.170	15.62	.2837	2.3	630.1	20303.56
50.2	2.4	.217	18.26	.3071	3.6	677.3	19881.56
60.2	3.4	.268	20.23	.3351	5.2	725.5	19459.56
70.2	4.7	.323	21.56	.3675	7.0	769.6	19037.56
80.2	6.1	.383	22.33	.4041	9.2	805.1	18615.56
90.2	7.7	.448	22.61	.4445	11.6	828.3	18193.56
100.2	9.5	.520	22.50	.4887	14.1	837.2	17771.56
110.2	11.5	.600	22.05	.5367	16.8	831.2	17349.56
120.2	13.6	.687	21.34	.5884	19.6	811.4	16927.56
130.2	15.8	.783	20.40	.6437	22.5	779.8	16505.56
140.2	18.0	.889	19.30	.7027	25.3	739.5	16083.56
150.2	20.4	1.005	18.06	.7655	28.0	693.7	15661.56
160.2	22.8	1.132	16.70	.8320	30.6	645.6	15239.56
170.2	25.2	1.271	15.26	.9023	32.9	598.2	14817.56
180.2	27.5	1.422	13.75	.9765	35.0	553.7	14395.56
190.2	29.8	1.587	12.19	1.0546	36.8	514.3	13973.56
200.2	32.0	1.765	10.58	1.1366	38.2	481.3	13551.56
210.2	34.0	1.958	8.94	1.2226	39.3	456.0	13129.56
220.2	35.7	2.167	7.28	1.3127	39.9	439.7	12707.56
230.2	37.3	2.391	5.59	1.4070	40.1	433.9	12285.56
240.2	38.5	2.632	3.90	1.5055	40.1	440.5	11863.56
250.2	39.4	2.890	2.76	1.6093	40.3	460.0	11441.56
260.2	40.0	3.165	1.72	1.7178	40.5	491.4	11019.56
270.2	40.4	3.459	.78	1.8311	40.5	537.4	10597.56
280.2	40.5	3.773	-.07	1.9496	40.5	602.4	10175.56
290.2	40.3	4.106	-.82	2.0736	40.5	692.4	9753.56
300.2	39.9	4.460	-1.49	2.2033	40.6	816.5	9331.56
310.2	39.2	4.837	-2.08	2.3392	40.8	988.0	8909.56
320.2	38.2	5.236	-2.58	2.4816	41.3	1227.0	8487.56
330.2	37.0	5.660	-3.02	2.6310	42.2	1563.2	8065.56
340.2	35.4	6.109	-3.38	2.7878	44.0	2042.1	7643.56
350.2	33.7	6.585	-3.66	2.9525	47.2	2732.7	7221.56
360.2	31.7	7.088	-3.88	3.1254	53.6	3741.1	6799.56
370.2	29.5	7.622	-4.03	3.3065	68.3	5229.2	6377.56
380.2	27.0	8.186	-4.11	3.4955	116.1	7442.6	5955.56
Final Values							
384.2	26.0	8.421	-4.13	3.5730	172.4	8608.3	5786.76

Circularization ΔV = 1469 km/sec Final Mass = 5504.9 kg

MARS LAUNCH TRAJECTORY - Trajectory Number 4

INITIAL CONDITIONS

TTURN (SEC)	PRATE (DEG/S)	MDOT (KG/S)	MASSO (KG)	ISP (SEC)	AREA (M SQ)	ALTP (KM)	L-AZ (DEG)	INCP (DEG)	STEP (SEC)
240.0	.45	42.2	22000.0	300.0	14.9	170.0	90.00	.00	.2

T (SEC)	ALT (KM)	PHI (DEG)	GAM (DEG)	VEL (KM/S)	APO (KM)	q (N/M2)	MASS (KG)
.2	.0	-.000	.08	.2421	.0	533.2	21991.56
10.2	.1	.041	4.30	.2446	.1	539.6	21569.56
20.2	.4	.083	8.43	.2531	.5	561.8	21147.56
30.2	.8	.125	12.15	.2674	1.2	598.6	20725.56
40.2	1.5	.171	15.25	.2874	2.2	647.2	20303.56
50.2	2.3	.219	17.62	.3126	3.5	703.4	19881.56
60.2	3.4	.271	19.27	.3428	5.0	762.0	19459.56
70.2	4.6	.328	20.25	.3775	6.8	818.0	19037.56
80.2	6.0	.390	20.65	.4164	8.8	866.6	18615.56
90.2	7.5	.458	20.56	.4595	10.9	904.3	18193.56
100.2	9.2	.534	20.07	.5065	13.2	929.1	17771.56
110.2	11.0	.618	19.26	.5574	15.5	940.7	17349.56
120.2	12.9	.711	18.19	.6122	17.7	940.3	16927.56
130.2	14.8	.813	16.92	.6707	19.9	930.2	16505.56
140.2	16.8	.925	15.48	.7330	21.9	913.5	16083.56
150.2	18.7	1.049	13.92	.7991	23.7	894.0	15661.56
160.2	20.6	1.184	12.26	.8690	25.3	875.4	15239.56
170.2	22.4	1.332	10.52	.9427	26.5	861.6	14817.56
180.2	24.0	1.494	8.72	1.0203	27.4	856.7	14395.56
190.2	25.5	1.669	6.87	1.1017	27.9	865.1	13973.56
200.2	26.6	1.858	4.99	1.1869	28.2	892.3	13551.56
210.2	27.5	2.062	3.08	1.2760	28.2	945.9	13129.56
220.2	28.0	2.282	1.14	1.3689	28.1	1037.2	12707.56
230.2	28.0	2.518	-.81	1.4655	28.1	1184.3	12285.56
240.2	27.6	2.770	-2.76	1.5660	28.5	1418.4	11863.56
250.2	26.6	3.039	-3.85	1.6728	28.7	1777.5	11441.56
260.2	25.3	3.326	-4.84	1.7836	29.2	2304.4	11019.56
270.2	23.6	3.631	-5.73	1.8983	30.0	3093.8	10597.56
280.2	21.5	3.956	-6.53	2.0167	31.3	4304.6	10175.56
290.2	19.0	4.300	-7.24	2.1382	33.3	6209.0	9753.56
300.2	16.1	4.664	-7.87	2.2615	36.1	9279.4	9331.56
310.2	12.8	5.048	-8.44	2.3842	40.1	14343.8	8909.56
320.2	9.1	5.452	-8.93	2.5015	45.2	22844.0	8487.56
330.2	5.1	5.874	-9.37	2.6047	51.1	37193.4	8065.56
340.2	.7	6.311	-9.77	2.6778	56.3	61027.0	7643.56
350.2	-4.0	6.756	-10.14	2.6939	57.1	98378.0	7221.56
360.2	-8.8	7.197	-10.53	2.6159	49.2	Error.	6799.56
370.2	-13.5	7.614	-10.99	2.4103	32.9	Error.	6377.56
380.2	-17.9	7.987	-11.60	2.0815	14.5	Error.	5955.56
390.2	-21.8	8.299	-12.47	1.6928	-.5	Error.	5533.56
Final Values							
399.8	-25.1	8.538	-13.64	1.3425	-10.6	Error.	5128.44

Circularization ΔV = 2.3607 km/sec Final Mass = 2298.8 kg

MARS LAUNCH TRAJECTORY - Trajectory Number 5

INITIAL CONDITIONS

TTURN (SEC)	PRATE (DEG/S)	MDOT (KG/S)	MASSO (KG)	ISP (SEC)	AREA (M SQ)	ALTP (KM)	L-AZ (DEG)	INCP (DEG)	STEP (SEC)
220.0	.40	42.2	22000.0	300.0	14.9	170.0	90.00	.00	.2

T (SEC)	ALT (KM)	PHI (DEG)	GAM (DEG)	VEL (KM/S)	APO (KM)	q (N/M2)	MASS (KG)
.2	.0	-.000	.08	.2421	.0	533.2	21991.56
10.2	.1	.041	4.31	.2444	.1	538.5	21569.56
20.2	.4	.082	8.49	.2521	.5	557.4	21147.56
30.2	.8	.125	12.33	.2653	1.3	588.8	20725.56
40.2	1.5	.170	15.62	.2837	2.3	630.1	20303.56
50.2	2.4	.217	18.26	.3071	3.6	677.3	19881.56
60.2	3.4	.268	20.23	.3351	5.2	725.5	19459.56
70.2	4.7	.323	21.56	.3675	7.0	769.6	19037.56
80.2	6.1	.383	22.33	.4041	9.2	805.1	18615.56
90.2	7.7	.448	22.61	.4445	11.6	828.3	18193.56
100.2	9.5	.520	22.50	.4887	14.1	837.2	17771.56
110.2	11.5	.600	22.05	.5367	16.8	831.2	17349.56
120.2	13.6	.687	21.34	.5884	19.6	811.4	16927.56
130.2	15.8	.783	20.40	.6437	22.5	779.8	16505.56
140.2	18.0	.889	19.30	.7027	25.3	739.5	16083.56
150.2	20.4	1.005	18.06	.7655	28.0	693.7	15661.56
160.2	22.8	1.132	16.70	.8320	30.6	645.6	15239.56
170.2	25.2	1.271	15.26	.9023	32.9	598.2	14817.56
180.2	27.5	1.422	13.75	.9765	35.0	553.7	14395.56
190.2	29.8	1.587	12.19	1.0546	36.8	514.3	13973.56
200.2	32.0	1.765	10.58	1.1366	38.2	481.3	13551.56
210.2	34.0	1.958	8.94	1.2226	39.3	456.0	13129.56
220.2	35.7	2.167	7.28	1.3127	39.9	439.7	12707.56
230.2	37.3	2.391	5.91	1.4072	40.5	432.5	12285.56
240.2	38.6	2.631	4.65	1.5060	41.0	433.4	11863.56
250.2	39.7	2.889	3.50	1.6093	41.3	443.2	11441.56
260.2	40.6	3.164	2.47	1.7172	41.5	463.0	11019.56
270.2	41.2	3.458	1.53	1.8301	41.6	494.6	10597.56
280.2	41.6	3.771	.68	1.9482	41.7	540.7	10175.56
290.2	41.7	4.104	-.07	2.0719	41.7	605.2	9752.56
300.2	41.5	4.458	-.74	2.2012	41.7	693.8	9331.56
310.2	41.1	4.834	-1.33	2.3368	41.8	814.9	8909.56
320.2	40.4	5.233	-1.84	2.4791	42.0	980.7	8487.56
330.2	39.5	5.657	-2.27	2.6285	42.5	1208.6	8065.56
340.2	38.4	6.105	-2.63	2.7857	43.5	1524.7	7643.56
350.2	37.0	6.580	-2.92	2.9511	45.6	1966.7	7221.56
360.2	35.4	7.084	-3.14	3.1255	49.8	2590.9	6799.56
370.2	33.5	7.617	-3.28	3.3093	60.1	3479.1	6377.56
380.2	31.6	8.182	-3.36	3.5031	98.0	4751.5	5955.56
Final Values							
385.0	30.6	8.465	-3.38	3.5997	171.0	5546.2	5753.00

Circularization ΔV = .1132 km/sec Final Mass = 5535.8 kg

MARS LAUNCH TRAJECTORY - Trajectory Number 6

INITIAL CONDITIONS

TTURN (SEC)	PRATE (DEG/S)	MDOT (KG/S)	MASSO (KG)	ISP (SEC)	AREA (M SQ)	ALTP (KM)	L-AZ (DEG)	INCP (DEG)	STEP (SEC)
200.0	.40	42.2	22000.0	300.0	14.9	170.0	90.00	.00	.2

T (SEC)	ALT (KM)	PHI (DEG)	GAM (DEG)	VEL (KM/S)	APO (KM)	q (N/M2)	MASS (KG)
.2	.0	-.000	.08	.2421	.0	533.2	21991.56
10.2	.1	.041	4.31	.2444	.1	538.5	21569.56
20.2	.4	.082	8.49	.2521	.5	557.4	21147.56
30.2	.8	.125	12.33	.2653	1.3	588.8	20725.56
40.2	1.5	.170	15.62	.2837	2.3	630.1	20303.56
50.2	2.4	.217	18.26	.3071	3.6	677.3	19881.56
60.2	3.4	.268	20.23	.3351	5.2	725.5	19459.56
70.2	4.7	.323	21.56	.3675	7.0	769.6	19037.56
80.2	6.1	.383	22.33	.4041	9.2	805.1	18615.56
90.2	7.7	.448	22.61	.4445	11.6	828.3	18193.56
100.2	9.5	.520	22.50	.4887	14.1	837.2	17771.56
110.2	11.5	.600	22.05	.5367	16.8	831.2	17349.56
120.2	13.6	.687	21.34	.5884	19.6	811.4	16927.56
130.2	15.8	.783	20.40	.6437	22.5	779.8	16505.56
140.2	18.0	.889	19.30	.7027	25.3	739.5	16083.56
150.2	20.4	1.005	18.06	.7655	28.0	693.7	15661.56
160.2	22.8	1.132	16.70	.8320	30.6	645.6	15239.56
170.2	25.2	1.271	15.26	.9023	32.9	598.2	14817.56
180.2	27.5	1.422	13.75	.9765	35.0	553.7	14395.56
190.2	29.8	1.587	12.19	1.0546	36.8	514.3	13973.56
200.2	32.0	1.765	10.58	1.1366	38.2	481.3	13551.56
210.2	33.9	1.958	8.94	1.2226	39.2	456.2	13129.56
220.2	35.7	2.167	7.43	1.3128	40.1	439.3	12707.56
230.2	37.3	2.391	6.06	1.4071	40.7	430.5	12285.56
240.2	38.7	2.631	4.80	1.5058	41.2	429.7	11863.56
250.2	39.9	2.889	3.65	1.6090	41.6	437.6	11441.56
260.2	40.8	3.164	2.62	1.7169	41.8	455.2	11019.56
270.2	41.4	3.458	1.68	1.8297	41.9	483.9	10597.56
280.2	41.8	3.771	.83	1.9477	42.0	526.3	10175.56
290.2	42.0	4.104	.08	2.0712	42.0	586.0	9753.56
300.2	41.9	4.458	-.59	2.2005	42.0	668.1	9331.56
310.2	41.5	4.833	-1.18	2.3361	42.1	780.1	8909.56
320.2	40.9	5.232	-1.69	2.4783	42.2	932.9	8487.56
330.2	40.1	5.655	-2.12	2.6278	42.7	1142.1	8065.56
340.2	39.0	6.104	-2.48	2.7850	43.6	1430.6	7643.56
350.2	37.7	6.579	-2.77	2.9506	45.4	1831.9	7221.56
360.2	36.1	7.082	-2.99	3.1252	49.3	2394.7	6799.56
370.2	34.4	7.616	-3.14	3.3095	58.8	3189.9	6377.56
380.2	32.5	8.181	-3.21	3.5040	94.4	4319.7	5955.56
Final Values							5744.56
385.2	31.5	8.476	-3.23	3.6052	171.7	5053.4	

Circularization ΔV = .1067 km/sec Final Mass = 5539.9 kg

MARS LAUNCH TRAJECTORY - Trajectory Number 7

INITIAL CONDITIONS

TTURN (SEC)	PRATE (DEG/S)	MDOT (KG/S)	MASSO (KG)	ISP (SEC)	AREA (M SQ)	ALTP (KM)	L-AZ (DEG)	INCP (DEG)	STEP (SEC)
180.0	.40	42.2	22000.0	300.0	14.9	170.0	90.00	.00	.2

T (SEC)	ALT (KM)	PHI (DEG)	GAM (DEG)	VEL (KM/S)	APO (KM)	q (N/M2)	MASS (KG)
.2	.0	-.000	.08	.2421	.0	533.2	21991.56
10.2	.1	.041	4.31	.2444	.1	538.5	21569.56
20.2	.4	.082	8.49	.2521	.5	557.4	21147.56
30.2	.8	.125	12.33	.2653	1.3	588.8	20725.56
40.2	1.5	.170	15.62	.2837	2.3	630.1	20303.56
50.2	2.4	.217	18.26	.3071	3.6	677.3	19881.56
60.2	3.4	.268	20.23	.3351	5.2	725.5	19459.56
70.2	4.7	.323	21.56	.3675	7.0	769.6	19037.56
80.2	6.1	.383	22.33	.4041	9.2	805.1	18615.56
90.2	7.7	.448	22.61	.4445	11.6	828.3	18193.56
100.2	9.5	.520	22.50	.4887	14.1	837.2	17771.56
110.2	11.5	.600	22.05	.5367	16.8	831.2	17349.56
120.2	13.6	.687	21.34	.5884	19.6	811.4	16927.56
130.2	15.8	.783	20.40	.6437	22.5	779.8	16505.56
140.2	18.0	.889	19.30	.7027	25.3	739.5	16083.56
150.2	20.4	1.005	18.06	.7655	28.0	693.7	15661.56
160.2	22.8	1.132	16.70	.8320	30.6	645.6	15239.56
170.2	25.2	1.271	15.26	.9023	32.9	598.2	14817.56
180.2	27.5	1.422	13.74	.9765	35.0	553.8	14395.56
190.2	29.8	1.587	11.79	1.0550	36.3	516.7	13973.56
[illegible]	31.8	1.766	10.00	1.1374	37.4	488.4	13551.56
210.2	33.7	1.959	8.36	1.2238	38.3	468.7	13129.56
220.2	35.4	2.168	6.85	1.3144	39.1	457.2	12707.56
230.2	36.8	2.393	5.47	1.4091	39.6	454.2	12285.56
240.2	38.1	2.634	4.22	1.5081	40.0	460.2	11863.56
250.2	39.0	2.892	3.07	1.6116	40.3	476.2	11441.56
260.2	39.8	3.168	2.04	1.7199	40.4	503.7	11019.56
270.2	40.3	3.463	1.10	1.8330	40.5	545.2	10597.56
280.2	40.5	3.776	.26	1.9513	40.5	604.3	10175.56
290.2	40.4	4.110	-.50	2.0750	40.5	686.5	9753.56
300.2	40.1	4.465	-1.16	2.2045	40.5	799.5	9331.56
310.2	39.5	4.841	-1.75	2.3402	40.7	954.9	8909.56
320.2	38.7	5.241	-2.26	2.4825	41.0	1169.5	8487.56
330.2	37.6	5.665	-2.69	2.6318	41.8	1468.2	8065.56
340.2	36.2	6.114	-3.05	2.7887	43.2	1888.6	7643.56
350.2	34.6	6.590	-3.34	2.9535	45.9	2486.5	7221.56
360.2	32.8	7.094	-3.55	3.1268	51.3	3346.3	6799.56
370.2	30.8	7.628	-3.70	3.3089	64.1	4594.5	6377.56
380.2	28.5	8.193	-3.78	3.4996	107.7	6419.2	5955.56
Final Values							
384.6	27.5	8.451	-3.80	3.5861	172.0	7472.1	5769.88

Circularization ΔV = .1313 km/sec Final Mass = 5518.1 kg

MARS LAUNCH TRAJECTORY - Trajectory Number 8

INITIAL CONDITIONS

TTURN (SEC)	PRATE (DEG/S)	MDOT (KG/S)	MASSO (KG)	ISP (SEC)	AREA (M SQ)	ALTP (KM)	L-AZ (DEG)	INCP (DEG)	STEP (SEC)
200.0	.40	42.2	22300.0	300.0	14.9	170.0	90.00	.00	.2

T (SEC)	ALT (KM)	PHI (DEG)	GAM (DEG)	VEL (KM/S)	APO (KM)	q (N/M2)	MASS (KG)
.2	.0	-.000	.08	.2421	.0	533.2	22291.56
10.2	.1	.041	4.13	.2443	.1	538.3	21869.56
20.2	.4	.082	8.13	.2518	.5	556.8	21447.56
30.2	.8	.125	11.83	.2645	1.2	587.7	21025.56
40.2	1.4	.170	15.01	.2824	2.1	628.5	20603.56
50.2	2.3	.217	17.57	.3051	3.4	675.5	20181.56
60.2	3.3	.268	19.49	.3325	4.9	724.4	19759.56
70.2	4.5	.322	20.79	.3640	6.6	770.3	19337.56
80.2	5.9	.382	21.54	.3997	8.7	808.8	18915.56
90.2	7.4	.447	21.82	.4392	10.9	836.4	18493.56
100.2	9.1	.519	21.70	.4825	13.3	850.7	18071.56
110.2	11.0	.597	21.26	.5295	15.8	851.1	17649.56
120.2	13.0	.684	20.56	.5801	18.4	838.1	17227.56
130.2	15.0	.779	19.64	.6343	21.1	813.5	16805.56
140.2	17.2	.884	18.54	.6922	23.7	779.8	16383.56
150.2	19.4	.999	17.31	.7538	26.2	740.3	15961.56
160.2	21.7	1.124	15.97	.8190	28.6	697.9	15539.56
170.2	23.9	1.261	14.54	.8880	30.8	655.5	15117.56
180.2	26.1	1.411	13.04	.9607	32.7	615.6	14695.56
190.2	28.3	1.573	11.49	1.0373	34.3	580.5	14273.56
200.2	30.3	1.749	9.90	1.1177	35.5	551.9	13851.56
210.2	32.1	1.940	8.21	1.2021	36.4	532.2	13429.56
220.2	33.7	2.145	6.67	1.2905	37.0	522.1	13007.56
230.2	35.1	2.366	5.26	1.3830	37.5	522.1	12585.56
240.2	36.2	2.603	3.97	1.4796	37.9	532.8	12163.56
250.2	37.1	2.856	2.79	1.5805	38.1	555.8	11741.56
260.2	37.7	3.127	1.72	1.6860	38.2	593.4	11319.56
270.2	38.1	3.416	.75	1.7961	38.2	648.8	10897.56
280.2	38.2	3.723	-.12	1.9111	38.2	727.5	10475.56
290.2	38.0	4.050	-.91	2.0313	38.2	836.9	10053.56
300.2	37.6	4.398	-1.61	2.1570	38.3	988.5	9631.56
310.2	36.8	4.766	-2.22	2.2883	38.5	1198.7	9209.56
320.2	35.8	5.157	-2.76	2.4258	39.0	1493.0	8787.56
330.2	34.5	5.571	-3.23	2.5696	39.9	1909.5	8365.56
340.2	32.9	6.010	-3.62	2.7202	41.6	2506.5	7943.56
350.2	31.1	6.474	-3.94	2.8777	44.5	3374.2	7521.56
360.2	29.0	6.965	-4.19	3.0422	50.0	4651.8	7099.56
370.2	26.6	7.484	-4.37	3.2133	61.0	6556.0	6677.56
380.2	24.1	8.032	-4.49	3.3902	87.6	9419.9	6255.56
Final Values							
389.6	21.5	8.575	-4.54	3.5596	172.6	13433.8	5858.88

Circularization ΔV = .1662 km/sec Final Mass = 5537.1 kg

Appendix F

Heating Effects Code

(Seybold)

```
C
C  CALINA'S PROGRAM 2
C
C  APPROXIMATE HEATING RATES AND TEMPERATURES
C
C NOTE:  THIS PROGRAM IS ONLY ONE OF THE HEATING CODES I
C WORKED WITH.  THE OTHERS WERE DIFFERENT ONLY IN THE
C DISTANCE RANGE FOR THE LAMINAR FLAT PLATE CALCULATIONS.
C
C  DEFINITION OF VARIABLES
C
      REAL RHO, VEL, RADIUS, C1, C2, ANGLE, LAMHT, STAGHT
      REAL TEMP, EMISS, DIST
C
C THE LAMINAR FLAT PLATE
C
      WRITE (*,*) 'INPUT A DENSITY IN KG/M3'
      WRITE (5,*) 'INPUT A DENSITY IN KG/M3'
      READ (*,*) RHO
      WRITE (5,*) RHO
      WRITE (*,*) 'INPUT THE VELOCITY IN M/S'
      WRITE (5,*) 'INPUT THE VELOCITY IN M/S'
      READ (*,*) VEL
      WRITE (5,*) VEL
      WRITE (*,*) 'INPUT THE LOCAL BODY ANGLE IN RAD'
      WRITE (5,*) 'INPUT THE LOCAL BODY ANGLE IN RAD'
      READ (*,*) ANGLE
      WRITE (5,*) ANGLE
      DIST=1
5     IF (DIST.LE.10) THEN
            C1=((2.53E-9)*(COS(ANGLE)**0.5)*SIN(ANGLE))/
     &      (DIST**0.5)
            LAMHT=C1*(RHO**0.5)*(VEL**3.2)
            WRITE (*,*) 'DIST = ', DIST, '  M AND LAMHT =', LAMHT,
     &      ' W/CM2'
            WRITE (5,*) 'DIST = ', DIST, ' M AND LAMHT =', LAMHT,
     &      ' W/CM2'
            DIST=DIST+1
            GOTO 5
      ELSE
            GOTO 10
      ENDIF
C
C THE STAGNATION HEATING
C
10    WRITE (*,*) 'INPUT THE NOSE RADIUS IN M'
```

```
      WRITE (5,*) 'INPUT THE NOSE RADIUS IN M'
      READ (*,*) RADIUS
      WRITE (5,*) RADIUS
      C2=(1.83E-8)/(RADIUS**0.5)
      STAGHT=C2*(RHO**0.5)*(VEL**3.0)
      WRITE (*,*) 'STAGNATION HEATING IS ', STAGHT, ' W/CM2'
      WRITE (5,*) 'STAGNATION HEATING IS ', STAGHT, ' W/CM2'
C
C  THE STAGNATION TEMPERATURE
C
      WRITE (*,*) 'INPUT THE EMISSIVITY OF THE MATERIAL'
      WRITE (5,*) 'INPUT THE EMISSIVITY OF THE MATERIAL'
      READ (*,*) EMISS
      WRITE (5,*) EMISS
      TEMP=((STAGHT/(EMISS*(5.67E-12)))**0.25)
      WRITE (*,*) 'THE TEMPERATURE IS ', TEMP, ' K AT THE NOSE'
      WRITE (5,*) 'THE TEMPERATURE IS ', TEMP, ' K AT THE NOSE'
      STOP
      END
```

Appendix G

Nozzle Design Code

(Amato)

Nozzle Design Code - Mike Amato

```
90 VC=250
100 LS=60
101  THRUST=26000!
102 DOC=.75
103 DIP=80
104 DENSO=90
105 DENSF=60
106 SIMP=300
107 VCF=.7
108 TC=5200
109  WMM=22
110 K=1.25
111 TCF=.96
112 PC=300
113 PE=1
114  AMTI=20
200 CF=(((2*K^2/(K-1))*(2/(K+1))^((K+1)/(K-1))*(1-(PE/PC)^((K-1)/K)))^.5)-
(((PE-.078)/PC)*25)
210  AT=THRUST*TCF/(CF*PC)
220 DT=(4*AT/3.1415)^.5
230  AEF=24*AT
240 DEGF=(4*AEF/3.1415)^.5
250 VE=3612.7*2.5
260 AEC=((THRUST*32.2*TC*1544)/((VE^2)*PC*WMM))*(PC/PE)^(1/K)
270 DEC=(4*AEC/3.1415)^.5
280  AC=(THRUST*32.2*1544*TC)/(VE*WMM*PC*VC)
285 DC=2*(AC/3.14)^.5
290  VOLC=LS*AT
300  FMT=THRUST*32.2/VE
310 FMO=FMT*1.62/(1.62+1)
320 FMF=FMT/(1.62+1)
330 AIO=((FMO/(DOC*(2*32.2*DIP*DENSO)^.5))/AMTI)
340 AIF=((FMF/(DOC*(2*32.2*DIP*DENSF)^.5))/AMTI)
350  VF=DOC*((2*32.2*DIP*144)/DENSF)^.5
360  VO=DOC*((2*32.2*DIP*144)/DENSO)^.5
370 REM FJA=ARCSIN((FMO*VO/(FMF*VF))*.342)
380 AMTP=((450*144*9.43)/(380*520))*(1.667/(1-((450*80)/3000)))
390 THICK=2*300*DC/(2*58000!)
400 WGT=((.3333*3.14*70*((DEGF+THICK)^2))-(.3333*3.14*70*(DEGF^2)))*.072
490 PRINT "CF=",CF
500 PRINT "THROAT AREA=", AT, "   THROAT DIAMETER=", DT
510 PRINT "FIGURE EXIT AREA=", AEF, "   EXIT DIAMETER=", DEGF
520 PRINT "EXIT VELOCITY=", VE
530 PRINT "EXIT AREA=", AEC, "EXIT DIAMETER=", DEC
```

```
540 PRINT "CHAMBER AREA=", AC, "CHAMBER VOLUME=", VOLC
542 PRINT "FUEL FLOW=",FMT
550 PRINT "FUEL AND OX MASS FLOW=", FMF, FMO
560 PRINT "EACH FUEL AND OX INJECTOR AREA=", AIF, AIO
570 PRINT "FUEL AND OX VELOCITY= ", VF, VO
580 PRINT " FUEL JET INCLINATION=", FJA
590 PRINT "AMT PRESSURANT =", AMTP
600 PRINT "THICKNESS MAX =", THICK
610 PRINT "Weight Of Engine =", WGT
```

Where:

VC=chamber velocity
LS=chamber volume to throat ratio = 60
DOC=injector discharge coefficient =0.75
DIP= injection pressure drop = 80 psi (the oxidizer and fuel injection velocities are 80 ft/s and 62 ft/s respectively for ascent which justifies a DIP of 80 psi)
DENSO=density of oxidizer = 90 lb/in
DENSF=density of fuel = 60 lb/in
SIMP=specific impulse= 300 s
VCF=velocity correction factor=0.7
TC=combustion temperature = 5200 F
WMM=mean molecular weight of exhaust gas = 22 lb/mole assuming frozen flow
K=specific heat ratio = 1.25 assuming frozen flow
TCF=thrust correction factor = 0.96
PC=combustion pressure = 300 psi
CF=thrust coefficient
AT,DT=throat area and diameter
AEC,DEC=exit area and diameter
AC,DC,VOLC=chamber area , diameter and volume
FMT,FMO,FMF=total,oxidizer and fuel mass flows
AIO,AIF=area of each injector
VO,VF=oxidizer and fuel injection velocities
FJA=fuel injection angle (picking a ox. in. angle)
AMTP=amount of helium pressurant needed
WGT=weight of engine using cone approximation and assuming whole cone is maximum thickness and a safety factor of 2
AMTI=number of fuel and oxidizer injectors

Appendix H

Battin's Universal Formulas Code

(Ryan)

```
C     DARREN RYAN
C
C     BATTIN'S UNIVERSAL FORMULAS
C
C     THIS PROGRAM COMPUTES THE FINAL POSITION AND FINAL
C     VELOCITY OF A SPACECRAFT AFTER A GIVEN TIME PERIOD,
C     IF THE INITIAL POSITION AND INITIAL VELOCITY ARE KNOWN.
C     THIS METHOD USES AN ITERATION TECHNIQUE AND BATTIN'S
C     UNIVERSAL FORMULAS.
C
C     -DECLARATION OF VARIABLES
C
      REAL N,R,V,A,AI,MU,T0,T
      REAL RR,RI,RJ,ALPHA,VR,VI,VJ,BETA
      REAL RDOTV,ANGLE
      REAL X(100),B(100),C(100),F(100),G(100),S(100)
C
C     -DEFINITION OF VARIABLES
C
C     -N =ITERATION VARIABLE
C     -R =INITIAL RADIUS
C     -V =INITIAL VELOCITY
C     -A =SEMI-MAJOR AXIS OF ORBIT
C     -AI =INVERSE OF SEMI-MAJOR AXIS
C     -MU =GRAVITATIONAL COEFFICIENT OF THE SUN
C     -T0 =INITIAL TIME, THE TIME AT THE STARTING POINT OF THE
ORBIT
C     -T =TOTAL TIME DURATION OF ORBIT TRAJECTORY
C     -RR =FINAL RESULTANT RADIUS VECTOR
C     -RI =X-COMPONENT OF THE RESULTANT RADIUS VECTOR RR
C     -RJ =Y-COMPONENT OF THE RESULTANT RADIUS VECTOR RR
C     -ALPHA =ANGLE FORMED BETWEEN THE FINAL RADIUS
VECTOR
C              RR AND THE X-AXIS
C     -VR =FINAL RESULTANT VELOCITY VECTOR
C     -VI =X-COMPONENT OF THE RESULTANT VELOCITY VECTOR VR
C     -VJ =Y-COMPONENT OF THE RESULTANT VELOCITY VECTOR VR
C     -BETA =ANGLE FORMED BETWEEN THE FINAL VELOCITY
VECTOR
C             VR AND THE X-AXIS
C     -RDOTV =SCALAR QUANTITY OF THE DOT PRODUCT OF
VECTORS
C              R & V
C     -ANGLE =ANGLE FORMED BETWEEN THE VECTORS R & V
C
```

```
      N=2.0
      MU=1.3267E+11
      T0=0.0
C
C     INPUT OF INITIAL VARIABLES
C
      WRITE(*,*) 'ENTER AN INITIAL VELOCITY (KM/SEC).'
      READ(*,*) V
      WRITE(*,*) 'ENTER AN INITIAL RADIUS (KM).'
      READ(*,*) R
      WRITE(*,*) 'ENTER THE ANGLE BETWEEN THE TWO VECTORS.'
      READ(*,*) ANGLE
      ANGLE=ANGLE*3.141592654/180
      WRITE(*,*) 'ENTER THE TIME OF FLIGHT IN DAYS.'
      READ(*,*) T
C
C     - CONVERTS TIME IN DAYS TO TIME IN SECONDS
      T=T*8.64E+04
C
C     -CALCULATION OF THE DOT PRODUCT OF VECTORS R & V
      RDOTV=R*V*COS(ANGLE)
C
      WRITE(*,*) 'ENTER AN INITIAL VALUE OF X.'
      READ(*,*) X(N)
C
C     -COMPUTATION OF SEMI-MAJOR AXIS 'A'.
      A=1/((2/R)-(V**2/MU))
C
      AI=1/A
C
C     -ITERATION LOOP TO DETERMINE THE FUNCTIONS S(N),C(N),
C      G(N),F(N), AND THE FINAL VALUE OF X.
C
      DO 10 I=1,15
      B(N)=AI*X(N)**2
      IF (B(N) .GT. 0.0) THEN
      S(N)=(SQRT(B(N))-SIN(SQRT(B(N))))/((SQRT(B(N)))**3)
      C(N)=(1-(COS(SQRT(B(N)))))/B(N)
      ELSE IF (B(N) .LT. 0.0) THEN
      S(N)=(SINH(SQRT(-B(N)))-SQRT(-B(N)))/((SQRT(-B(N)))**3)
      C(N)=((COSH(SQRT(-B(N))))-1)/(-B(N))
      ENDIF
      F(N)=(RDOTV/SQRT(MU))*(X(N)-(AI*(X(N)**3)*S(N)))+(1-
R*AI)*(X(N)**2)*C(N)     G(N)=(RDOTV/SQRT(MU))*(X(N)**2)*C(N)+(1-
R*AI)*(X(N)**3)*S(N)+R*X(N)
      N=N+1
```

```
      X(N)=X(N-1)-((G(N-1)-(SQRT(MU)*T))/F(N-1))
 10   CONTINUE
C
C     - PRINT OUT COMPUTED VARIALBES
C
      WRITE(*,*) 'A=',A
      WRITE(*,*) 'AI=', AI
      WRITE(*,*) 'X=', X(N-1)
C
C     - CALCULATION OF RI,RJ,RR,ALPHA
C
      RI=(1-((X(N-1)**2)/R)*C(N-1))*R
      RJ=(T-((X(N-1)**3)/(SQRT(MU)))*S(N-1))*V
      RR=SQRT((RI**2)+(RJ**2))
      ALPHA=ACOS(RI/RR)*180/3.141592654
C
C     - CALCULATION OF VI,VJ,VR,BETA
C
      VI=(SQRT(MU)/(RR*R))*((AI*(X(N-1)**3)*S(N-1))-X(N-1))*R
      VJ=(1-((X(N-1)**2)/RR)*C(N-1))*V
      VR=SQRT((VI**2)+(VJ**2))
      BETA=ACOS(VI/VR)*180/3.141592654
C
C     - PRINTS OUT FINAL VARIABLES
C
      WRITE(*,*) 'R(T)=',RI,'i + ',RJ,'j'
      WRITE(*,*) 'V(T)=',VI,'i + ',VJ,'j'
      WRITE(*,*) ' '
      WRITE(*,*) 'R=',RR
      WRITE(*,*) 'ALPHA=',ALPHA
      WRITE(*,*) 'V=',VR
      WRITE(*,*) 'BETA=',BETA
      STOP
      END
```

Appendix I

Planet Position Determination Code

(Ryan)

```
C     DARREN RYAN
C
C     PLANET POSITION DETERMINATION PROGRAM
C
C     THIS PROGRAM COMPUTES THE HELIOCENTRIC COORDINATES
OF
C     THE PLANETS VENUS, EARTH, AND MARS, GIVEN AN INITIAL
MONTH,
C     DATE AND YEAR STARTING WITH THE YEAR 2000.  THE
PROGRAM ASSUMES
C          CIRCULAR AND COPLANAR ORBITS, AND PERTURBATIONS
IN THESE ORBITS ARE
C     ARE NOT ACCOUNTED FOR.
C
C     -DECLARATION OF VARIABLES
C
      REAL YEAR,MONTH,DAY,LEAP,MU,PI
      REAL AMARS,AEARTH,AVENUS,MHELIO,EHELIO,VHELIO
      REAL MPER,EPER,VPER,MREF,EREF,VREF
C
C     -DEFINITION OF VARIABLES
C
C     MU=GRAVITATIONAL COEFFICIENT OF THE SUN
C     YEAR= INPUT YEAR (2000- )
C     MONTH= INPUT MONTH (1-12)
C     DATE= INPUT DATE (1-31)
C     AMARS=SEMI-MAJOR AXIS OF MARS ABOUT THE SUN
C     AEARTH= SEMI-MAJOR AXIS OF EARTH ABOUT THE SUN
C     AVENUS= SEMI-MAJOR AXIS OF VENUS ABOUT THE SUN
C     MREF= HELIOCENTRIC REFERENCE ANGLE OF MARS ON YEAR
2000
C     EREF= HELIOCENTRIC REFERENCE ANGLE OF EARTH ON YEAR
2000
C     VREF= HELIOCENTRIC REFERENCE ANGLE OF VENUS ON YEAR
2000
C     LEAP= NUMBER OF LEAP DAYS BETWEEN THE ENTERED YEAR
AND
C          YEAR 2000
C     TIME= AMOUNT OF TIME IN SECONDS FROM YEAR 2000 TO
INPUTE
C          YEAR
C     MPER= PERIOD OF MARS ABOUT THE SUN
C     EPER= PERIOD OF EARTH ABOUT THE SUN
C     VPER= PERIOD OF VENUS ABOUT THE SUN
C     MANGLE= HELIOCENTRIC DISPLACEMENT ANGLE OF MARS
FROM
```

```
C                    HELIOCENTRIC REFERENCE ANGLE MREF
C      EANGLE= HELIOCENTRIC DISPLACEMENT ANGLE OF EARTH
FROM
C                    HELIOCENTRIC REFERENCE ANGLE EREF
C      VANGLE= HELIOCENTRIC DISPLACEMENT ANGLE OF VENUS
FROM
C                HELIOCENTRIC REFERENCE ANGLE VREF
C      MHELIO=HELIOCENTRIC ANGLE OF MARS AT SPECIFIED DATE
C      EHELIO=HELIOCENTRIC ANGLE OF EARTH AT SPECIFIED DATE
C      VHELIO=HELIOCENTRIC ANGLE OF VENUS AT SPECIFIED DATE
C
       AMARS=2.275E+11
       AEARTH=1.495E+11
       AVENUS=1.082E+11
       MU=1.3267E+20
       MREF=357.9
       EREF=99.27
       VREF=180.79
       PI=3.14159
C
C      INPUT OF REQUIRED DATA
C
       WRITE(*,*) 'ENTER THE SPECIFIED YEAR.'
       READ(*,*) YEAR
       WRITE(*,*) 'ENTER THE SPECIFIED MONTH (1-12).'
       READ(*,*) MONTH
       WRITE(*,*) 'ENTER THE SPECIFIED DATE (1-31).'
       READ(*,*) DAY
C
C      CONVERSION OF THE NUMERICAL VALUE OF MONTH INTO
NUMBER
C      OF DAYS SINCE JANUARY 1ST
C
       IF (MONTH .EQ. 1) THEN
             MONTH=0.0
       ELSE IF (MONTH .EQ. 2) THEN
             MONTH=31.0
       ELSE IF (MONTH .EQ. 3) THEN
             MONTH=59.0
       ELSE IF (MONTH .EQ. 4) THEN
             MONTH=90.0
       ELSE IF (MONTH .EQ. 5) THEN
             MONTH=120.0
       ELSE IF (MONTH .EQ. 6) THEN
             MONTH=151.0
       ELSE IF (MONTH .EQ. 7) THEN
```

```
            MONTH=181.0
        ELSE IF (MONTH .EQ. 8) THEN
            MONTH=212.0
        ELSE IF (MONTH .EQ. 9) THEN
            MONTH=243.0
        ELSE IF (MONTH .EQ. 10) THEN
            MONTH=273.0
        ELSE IF (MONTH .EQ. 11) THEN
            MONTH=304.0
        ELSE IF (MONTH .EQ. 12) THEN
            MONTH=334.0
        ENDIF
C
        LEAP=INT((YEAR-2000)/4))
C
        TIME=(((YEAR-2000)*365)+MONTH+DAY+LEAP)*8.64E+04
C
        MPER=2*PI*(SQRT(AMARS**3)/MU)
        EPER=2*PI*(SQRT(AEARTH**3)/MU)
        VPER=2*PI*(SQRT(AVENUS**3)/MU)
C
        MANGLE=((TIME/MPER)-INT(TIME/MPER))*360
        EANGLE=((TIME/EPER)-INT(TIME/EPER))*360
        VANGLE=((TIME/VPER)-INT(TIME/VPER))*360
C
C       CALCULATION OF THE HELIOCENTRIC ANGLE OF MARS ON THE
C       SPECIFIED DATE
C
        IF ((MREF+MANGLE) .GE. 360) THEN
            MHELIO=(MREF+MANGLE)-360
        ELSE
            MHELIO=MREF+MANGLE
        ENDIF
C
C       CALCULATION OF THE HELIOCENTRIC ANGLE OF EARTH ON
THE
C       SPECIFIED DATE
C
        IF ((EREF+EANGLE) .GE. 360) THEN
            EHELIO=(EREF+EANGLE)-360
        ELSE
            EHELIO=EREF+EANGLE
        ENDIF
C
C       CALCULATION OF THE HELIOCENTRIC ANGLE OF VENUS ON
THE
```

```
C       SPECIFIED DATE
C
        IF((VREF+VANGLE) .GE. 360) THEN
              VHELIO=(VREF+VANGLE)-360
        ELSE
              VHELIO=VREF+VANGLE
        ENDIF
C
C       PRINT'S OUTPUT TO THE SCREEN
C
        WRITE(*,*) VHELIO,EHELIO,MHELIO
        STOP
        END
```

Appendix J

Waverider Generation Data

(McCartney, Martin)

WAVERIDER OPTIMIZED FOR MAX VOL WITHOUT CHEMISTRY - VENUS: M=49.7, ALT=30 km

---------- FLIGHT CONDITIONS ----------

Mach No.	=	4.97000E+01
Pressure	=	9.55000E-05 N/m2
Density	=	1.01500E-01 kg/m3
Temperature	=	4.91581E-06 K
Dynamic press	=	1.44839E-01 N/m2

---------- GENERATING BODY FOR FLOWFIELD ----------

Length	=	1.56096E+02 m
Cone angle	=	7.50000E+00 degrees
Shock angle	=	7.99376E+00 degrees

---------- AIRCRAFT DIMENSIONS ----------

Aircraft length	=	8.00000E+01 m
Base height / length	=	1.27431E-01
Semi-span / length	=	1.76599E-01
Planform area	=	1.36388E+03 m2
Base area	=	1.79097E+02 m2
Wetted area (upper)	=	1.45291E+03 m2
Wetted area (lower)	=	1.42887E+03 m2
Total wetted area	=	2.88178E+03 m2
Aircraft volume	=	5.29994E+03 m3
Volumetric Efficiency	=	2.22879E-01

---------- INVISCID AERODYNAMICS ----------

CLpl = 3.53538E-02	CDpl = 5.12784E-03	
CLpu = -6.59354E-04	CDpu = 0.00000E+00	CMpl = -2.17325E-02
CLpb = 0.00000E+00	CDpb = -8.65825E-05	CMpd = -3.42132E-04
CLp = 3.46944E-02	CDp = 5.04126E-03	CMp = -2.20747E-02
L/D = 6.88209E+00		

---------- VISCOUS AERODYNAMICS ----------

Local transition Reynolds number = Inf
Upper surface transition dist from LE = Inf m

CLfl = -7.92499E-10	CDfl = 6.65062E-09	CMfl = 2.99203E-11
CLfu = 0.00000E+00	CDfu = 2.24621E-07	CMfu = -5.18748E-09
CLf = -7.92499E-10	CDf = 2.31272E-07	CMf = -5.15756E-09
CL = 3.46944E-02	CD = 5.04149E-03	CM = -2.20747E-02
L/D = 6.88178E+00		

---------- HEAT TRANSFER DATA ----------

Aircraft wall temperature = 7.85000E+02

Index of Authors